ASPECTS OF BUBBLE BEHAVIOUR IN FLUIDIZED BEDS

A Thesis Submitted for the

Degree of Doctor of Philosophy

of the

University of London

by

MANSOUR MOTAMEDI-LANJANI

M.Sc.,D.I.C.

Department of Chemical Engineering and Chemical Technology

Imperial College of Science and Technology

London S.W.7.

England

AUGUST 1970

TO MY WIFE

ABSTRACT

This work consists of two parts. Part one is mainly concerned with the problems of the division of the flow between various phases, bubble population properties and bubble growth. Experimental evidence is presented in support of the theory put forward by LOCKETT, DAVIDSON, and HARRISON. It is shown that the bubble size distribution and also the distribution of α (the ratio of bubble velocity to the remote interstitial gas velocity) follow normal distribution curves. The growth of a single bubble is also studied experimentally and theoretically.

In the second part the pressure distribution around bubbles in beds of spherical ballotini and irregular sand is studied. The stability of the bubble boundary is explained in the light of the pressure gradient information. Finally some of the anomalies reported in literature are satisfactorily explained.

ACKNOWLEDGMENTS

The author wishes to express his sincere gratitude to Dr. G.J. Jameson for his continued supervision and interest throughout the course of this work.

Thanks are also due to Mr. J. Oakley, Mr. A. Tyley and Mr. D.P. Roch and many members of their staff for their help in the construction of the apparatus, and the electronic components.

My sincere thanks are extended to my wife, Pari, for her lasting tolerance and patience, and to my parents for their encouragement whilst the work was being completed.

The author would like to express his appreciation for the Scholarship awarded by The Ministry of Higher Education of Imperial Iranian Government.

TABLE OF CONTENTS

NOMENCLATURE

A	cross-sectional area of bed; radius of circle of penetration
a	radius of bubble
$d\bar{A}$	vector of an element of area
$d\bar{a}$	vector area of element of bubble surface
B_o	flow through bubbles at a cross section
$\triangle B_o$	flow through a cross section of a fixed bubble
$\triangle B_M$	flow through a cross section of a moving bubble
C_{RT}	coefficient
C_{RB}	coefficient
d_i	part of a cross section inside i_{th} bubble
D_B	bubble diameter
F_p	flow through particulate phase
g	acceleration of gravity
h	height
J	pressure gradient at infinity
k	constant
K	constant of DARCY'S law; constant of bubble velocity diameter relationship
L	width of bed; length of a fixed bed
m, n	number of frames
P	pressure
$\triangle P$	pressure drop
p_f	fluid pressure
p_p	interparticle pressure
Q_B	visible bubble flow rate
Q_{mf}	minimum fluidization flow rate
q	velocity in space
R_B	bubble radius

r	bubble radius; polar co-ordinate
s	$\frac{r}{a}$
S	thickness of bed
U	superficial velocity of fluidizing fluid
U_o, U_{mf}	incipient fluidization velocity (superficial)
U_{bp}	velocity at bubbling point
$\bar{u}$	interstitial fluid velocity
$\bar{u}_f$	interstitial fluid velocity with particles fixed
$\bar{u}_R$	interstitial fluid velocity at surface of fixed bubble
U_B, U_b	bubble velocity
U_{Bi}	velocity of the i_{th} bubble
$\bar{v}$	particle velocity
V_B	volume of bubble
V_{cp}	cloud space volume
Z	distance in vertical direction
ε_o, ε_{mf}	mean voidage fraction at incipient fluidization
ε_b, ε_B	bubble fraction in bed
δ	fraction of cross section taken by bubbles
μ	viscosity of fluid
α	ratio of bubble velocity to remote gas interstitial velocity
β	U_{B/U_o}
θ	polar co-ordinate
ψ	stream function
ρ	density

P A R T O N E

CHAPTER 1

INTRODUCTION

Fluidization is the phenomenon in which the drag force acting on a dense swarm of particles due to an upward fluid flow through them is counteracted by the gravitational force and hence the particles are kept in a more or less floating state. The properties of gas fluidized systems have attracted enormous attention and interest, both in theoretical and practical sense. This is because a gas fluidized system is not only a field with a high capability for attracting theoretical treatment, but also because such systems have particular properties which offer suitable solutions to a wide range of industrial problems. These properties are namely good heat transfer characteristics, good mixing and good gas solid contacting under suitable conditions. Let us examine the main reason behind all these features of gas fluidized systems. The continuous movement of the particles disturbs the thermal equilibrium near a wall and hence by maintaining a steep temperature gradient ensures a high rate of heat transfer, BOTTERILL et al (1). Neglecting the mechanical stirring of the solids, this would have been impossible without bubbles. Bubbles are also responsible for the good degree of mixing achieved in gas fluidized beds, ROWE et al (2). When a slow reaction is to be carried out the role of bubbles becomes significant in regard to gas-solid contact too. Thus bubbles are the cause of many of the most useful features of fluidized beds. Without bubbles the engineering and the design of gas fluidized systems would have been much easier, however, their application would

have been much more limited.

Bubbles appear when the upward flow of gas through a bed of particles exceeds the critical value necessary to keep the particles in suspension . It is from this point where the interest and associated problems in gas fluidization become significant. It is highly desirable to know, for instance, how the flow is divided into different phases, i.e. particulate and bubble phase s. Also it is extremely important to know how bubbles grow, and the bubble population properties. All these questions are of immediate interest in the understanding and design of gas-fluidized systems and have attracted a vast amount of effort in theory and practice. A basic knowledge of some of the problems has been provided, but a complete and clear picture is not still available. The aim of the present work is to investigate some of the most important aspects of bubbles in gas-fluidized systems with regard to the understanding and design of such systems. The first part is mainly concerned with the problems of the division of flow between various phases, bubble population properties and growth. In addition a good deal of by-product information is presented.

CHAPTER 2

LITERATURE SURVEY

2.1 INTRODUCTION

TOOMEY & JOHNSTONE (3) proposed that in an aggragatively fluidized system the total flow of gas is equal to the flow in the rising bubbles and the flow required for incipient fluidization. DAVIDSON & HARRISON (4) pointed out that a model of aggregative fluidization may be set up by considering a bed as a two-phase system consisting of:

(a) a particulate phase in which the flow-rate is equal to the flow rate for incipient fluidization, i.e. the voidage fraction is essentially constant at ε_o (where ε_o = mean voidage fraction at incipient fluidization), and

(b) a bubble phase which carries the additional flow of the fluidizing fluid.

The model was discussed at some length by DAVIDSON & HARRISON who found that there was considerable experimental work of differing techniques in support of the theory. They also found out that there was remarkable agreement between the theory and experiment when the model was applied to the cases of slug flow (4) and bubble formation at a single orifice in a fluidized bed (4).

It was pointed out that the contradictory experimental results of some workers (cf. BAUMGARTEN & PIGFORD (5); LANNEAU (6)) was due to the measuring techniques they employed.

ROWE & SUTHERLAND (7) showed that bubbling did not start at

gas velocities up to about 1.2 Uo (where Uo is the incipient fluidization velocity) which suggested that the dense phase could absorb a velocity greater than Uo. DAVIES & RICHARDSON (8) noticed that when the background velocity was 1.5 Uo, gas was transferred from the bubble to the continuous phase for injection rates of bubbles less than 400 ml/min. It was also noticed that the interstitial velocity at which bubble formation first occurs, U_{bp}, could be as high as 2.8 Uo. They also showed that the effective gas velocity in the continuous phase approached the minimum value of Uo asymptotically.

TURNER (9) questioned the common "two-phase" assumption of fluidization that the excess fluid above that necessary for incipient fluidization of a bed of particles passes through the bed as visible bubble flow. DAVIDSON & HARRISON (10) gave a new theory which partly justified the assumption. They showed that

$$U\,A = k\,Uo\,A + Q_B \qquad \text{Eq.(1)}$$

where

U = the superficial fluid velocity,

U_o = the superficial fluid velocity at incipient fluidization,

k = a parameter depending on the concentration of the bubble,

A = the cross-sectional area of the bed,

Q_B = the visible bubble flow.

PARTRIDGE & ROWE (11) devised a theory which showed that k = 1 always, and therefore confirmed the strict "two-phase" assumption. LOCKETT et al (12) gave an alternative method of calculating k in Eq.(1). Their theory, assuming constant voidage fraction between bubbles, showed that for a regular array of bubbles, $k = 1 + \varepsilon_b$, for a two-dimensional system, where

$$\varepsilon_b = \frac{\text{Total volume of the bubbles in the bed}}{\text{bed volume}}$$

was small. For three-dimensional systems it was inferred that $k = 1 + 2\varepsilon_b$. They concluded that for systems operated under flow conditions distinctly above the incipient fluidization velocity (i.e. large Q_B) the two-phase assumption - though formally incorrect - was a reasonable model of the experimental situation.

PYLE & HARRISON (13) discussed the experimental evidence for the two-phase theory from two points of view. First, they measured the volume flow rate of bubbles in a two-dimensional fluidized bed and compared them with theory. Second, an expression for the minimum height of fluidized bed on the basis of NICKLIN'S (14) theory for bubbling two-phase systems was developed. Their conclusion was that in both two- and three-dimensional fluidized beds interstitial velocities several times greater than the incipient value may be found, particularly near the bottom of the bed. GRACE & HARRISON (15) presented experimental evidence which indicated that the analysis of LOCKETT, DAVIDSON and HARRISON gives a better estimate of flow in the bubble phase than the earlier theory of TOOMEY and JOHNSTONE. However, it was pointed out that, the bubble through flow velocities appear to be greater than predicted by the available theories. GELDART (16) presented evidence in support of the view that the visible bubble flow rate was less than the difference between the total flow rate and that necessary for minimum fluidization.

The fundamental objective of the present work is to obtain experimental evidence for testing the two-phase theory. The relation between this experimental evidence and the new theory proposed by DAVIDSON & HARRISON (10) will be discussed. Next a short account of the above mentioned theory will be given.

2.2 THEORY

The following theory is given by DAVIDSON & HARRISON (10).

The analysis of the fluid flow in a continuously bubbling fluidized bed is presented based on the following assumptions:

(i) The voidage fraction in the dense phase is assumed to be constant and equal to its value at incipient fluidization.

(ii) DARCY'S Law is assumed to govern the relative motion between the fluid and particles. Neglecting the fluid inertia

$$\bar{u} = \bar{v} - K \text{ grad } P \qquad \text{Eq.(2)}$$

where $\bar{u}$ and $\bar{v}$ are the fluid and the particle velocity respectively; P the fluid pressure; and K is the constant of DARCY'S Law.

(iii) The fluidizing fluid is assumed to be incompressible.

Continuity equations for fluid and particles are

$$\begin{aligned} \text{div } \bar{u} &= 0 \\ \text{div } \bar{v} &= 0 \end{aligned} \qquad \text{Eq.(3)}$$

even for unsteady flow. From Eqs. (2 & 3) it follows that

$$\text{div grad } P = 0 \qquad \text{Eq.(4)}$$

which gives the important information that the pressure distribution is independent of the particle motion for given boundary conditions.

Now consider a freely bubbling bed Fig.(1) fluidized by a superficial fluid velocity U. According to the above argument the pressure distribution in the bed would be exactly the same if all particles, and hence the bubbles, were held fixed by an external force, provided

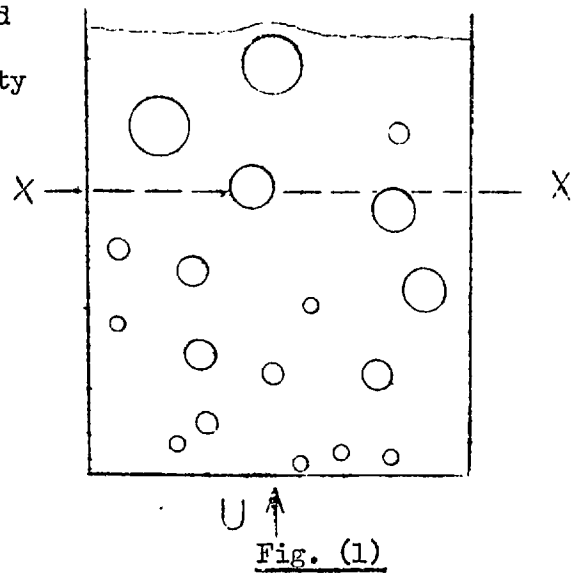

Fig. (1)

the pressure just above the distributor was the same in both situations.

In order to get the total flow through the bed, we integrate the contribution of the particulate phase and the bubble phase across a typical cross section such as X-X. In the fixed particle case we have:

$$\text{Total flow through the bed} = \varepsilon_o \int_p \bar{u}_f \cdot d\bar{A} + B_o$$

$$= F_p + B_o \qquad \text{Eq.(5)}$$

where $\bar{u}_f$ is the interstitial velocity (vector) and $d\bar{A}$ is an upward pointing vector representing an element of area; B_o is the flow through the bubbles intersected by X-X, F_p is the contribution of the particulate phase, and the integral is over the area of particles cut by X-X.

Now consider the same cross-section but in the case where particles are moving with velocity $\bar{v}$. The pressure distribution is unaffected by the motion of the particles. In this case the fluid velocity at any point is $\bar{u}_f + \bar{v}$, and the flow due to the particulate phase cut by X-X is $\varepsilon_o \int_p (\bar{u}_f + \bar{v}) \cdot d\bar{A}$. But $\int_p \bar{V} \cdot dA = 0$ because there is no net motion of the particles when integration is carried out across an area large compared with the size of the bubbles. Therefore the flow due to the particulate phase is still F_p. Next consider one of the bubbles cut by X-X Fig.(2). If the bubble is fixed, the fluid interstitial velocity at the surface of the bubble is $\bar{u}_R$ and therefore the flow across A-C is given by

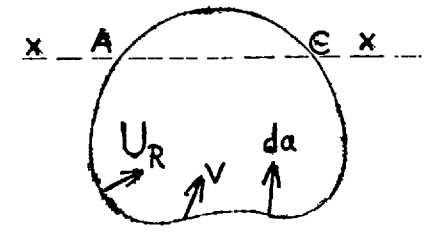

Fig(2)

$$\Delta B_o = \varepsilon_o \int_A^C \bar{u}_R \cdot d\bar{a} \qquad \text{Eq.(6)}$$

where $d\bar{a}$ is a vector representing an element of the bubble surface, and $\bar{u}_R$ is parallel to $d\bar{a}$.

If bubble is moving this means that the particles at the boundary of the bubble have a velocity $\bar{v}$, and with the pressure distribution being unaffected by this motion, fluid at the bubble boundary has a velocity of $(\bar{u}_R + \bar{v})$. The contribution to the flow across X-X between AC is

$$\varepsilon_o \int_A^C (\bar{v} + \bar{u}_R) \cdot d\bar{a}$$

plus the contribution due to the fluid displacement caused by the motion of the particles at the bubble boundary:

$$(1 - \varepsilon_o) \int_A^C \bar{v} \cdot d\bar{a}$$

and so for a single bubble the total flow across X-X between A & C.

$$\Delta B_M = \varepsilon_o \int_A^C \bar{u}_R \cdot d\bar{a} + \int_A^C \bar{v} \cdot d\bar{a} \qquad \text{Eq.(7)}$$

or from Eq.(6)

$$\Delta B_M = \Delta B_o + \int_A^C \bar{v} \cdot d\bar{a} \qquad \text{Eq.(8)}$$

If we sum all the contributions due to the bubbles cut by X-X we get the total flow due to bubbles across X-X:

$$= B_o + \sum_{\text{all bubbles}} \int_A^C \bar{v} \cdot d\bar{a} \qquad \text{Eq.(9)}$$

If we add the flow due to particulate phase F_p to the Eq.(9) we get the total flow in a freely bubbling bed:

$$A\,U = B_o + F_p + \sum \int_A^C \bar{v} \cdot d\bar{a}$$

$$= A\,k\,U_o + Q_B \qquad \text{Eq.(10)}$$

where Q_B is the observed bubble flow.

DAVIDSON & HARRISON (10) suggested that since k was unlikely to be very different from unity, unless bubbles were extremely close together, the assumption that the total flow = (flow at incipient fluidization) plus (bubble flow) would seem to have good theoretical justification.

LOCKETT et al (12) devised a method for the numerical calculation of k for a two-dimensional system and obtained an expression which enabled them to calculate k for different bubble spacings.

An alternative method was given by LOCKETT et al (12) following the approach adopted by PARTRIDGE & ROWE (11), and applying the theory given by DAVIDSON & HARRISON (4).

Consider a freely bubbling bed, fluidized by a superficial velocity U, in which the fraction of the bed volume taken by bubbles is ε_b. Then in a typical cross-section such as X-X normal to the vertical axis of the bed, the area taken by bubble and particulate phases are $\varepsilon_b A$ and $(1 - \varepsilon_b)A$ respectively, where A is the cross-sectional area of the bed. Now we assume that:

(i) fluid interstitial velocity is U_o,

(ii) the flow associated with a bubble is the same for a bubble rising in a swarm or array of bubbles as it is for a single isolated bubble rising in an infinitely wide bed.

From assumption (i) it follows that the flow due to particulate phase across the cross-section X-X is $A(1 - \varepsilon_b)U_o$. From assumption (ii) and the theory given by DAVIDSON & HARRISON (4) it follows that through flow associated with the bubble phase is $2U_o A\varepsilon_b$ and $3U_o A\varepsilon_b$ for two-dimensional and three-dimensional respectively. Denoting the visible bubble flow by Q_B and equating the total flow across a cross-section X-X with the total flow of the fluidizing fluid into

the bed we get:

$$A(1 - \varepsilon_b)\, U_o + 2U_o A\, \varepsilon_b + Q_B = AU \qquad \text{Eq.(11)}$$

for two-dimensional case, and

$$A(1 - \varepsilon_b)\, U_o + 3U_o A\, \varepsilon_b + Q_B = AU \qquad \text{Eq.(12)}$$

for three-dimensional case, where the first, second and third terms on the left of Eq.(11) and Eq.(12) are emulsion flow, bubble through flow, and visible bubble flow respectively. By rearrangement of the terms we get:

$$U = (1 + \varepsilon_b)\, U_o + \frac{Q_B}{A} \qquad \text{Eq.(13)}$$

and

$$U = (1 + 2\,\varepsilon_b)\, U_o + \frac{Q_B}{A} \qquad \text{Eq.(14)}$$

Comparison of Eq.(13) and Eq.(14) with Eq.(10) shows that:

$k = 1 + \varepsilon_b$ for two-dimensional case

and $k = 1 + 2\varepsilon_b$ for three-dimensional case

It is the purpose of the present work to provide experimental evidence to check the validity of the equation stated above for the two dimensional case. If it is shown that k is not very different from unity and in particular if it does not take values much greater than 1.4, for a system operated under flow conditions distinctly above the incipient fluidization (i.e. large Q_B), then according to LOCKETT et al (12) the "two-phase" assumption - though formally incorrect - is a reasonable model of the experimental situation.

CHAPTER 3

EXPERIMENTS

3.1 MODEL FOR THE ANALYSIS OF THE DATA

In Fig.(3) a sketch of a typical two-dimensional freely bubbling fluidized bed is given. Consider a cross-section such as X-X normal to the vertical axis of the bed at level h. Suppose that X-X cuts n bubbles. A typical bubble cut by X-X is denoted by i. We assume:

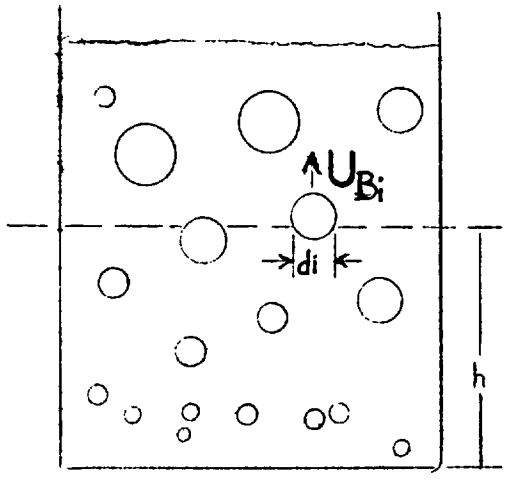

Fig (3)

di = part of the cross-section X-X inside i_{th} bubble

U_{Bi} = velocity of i_{th} bubble

L = width of the bed

S = thickness of the bed

We also assume that bubbles are extended from the front face to the rear face of the bed and also there are no particles inside the bubble. Three groups of investigators, (17), (18), (19) using different experimental techniques independently found that on average 0.2 to 1% solids are present in the bubble phase. However, with negligible error it is possible to ignore this and take the bubble phase to be solid free. It follows that:

S di = cross-section cut by i_{th} bubble at level h,

$$\frac{S\ di}{SL} = \frac{di}{L} = \delta i = \text{fraction of the cross-section taken by } i_{th} \text{ bubble} = \varepsilon_{bi}$$

$$\delta = \sum_{i=1}^{n} \delta i = \sum_{i=1}^{n} \varepsilon_{bi} = \varepsilon_b = \text{fraction of the cross-section taken by all bubbles}$$

$$\therefore \quad \delta = \frac{1}{L} \sum_{i=1}^{n} di \qquad \text{Eq.(15)}$$

(We note that the fractional area of bubbles in two-dimensions is also the fractional volume of bubbles in a three-dimensional system (20)).

Now if the two-phase model is correct, it follows that the velocity of the gas in the particulate phase is U_o, the velocity at incipient fluidization. Therefore, we have for the contribution to the flow across X-X, due to particulate phase:

$$A(1 - \delta)U_o = \text{flow due to particulate phase} \qquad \text{Eq.(16)}$$

where A is the bed cross-sectional area.

Now we investigate the flow of fluid across X-X due to a typical bubble cut by X-X. DAVIDSON & HARRISON (4) showed that the average velocity for percolation through a two-dimensional void (circle) is $2U_o$ where U_o is the interstitial fluid velocity. PARTRIDGE & ROWE (11) obtained from MURRAY'S (21) stream function the value of U_o for the flow of gas through the bubble relative to an observer moving with the bubble velocity. LOCKETT et al (12) reported the value at 5.1 U_o for the flow inside a two-dimensional bubble actually measured by JUDD (22) and suggested that this may be compared with the value $4U_o$ obtained from the analysis given by DAVIDSON & HARRISON (4) in contrast to the value of 2.2 U_o implied by MURRAY'S stream function.

In the present analysis, in the light of above argument, we

take the value of $2U_o$ for the average velocity of gas through a two-dimensional bubble. This velocity is relative to an observer moving with the bubble velocity U_B. Therefore, the velocity of the gas through a bubble relative to a fixed frame is $(U_B + 2U_o)$ where U_B is the bubble velocity. At the cross-section X-X the fractional area taken by the i_{th} bubble was shown to be $\delta i = \frac{di}{L}$. Now if the velocity of the i_{th} bubble is U_{Bi}, then it follows that the contribution of the i_{th} bubble to the flow across X-X is given by

$$(U_{Bi} + 2U_o)\, \delta i\, S\, L$$

by rearrangement we get:

$$\text{flow due to } i_{th} \text{ bubble} = S\, di\, (U_{Bi} + 2U_o) \qquad \text{Eq.(17)}$$

(The relative magnitude of the U_{Bi} and U_o will be discussed later). Now summing equations like Eq.(16) for all the bubble cut by X-X gives the total flow due to the bubbles at a level h:

$$\begin{aligned}(\text{total flow due to bubbles across X-X}) &= \sum_{i=1}^{n} S\, di\, (U_{Bi} + 2U_o) \\ &= S \sum_{i=1}^{n} di\, (U_{Bi} + 2U_o) \\ &= S \sum_{i=1}^{n} di\, U_{Bi} + 2SU_o \sum_{i=1}^{n} di \qquad \text{Eq.(19)}\end{aligned}$$

Adding equations (19) and (16) gives the total flow due to particulate (or emulsion) phase and bubble phase across X-X. Equating this total flow to the total flow of the fluidizing fluid into the bed we get:

$$AU_o(1 - \delta) + 2SU_o \sum_{i=1}^{n} di + S \sum_{i=1}^{n} di U_{Bi} = AU \qquad \text{Eq.(20)}$$

where $\delta = \frac{1}{L} \sum_{i=1}^{n} di$. The first, second and third terms on the left of the Eq.(20) are flow due to particulate phase, flow through the

bubble phase and visible bubble flow rate respectively.

By substitution into Eq.(20) from Eq.(15) we get:

$$A(1 - \delta)U_o + 2SL\delta\, U_o + S \sum_{i=1}^{n} di\, U_{Bi} = AU$$

but SL is the bed cross-sectional area, A. Substitution and rearrangement gives:

$$(1 + \delta)\, AU_o + S \sum_{i=1}^{n} di\, U_{Bi} = AU \qquad \text{Eq.(21)}$$

On comparing Eq.(21) with Eq.(13) and also noticing that

$$1 + \delta = 1 + \varepsilon_b = k \qquad \text{Eq.(21-a)}$$

where $\varepsilon_b = \delta$ = volume fraction of the bed taken by bubbles,

and $Q_B = S \sum_{i=1}^{n} di\, U_{Bi}$ = visible bubble flow, it is concluded that Eq.(13) and Eq.(21) are identical. Here Eq.(21) is taken to be the the model representing the situation. The degree of the success or failure of Eq.(21) in correlating the experimental data would be a test for the degree of validity and applicability of the underlying principle used in the development of this equation, namely the two-phase theory.

3.2 METHOD OF THE ANALYSIS OF THE DATA

Before applying the model proposed above to our experimental data, attention is drawn to the following points.

There are a number of experimental difficulties involved in the measurement of the various terms in Eqs.(20), (21). This has been acknowledged by other investigators as well. LOCKETT et al (12) pointed out that

(a) the incipient fluidizing velocity Uo was notoriously hard to measure with any degree of accuracy,

(b) measurement of the total bubble flow rate was difficult.

PYLE & HARRISON (13) noticed that the rapid growth and acceleration of some of the bubbles near the surface of the bed and also the uncertainty about the size of some bubbles on the point of bursting made the measurement more difficult.

The method of the measurement of the incipient fluidizing velocity will be discussed later on. Here we only point out that by the method devised it is possible to get unambiguous and reproducible results for Uo for different types of particles. The other difficulty, namely the assessment of the total bubble flow, was overcome by using the expression $\sum_{i=1}^{n} di\, U_{Bi}$ in Eq.(20) for the evaluation of the visible bubble flow. This did not involve the measurement of the bubble area which was a source of uncertainty in the experimental work of PYLE & HARRISON (13).

What we measured was the part of a cross-section such as X-X (Fig.(3)) which was inside the bubbles, and also the velocity of each single bubble at the cross-section. Although there was some difficulty involved in the measurement of the bubble velocity due to the change in the shape of the bubble from one frame to another frame, it was always possible to average the distance travelled by different points

on the boundary of the bubble, usually the highest and lowest, and get a true magnitude for the bubble velocity.

Clearly an experimental work of this nature produces results with some scatter. By increasing the number of experiments the standard error is decreased. In order to get reliable results one should increase the number of experiments to such a level that further increase does not produce any appreciable change in the magnitude of the scatter. In order to achieve a high degree of reproducibility we have to average the magnitude of the terms in Eq.(20) over a large period of time.

Operation of the bed at various values of U/Uo was recorded on a cine film (16 frames/sec.). The film was projected on a screen and the required measurements were carried out on between 50 to 70 frames for each value of U at each selected height (10 cm. interval). The results obtained for each height was averaged. It is important to notice that the period of time over which averaging process was carried out, was at least 5 times the time required for a bubble of medium size to travel the whole bed. The cumulative average of the measured quantities were assessed at 10-frame intervals and it was satisfactorily concluded that the time period over which the data were averaged was long enough to give reproducible results.

To show the terms of the Eq.(20) in time-averaged form, we have

$$(\text{Total visible bubble flow})_{ave} = S \left(\frac{1}{m} \sum_{j=1}^{m} \sum_{i=1}^{n} dij\, U_{Bij} \right) \qquad \text{Eq.(22a)}$$

and

$$(\text{Total bubble through flow})_{ave} = 2\, S\, U_o \left(\frac{1}{m} \sum_{j=1}^{m} \sum_{i=1}^{n} dij \right) \qquad \text{Eq.(22b)}$$

and,

$$= \frac{1}{m} \sum_{j=1}^{m} \sum_{i=1}^{n} \delta_{ij} = \frac{1}{L} \left(\frac{1}{m} \sum_{j=1}^{m} \sum_{i=1}^{n} dij \right) \qquad \text{Eq.(22c)}$$

where,

m = number of frames over which averaging was carried out

n = number of bubbles cut by the cross-section X-X at level h

$\overline{\delta}$ = δ averaged over m frames

Adding Eqs.(22,a,b,c) we get:

$$A(1 - \overline{\delta})\, Uo + 2\, S\, Uo \left(\frac{1}{m} \sum_{j=1}^{m} \sum_{i=1}^{n} dij \right) + S \left(\frac{1}{m} \sum_{j=1}^{m} \sum_{i=1}^{n} dij\, U_{Bij} \right) = AU$$

which is an averaged form of Eq.(20). We may represent this equation in a compact form by putting

$$\frac{1}{m} \sum_{j=1}^{m} \sum_{i=1}^{n} di = \left(\overline{\sum} di \right)$$

and

$$\frac{1}{m} \sum_{j=1}^{m} \sum_{i=1}^{n} dij\, U_{Bij} = \left(\overline{\sum di\, U_{Bi}} \right)$$

and so we get

$$A(1 - \overline{\delta})\, Uo + 2\, S\, Uo \left(\overline{\sum} di \right) + S \left(\overline{\sum di\, U_{Bi}} \right) = AU \qquad \text{Eq.(23)}$$

3.3 APPARATUS

The apparatus is a conventional two-dimensional transparent walled bed (a). Two sheets of perspex 83" x 31" x $\frac{1}{2}$" were held $\frac{1}{2}$" apart by perspex spacings. Paper gasketting was used between the surfaces directly in contact to reduce the possibility of leakage. The air distribution unit (b) consisted of a brass vessel on the top of which a piece of porous plastic, vion was fitted. This assembly was placed between the perspex sheets. The apparatus was held together by bolts at 2" intervals and $\frac{1}{2}$" away from the sides and lower edges. The distribution unit served as the support for the particles. A hole in the rear side of the bed provided the air entry to the distribution unit. A side view of the vertical section taken along the centre line is given in Fig.(4). The section taken along the centre line of the distribution assembly is also provided. On the rear wall at one side, holes (c) were drilled and tapped at 10" distances along the height of the bed, which provided the housing for the pressure tappings. Along the vertical central line of the bed holes (d) of different size were drilled to provide housing for pressure probes.

Air was passed through a primary filter (e) and after being reduced to about 20 psig pressure by a reducing valve (f) was passed through another filter (g). Clean air was passed through a set of rotameters (h) which made possible the gross and fine adjustment (i) of the flow. A pressure gauge (j) measured the air pressure, necessary for the determination of the flow rate. The air was then passed

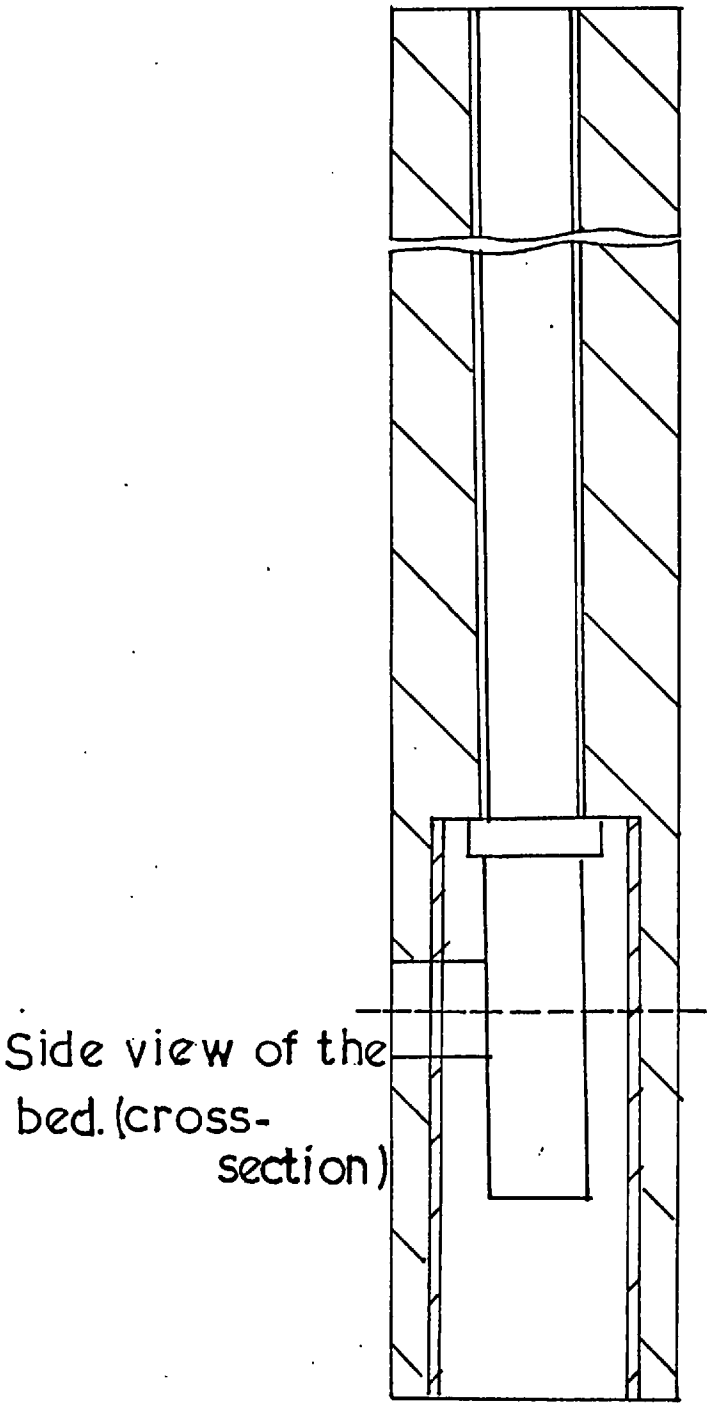

Side view of the bed. (cross-section)

(Graphs are not to scale.)

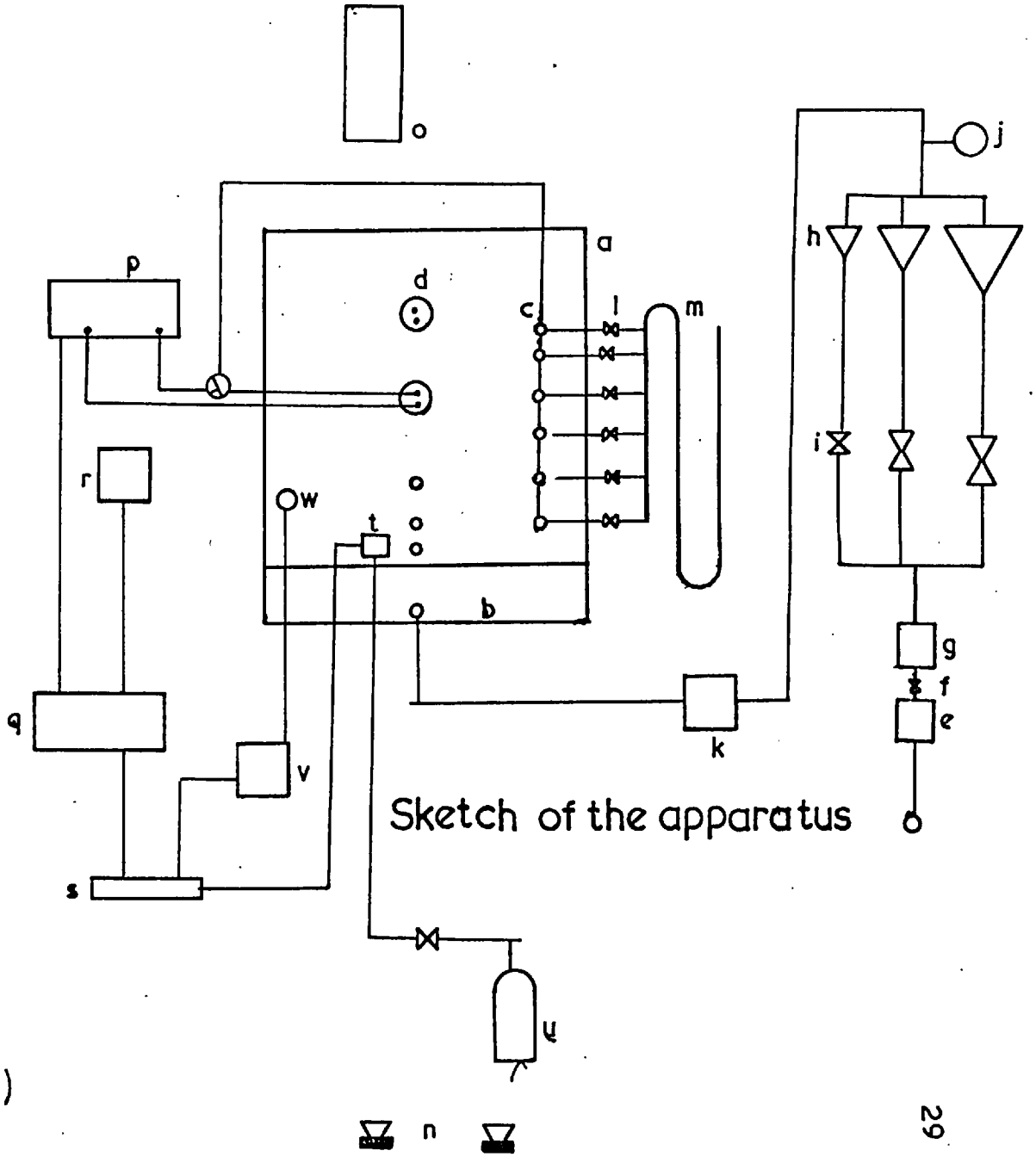

FIG. (4)

through a humidifier (k) and then introduced to the distribution unit (b). From there it was uniformly distributed through a strip of porous plastic which covered the bed width on breadth. The pressure tappings were connected to a manifold (1) which in turn was connected to a U (m) tube manometer. Water and TETRABROMOETHANE were used in the U tube according to the type of experiment. The other end of the U tube was connected to an alternative pressure tapping or was open to air according to the type of the experiment.

Rear illumination was employed, a cine camera (O) recorded the bed operation.

Glass particles ballotini grades 8, 10 and 14 and also two types of sand particles (density 2.5 g./cc.) were used. The size distribution of the particles are as follows:

	Approximate diameter (mm)	U_o cm/sec
ballotini grade 8	0.452 - 0.520	25.8
" " 10	0.249 - 0.318	8.5
" " 14	0.090 - 0.102	2.5

For sand particles:

Nominal Aperture (mm)	Percentage retained	
	COARSE SAND	FINE SAND
0.599	4.4	-
0.500	37.6	-
0.422	53.7	-
0.353	4.3	3.0
0.251	-	65.6
0.152	-	26.4
0.104	-	5.0
U_o cm/sec	235	11.5

3.4 EXPERIMENTAL RESULTS AND DISCUSSION

The necessary information for the assessment of the various terms in Eq.(23) which are taken from experimental results is as follows:

di, part of the cross-section taken by i_{th} bubble at a selected height.

U_{Bi}, velocity of the same bubble

m, number of frames to be selected in such a way that the time-averaged terms approach towards their true magnitude

The representation and the discussion of the measurements of Ui and di are included in this part. The results and the discussion of Uo measurements will be given later.

3.4.1 FRACTION OF THE CROSS-SECTION TAKEN BY BUBBLES

The experimental results of the measurement of di is expressed as the percentage of the cross-section taken by the bubbles (i.e. $\frac{(\sum di)}{L} \times 100$) as a function of the distance of the cross-section from the distributor, in Figs. (5a,b,c,d,e), at various values of $\frac{U}{Uo}$ for various particles.

The convergence diagrams for one type of particle used is given in Fig. (6) In this diagram the ratio:

$$\frac{(\overline{\sum} di) \text{ averaged over m frames}}{(\sum di) \text{ averaged over all the frames analysed}}$$

is plotted as a function of m. It is seen that for m about 50 there is no marked change in the degree of the scatter around final value. Indeed the variance is very small after m = 30 frames. This satisfactorily suggests that the number of the frames analysed is large enough to give a good representation of the measured quantity. In particular we notice that it is possible to conclude from the general shape of the graph in Fig.(6) that the general conditions necessary for the estimation to be the maximum likelihood estimation exist. (23)

It can be seen from Figs.(5a,b,c,d,e) that the percentage of the cross-section taken by bubbles at a given level is a decreasing function of the distance of the level from the distributor. In attempting to express this relationship in an analytical form we notice that in most of the cases:

(i) the relationship is very nearly linear,

(ii) variation of the data around a line drawn through them is almost constant for all values of the distance from the distributor,

(iii) we can justifiably assume that different observations are

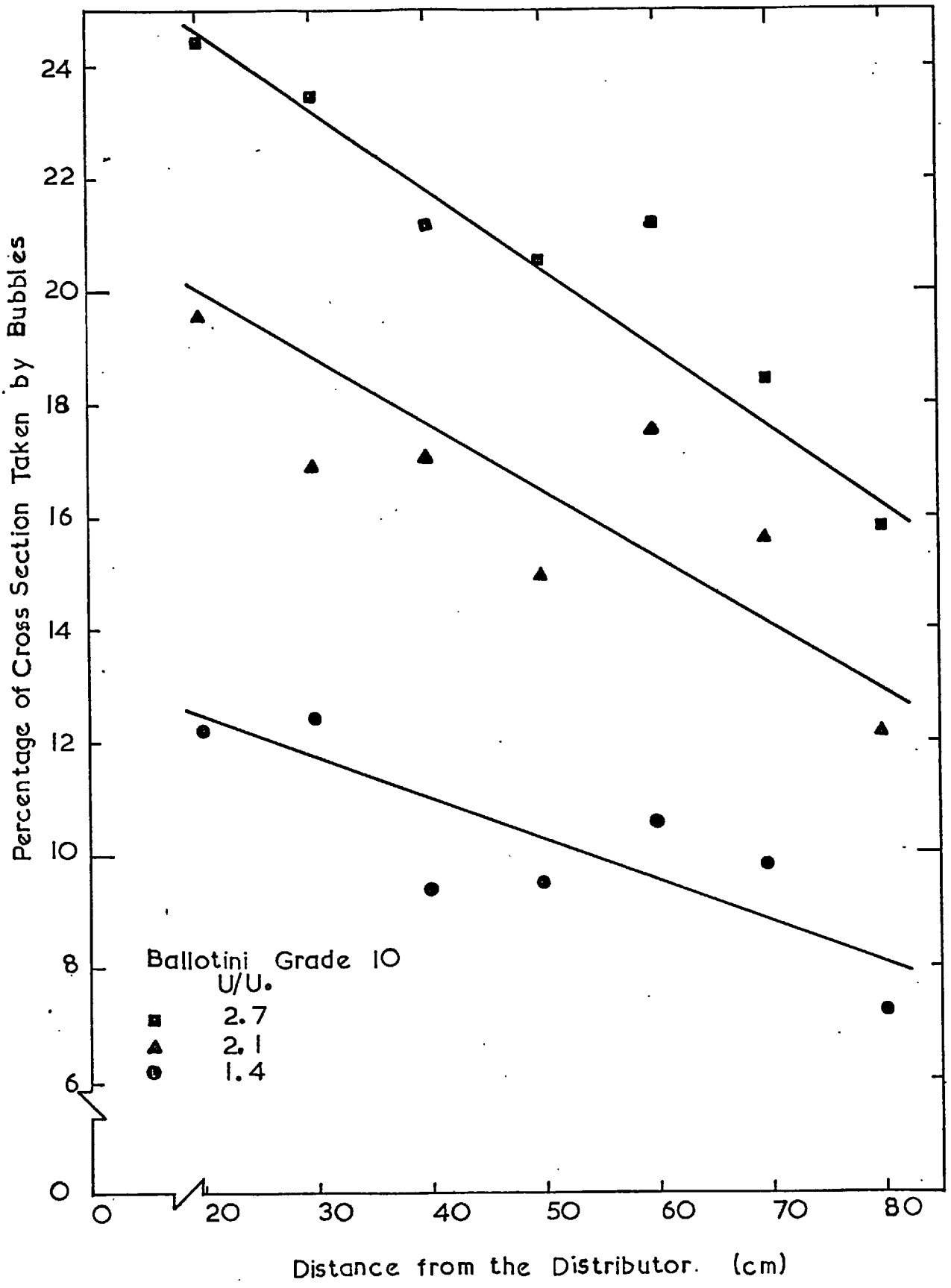
Percentage of Cross Section Taken by Bubbles
24
22
20
18
16
14
12
10
8
6
0
0
20
30
40
50
60
70
80
Distance from the Distributor. (cm)
Ballotini Grade 10
U/U.
2.7
2.1
1.4

Fig. (5-a)

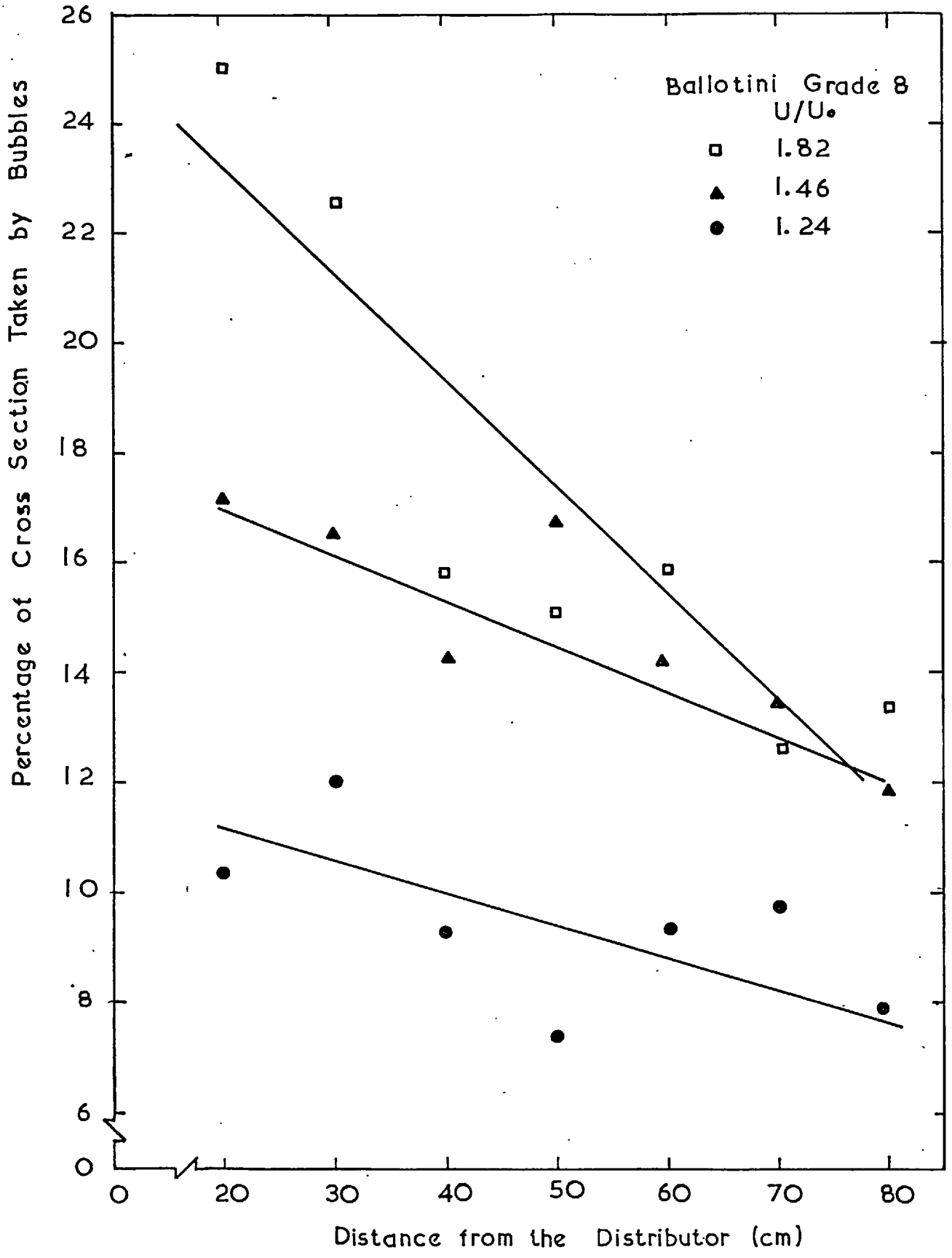
Ballotini Grade 8
U/Uo
1.82
1.46
1.24
Percentage of Cross Section Taken by Bubbles
26
24
22
20
18
16
14
12
10
8
6
0
0
20
30
40
50
60
70
80
Distance from the Distributor (cm)

Fig. (5-b)

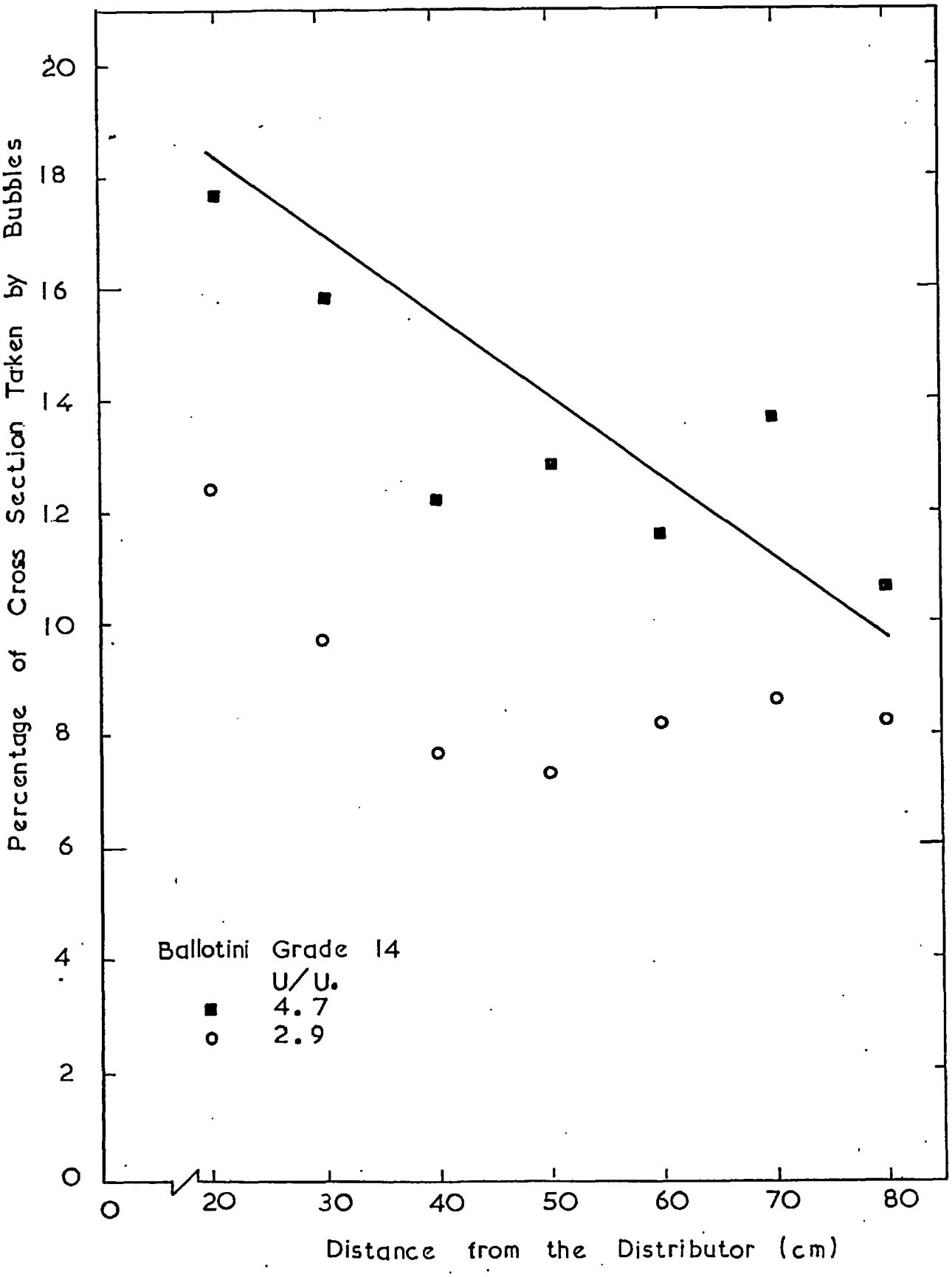
Percentage of Cross Section Taken by Bubbles
20
18
16
14
12
10
8
6
4
2
0
0
20
30
40
50
60
70
80
Distance from the Distributor (cm)
Ballotini Grade 14
U/U.
4.7
2.9

Fig. (5_c)

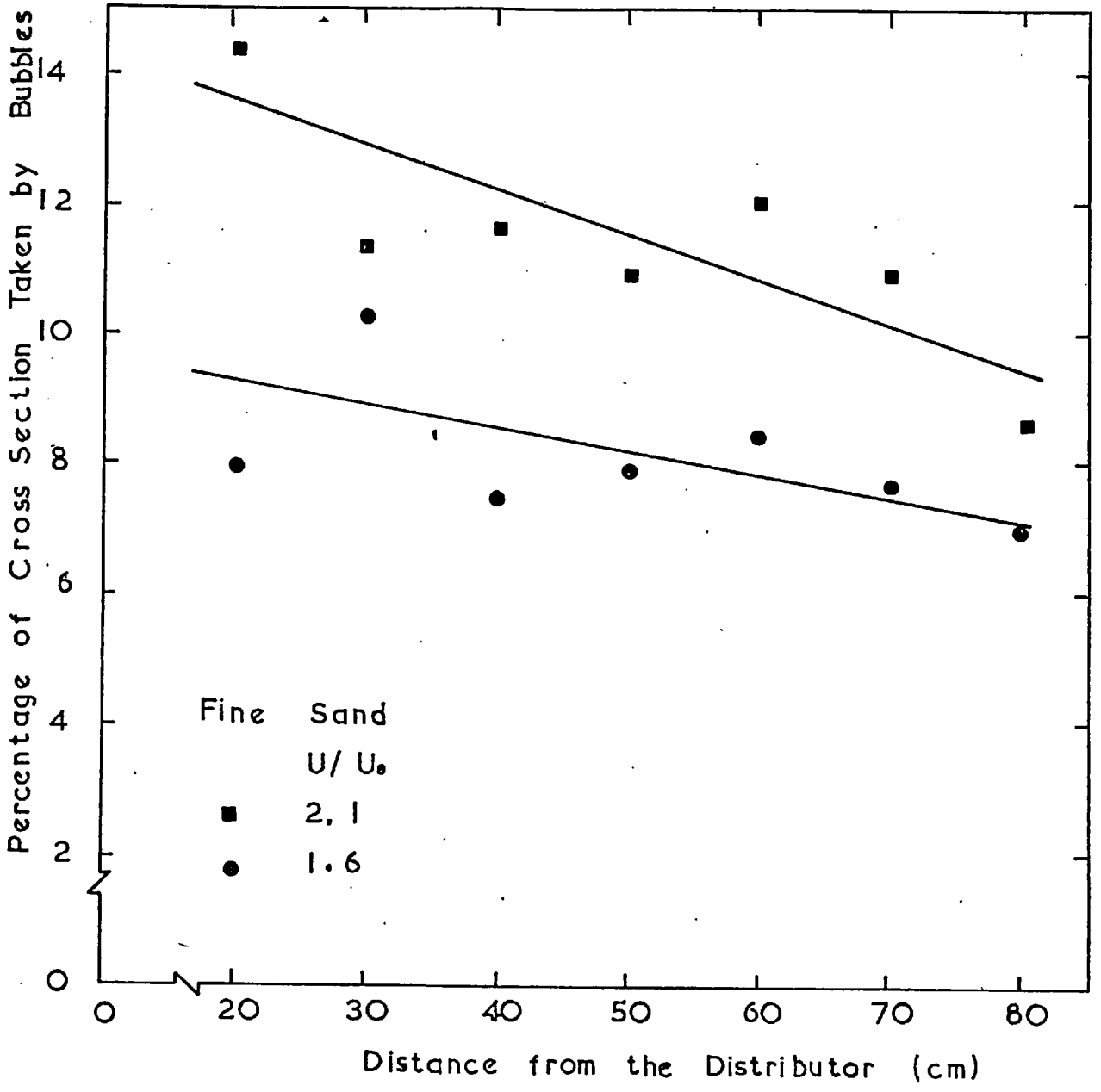
Percentage of Cross Section Taken by Bubbles
0
2
4
6
8
10
12
14
0
20
30
40
50
60
70
80
Distance from the Distributor (cm)
Fine Sand
U/ U₀
2.1
1.6

Fig (5-d)

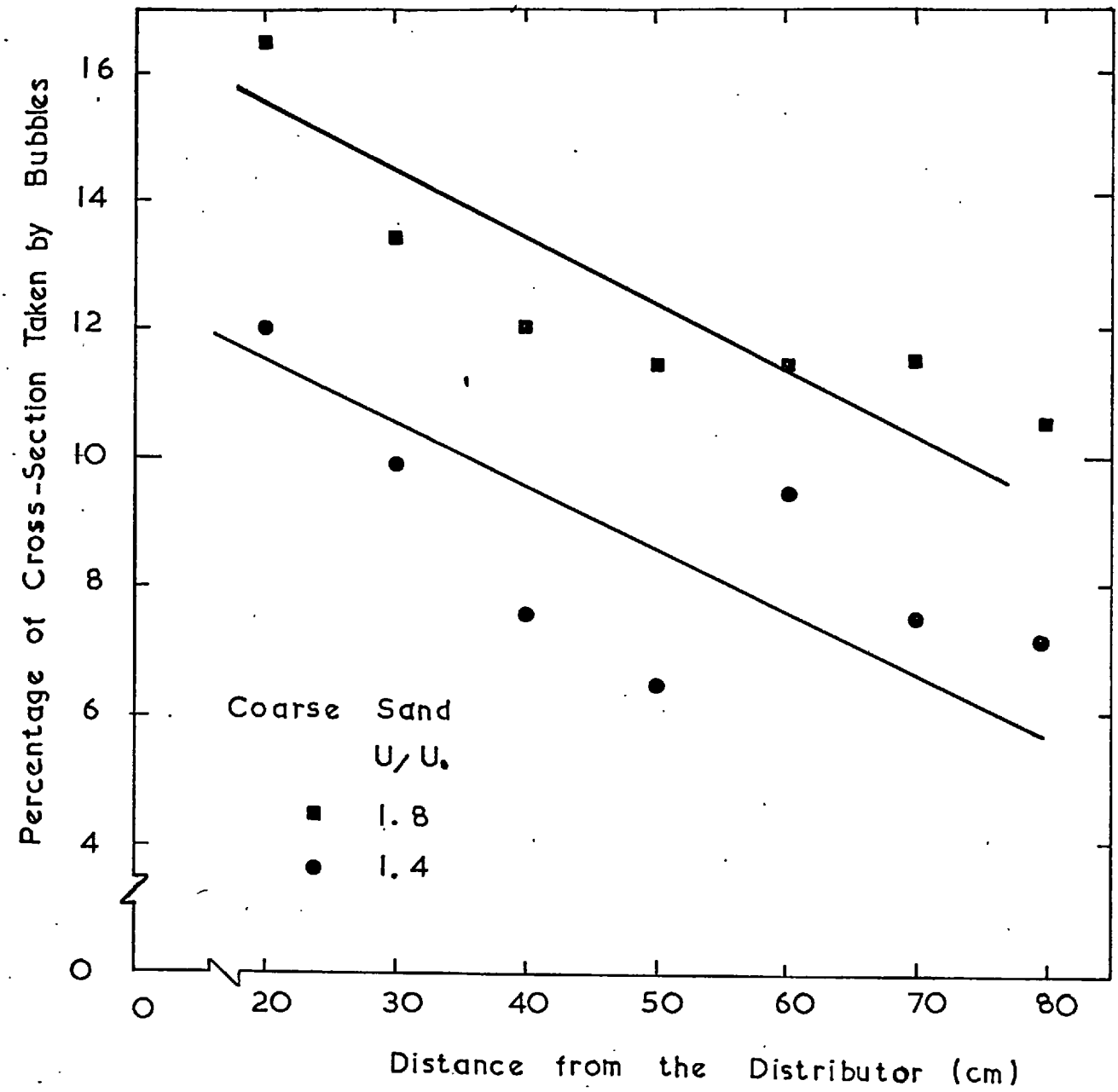
Percentage of Cross-Section Taken by Bubbles
16
14
12
10
8
6
4
0
0
20
30
40
50
60
70
80
Distance from the Distributor (cm)
Coarse Sand
U/ U.
1.8
1.4

Fig. (5-e)

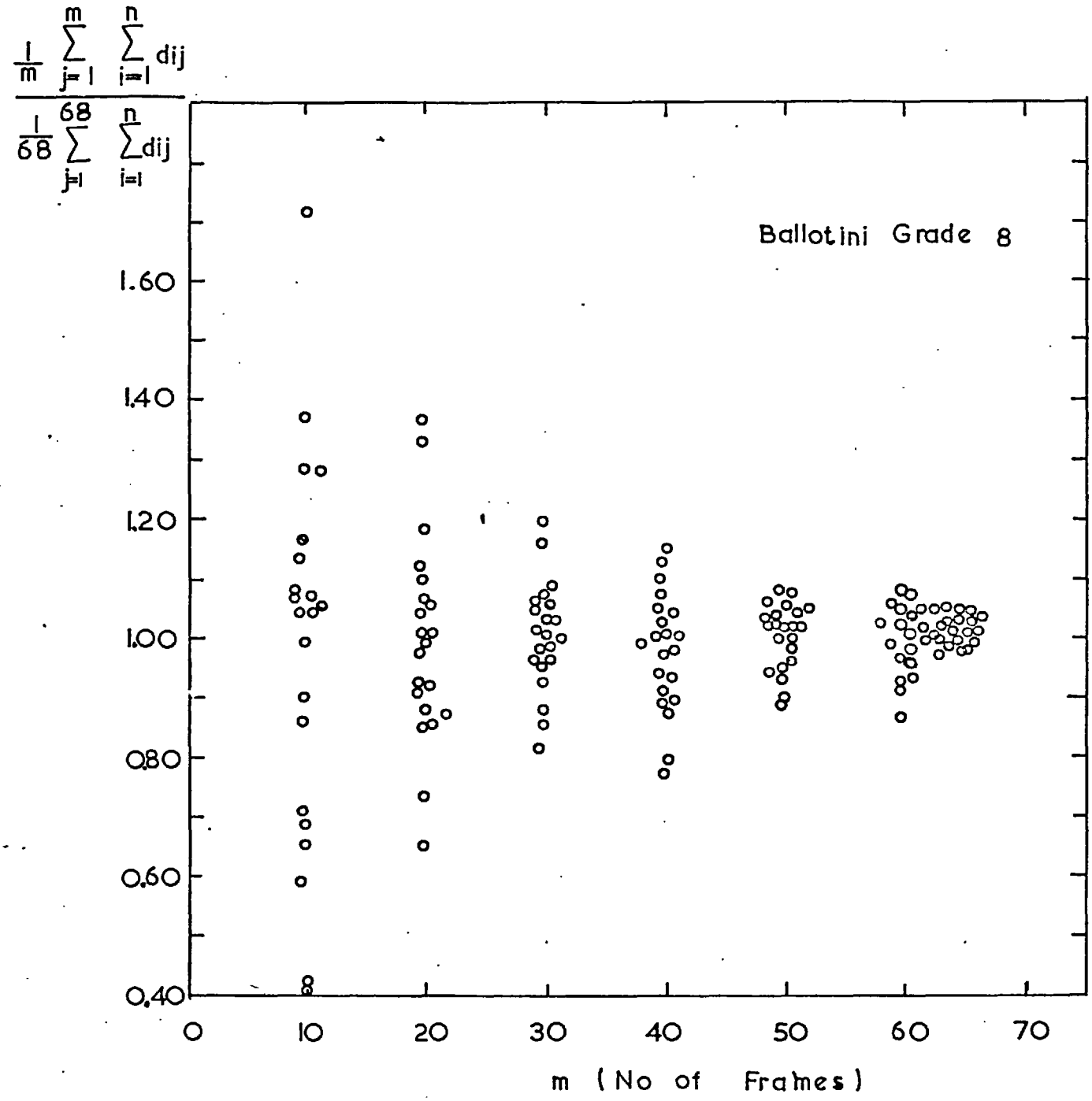
$\frac{1}{m}\sum_{j=1}^{m}\sum_{i=1}^{n} dij$
$\frac{1}{68}\sum_{j=1}^{68}\sum_{i=1}^{n} dij$
Ballotini Grade 8
1.60
1.40
1.20
1.00
0.80
0.60
0.40
0
10
20
30
40
50
60
70
m (No of Frames)

Fig. (6)

independent, i.e. deviations around a straight line are independent of one another,

(iv) deviations have a normal distribution about the straight line (cf. Fig. (6)).

The above assumptions enable us to apply linear regression between ($\overline{\sum di}$) and the distance from the distributor (23),(24). In order to be able to use all the data, obtained from various cases, for the evaluation of the regression coefficient, we proceed as follows:

Each set of the data (i.e. one type of particle, one U/Uo) is taken and the value of each point is expressed as the percentage of the mean value of the set. Justification for this process of pooling the data is that at this instance we are not interested in the behaviour of each type of particle at each value of U/Uo. What we are interested in is the macroscopic behaviour of the system. Therefore although by pooling the data some information may be lost, gross behaviour is unaffected. Now if we plot all the data obtained by the method explained above in the same diagram we get the scatter diagram given in Fig.(7). Expressing the relationship as

$$Y = \beta X + \alpha \qquad \text{Eq.(24)}$$

where Y = percentage of the cross-section taken by bubbles at a selected level.

X = distance of the level from the distributor.

α & β = const.

and applying the method of least squares to the set of X and Y (values of Y averaged for each value of X) we get:

$$\beta = -0.618 \quad \text{and} \quad \alpha = 130.83$$

By substitution of the values of α and β into Eq.(24) we get:

$$Y = -0.618X + 130.83 \qquad \text{Eq.(25)}$$

The details of the statistical analysis of the data are given in the

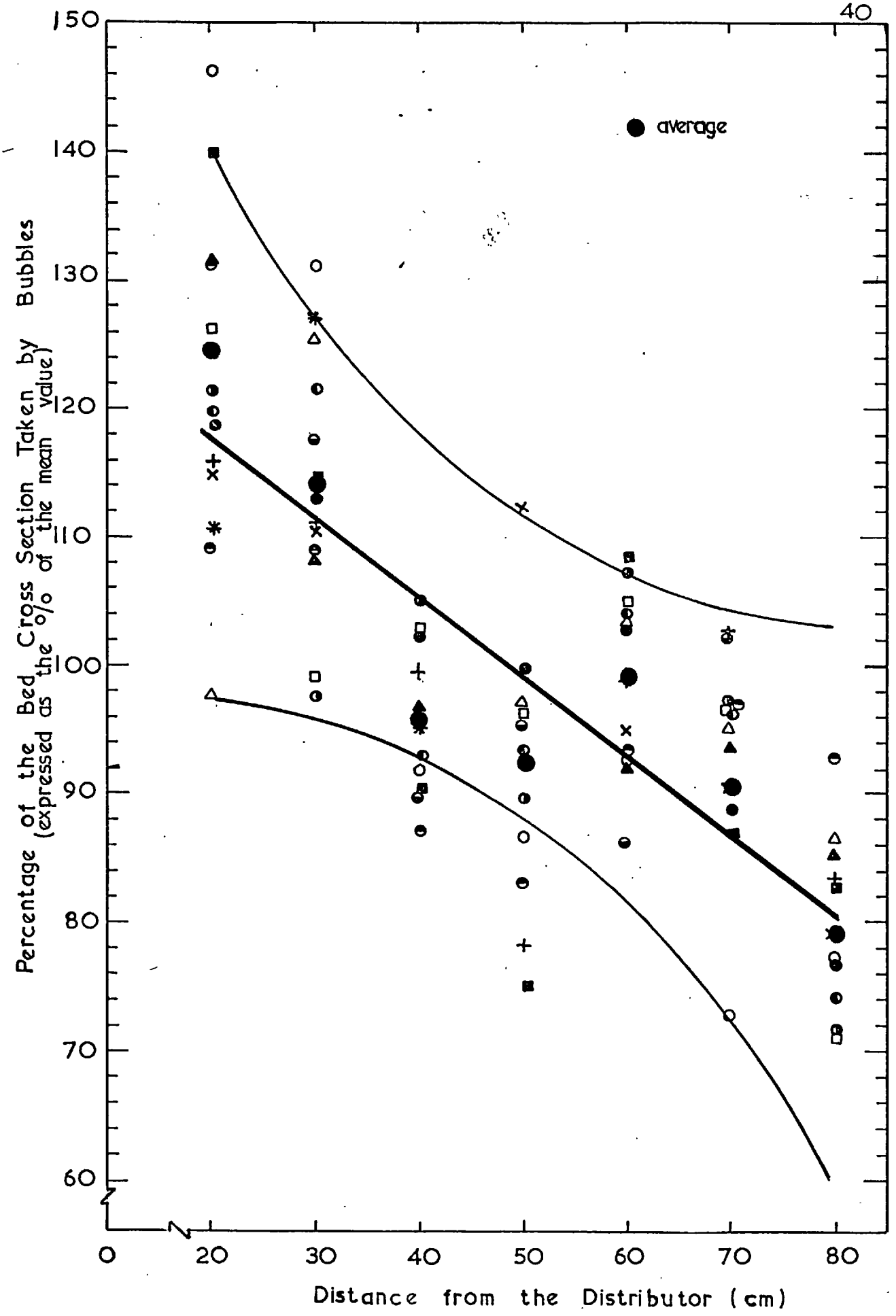
150
140
130
120
110
100
90
80
70
60
0
20
30
40
50
60
70
80
average
Percentage of the Bed Cross Section Taken by Bubbles (expressed as the % of the mean value)
Distance from the Distributor (cm)

Fig.(7)

APPENDIX (1). It is shown that

$$0.2\ \% < \Pr\ (\beta = o) < 1\ \%$$

where Pr (β = o) is the probability of β = o. The conclusion is that β is significantly different from zero at 99 % level, i.e. the relationship between Y and X exists. Eq.(25) and also the 99 % confidence limits are given in Fig.(7).

In the light of the evidence given above one has no doubt in saying that the percentage of the cross-section taken by bubbles is a decreasing function of the distance of the level from the distributor. This of course is also intuitively correct. In a freely bubbling fluidized bed, there are a large number of rapidly growing bubbles just above the distributor, occupying a large fraction of the cross-section. These bubbles get bigger (mainly by coalescence) as they move up the bed so that there are a fewer but larger bubbles in the top of the bed, occupying a relatively smaller fraction of the cross-section. It is a simple matter to show that for an idealized situation (i.e. constant bubble size at each level) the ratio of the cross-section occupied by bubbles at two different heights is proportional to the square root of the ratio of the bubble frequencies at those heights.

A very slight extra scatter around the central portion of some of the graphs presented in Figs.(5a,b,c,d,e) is noticeable. Also, some of the points in the scatter diagram fall out of the regression line confidence limits. This could be explained as follows. As was pointed out before the decrease of the fractional area taken by bubbles is due to coalescence. It may be that in some region in the central portion of the bed splitting of bubbles becomes also an influencing factor. The result of this could be an equilibrium between bubble coalescence and splitting in such a way that the

fractional area taken by bubbles varies around a constant central value in that region of the bed. As bubbles travel further up the bed the coalescence again becomes the dominant factor and therefore $(\overline{\sum} di)$ keeps on decreasing with height. However, the overall conclusion is that $(\overline{\sum} di)$ is a decreasing function of height.

As was mentioned earlier the fractional area of bubbles in two-dimensions is also the fractional volume of bubbles in a three-dimensional system (20). The fraction of the area taken by all bubbles in a vertical cross-section of the bed was also measured. The procedure was as follows: The area of each individual bubble on a typical frame taken from the cine film was measured either by tracing the boundary of the bubble with a planimeter or/and by a weighing technique. This was repeated for all bubbles in the frame. Up to 50 frames were analysed and it was satisfactorily concluded that 15 frames would give an accurate representation of the quantity. It was also found that the different measuring techniques produced results with no significant error of the measurement. The results of this experiment are expressed as bubble hold up as a function of U/Uo for various particles in Fig.(8). Two points are noticeable:

(i) In the same figure are given data obtained from the measurement of $(\overline{\sum} di)$. There is a remarkable agreement between the results obtained by two entirely different methods. This is an indication of the accuracy of measurements and also the fact that $(\overline{\sum} di)$ indeed is a true estimate of the occupied cross-section by bubbles. This in turn is an indication of the suitability of the proposed model for the analysis of the data, i.e. Eq.(20). Due to this remarkable agreement measurements of bubble hold up by the latter method were not carried further and it was assumed that $(\overline{\sum} di)$ is the representative of the bubble hold up.

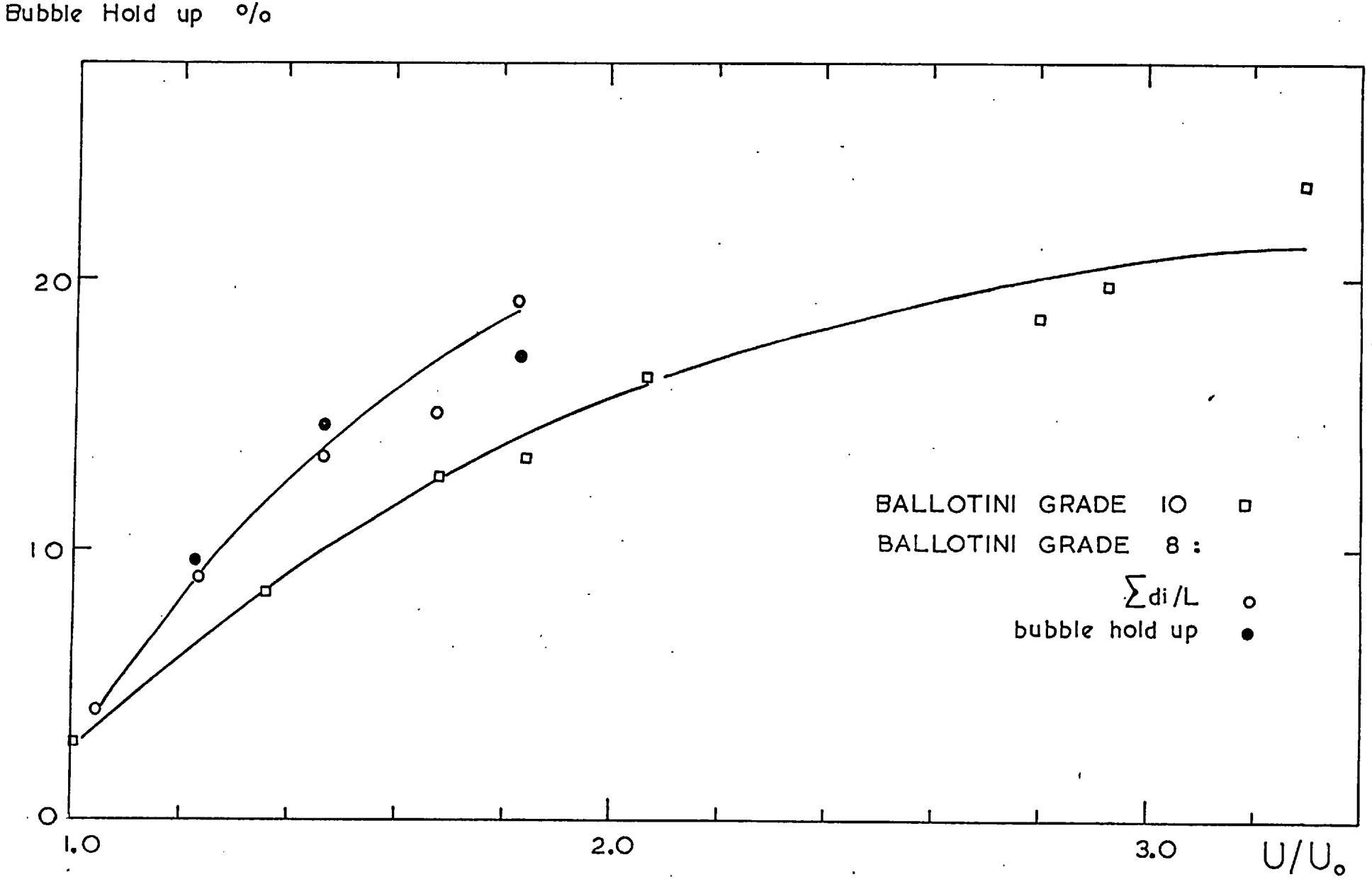
Bubble Hold up %
20
10
0
1.0
2.0
3.0
U/U₀
BALLOTINI GRADE 10
BALLOTINI GRADE 8 :
∑di /L
bubble hold up

Fig(8)

(ii) Fig.(8) shows that for the value of U/Uo between 1 and 2 the bubble hold up is an increasing linear function of U/Uo. For $\frac{U}{Uo} > 2$ the asymptotic approach of bubble hold up towards its terminal value is detectable. This again is intuitively correct. For very large values of U/Uo the fluidizing fluid takes only one (usually central) path up the bed. Clearly at such a situation an increase in the flow does not change the bubble hold up. The asymptotic nature of the bubble hold up is also apparent from the data of BAUMGARTEN & PIGFORD (5) who worked at value of U/Uo up to 15. Their Fig.(13) showed how bubble hold up becomes constant after U/Uo has reached a value of 7.

The immediate consequences which follow from the experimental results of $(\sum di)$ presented above are as follows:

(i) According to Eq.(22-a) we have

$$\text{Total bubble through flow} = 2\,S\,Uo\,\left(\frac{1}{m}\sum_{j=1}^{m}\sum_{i=1}^{n} dij\right)$$

$$= 2\,S\,Uo\,\left(\overline{\sum di}\right)$$

We have shown that $(\overline{\sum di})$ is a decreasing function of the height. Therefore $2\,S\,Uo\,(\overline{\sum di})$ is also a decreasing function of the height.

(ii) According to Eq.(23) we have

$$A(1-\bar{\delta})\,Uo + 2\,S\,Uo\left(\overline{\sum di}\right) + S\left(\overline{\sum di U_{Bi}}\right) = AU \qquad \text{Eq.(23)}$$

where, the first, second, and third terms on the left of the equation are: emulsion flow, bubble through flow, and visible bubble flow respectively, and UA is the total flow into the bed. Substitution of the value of $\bar{\delta}$ from Eq.(22-c):

$$\bar{\delta} = \frac{1}{L}\left(\sum_{j=1}^{m}\sum_{i=1}^{n} dij\right)\frac{1}{m} = \frac{1}{L}\left(\overline{\sum di}\right) \qquad \text{Eq.(22-c)}$$

into Eq.(23) and rearrangement gives:

$$A(1+\bar{\delta})\,Uo + S\left(\overline{\sum di\,U_{Bi}}\right) = AU \qquad \text{Eq.(26)}$$

Since the fraction of the cross-section occupied by bubbles, i.e. $\bar{\delta}$ (or $\frac{1}{L}(\overline{\sum di})$), decreases with height, therefore the term $A(1+\bar{\delta})Uo$ in Eq.(26) is also a decreasing function of height. Now AU is constant. This means that the term $S(\overline{\sum di\ U_{Bi}})$ in Eq.(26), i.e. the visible bubble flow rate should be an increasing function of the height. The experimental results of the measurement of the visible bubble flow, which will be given next, confirms this conclusion.

3.4.2 VISIBLE BUBBLE FLOW RATE

Eq.(22-a) states that:

$$\text{(Total visible bubble flow)} = S\left(\frac{1}{m}\sum_{j=1}^{m}\sum_{i=1}^{n} dij\, U_{Bij}\right)$$

$$= S\left(\overline{\sum di\, U_{Bi}}\right) \qquad \text{Eq.(22-a)}$$

where dij = part of a cross-section cut by i_{th} bubble in j_{th} frame

U_{Bij} = velocity of the same bubble

n = number of the bubbles at the cross-section

m = number of the frames analysed

S = bed thickness

Experimental results of the measurement of $\left(\overline{\sum di\, U_{Bi}}\right)$ for various particles at various values of U/Uo are given at different heights from the distributor in Table (1). All these results are also given in Fig.(9). The points are plotted in this way. For each set of observations (i.e. one type of particle at one value of U/Uo), $\left(\overline{\sum di\, U_{Bi}}\right)$ at different heights is given as the percentage of the mean value of the set of the observations. This procedure is repeated for a number of cases and the results are plotted on the same diagram as a function of height from the distributor. In this way it is possible to use all the data in order to investigate the overall relationship between $\left(\overline{\sum di\, U_{Bi}}\right)$ and the height. The average of all the points at each height is taken and the method of the least squares is applied. All the necessary assumptions are exactly the same as was described in the regression analysis of $\left(\overline{\sum di}\right)$ and height. In particular, we notice that the justification for such assumptions are apparent from the examination of the data given in Fig. (10) where the ratio

$$\frac{\left(\overline{\sum di\, U_{Bi}}\right) \text{ averaged over m frames}}{\left(\overline{\sum di\, U_{Bi}}\right) \text{ averaged over all the frames analysed}}$$

is given as a function of m. The results of the regression analysis

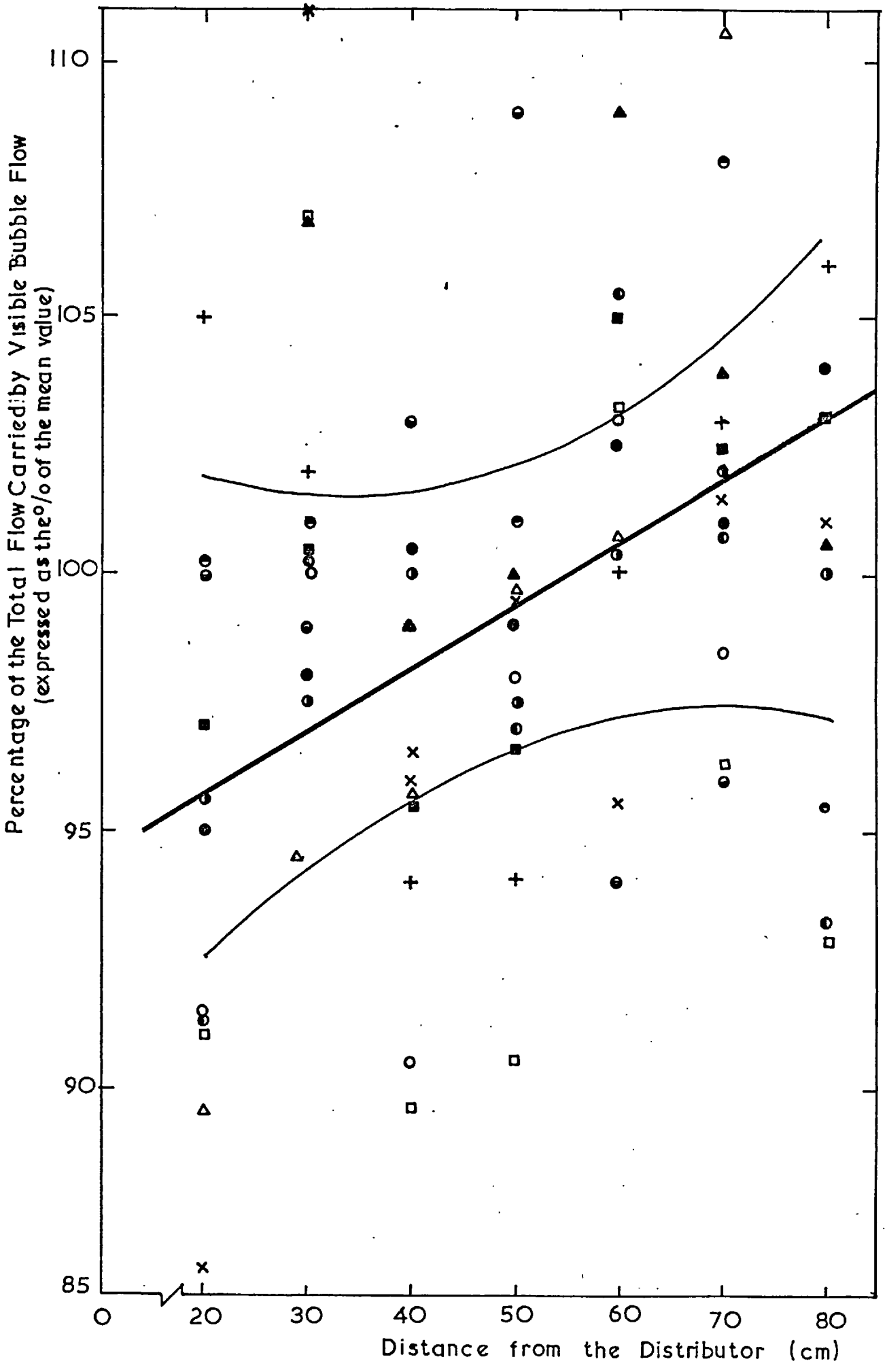
Percentage of the Total Flow Carried by Visible Bubble Flow
(expressed as the % of the mean value)
110
105
100
95
90
85
0
20
30
40
50
60
70
80
Distance from the Distributor (cm)

Fig. (9)

$$\frac{\frac{1}{m}\sum_{j=1}^{m}\sum_{i=1}^{n} d_{ij}\, U_{B_{ij}}}{\frac{1}{68}\sum_{}^{m}\sum^{n} d_{ij}\, U_{B_{ij}}}$$

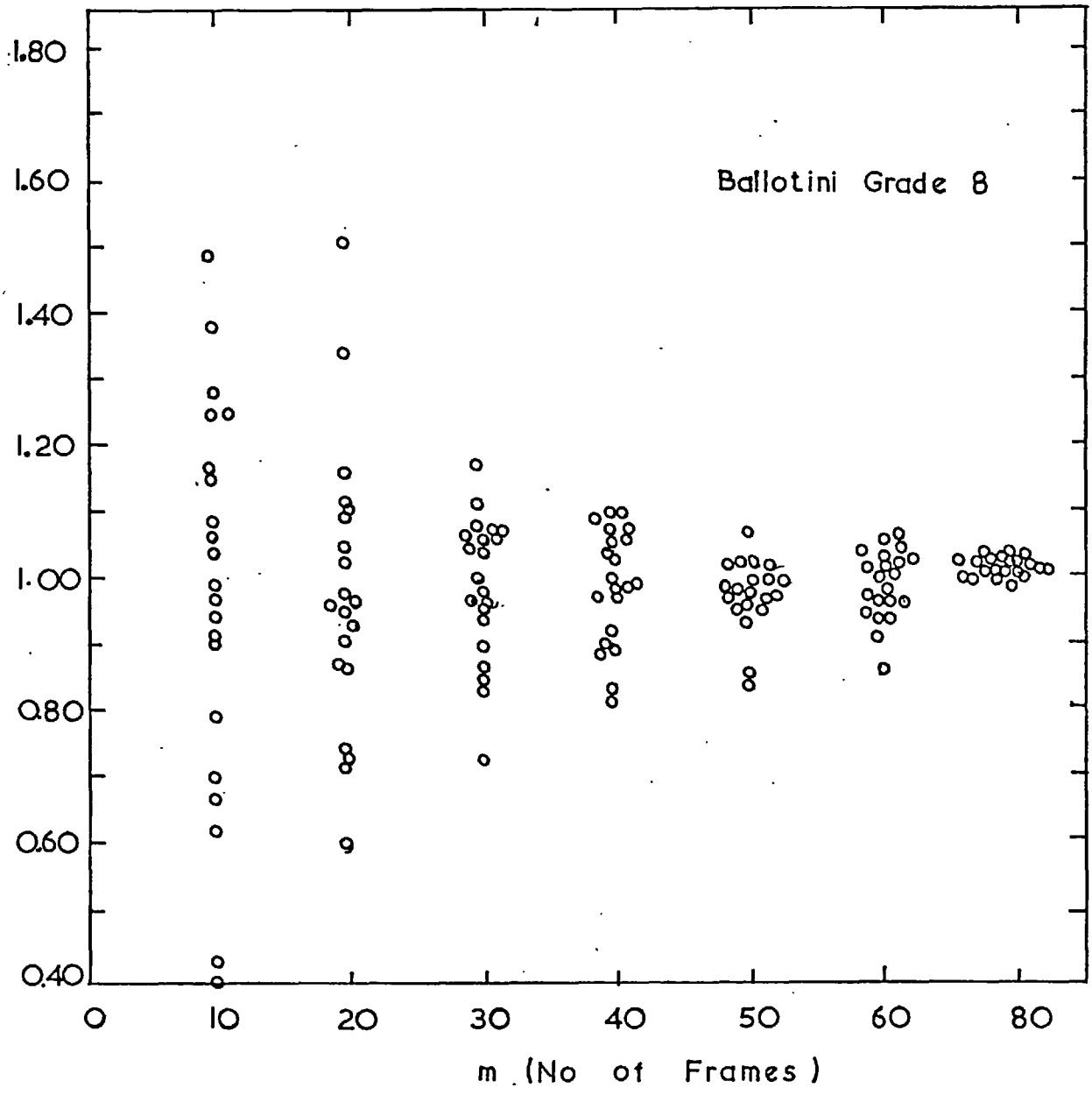

Fig. (10)

between $(\overline{\sum di\ U_{Bi}})$ and height are as follows:

$$\beta = 0.123$$

$$\alpha = 93.3$$

where α and β are the constants in the least squares line

$$Y = \beta X + \alpha$$

where

$Y = (\overline{\sum di\ U_{Bi}})$ visible bubble flow rate at a given level

X = distance of the level from the distributor

Putting the values of α and β into the regression line we get

$$Y = 0.123\ X + 93.3 \qquad \text{Eq.(27)}$$

Details of the statistical analysis of the data are given in the APPENDIX (1). It is shown that the probability of the Null Hypothesis being true (i.e. $\beta = \beta o = o$) is about 5%. So we reject the hypothesis of $\beta = o$. This means that the relationship between $(\overline{\sum di\ U_{Bi}})$ and height exists with a probability of 95%. The regression line Eq.(27) and also the 95% confidence limits are given in Fig.(9). Examination of the above analysis and also Fig.(9) shows that the visible bubble flow at various levels in a fluidized bed is an increasing function of the height of the level above the distributor.

The results presented above agree well with the experimental results of the measurement of $(\overline{\sum di})$. As was pointed out earlier, since the term $A(1 + \bar{\delta})\ Uo$ in Eq.(26) decreases with height we expect that $S(\overline{\sum di\ U_{Bi}})$, i.e. the visible bubble flow increases with height. We have shown that this is so. The agreement between the results is another indication of the suitability and consistency of the model and accuracy of the measurements.

Returning to Eq.(23):

$$A(1 - \bar{\delta})Uo + 2\ S\ Uo(\overline{\sum di}) + S(\overline{\sum di\ U_{Bi}}) = AU \qquad \text{Eq.(23)}$$

by rearrangement we have

$$A(1 - \overline{\delta})Uo + S\ (2\ Uo(\overline{\sum di}) + (\overline{\sum di\ U_{Bi}})) = AU$$

where

$A(1 - \overline{\delta})Uo$ = flow due to the emulsion phase,

AU = total flow of the fluidizing fluid into the bed, and

$S\ (2\ Uo(\overline{\sum di}) + (\overline{\sum di\ U_{Bi}}))$ = bubble through flow + visible bubble flow = total flow associated with bubbles.

$\overline{\delta}$, the fraction of the cross-section taken by bubbles was shown to be a decreasing function of the distance from the distributor. Therefore the term $A(1 - \overline{\delta})\ Uo$ (i.e. emulsion flow) is an increasing function of the distance from the distributor. Since AU is constant, then the total flow associated with bubbles, i.e. (bubble visible flow) + (bubble through flow) must be a decreasing function of the height. This conclusion is supported by the experimental results of the total flow associated with bubbles which is considered next.

TABLE (1)

DIVISION OF FLOW BETWEEN VARIOUS PHASES

BALLOTINI GRADE 8

U/Uo = 1.2

h* cm	$\frac{(\sum di)}{L}$ =	$(\overline{\sum di\ U_{Bi}})$ cm^2/sec	Total Bubble Flow % Visible	% Through	Total Flow cm^3/sec
20	0.104	155.2	8.9	17.2	2916.2
30	0.120	208.6	11.4	19.0	2314.2
40	0.093	169.6	9.7	15.4	2215.5
50	0.071	140.8	8.3	12.6	2141.2
60	0.093	182.4	10.4	15.3	2231.7
70	0.097	217.6	12.1	15.5	2282.2
80	0.079	193.6	11.1	13.0	2219.0
Average	0.094	181.1	10.3	15.5	2231.4
		U/Uo = 1.5			
20	0.172	361.6	17.6	24.2	2603.0
30	0.165	364.3	17.8	23.3	2592.9
40	0.142	363.7	18.1	20.3	2549.1
50	0.167	393.1	19.0	23.2	2632.4
60	0.142	324.8	16.5	20.7	2490.7
70	0.134	332.4	16.9	19.7	2497.6
80	0.118	326.1	16.8	17.6	2460.1
Average	0.148	352.3	17.6	21.3	2547.8
		U/Uo = 1.8			
20	0.250	643.5	26.3	29.5	3106.6
30	0.226	714.0	28.8	26.2	3148.3
40	0.158	588.4	26.1	20.1	2864.2
50	0.151	654.5	28.3	18.8	2934.6
60	0.159	703.7	29.6	19.4	3015.3
70	0.125	644.1	28.4	15.9	2877.3
80	0.133	837.9	33.9	15.5	3134.9
Average	0.172	683.7	28.8	20.9	3011.5

h* = height above the distributor.

TABLE (1) cont'd

DIVISION OF FLOW BETWEEN VARIOUS PHASES

BALLOTINI GRADE 10

U/Uo = 1.4

h* cm	$\frac{(\sum di)}{L}$ =	$(\overline{\sum di\ U_{Bi}})$ cm^2/sec	Total Bubble Flow % Visible	% Through	Total Flow cm^3/sec
20	0.122	196.8	27.2	15.6	923.6
30	0.124	233.6	30.8	15.2	971.2
40	0.095	204.8	28.6	12.8	917.5
50	0.095	214.4	29.1	12.5	929.7
60	0.106	222.4	29.9	13.5	946.2
70	0.099	248.0	32.4	11.4	974.3
80	0.072	195.2	27.8	9.7	891.1
Average			29.2	13.2	936.1
		U/Uo = 2.1			
20	0.197	465.6	45	18.4	1310.6
30	0.169	467.2	45.8	15.7	1294.9
40	0.170	494.4	47.1	15.5	1331.0
50	0.149	456.0	45.6	14.2	1268.9
60	0.174	547.2	49.6	15	1400.0
70	0.156	508.8	48.1	14.2	1340.4
80	0.120	468.8	47.0	11.4	1268
Average	0.162		47.0	14.8	1316.3
		U/Uo = 2.7			
20	0.244	729.6	55.4	17.6	1673.8
30	0.233	776.0	57.1	16.1	1726.4
40	0.212	812.8	58.5	14.6	1759.8
50	0.206	780.8	57.7	14.6	1716.3
60	0.212	841.6	59.7	13.9	1796.4
70	0.183	796.8	58.6	12.9	1722.4
80	0.158	824.0	60.5	10.5	1741.7
Average	0.207		58.2	14.3	1733.8

h* = height above the distributor.

TABLE (1) cont'd

DIVISION OF FLOW BETWEEN VARIOUS PHASES

BALLOTINI GRADE 14

U/Uo = 2.9

h* cm	$\frac{(\overline{\sum di})}{L} =$	$(\overline{\sum di\ U_{Bi}})$ cm^2/sec	Total Bubble Flow % Visible	% Through	Total Flow cm^3/sec
20	0.124	251.2	62	8.5	514.6
30	0.097	224.0	60	7.1	475.3
40	0.077	182.4	55.3	6.5	418.9
50	0.073	180.8	55.0	6.4	416.3
60	0.082	190.4	56.2	6.8	429.9
70	0.086	220.8	59.7	6.5	469.3
80	0.082	249.6	62.5	5.8	507.1
Average	0.088	214.2	58.9	6.8	461.7
		U/Uo = 4.7			
20	0.177	443.2	73.2	8.2	768.3
30	0.159	416	72.3	7.7	730.6
40	0.122	369.6	70.6	6.5	664.8
50	0.129	417.6	72.9	6.3	727.1
60	0.116	414.4	73.0	5.7	720.8
70	0.137	484.8	75.6	6.0	814.2
80	0.107	435.2	71.0	5.1	745.6
Average	0.135	425.8	73.2	6.5	738.8

h* = height above the distributor

TABLE (1) cont'd

DIVISION OF FLOW BETWEEN VARIOUS PHASES

FINE SAND

U/Uo = 1.6

h* cm	$\frac{(\sum di)}{L}$ =	$(\sum di\ U_{Bi})$ cm^2/sec	Total Bubble Flow % Visible	% Through	Total Flow cm^3/sec
20	0.079	149.0	17.7	12.0	1068.7
30	0.102	214.3	23	14.5	1170.9
40	0.077	187.5	21.3	11.3	1116.3
50	0.079	189.9	21.5	11.5	1120.6
60	0.084	213.1	23.4	11.9	1154.8
70	0.077	200	22.4	11.1	1132.2
80	0.070	188.7	21.6	10.2	1111.9
Average	0.081	191.8	21.7	11.6	1125.1
		U/Uo = 2.1			
20	0.143	339.0	31.6	17.1	1363.0
30	0.113	344.8	32.6	13.6	1345.1
40	0.116	325.7	31.2	14.3	1324.3
50	0.109	326.9	31.5	13.5	1319.8
60	0.120	373.2	34.2	14.1	1387.2
70	0.109	356.8	33.4	13.1	1357.8
80	0.080	350.9	33.6	9.9	1326.4
Average	0.113	345.2	32.6	13.7	1346.2

h* = height above the distributor.

TABLE (1) cont'd

DIVISION OF FLOW BETWEEN VARIOUS PHASES

COARSE SAND

U/Uo = 1.4

h* cm	$\frac{(\overline{\sum di})}{L}$ =	$(\overline{\sum di\ U_{Bi}})$ cm^2/sec	Total Bubble Flow % Visible	% Through	Total Flow cm^3/sec
20	0.120	203.2	12.1	18.9	2124.7
30	0.098	225.6	13.5	15.5	2116.5
40	0.077	180.8	11.3	12.7	2024.6
50	0.065	179.2	11.4	10.7	2000.8
60	0.093	211.2	12.8	14.8	2090.3
70	0.075	193.6	12.1	12.3	2038.3
80	0.071	184.0	11.6	11.8	2021
Average	0.086	196.8	12.8	13.9	2059.5
		U/Uo = 1.8			
20	0.163	342.3	18.4	22.8	2375.7
30	0.134	361.2	19.5	19.1	2349.8
40	0.120	362.5	19.8	17.2	2327.2
50	0.115	376.2	20.5	16.4	2334.9
60	0.115	384.6	20.8	16.3	2345.5
70	0.116	435.3	22.9	16.1	2414.2
80	0.106	444.3	23.4	14.6	2406.6
Average	0.124	386.6	20.7	17.5	2364.8

h* = height above the distributor.

3.4.3 TOTAL FLOW ASSOCIATED WITH BUBBLES

It was pointed out earlier that the total flow associated with bubbles is given by:

$$S\left[2\,U_o\,\overline{\left(\sum d_i\right)} + \overline{\left(\sum d_i\,U_{Bi}\right)}\right]$$

where the first term is the bubble through flow and the second term is the visible bubble flow. Assessment of the above expression is possible because all necessary terms are available from previous measurements. The total bubble flow for various particles at various values of U/Uo are given in Figs.(11a,b,c,d,e) at different heights as a fraction of the total flow carried by bubbles (i.e. through flow + visible bubble flow). The corresponding scatter diagram is given for all the results in Fig.(12). Each point value in this diagram is given as the percentage of the mean value of the set of the observation from which the point was taken. The average of different points for different cases at each level is taken and the method of the least squares is applied. The requisite assumptions and the corresponding justifications are as discussed previously. Details of the statistical analysis are given in APPENDIX (I). The summarized results of the regression analysis are given below:

$$\beta = -0.17$$

$$\alpha = 109.1$$

where α and β are the constants in equation

$$Y = \beta X + \alpha$$

and Y = total flow associated with bubbles at a level

X = height of the level above the distributor.

The relationship is given as a diagram in Fig.(12). Also there are included the 95% confidence limits. The test statistic calculated from Eq.(A.I.5) is equal to -2.6, i.e. t = -2.6. The probability of β being significantly different from zero is more than 95%. The null

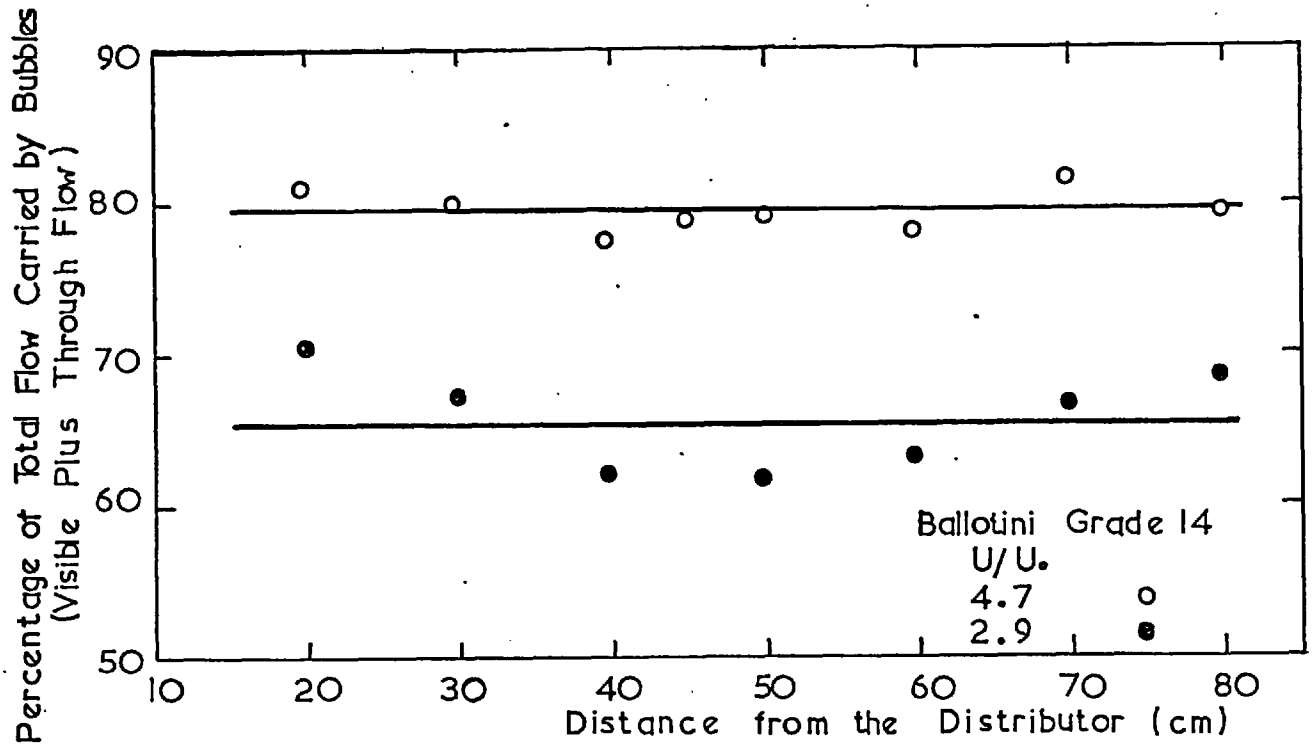

Fig.(II-a)

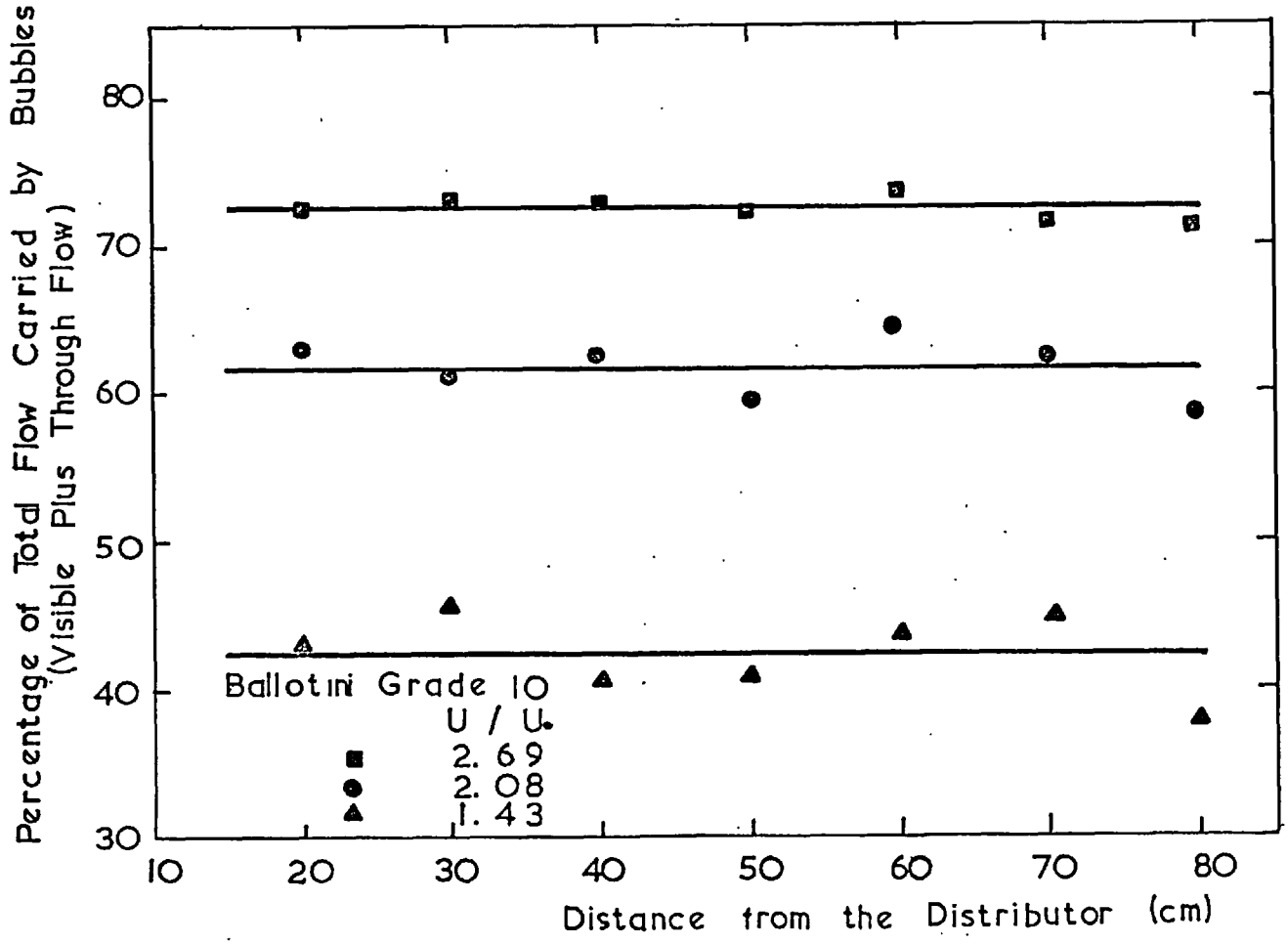

Fig. (II-b)

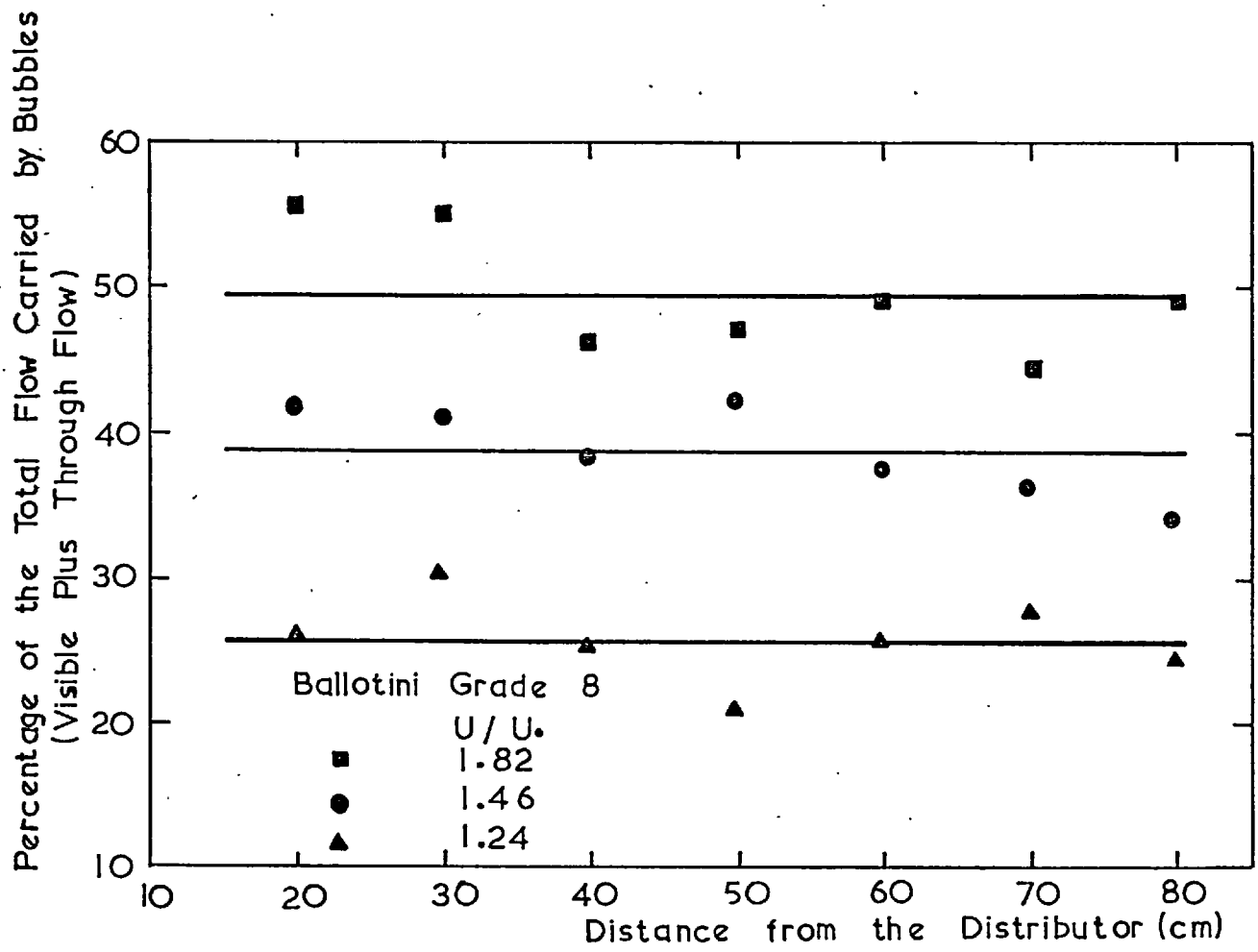
Percentage of the Total Flow Carried by Bubbles
(Visible Plus Through Flow)
60
50
40
30
20
10
10
20
30
40
50
60
70
80
Distance from the Distributor (cm)
Ballotini Grade 8
U / U.
1.82
1.46
1.24

Fig.(11-c)

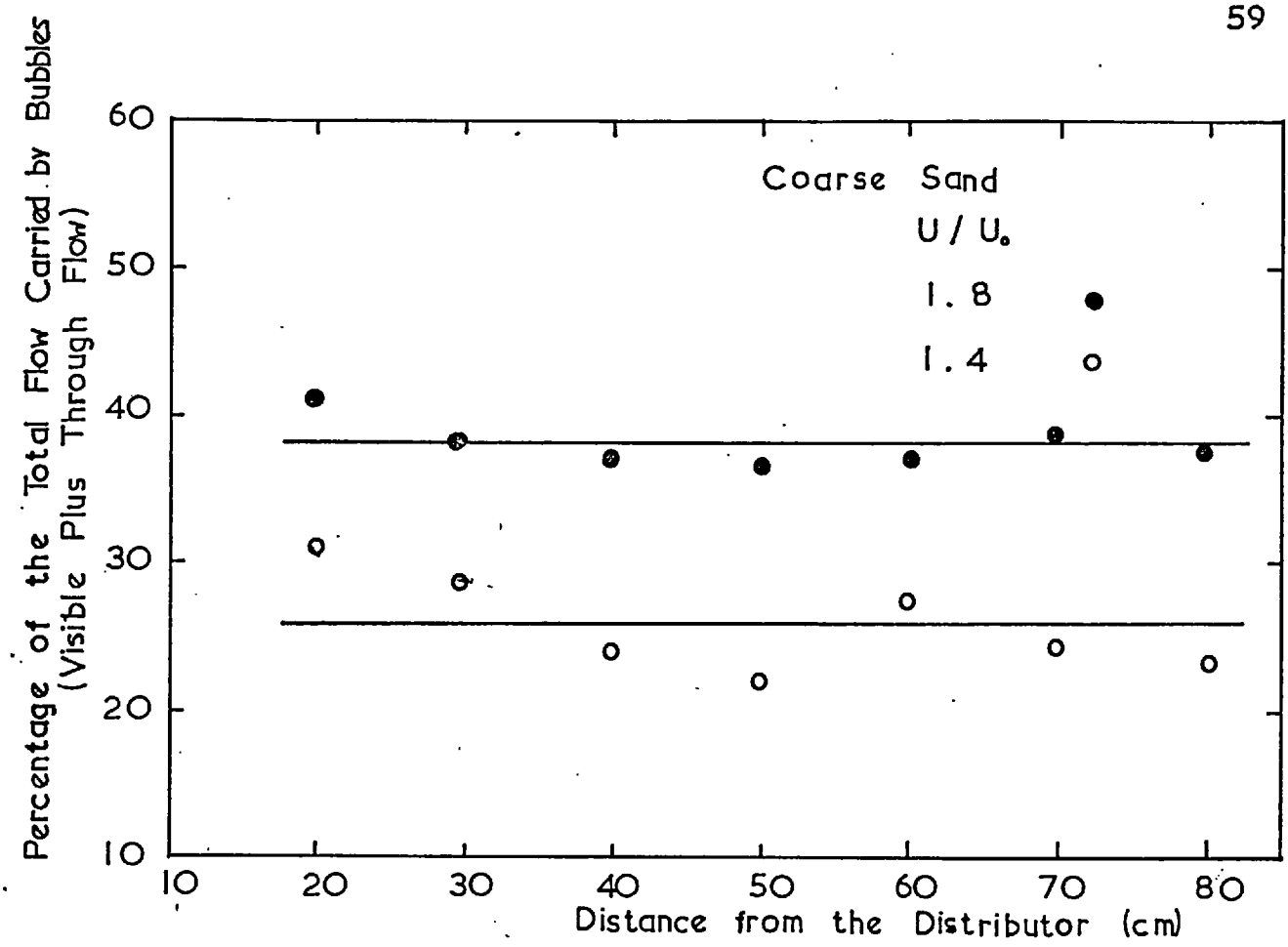

Fig. (11-d)

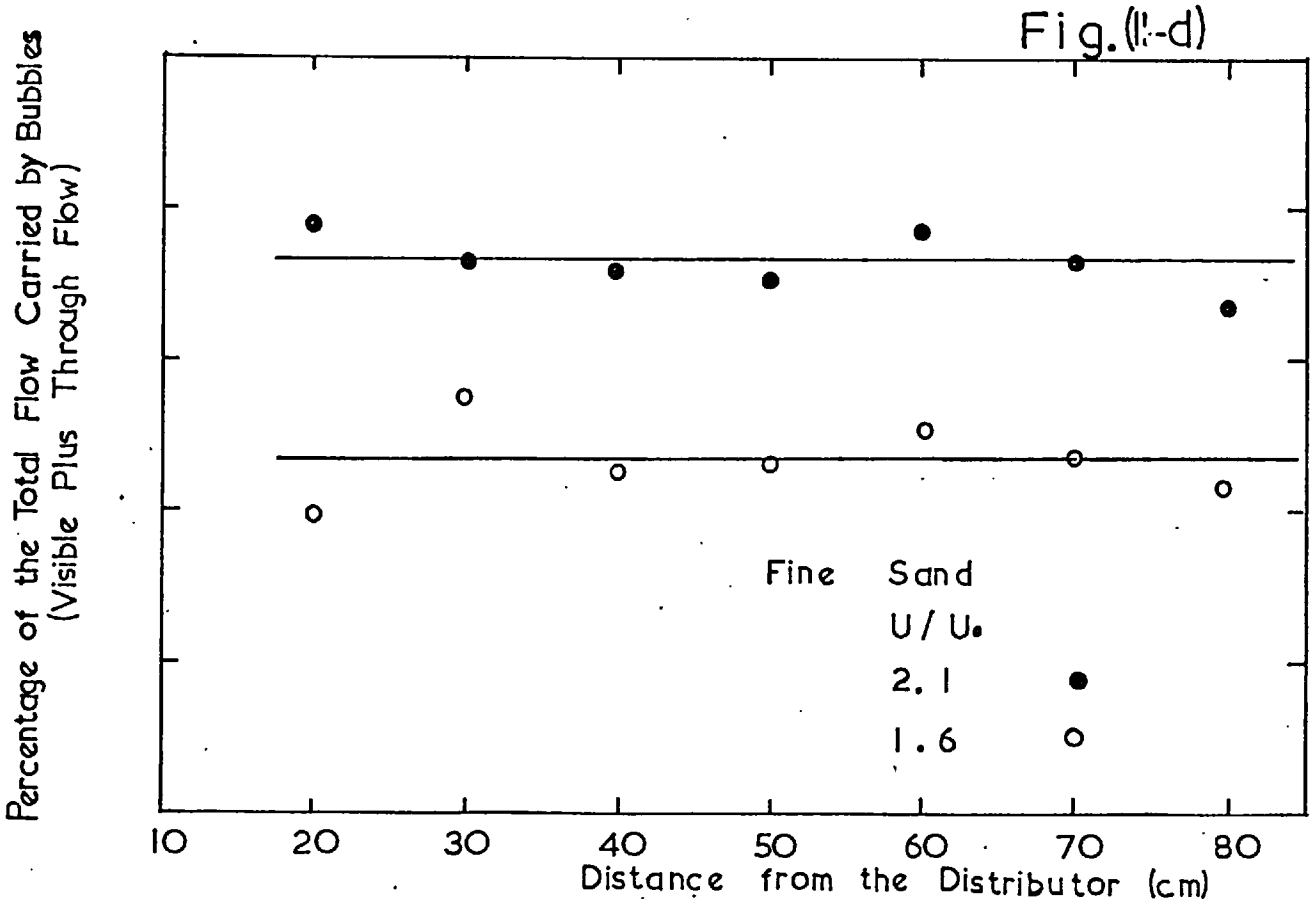

Fig. (11-e)

hypothesis is rejected and it is concluded that the relationship between Y and X exists with a probability of 95%.

The immediate conclusion which could be drawn from the above argument and also Fig.(12) is that the total flow associated with bubbles is a decreasing function of the height. This conclusion is in agreement with the experimental results obtained previously.

From the results given in Fig.(12) and the accompanying analysis it is very clear that the total flow associated with bubbles is a decreasing function of height. However, for each individual case (i.e. one type of particle at one value of U/Uo) the examination of the graphs given in Figs.(11a,b,c,d,e) shows that it can be stated, with small error, that the total flow associated with bubbles is constant at various heights above the distributor. At the same time we notice from Fig.(12) that the maximum change in the flow at various height is about 10%. It is emphasised that the assumption made above, that the total flow associated with bubbles is almost constant, is not contradictory with the results of the experiments. Analysis of the data given in Fig.(12) is only concerned to find out if the total bubble flow is a function of height, no matter how weak this functional relationship might be. Indeed the statistical technique employed is very successful in detecting this functional relationship with a very good level of confidence. Here, in contrast, and in the light of the experimental data given in Fig.(12) and Figs.(11a,b,c,d,e) we take the total bubble flow for each individual case to be very nearly constant. The maximum error which might be caused by this assumption is 10%. An error of this magnitude is very infrequent, and this is apparent from the data given in Figs.(11a,b,c,d,e).

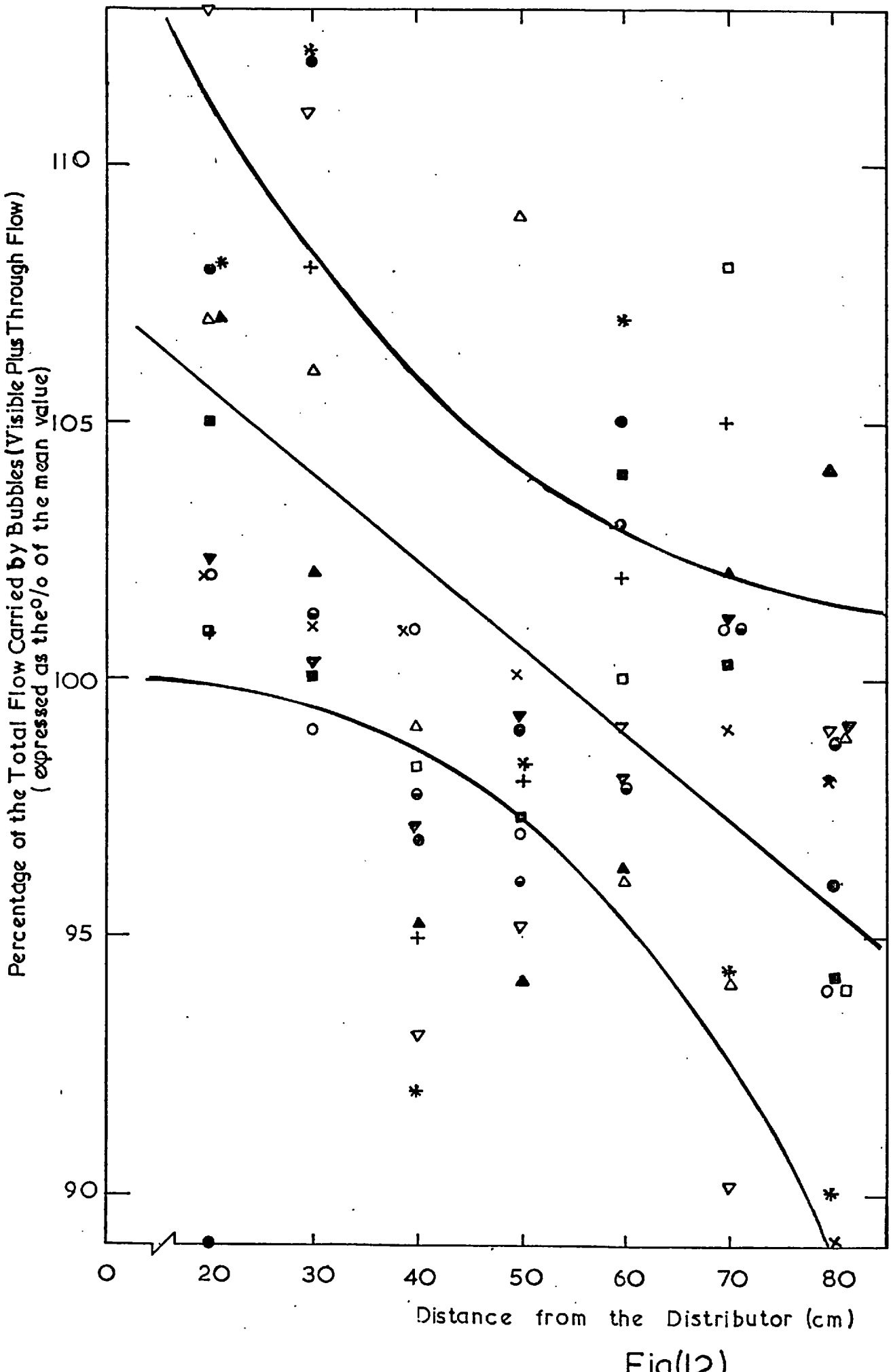
Percentage of the Total Flow Carried by Bubbles (Visible Plus Through Flow)
(expressed as the% of the mean value)
110
105
100
95
90
0
20
30
40
50
60
70
80
Distance from the Distributor (cm)

Fig(12)

3.4.4 DIVISION OF THE TOTAL FLOW TO VISIBLE & THROUGH FLOW

At this point it is necessary to look more closely at the relative magnitude of different contributions to the total bubble flow, i.e. bubble through flow and visible bubble flow. LOCKETT et al (12) by considering the treatment given by DAVIDSON & HARRISON (4) arrived at the conclusion that for a two-dimensional case, the through bubble flow was given by $2\ Uo\ A\ \varepsilon_b$

where ε_b = fraction of the cross-section taken by bubbles,

A = bed cross-section,

Uo = incipient fluidization velocity at superficial basis.

In this work it is assumed that the total flow associated by all the bubbles at a typical cross-section in a two-dimensional fluidized bed is given by Eq.(19):

Total flow due to bubbles across X-X =

$$= S \sum_{i=1}^{n} di\ (U_{Bi} + 2\ Uo)$$

$$= S \sum_{i=1}^{n} di\ U_{Bi} + 2\ S\ Uo \sum_{i=1}^{n} di \qquad \text{Eq.(19)}$$

When Eq.(19) is averaged over a period of time we get:

$$\left(\text{Total flow due to bubbles across X-X}\right)_{av} = \frac{S}{m}\left[\left(\sum_{j=1}^{m} \sum_{i=1}^{n} dij\ U_{Bij} \right)\right] +$$

$$+ \frac{2\ S\ Uo}{m}\left[\left(\sum_{j=1}^{m} \sum_{i=1}^{n} dij \right)\right]$$

which is sum of Eqs.(22-a) and (22-b). The implied assumption in the above statement is that there always is a through flow associated with each bubble, contributing to the total flow across the cross-section X-X.

It has been shown by DAVIDSON & HARRISON (4) on theoretical

grounds that in a fluidized bed when the velocity of a bubble U_B is greater than the interstitial velocity at incipient fluidization Uo then fluid within the bubble stays with the bubble, but makes regular excursions into the surrounding particulate phase without going beyond the surface of a circle concentric with the bubble (cloud). This is in contrast to the case where $U_B < Uo$ and the velocity of the fluid within the bubble is 2 Uo with respect to an observer moving with the velocity of the bubble. Experimental work of DE KOCK & DAVIDSON (25), and ROWE (26) and ROWE & WACE (27) provided the proof for the validity of the theoretical considerations stated above. JACKSON (28) and MURRAY (21) employed more elaborate analysis and produced the same conclusion.

Now in a freely bubbling fluidized bed there is a distribution of bubble size and velocity at each level at various values of U/Uo. This will be discussed in some length later on. A typical cross-section over a period of time cuts bubbles of a distribution of size. (Dependence of the bubble velocity on the bubble size has been established (e.g. 4)). The work which is most relevant to the present work is the investigation carried out by PYLE & HARRISON (29) who measured the velocity of the rise of a bubble in a two-dimensional fluidized bed as a function of the area of the bubble and found that

$$U_B = 15.9\ A_B^{\frac{1}{4}}$$

where $A_B(cm^2)$ and $U_B(cm/sec)$ are the area and the velocity of the bubble respectively).

Now in a cross-section for those bubbles with $U_{Bi} < Uo$ the total flow is given by Eq.(19), $S \sum_{i=1}^{n} di\ (U_{Bi} + 2\ Uo)$. But for the case of fast bubbles where $U_{Bi} \gg Uo$, the contribution of the through flow becomes negligible. In fact, strictly speaking for a fast bubble the effect of the downward flowing gas in the cloud region

should be taken into account where the flow across the cross-section is considered. In such a case the fluidizing fluid leaves the roof of the bubble and, after making a circuit within the particles returns to the bubble. We see that for large and fast bubbles the bubble through flow has, effectively, no contribution to the flow across the cross-section. Therefore the assumption that there always is a through flow associated with each bubble (implied in Eq.(19)) is strictly correct where there are a large number of small and slow bubbles, and not strictly correct when there are too many large and hence fast bubbles. However, the error due to this assumption is negligible and this can be proved by the examination of the data given in Figs.(9,12).

Fig.(9) shows that the visible bubble flow increases as the distance from the distributor is increased. Fig.(12) shows that the total flow associated with bubbles decreases with height above the distributor. The conclusion is that the through flow is a strong (relatively) function of height and in particular decreases with height. This means that the contribution of the bubble through flow to the total bubble flow and hence to the total flow across the cross-section X-X is mainly near the foot of the fluidized bed, where there are large numbers of small bubbles and very few large ones.

In the light of the argument presented above it can be seen that the inclusion of the term 2 Uo $\sum$ di (bubble through flow) in Eq.(19) does not cause any appreciable error because the contribution of this term to the flow across a cross-section is mainly in the foot of the fluidized bed, in which region inclusion of the term in Eq.(19) is justified.

CHAPTER 4

EXAMINATION OF THE TWO-PHASE MODEL

Eq.(23) states that:

$$A(1-\bar{\delta})\,Uo + 2\,S\,Uo\,(\overline{\textstyle\sum} di) + S\,(\overline{\textstyle\sum di\,U_{Bi}}) = AU \qquad \text{Eq.(23)}$$

where the first, second, and the third terms on the left of Eq.(23) are the emulsion flow, bubble through flow, and the visible bubble flow and also

$(\overline{\sum} di)$ = part of the cross-section occupied by all the bubbles at a given level averaged over a long period of time,

$S\,(\overline{\sum di\,U_{Bi}})$ = visible bubble flow rate due to all the bubbles at the same level, averaged over a long period of time,

$\bar{\delta} = \bar{\varepsilon}\,b = \frac{(\overline{\sum} di)}{L}$ = fraction of the cross-section taken by all the bubbles at that level.

By now we have obtained all the information concerning the different terms in Eq.(23) and we are able to verify the validity of this equation. We have shown and discussed the relative magnitude and the behaviour of the various terms in Eq.(23) as a function of height, for each type of particle and each value of U/Uo.

It has also been shown that the total bubble flow can be assumed, with negligible error to be constant at various height. Now if we consider the average value of this quantity over the whole length of the bed as the representative of the total bubble flow in the bed, the effect of this averaging would be to reduce the error due to random variation and therefore this may partly or totally compensate the error which is caused by the assumption made above (i.e. the total

bubble flow is constant at various heights). In the same way it is possible to show that it is justifiable to average the magnitude of the emulsion flow at various heights and take the average value as the estimate of the emulsion flow.

If we use the average value of the total bubble flow (visible + through) and the emulsion flow in Eq.(23) we get:

$$A(1 - \overline{\delta}_{ave}) Uo + 2 S Uo \left(\overline{\sum di}\right)_{ave} + S \left(\overline{\sum di\, U_{Bi}}\right)_{ave} = UA \qquad \text{Eq.(27)}$$

where suffix "ave" means that the quantity is averaged over the whole length of the bed. Now the experimental data will be used to check Eq.(27). As was previously mentioned the degree of the success or failure of this equation would be a critical check for the validity of the underlying assumption, i.e. the two-phase model of fluidization. If this model is the true representative of the situation then we expect the sum of the terms on the left side of equation (27), i.e. emulsion flow, bubble through flow, and bubble visible flow to be equal (within the range of experimental error) to the value of the term on the right side of Eq.(27), i.e. the total flow of the fluid into the bed.

Eq.(13): $U = (1 + \varepsilon_b) Uo + Q_B/A$ in an averaged form is:

$$U = (1 + \overline{\varepsilon}_{b_{ave}}) Uo + \overline{Q_B}_{ave/A} \qquad \text{Eq.(28)}$$

or

$$U = Uo\, \overline{k}_{ave} + \overline{Q_B}_{ave/A} \qquad \text{Eq.(29)}$$

where $$\varepsilon_{b_{ave}} = \frac{\left(\overline{\sum di}\right)_{ave}}{L},$$

$$\overline{Q_B}_{ave} = S \left(\overline{\sum di\, U_{Bi}}\right)_{ave} + 2 S Uo \left(\overline{\sum di}\right)_{ave}$$

and $$\overline{k}_{ave} = 1 + \varepsilon_{b_{ave}} = 1 + \overline{\delta}_{ave}$$

(Averaging is carried over the time and the height. From now on the

averaging sign is dropped for the reason of simplicity and it is understood that all terms are averaged).

We are also going to find out the value of k from Eq.(29) by using our experimental data. Another check for the two-phase model would be the comparison of k so obtained with the theoretical value given by LOCKETT et al (12). If we find out that the value of k evaluated from the data is not significantly greater than 1.4, then we would conclude according to LOCKETT et al (12) that the two-phase model is a valid representative of the situation.

First the results of the examination of Eq.(27) will be presented.

4.1 COMPARISON OF THE TOTAL FEED WITH THE TOTAL MEASURED FLOW IN VARIOUS PHASES

In Figs.(13a,b,c,d,e) the values of the various terms in Eq.(27) are given for different values of U/Uo for various particles. The horizontal co-ordinate is graded in multiples of Uo, the incipient fluidization velocity. On the vertical co-ordinate the percentage of the measured total flow is given. Therefore at each value of U/Uo the sum of the visible bubble flow, bubble through flow, and the emulsion flow is equal to 100. On each graph the 99% confidence limits for the sum of measured quantities are also included and given as the percentage of the total measured flow.

Starting with Fig.(13a) for ballotini grade 8, we see that there is a remarkable agreement between the sum of terms, emulsion flow, visible flow, and through flow on one hand and the value of the actual flow (actual feed) into the bed on the other hand. Only in one case the value of actual feed is slightly outside the confidence limits of the measured total flow. The significance of this point will be discussed later on. For ballotini grade 10 also there is an extremely good agreement between the total flow and the actual feed, Fig.(13b). For ballotini grade 14 also the agreement is very good, Fig.(13c). For the cases of the coarse sand and fine sand Fig.(13d) and Fig.(13e) the agreement is not as good as the case of the spherical particles, the value of the actual feed is outside the confidence intervals of the total flow.

The general features of these curves are as follows: As the ratio of U/Uo is increased the percentage of the total flow carried by the visible bubble flow is increased, and the percentage carried by the emulsion phase is decreased. The percentage of the bubble through flow remains almost constant.

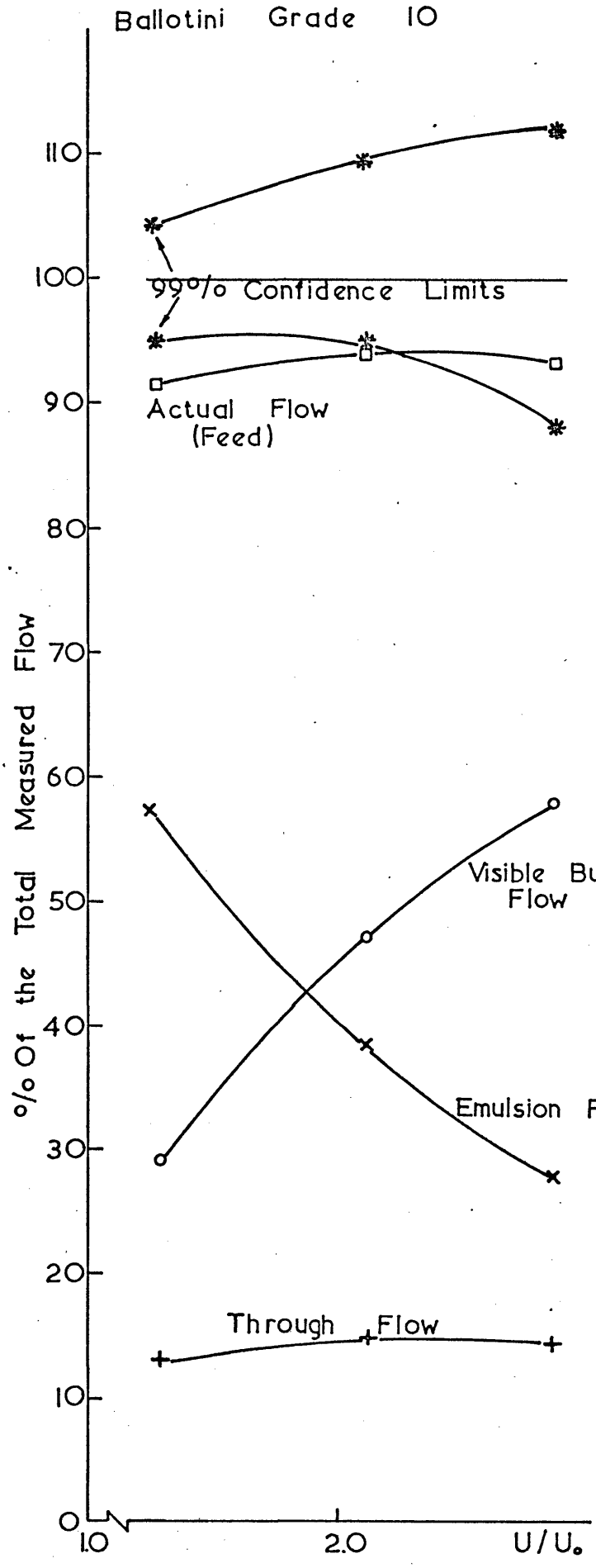

Fig(13-b)

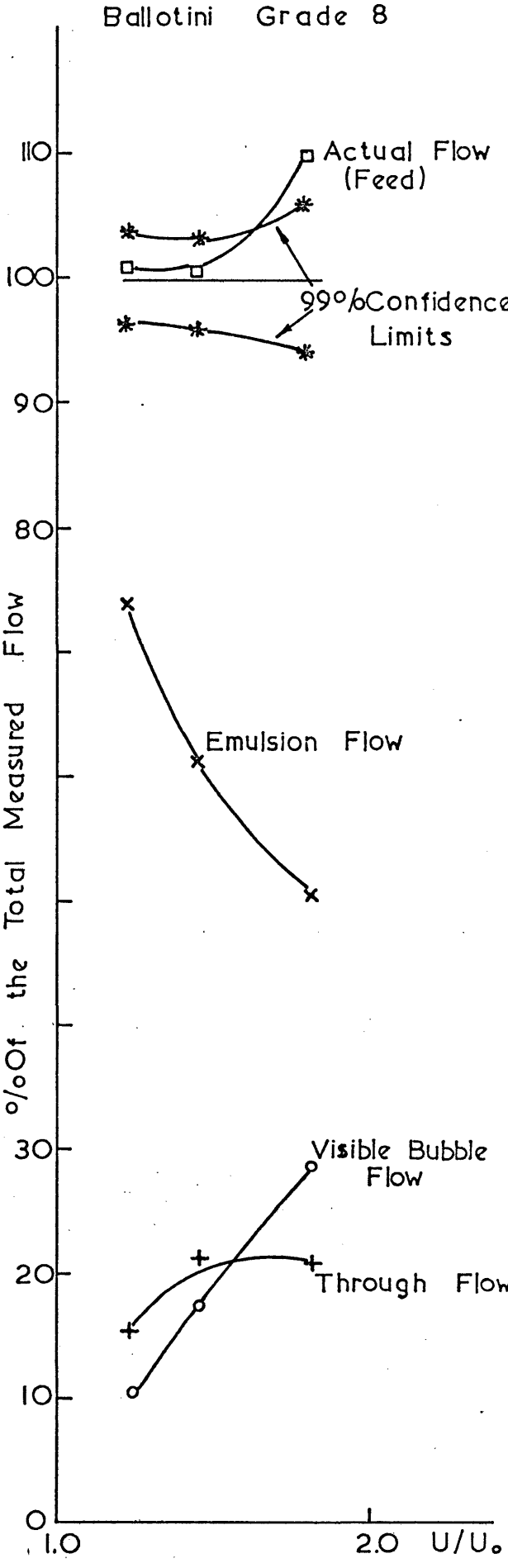

Fig.(13-a)

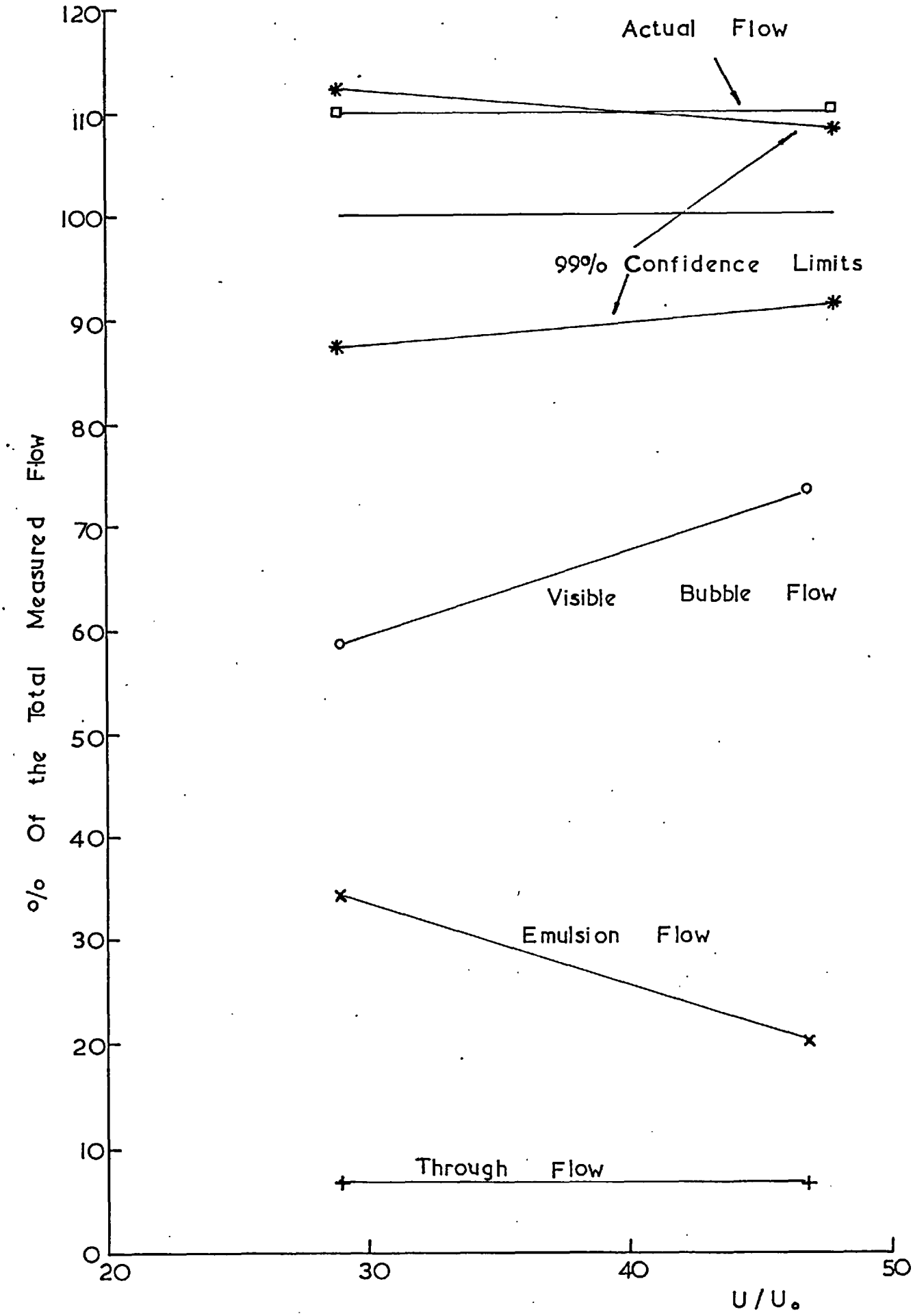
Ballotini Grade 14
Actual Flow
99% Confidence Limits
Visible Bubble Flow
Emulsion Flow
Through Flow
% Of the Total Measured Flow
U/U₀
120
110
100
90
80
70
60
50
40
30
20
10
0
20
30
40
50

Fig.(3-c)

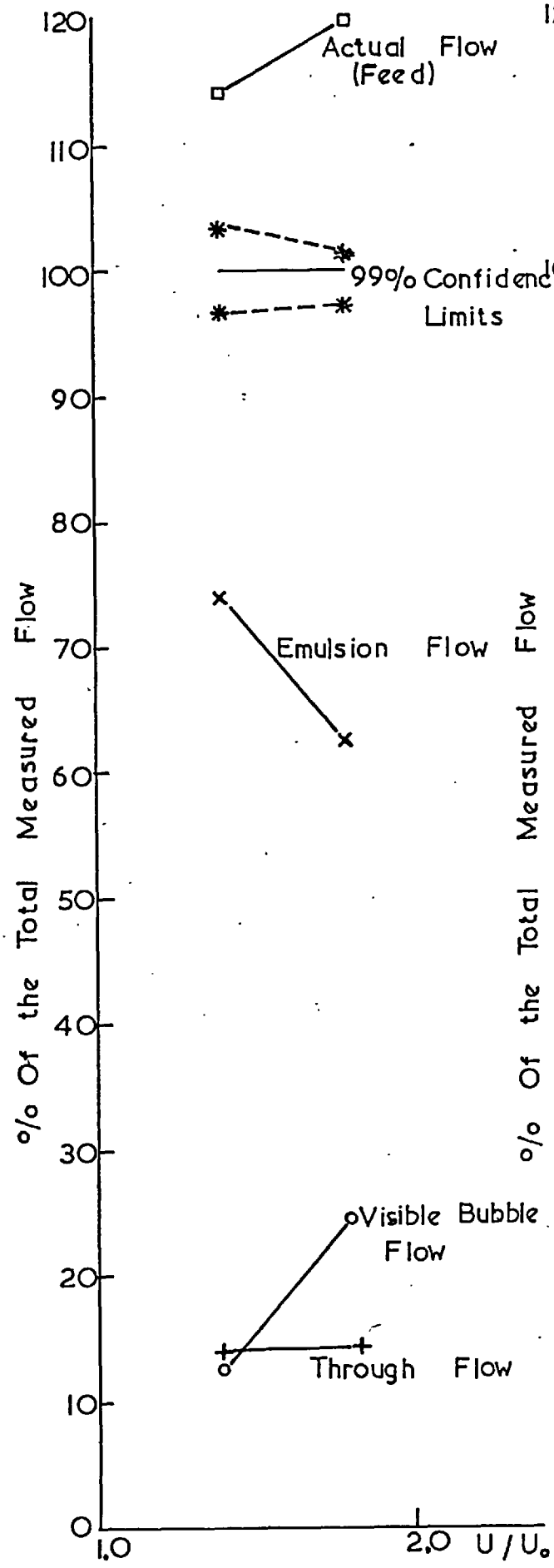

Fig (13-d)

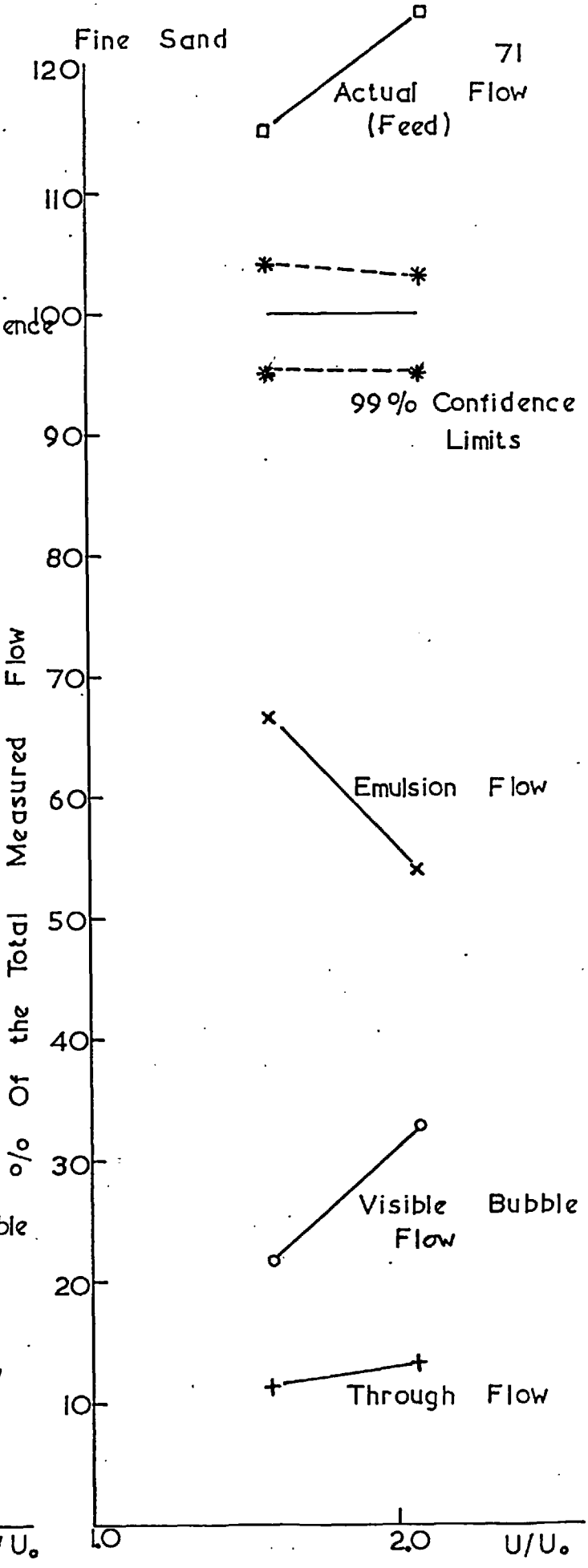

Fig (13-e)

For the case of ballotini grade 10 the actual feed falls below the total flow measured. Only in one case, i.e. at U/Uo = 1.43, there is a significant difference between the feed and the total flow measured. From Eq.(26) it can be seen that one of the factors which may have caused this difference is the estimated value of the interstitial velocity which is assumed to be at the incipient fluidization value.

Now we are looking to see if the magnitude of the interstitial velocity which according to two-phase model is assumed to remain at its incipient value is really equal to Uo. In particular we want to determine if Ui is greater than Uo, because this is the most commonly held argument against the two-phase model. Now the fact that the sum of the terms on the left of Eq.(26) over-estimates the term on the right of the equation shows that, if anything, we are over-estimating the magnitude of the interstitial velocity by assuming it to be equal to Uo. Now the over-estimation of Ui by assuming it to be equal to Uo is not the question. Therefore we conclude that the observed discrepancy is not against the two-phase model and indeed the closeness of the results is in favour of the model.

In Fig.(13,d,e) we have the experimental results of the sand particles. The closeness of the results in these cases is not as good as the cases of spherical particles. One possible explanation is that the measurement of Uo is more subject to error in these cases because of the geometry of particles and their size distribution. Also the measurements of visible bubble flow is subjected to more error because of frequent splitting and particle raining through. However, a general feature of the curves is that for higher values of U/Uo the closeness of the results decreases.

Now we look more closely at the situation and examine what

happens when the ratio of U/Uo is increased. Eq.(26) states that:

$$A(1 + \overline{\delta}) Uo + S (\overline{\sum} di\ U_{Bi}) = AU \qquad \text{Eq.(26)}$$

or in averaged form (over height also)

$$A(1 + \overline{\delta}_{ave}) Uo + S (\sum di\ U_{Bi})_{ave} = AU \qquad \text{Eq.(28)}$$

the first term being (emulsion + through bubble) flow and the second term visible bubble flow. Now we have shown that as the ratio of U/Uo is increased the $\overline{\delta}_{ave}$ is increased, Fig.(8). This also is apparent from the examination of Fig.(14) where the value of $(1 + \varepsilon_{b_{ave}}) = (1 + \overline{\delta}_{ave})$ is plotted for various particles at different values of U/Uo.

Now it might be argued that if there is an error in the assumption that the interstitial velocity is equal to Uo and in particular if we are <u>under-estimating</u> the value of Ui by putting Uo in term $A(1 + \overline{\delta}_{av}) Uo$, then this is likely to produce an under-estimation of the actual feed. Accordingly this under-estimation, it might be argued, is going to be greater when the factor $(1 + \overline{\delta}_{ave})$ is bigger. Now it was shown that $(1 + \overline{\delta}_{ave})$ is greater at high U/Uo and also a greater under-estimation of the actual feed at higher U/Uo. According to the above argument it may be concluded that we are under-estimating the value of Ui by putting it equal to Uo, and this error (i.e. under-estimation) is more accentuated at high values of U/Uo.

The above conclusion is not correct because the argument leading to this conclusion is partly wrong. In fact, the above argument overlooks one important fact. It is true that at higher values of U/Uo the factor $1 + \overline{\delta}_{ave}$ is greater, but the important point is that the distribution of the total feed between different phases contributing to the flow through the bed is such that as the ratio U/Uo increases, the flow due to emulsion phase plus bubble through flow decreases. This point is quite clear and apparent from graphs given in Fig.(13,a,b,c,d)

From Fig.(13b), for instance, we find that for a 100% increase in U/Uo the flow due to emulsion phase + bubble through flow decreases about 25%. Now if by the assumption that the interstitial velocity of gas is equal to Uo we are under-estimating the term $(A(1 + \bar{\delta}_{av}) Uo)$ in Eq.(26) then we would expect this under-estimation to be more distinct when the relative magnitude of $A(1 + \bar{\delta}_{ave}) Uo$ is greater, (i.e. at smaller values of U/Uo). In other words, if assumption Ui = Uo was wrong we would have expected to get a smaller error at higher ratios of U/Uo, i.e. when the relative magnitude of $A(1 + \bar{\delta}_{ave})Uo$ is smaller. So clearly the fact that at high values of U/Uo we do not get a very good agreement between the actual flow and the sum of flow due to various flow phases, is not an evidence for the breakdown of the two-phase model at higher U/Uo. One possible explanation for the discrepancy between the two sides of Eq.(26) can be stated as follows:

We expect to make some errors in the measurements of the di and U_{Bi}. By increasing the number of observations the scatter of the measured quantities around their limiting magnitude is decreased. In order that the magnitude of error remains constant at various values of the independent variable, i.e. U/Uo, the quantity to be measured must subject itself to the measurement in a manner which is irrespective of the magnitude of the independent variable. Now it is an observational fact that as the magnitude of U/Uo is increased the motion of bubbles becomes very erratic. This is mainly because of the large number of coalescences that a bubble may experience. When two bubbles are close enough coalescence occurs. The result is that the shape and the velocity of the lower bubble is greatly influenced. TOEI & MATSUMO (30) investigated the problem of coalescence and found that when the distance between the roofs of two bubbles is approximately

equal to the sum of their diameters they can affect each other. The lower bubble is accelerated and when it enters the wake of the upper bubble, its velocity is increased up to 1.7 times the velocity of the upper bubble. The velocity of the upper bubble also may be increased by up to 10%. The shape of the lower bubble, during the process of coalescence gradually becomes elongated and that of the upper bubble becomes flat. This is very apparent from the tracing given in Plate (2). In short, the effect of high degree of coalescence at high values of U/Uo is that the shape and the velocity of the bubbles change very drastically. It becomes difficult to measure the size and the velocity of the bubble which is at the point of coalescence. Bubble splitting and raining of the particles through the bubble become also influencing factors. For instance, in the case of fine sand, collapse of the bubble roof and raining of the particles was very severe and the measurement of the size and the velocity of bubbles was difficult. Now these difficulties in the measurements are very likely to have produced a systematic error (quite apart from the usual errors of measurements) in the estimation of the measured quantity. We notice that the quantity to be measured does not subject itself to measurement, uniformly, and in particular the cause for error is greater at higher values of the independent variable. What follows is that the relatively greater deviation at higher U/Uo is most probably due to the systematic error which is inherent in the measurements at higher U/Uo.

4.2 EVALUATION OF k

Another relevant investigation and also test for the justification of the two-phase model is the magnitude of the constant k in the Eq.(13).

$$U = (1 + \varepsilon_b)\, U_o + Q_{B/A}$$

where ε_b = fraction of the bed taken by bubbles,

and $k = 1 + \varepsilon_b$.

LOCKETT et al (12) produced a theory from which they calculated the value of the k in Eq.(10).

$$AU = A\, k\, U_o + Q_B$$

where Q_B = observed bubble flow.

They also showed by a less rigorous analysis that in a fluidized bed:

$k = 1 + \varepsilon_b$ for a two-dimensional case

and $k = 1 + 2\varepsilon_b$ for three-dimensional case.

They suggested that if k did not take values much greater than 1.4 (i.e. when $\varepsilon_b = 0.4$) then for systems operated under flow conditions distinctly above the incipient fluidization velocity (i.e. large Q_B), the two-phase assumption is a reasonable model of the experimental situation.

From Eq.(21-a),

$k = 1 + \delta$

where $\delta = \varepsilon_b = \dfrac{\sum_{i=1}^{n} di}{L}$, fraction of a typical cross-section X-X which falls into the bubbles at that cross-section.

L = width of the bed.

First we represent the experimental results for $k(= 1 + \delta)$ as a function of U/U_o (δ is averaged over a period of time and also

across the whole length of the bed) for various particles in Fig.(14) and also in Table (2). For ballotini grade 8 and grade 10 the value of $(1 + \delta)$ obtained from the bubble hold up measurements are also included. From Fig.(14) following points are noticeable:

(i) For all different cases which were examined the value of k obtained from the measurements of δ (i.e. $k = 1 + \delta = 1 + \frac{\sum_{i=1}^{n} di}{L}$) is smaller than 1.22.

(ii) Values of k obtained from the measurements of δ and bubble hold up agree very well. This, as was previously mentioned, shows that the value of δ is a true and accurate estimate of ε_b, i.e. the fraction of the bed taken by bubbles.

(iii) For an equal percentage change in the magnitude of U/Uo the percentage change in the value of $1 + \delta$ is greater for the larger particle size. This shows the reason for the observed mixing behaviour of the particles of various size where with fine material, where the minimum fluidization velocity is much less than the bubble velocity, an increase in gas flow rate will produce less bubbles and therefore less mixing than the same percentage increase with coarse particles. (ROWE & SUTHERLAND (7)).

From Eq.(21) by rearrangement we get

$$(1 + \delta) = \frac{AU - S \sum_{i=1}^{n} di\, U_{Bi}}{A\, Uo}$$

or from Eq.(28) in an averaged form we get

$$(1 + \delta) = \frac{\text{Total Feed - VISIBLE BUBBLE FLOW}}{\text{FLOW AT INCIPIENT FLUIDIZATION}} \qquad \text{Eq.(29)}$$

where $(1 + \delta) = k$

(averaged over a period of time and the height of the bed also).

The value of k obtained from Eq.(29) would be different, obviously, from what was previously obtained from the measurement of

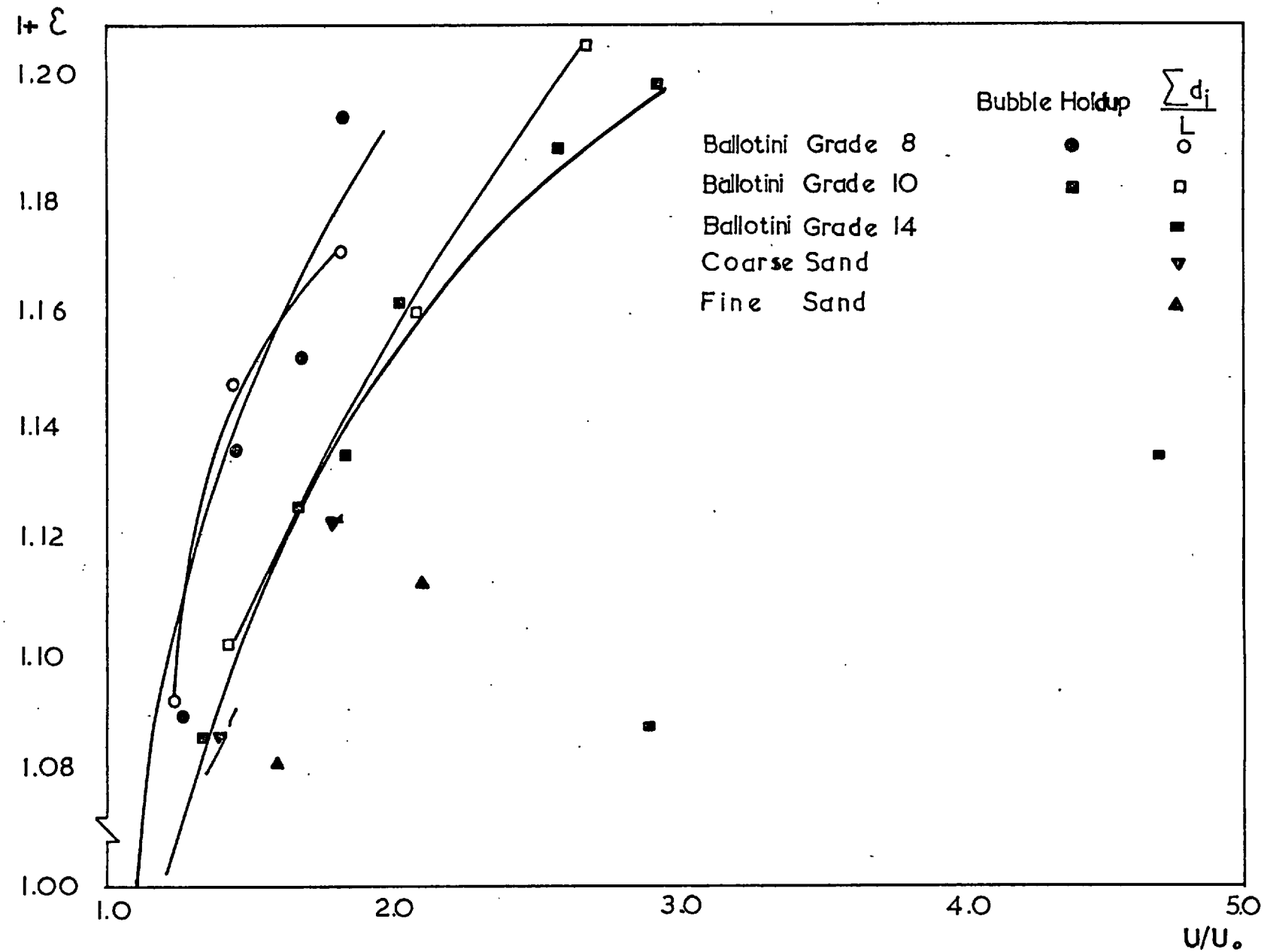
1+ ε
1.20
1.18
1.16
1.14
1.12
1.10
1.08
1.00
1.0
2.0
3.0
4.0
5.0
U/U.
Bubble Holdup
$\frac{\sum d_i}{L}$
Ballotini Grade 8
Ballotini Grade 10
Ballotini Grade 14
Coarse Sand
Fine Sand

Fig (14)

TABLE (2)

$(1 + \delta)$ FROM THE EXPERIMENTAL RESULTS AT VARIOUS VALUES OF U/Uo

Height From Distributor cm	BALLOTINI								SAND			
	Grade 8			Grade 10			Grade 14		FINE		COARSE	
	U/Uo			U/Uo			U/Uo		U/Uo		U/Uo	
	1.24	1.46	1.82	1.43	2.08	2.69	2.9	4.7	1.6	2.1	1.4	1.8
20	1.104	1.172	1.250	1.122	1.197	1.244	1.124	1.177	1.079	1.143	1.120	1.163
30	1.120	1.165	1.226	1.124	1.169	1.233	1.097	1.159	1.102	1.113	1.099	1.134
40	1.093	1.142	1.158	1.095	1.170	1.212	1.077	1.122	1.077	1.116	1.077	1.120
50	1.074	1.167	1.151	1.095	1.149	1.206	1.073	1.129	1.079	1.109	1.065	1.115
60	1.093	1.142	1.159	1.106	1.174	1.212	1.082	1.116	1.084	1.120	1.093	1.115
70	1.097	1.134	1.125	1.099	1.156	1.83	1.086	1.137	1.077	1.109	1.075	1.116
80	1.097	1.118	1.133	1.072	1.120	1.158	1.082	1.107	1.070	1.081	1.071	1.106
Average over height	1.094	1.148	1.172	1.102	1.162	1.207	1.088	1.135	1.081	1.113	1.086	1.124

δ. In fact, in previous cases the assumption that $k = 1 + \delta$ is a consequence of the implied assumption that the interstitial velocity remains constant at its incipient value Uo irrespective of the U/Uo, which in turn is a consequence of the two-phase model. Since the two-phase model is considered to be applicable in the assessment of k therefore the value of k so obtained cannot be used to make a rigorous test of the two-phase model. However, the value of k obtained from equation (29) can be used as a rigorous test of the model, because Eq.(29) is virtually the same as Eq.(10).

$$AU = B_o + F_p + \sum_{\text{all bubbles}} \int_A^C \bar{v} \; . \; d\bar{a} \; . = A \; k \; Uo + Q_B \qquad \text{Eq.(10)}$$

Although in the derivation of Eq.(10) it was assumed that the voidage remains constant at εo, i.e. the voidage at incipient fluidization, however taking Eq.(10) as:

$$AU = A \; k \; Uo + Q_B$$

it is quite possible to think of k as a constant the magnitude of which would be a deciding factor about the two-phase model. What Eq.(10) states is that the total flow introduced to the bed is carried in two phases:

(i) a visible bubble phase Q_B

(ii) an emulsion phase which is assumed

to be k times the amount of the flow at incipient fluidization. This is a statement of continuity and therefore the value of k obtained from Eq.(10) or Eq.(29) can be used as a rigorous test of the model.

The experimental results for k obtained from Eq.(29) for different cases are given in Table (3) for various heights in the bed. The average of k values over the height of the bed, for each case is also given in Fig.(15) as a function $\bar{\varepsilon}_{b_{av}}$. (For each case $\bar{\varepsilon}_{b_{av}}$ itself was taken from the corresponding measurement of $\bar{\delta}_{av}$). Also in Fig.(15) is given the graph obtained on theoretical ground from the relationship between k and ε_b by LOCKETT et al (12). The following points are noticed:

(i) Most of the points fall above the line of the theoretical relationship given by LOCKETT et al (12).

There are only two points which fall above the value of k = 1.4. In one case the particle size is very small (ballotini grade 14); in another case the shape of the particle is also irregular (fine sand). The same factors as given previously in the discussion of the graphs in Fig.(13) could have caused the scatter. Measurements of di and U_{Bi} are biased at high ratios of U/Uo, because bubble coalescence, splitting, and particle raining through the bubble, influence the bubble shape and velocity drastically at high U/Uo and in particular for smaller particle size. The difficulty in the measurements of Uo for fine and irregular particles might have contributed to the scatter. The above consideration leads to:

(ii) All values of k fall below the value of k = 1.4 except two points which are influenced by the experimental difficulties.

There is only one value of k which is less than k = 1. The statistical consideration shows that this point cannot be rejected as being an extreme value.

The immediate conclusions which could be drawn from the above experimental results are:

(i) The value of k obtained from these experimental results is

TABLE (3)

EXPERIMENTAL RESULTS FOR "k" FROM EQ.(29)

Height From Distributor cm	BALLOTINI								SAND			
	Grade 8			Grade 10			Grade 14		FINE		COARSE	
	U/Uo			U/Uo			U/Uo		U/Uo		U/Uo	
	1.2	1.5	1.8	1.4	2.1	2.7	2.9	4.7	1.6	2.1	1.4	1.8
20	1.131	1.210	1.375	1.012	1.087	1.145	1.108	1.480	1.360	1.46	1.255	1.443
30	1.095	1.209	1.372	0.935	1.084	1.047	1.307	1.677	1.259	1.545	1.238	1.429
40	1.122	1.209	1.414	0.995	1.027	0.970	1.612	2.017	1.300	1.575	1.272	1.428
50	1.141	1.189	1.368	0.975	1.108	1.037	1.624	1.670	1.297	1.573	1.273	1.418
60	1.113	1.236	1.334	0.958	0.915	0.909	1.554	1.689	1.260	1.501	1.249	1.411
70	1.088	1.230	1.375	0.904	0.996	1.004	1.331	1.173	1.281	1.527	1.262	1.373
80	1.105	1.235	1.241	1.016	1.081	0.94	1.120	1.530	1.298	1.535	1.270	1.366
Average over height	1.114	1.217	1.348	0.971	1.043	1.007	1.379	1.606	1.294	1.53	1.260	1.410
b_{av}= av	0.094	0.148	0.172	0.102	0.162	0.207	0.088	0.135	0.081	0.113	0.080	0.124

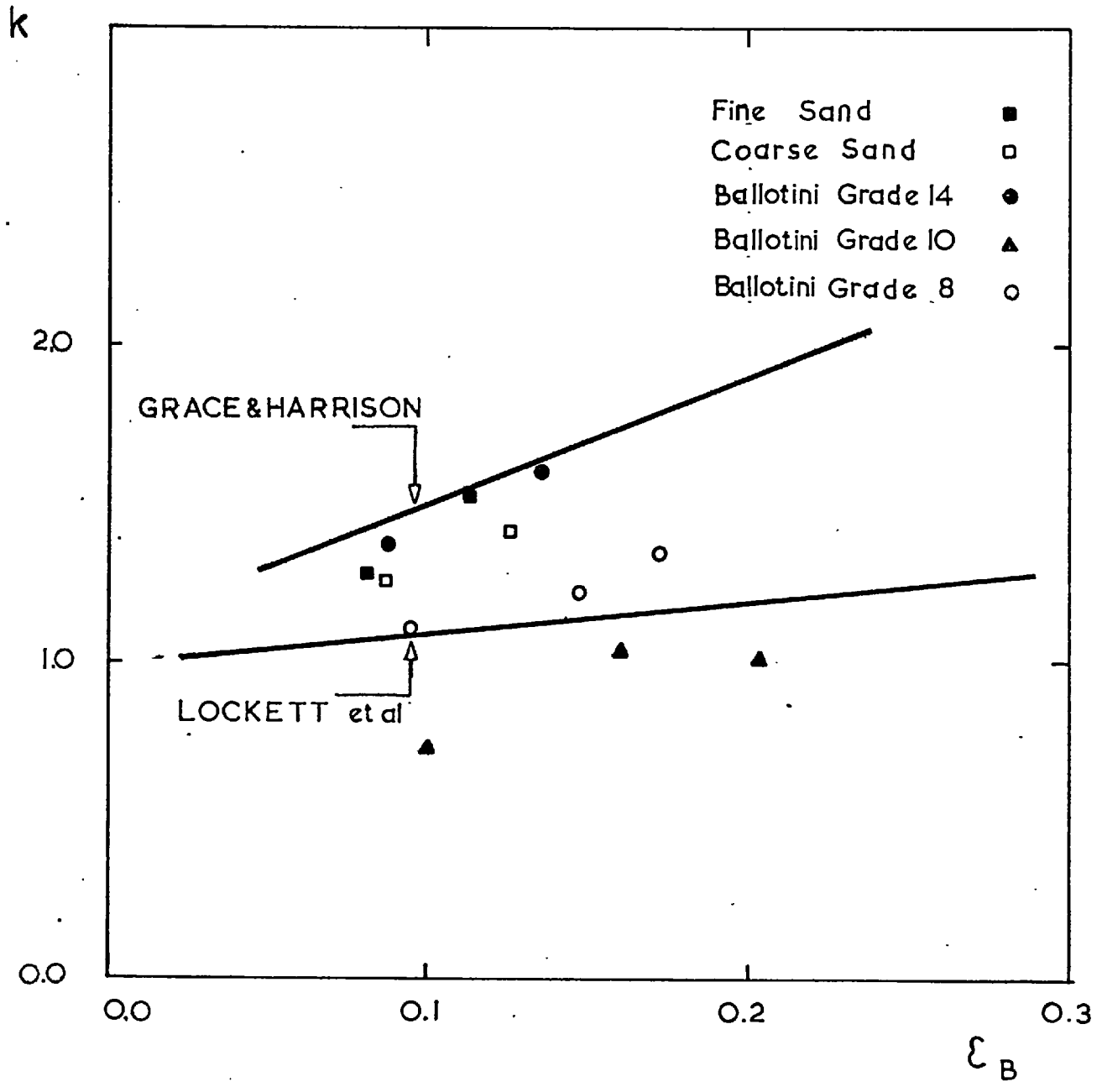
k
Fine Sand
Coarse Sand
Ballotini Grade 14
Ballotini Grade 10
Ballotini Grade 8
2.0
1.0
0.0
GRACE & HARRISON
LOCKETT et al
0.0
0.1
0.2
0.3
ε_B

Fig. (15)

in good agreement with the theoretical value obtained from the analysis given by LOCKETT et al (12).

(ii) In particular, as was mentioned earlier, except in two cases (where experimental difficulties were important) the value of k does not exceed 1.4. The agreement with the conditional magnitude of k, suggested by LOCKETT et al (12) is highly satisfactory.

(iii) Values of $k = 1 + n\,\varepsilon_B$, with n = 4.35 from the work of GRACE & HARRISON (15) overestimates all the results. The experimental data of the above mentioned authors seem not to be accurate because of the measuring techniques employed in the measurement of incipient flow and visible flow rates. The theoretical argument put forward in support of the high value of n also seems not to be logically consistent.

In connection to the conclusion (i) just mentioned, it is realised that in any attempt to estimate the true value of k from the above experimental data, there are three sources of error which could influence the so obtained estimation:

From Eq.(29) we have

$$k = \frac{\text{Total Feed - visible bubble flow}}{\text{Flow at incipient fluidization}}$$

If we represent the total feed as X,

visible bubble flow as Y,

and flow at incipient fluidization as Z,

we get:

$$k = \frac{X - Y}{Z} \quad \text{Eq.(29-a)}$$

Any error in the measurement of X, Y and Z would be reflected in the estimated value of k. To show this analytically if we take the variance of k as a measure of the scatter of the observations around its true value, we get:

$$\text{var}\,(k) = \text{var}\,\left(\frac{X - Y}{Z}\right)$$

$$= \left[\frac{E(X-Y)}{E(Z)}\right]^2 \left\{ \frac{Var(X-Y)}{\left[E(X-Y)\right]^2} - \frac{2\,Cov\left[(X-Y)^2\right]}{E(X-Y)E(Z)} + \frac{Var\,(Z)}{\left[E(Z)\right]^2} \right\} \quad \text{Eq.(30)}$$

where for a given variable X we have:

$$E(X) = \text{expected value of } X = \sum_{X=0}^{\infty} X\,P(X)$$

where P(X) = probability of X, and also

$$Var(X) = \text{variance of } X = \sum_{0}^{\infty} (X - \mu)^2\,P(X)$$

μ = average of X = ave(X)

and Cov(X,Y) = co-variance of X,Y

$$= ave(X - \mu_x)(Y - \mu_y)$$

Now since X,Y and Z are independent variables, therefore we have for equation (30)

$$Var(k) = Var\left(\frac{X - Y}{Z}\right)$$

$$= \left[\frac{E(X-Y)}{E(Z)}\right]^2 \left\{ \frac{Var(X-Y)}{\left[E(X-Y)\right]^2} + \frac{Var\,(Z)}{\left[E(Z)\right]^2} \right\} \quad \text{Eq.(31)}$$

and if there is no error in the measurement of Z (i.e. Uo) we have:

$$Var(k) = \left(\frac{1}{Z}\right)^2 Var(X-Y)$$

because in this case E(Z) = Z and Var(Z) = 0. Clearly we do have error in the measurements of Uo and therefore Eq.(31) is applicable. However, since X and Y are also independent (i.e. the measurements of X, Y and Z are mutually independent), we have:

$$Var(X-Y) = Var(X) + Var(Y)$$

and by substitution in Eq.(31) we get:

$$Var(k) = \left[\frac{E(X-Y)}{E(Z)}\right]^2 \left\{ \frac{Var(X)}{\left[E(X-Y)\right]^2} + \frac{Var(Y)}{\left[E(X-Y)\right]^2} + \frac{Var(Z)}{\left[E(Z)\right]^2} \right\} \quad \text{Eq.(32)}$$

In the measurements of X (i.e. the actual feed) we expect to make very small errors, because this measurement is done by taking direct readings

of the pressure gauge and the rotameters. The random variation of these readings could be assumed to be negligible. Now if we take our readings at the prescribed range of the application of the measuring instruments where the bias is supposed to be small, then we can assume that the variance of X (i.e. total feed) is very small and negligible. This leaves us with the variances of the measurements of Y (visible flow) and Z (i.e. Uo A). We have shown that by increasing the number of the frames analysed beyond 50 and up to 70 the scatter of the experimental results of the visible bubble flow is drastically reduced. The other contributing factor to the scatter of the values of k is the error involved in the measurements of Uo, the incipient fluidization velocity. In order to get an idea about the magnitude of var (k) we evaluate various terms in Eq.(32) for ballotini grade 10. The magnitude of variance of X is assumed to be zero.

From APPENDIX (2) we get:

$$\text{Var}\,(Q_{mf}) = \text{var}\,(Z) = 0.5 \text{ and } \left[E\,(Z)\right]^2 = 1226$$

The rest of the information is given in the following table:

$\frac{U}{U_o}$	Var(Y)	$E(X-Y)^2$	Var (k)	Standard Error
1.4	3.76	1149.2	0.003	0.05
2.1	9.0	1482.2	0.007	0.08
2.7	8.6	1339.6	0.007	0.08

As is seen var (Q_{mf}) is very small. Also it is seen that the Var (k) and the corresponding standard error are negligibly small.

CHAPTER 5

BUBBLE POPULATION PROPERTIES AND BUBBLE GROWTH

5.1 INTRODUCTION

According to DAVIDSON & HARRISON (4) who reviewed the relevant literature, there are at least three possible explanations for the growth of bubbles as they rise in a gas-fluidized bed:

(i) the effective hydrostatic pressure acting on the bubbles decreases as they rise.

(ii) bubbles may coalesce in vertical line, i.e. one bubble may catch up another; and

(iii) neighbouring bubbles in a similar horizontal plane may combine when they are very close to each other.

HARRISON & LEUNG (31) made an experimental study of the bubble growth by mechanism (ii) and concluded that the velocity of the upper bubble is not affected, that a bubble wake extends roughly 1.2 bubble diameters behind it and that the trailing bubble is affected by the leading one. TOEI & MATSUNO(30) produced a theoretical model for bubble coalescence in a two-dimensional fluidized bed and compared their experimental results with the model. Their conclusions are almost the same as HARRISON & LEUNG (31).

They also found that two bubbles side by side hardly coalesced and when one bubble was obliquely below the other bubble, coalescence occurred but the required time was longer.

WHITEHEAD & YOUNG (32) used a light source and light sensing device in a large scale fluidized bed to detect bubbles. They found,

among other things, that when two equal-sized adjacent bubbles rose past the probe and interacted before reaching the bed surface, two different mechanisms were evident:

(i) a single eruption occurred due to "collision coalescence,

(ii) two surface eruptions occurred, some distance apart, one much larger than the other, indicating gas transfer between the bubbles before reaching the surface.

The ultimate aim for any investigation of bubble coalescence is the prediction of bubble size as a function of height. HARRISON & LEUNG(31) studied the bubble size in a fluidized bed above an injection point at various heights. They measured the maximum size of bubbles at various levels above an injection orifice by cine photography of the surface of the bed. Their experimental results were in reasonable agreement with the theory. WHITEHEAD & YOUNG (32) also studied the bubble eruption by the motion picture technique at the surface of a large scale fluidized bed. They correlated their data by an expression which showed that the eruption size was a function of bed height and gas flow rate. It was also concluded that a freely bubbling fluidized bed always contains a wide range of bubble sizes. They also produced eruption diameter distribution histograms from which the effect of height and gas flow rate on eruption size was apparent. BOTTERILL et al (33) found that the diameter of the surface disturbance was observed to be nearly 50% greater than the diameter of the bubble causing it.

Here we are going to present some of our experimental evidence relevant to the phenomena of bubble coalescence and bubble size at various heights. In particular we are going to concentrate on the bubble size distribution and α distribution at each level for various particles at different values of U/U_o. Bubble size distribution and

"α" distribution are of primary importance in the design of the gas-fluidized reactors. The importance is fully appreciated when the analysis of chemical reaction in a bubbling gas-fluidized bed given by PARTRIDGE & ROWE(34) is considered. This was also stressed by RIETEMA (35) and ROWE (36).

5.2 BUBBLE SIZE DISTRIBUTION

As was pointed out earlier the bubble size is one of the most important factors in the design of gas-fluidized reactors.

Many investigators have studied the problem of the size of bubbles in gas-fluidized beds as a function of height for various particles and at different gas flow rates. KUNII& LEVENSPIEL (37) have reviewed the literature and the results are given in their Fig.(19). The general conclusion is that the size of a bubble is an increasing function of the distance of the bubble from the distributor. It is common to give as the estimate of the size of the bubble, the mean value of the bubble size distribution. It is also common to take the bubble size to be constant at each height. It is true that these commonly held assumptions simplify the complicated treatments of the fluidized systems; however, the analysis of PARTRIDGE & ROWE (34) shows very clearly the necessity of considering the bubble size distribution in the treatment of fluidized reactors.

In Fig.(16a-h) the bubble size distribution is given as histograms at various heights, various values of U/Uo and for different particles. (The rest of the relevant information is given in TABLE (4)). On the horizontal axis is given the square root of the area of the bubble and on the vertical axis the relative frequency/ cell interval is given. The corresponding cumulative relative frequency distribution diagrams are given in Figs.(17a-h). The horizontal axis again is the square root of the area of the bubble. The experimental data were obtained in this way. The cine film taken from the performance of the bed was projected on a screen (a sheet of paper) and the area of all bubbles passing a selected level was traced. This was carried on over a period of time. The area was measured by cutting the bubbles out of the sheet of paper and weighting them

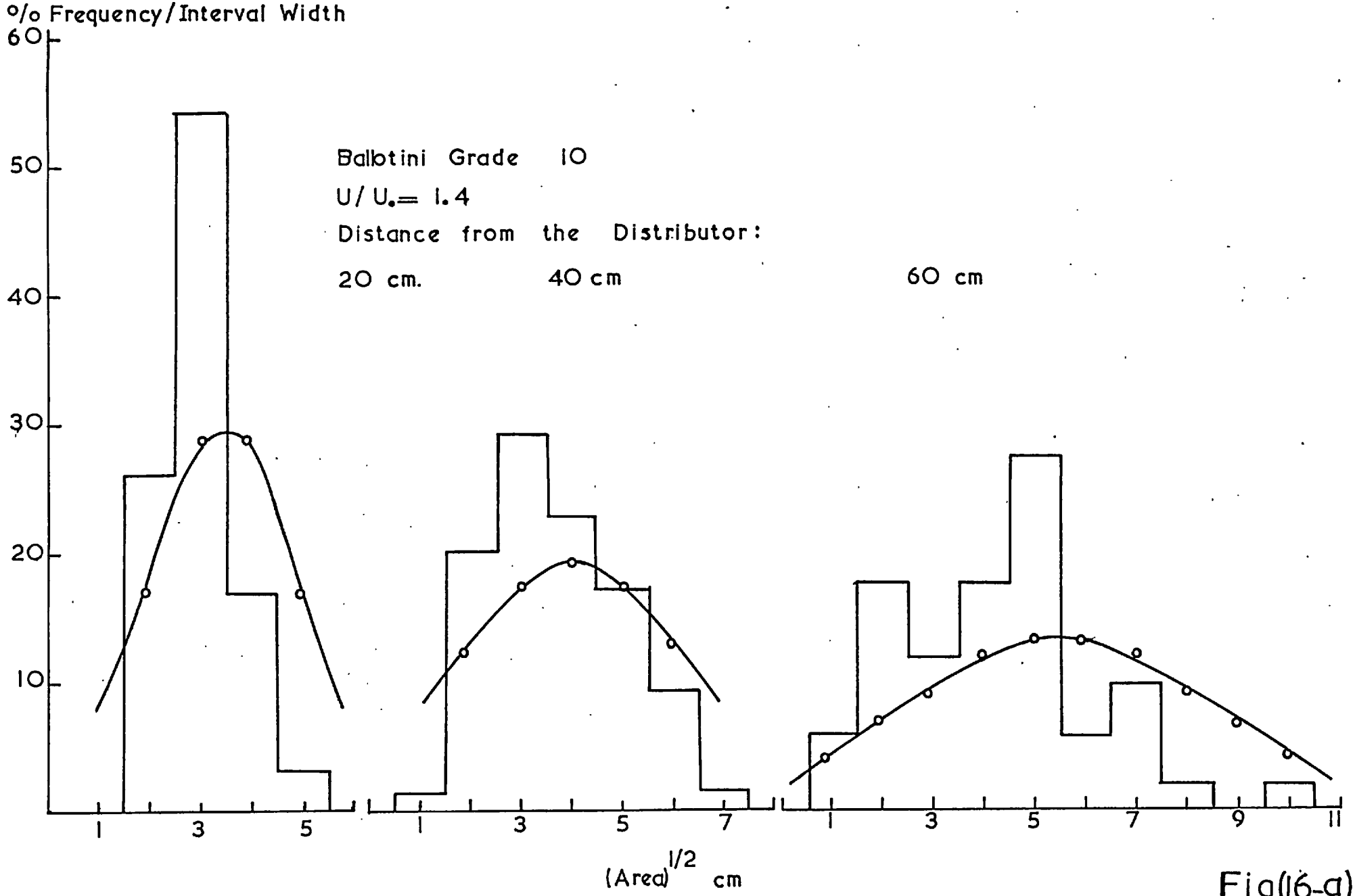
% Frequency / Interval Width
60
50
40
30
20
10
Balbtini Grade 10
U / U∞ = 1.4
Distance from the Distributor:
20 cm.
40 cm
60 cm
1
3
5
7
9
11
(Area)^1/2 cm

Fig.(16-a)

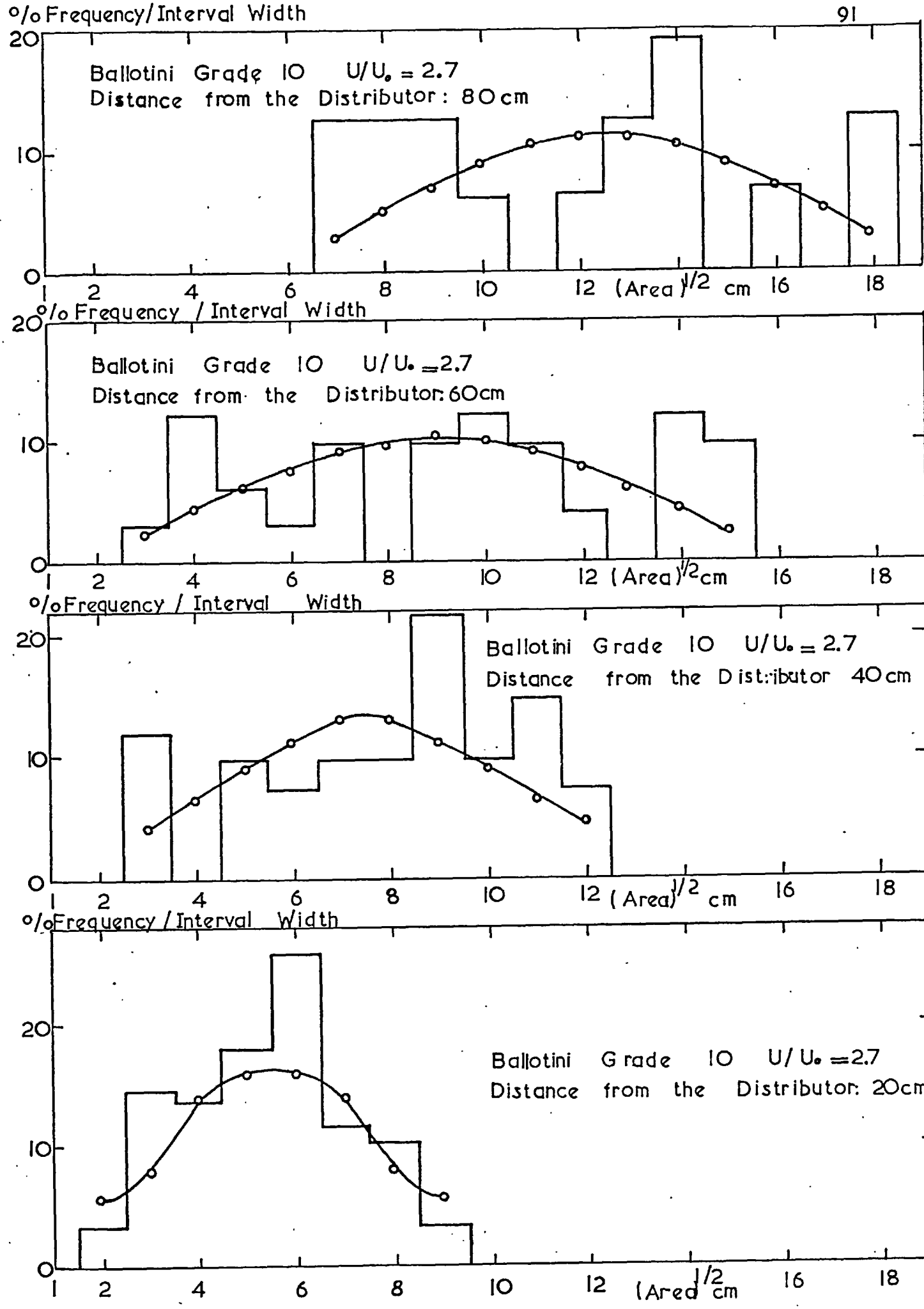
% Frequency / Interval Width
Ballotini Grade 10 U/U₀ = 2.7
Distance from the Distributor : 80 cm
(Area)^1/2 cm
% Frequency / Interval Width
Ballotini Grade 10 U/U₀ = 2.7
Distance from the Distributor: 60cm
(Area)^1/2 cm
% Frequency / Interval Width
Ballotini Grade 10 U/U₀ = 2.7
Distance from the Distributor 40 cm
(Area)^1/2 cm
% Frequency / Interval Width
Ballotini Grade 10 U/U₀ = 2.7
Distance from the Distributor: 20cm
(Area)^1/2 cm

Fig.(16-b)

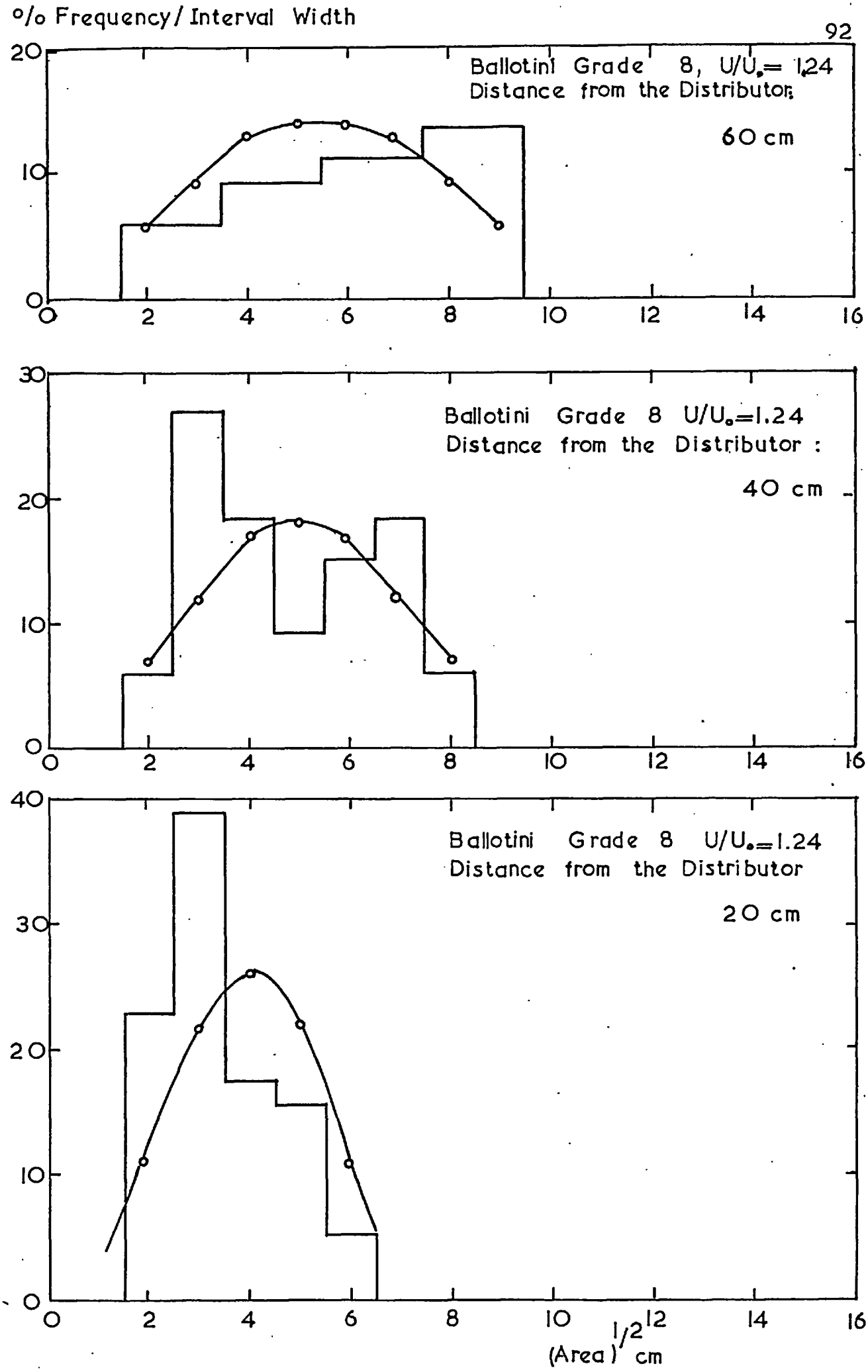
% Frequency / Interval Width
Ballotini Grade 8, U/U₀ = 1.24
Distance from the Distributor:
60 cm
Ballotini Grade 8 U/U₀=1.24
Distance from the Distributor :
40 cm
Ballotini Grade 8 U/U₀=1.24
Distance from the Distributor
20 cm
(Area)^1/2 cm

Fig.(16-c)

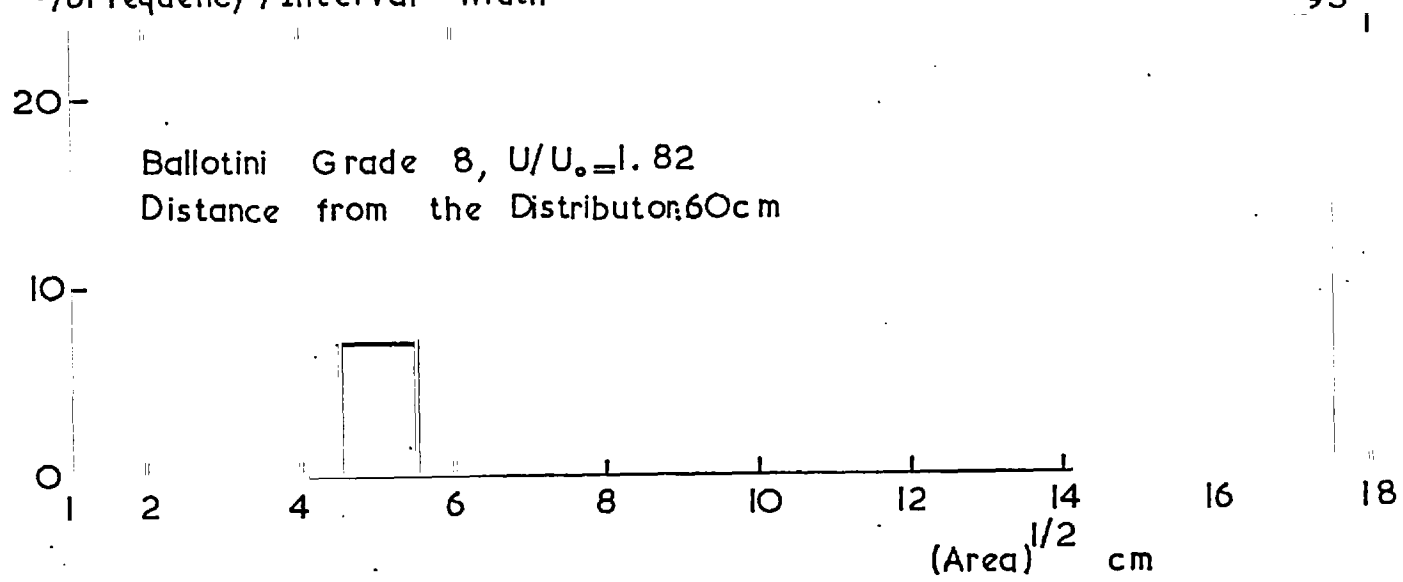
%Frequency / Interval Width
Ballotini Grade 8, U/U₀=1.82
Distance from the Distributor:60cm
(Area)^1/2 cm

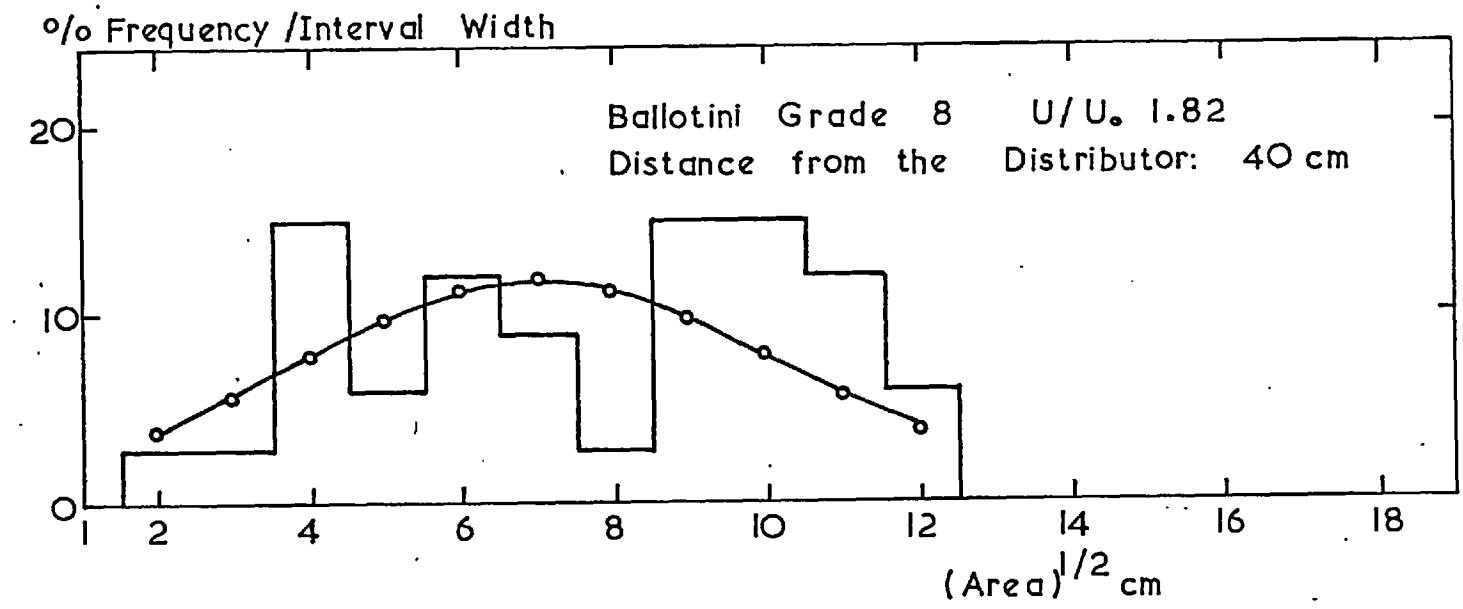
%Frequency /Interval Width
Ballotini Grade 8 U/U₀ 1.82
Distance from the Distributor: 40 cm
(Area)^1/2 cm

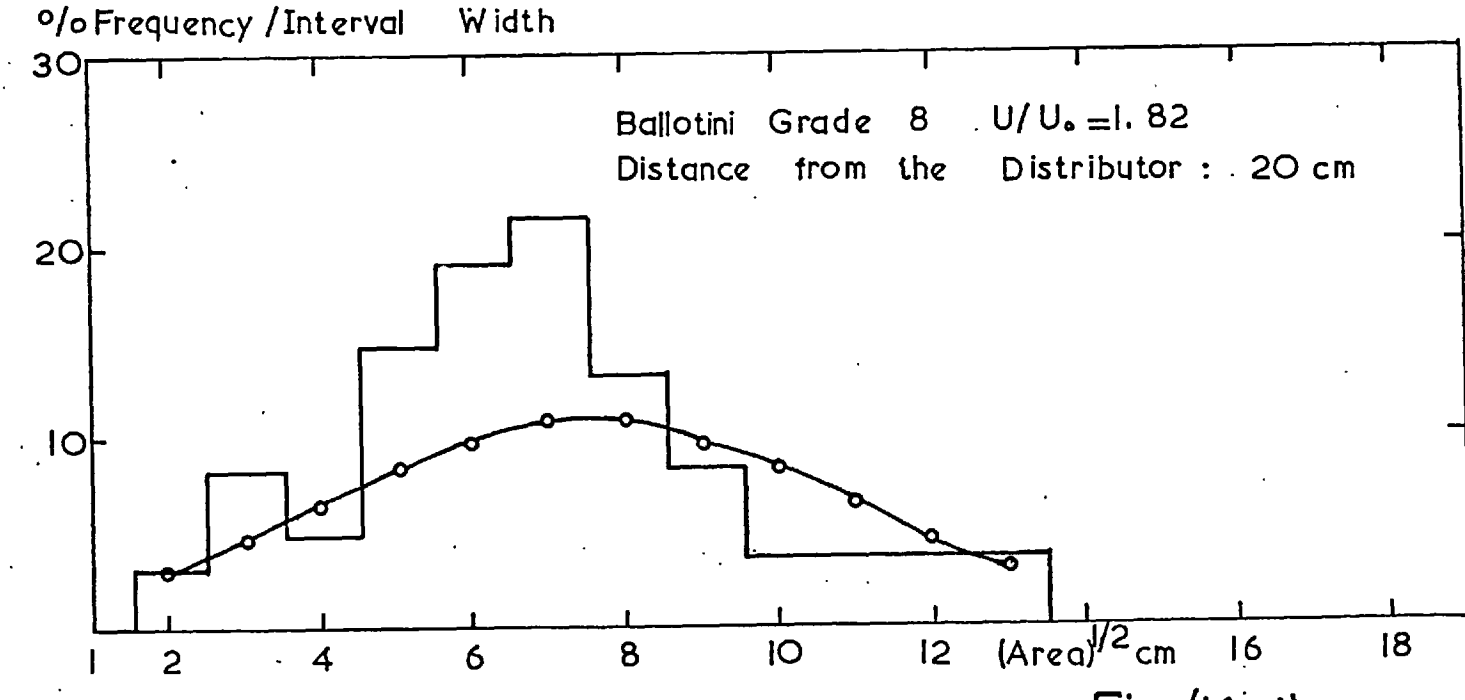
%Frequency /Interval Width
Ballotini Grade 8 U/U₀=1.82
Distance from the Distributor : 20 cm
(Area)^1/2 cm

Fig.(16-d)

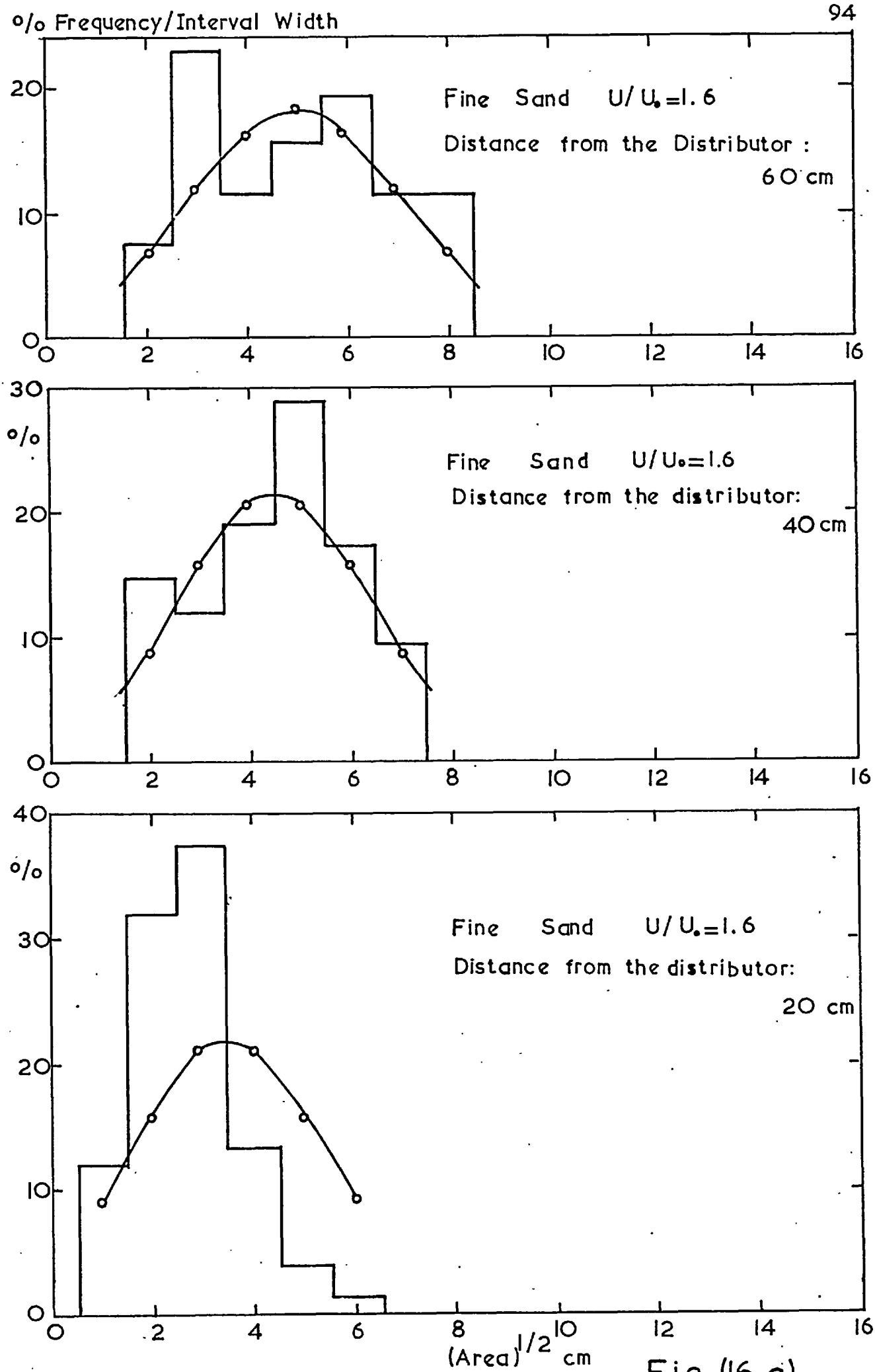
% Frequency/Interval Width
Fine Sand U/U₀=1.6
Distance from the Distributor :
60 cm
Fine Sand U/U₀=1.6
Distance from the distributor:
40 cm
Fine Sand U/U₀=1.6
Distance from the distributor:
20 cm
(Area)^1/2 cm

Fig. (16-e)

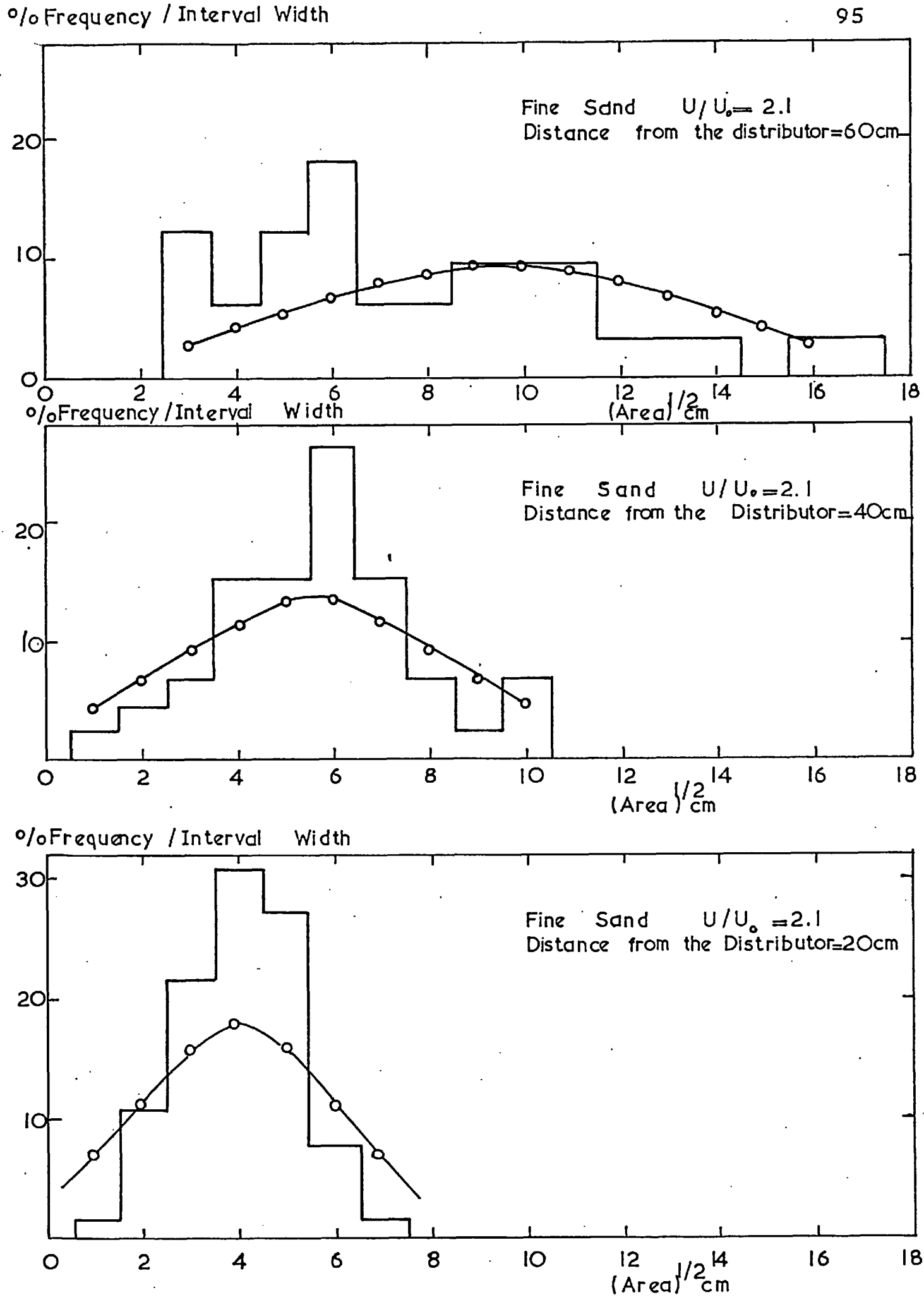
%Frequency / Interval Width
Fine Sand U/U₀= 2.1
Distance from the distributor=60cm
(Area)^1/2 cm
%Frequency / Interval Width
Fine Sand U/U₀=2.1
Distance from the Distributor=40cm
(Area)^1/2 cm
%Frequency / Interval Width
Fine Sand U/U₀ =2.1
Distance from the Distributor=20cm
(Area)^1/2 cm

Fig.(16-f)

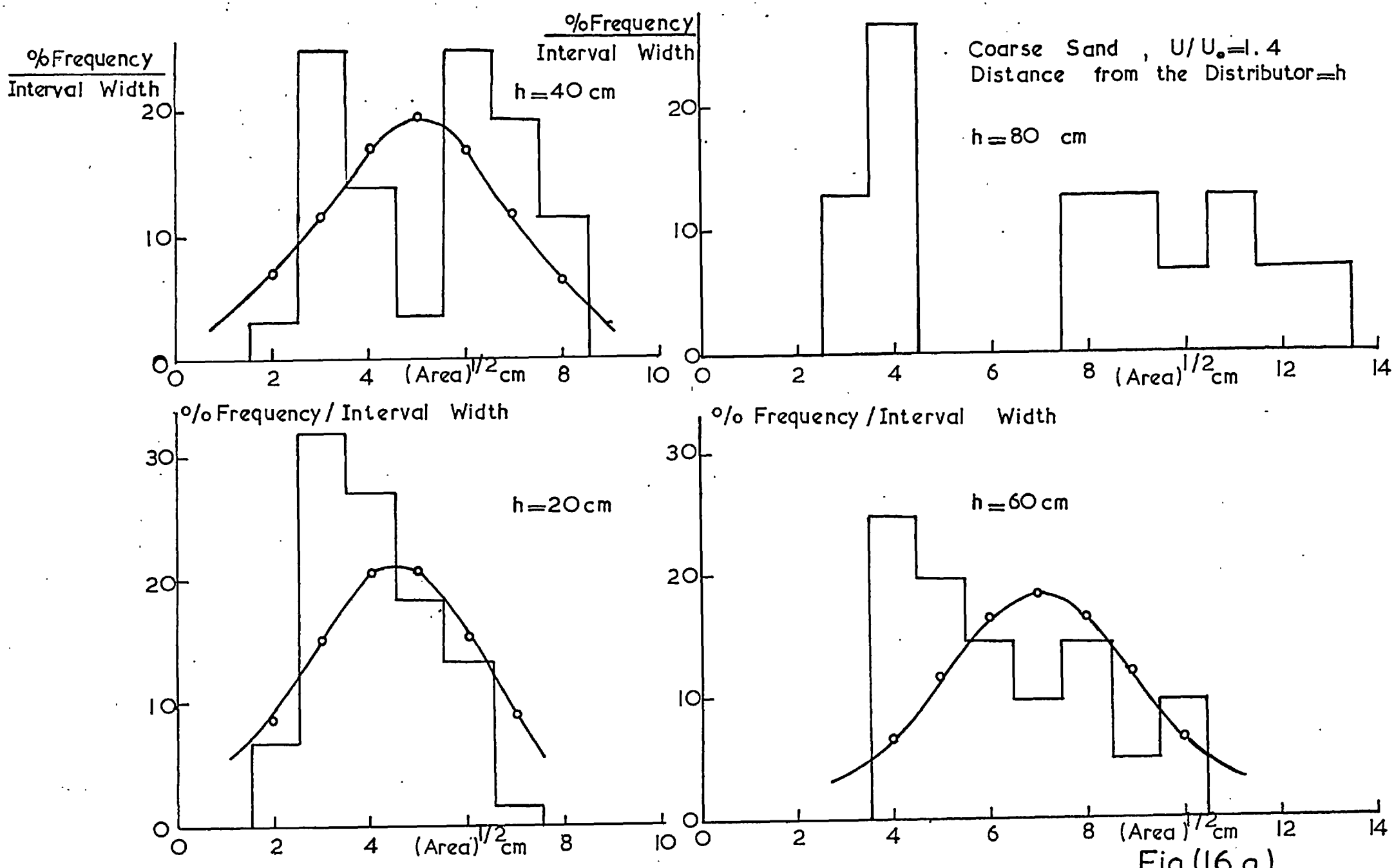
%Frequency / Interval Width
h=40 cm
20
10
0
0
2
4
(Area)^1/2 cm
8
10
%Frequency / Interval Width
Coarse Sand , U/U₀=1.4
Distance from the Distributor=h
h=80 cm
20
10
0
0
2
4
6
8
(Area)^1/2 cm
12
14
%Frequency / Interval Width
h=20 cm
30
20
10
0
0
2
4
(Area)^1/2 cm
8
10
%Frequency / Interval Width
h=60 cm
30
20
10
0
0
2
4
6
8
(Area)^1/2 cm
12
14

Fig.(16_g)

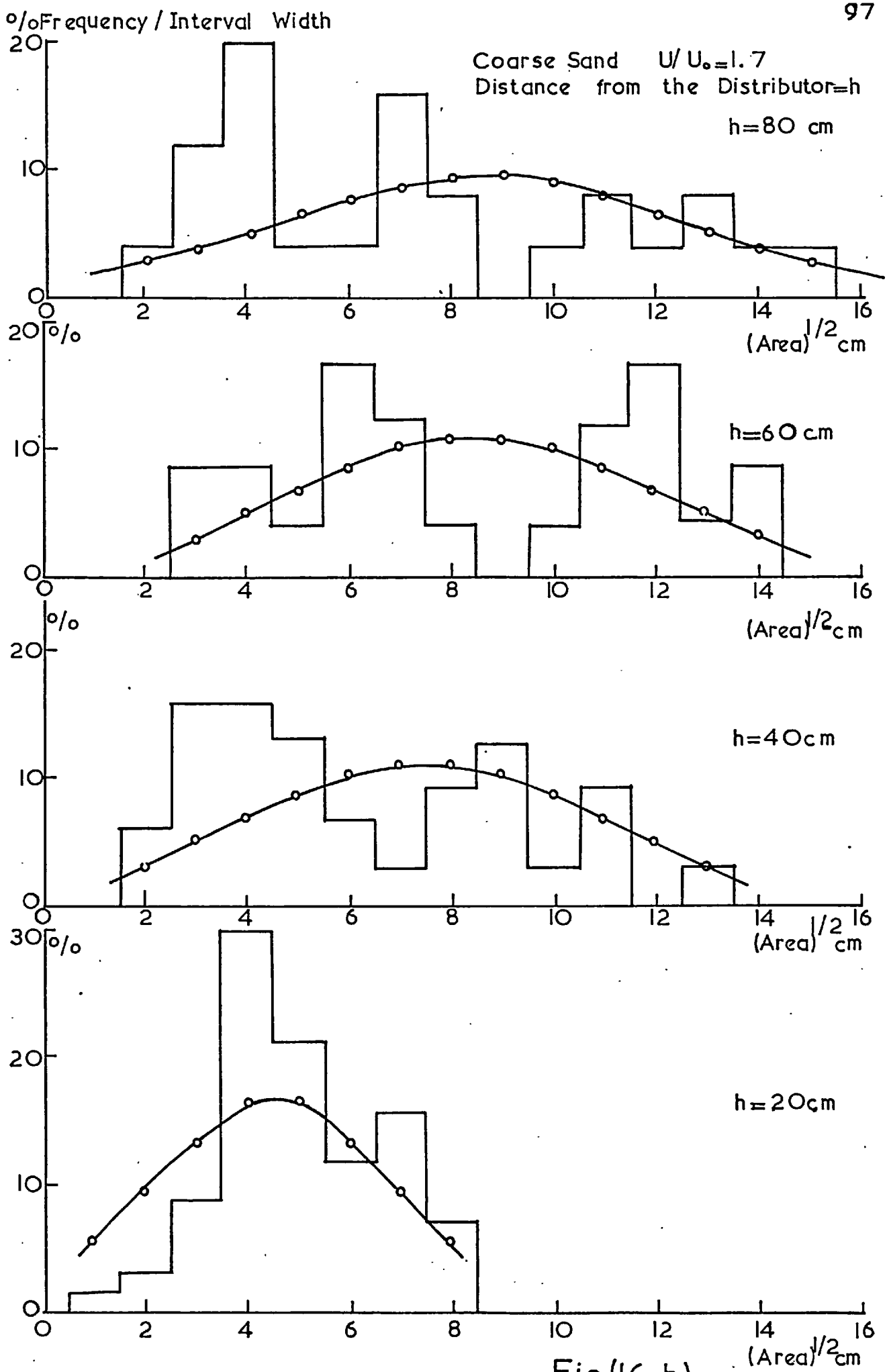
%Frequency / Interval Width
Coarse Sand U/ U₀=1.7
Distance from the Distributor=h
h=80 cm
h=60 cm
h=40cm
h=20cm
(Area)^1/2 cm
0
2
4
6
8
10
12
14
16
20
10
30

Fig.(16-h)

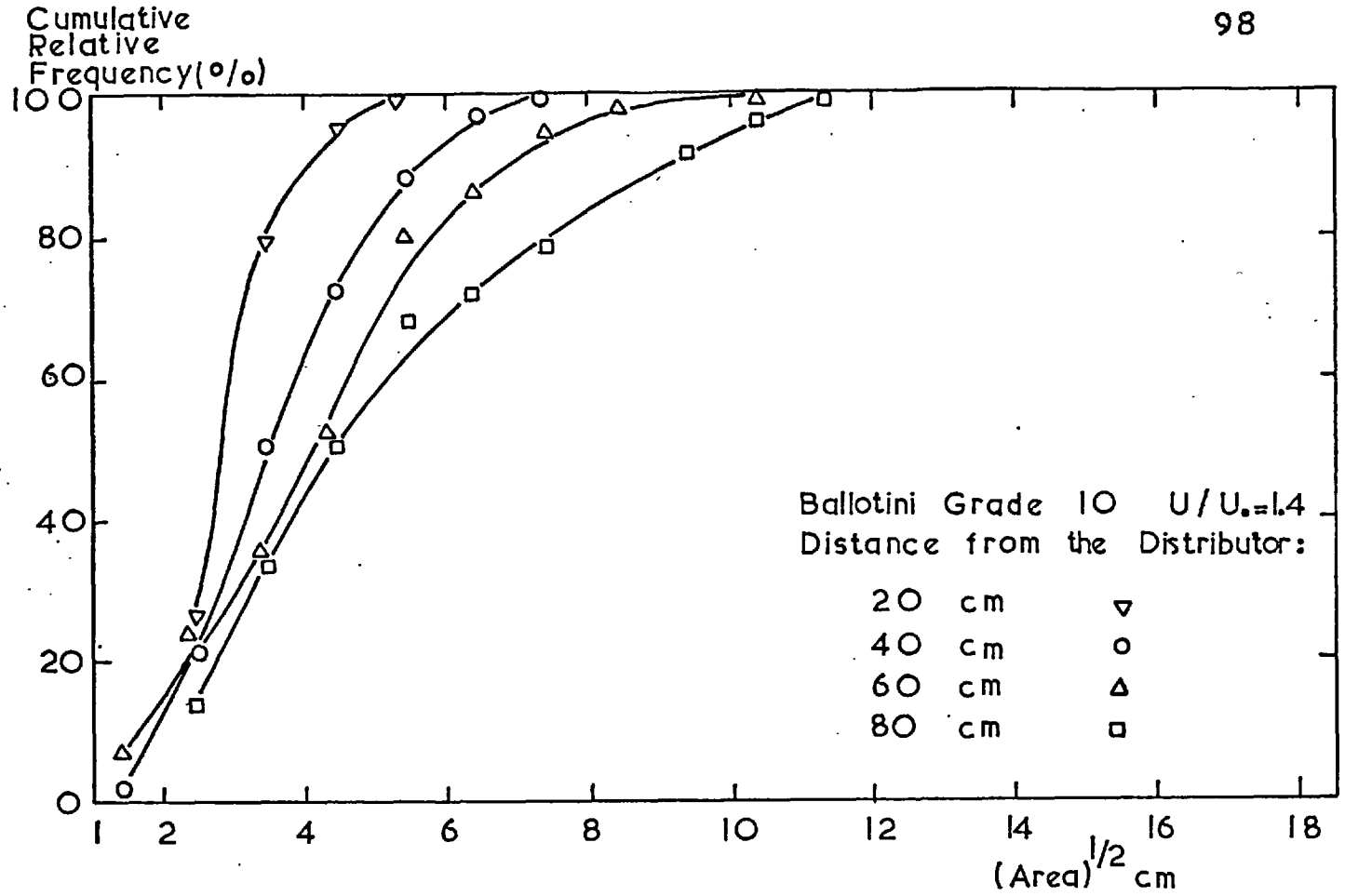

Fig.(17-a)

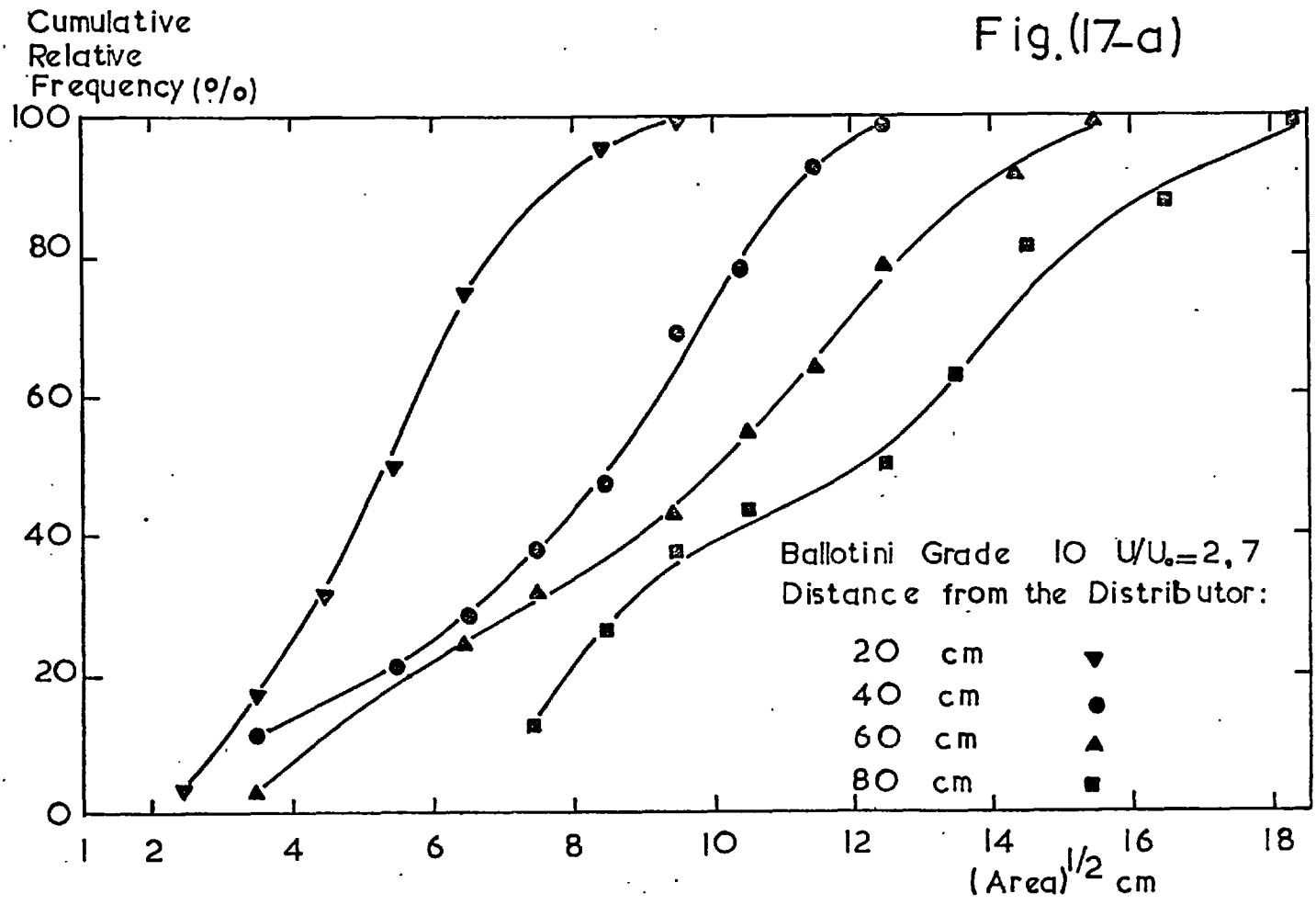

Fig. (17-b)

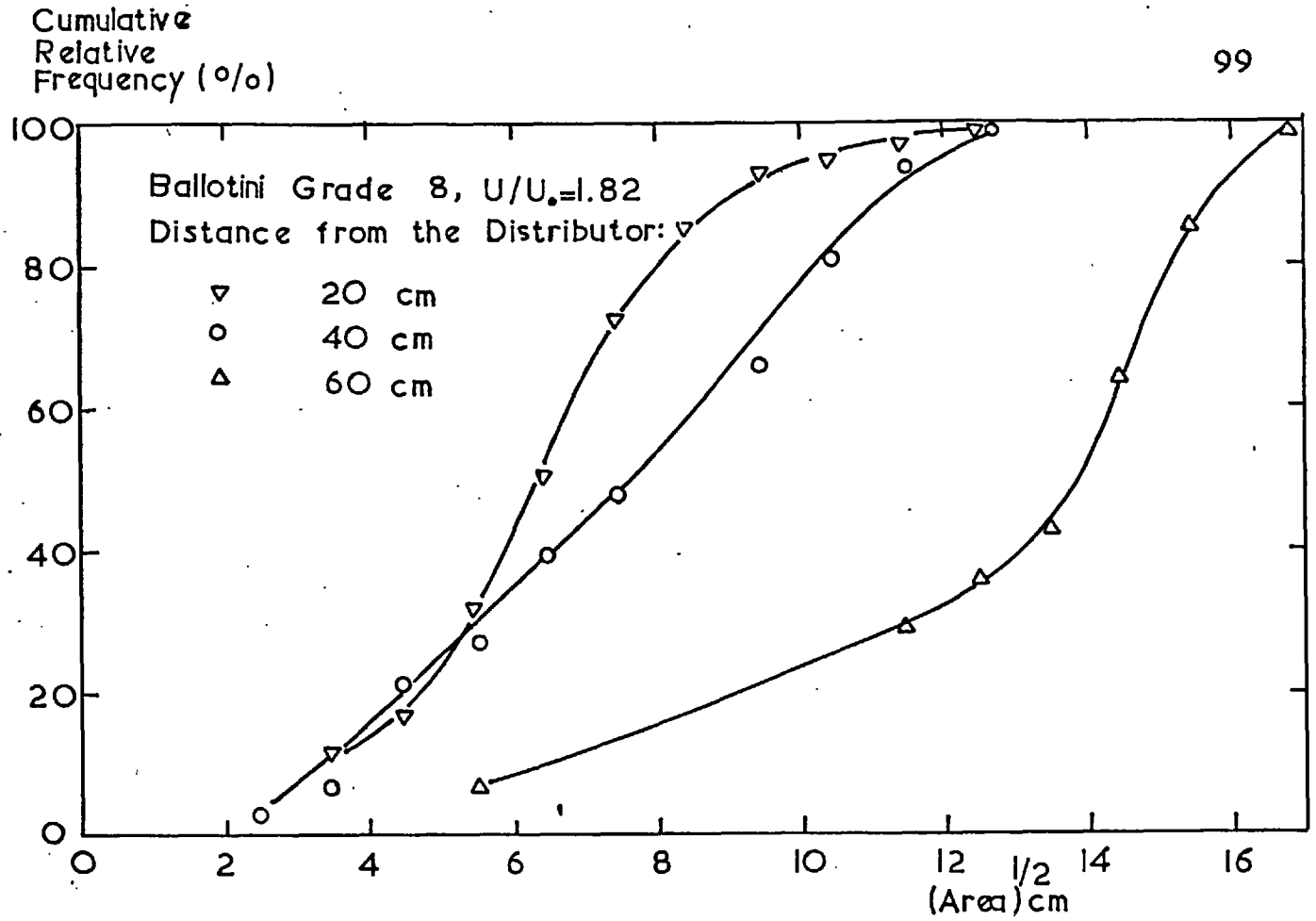

Fig.(17-c)

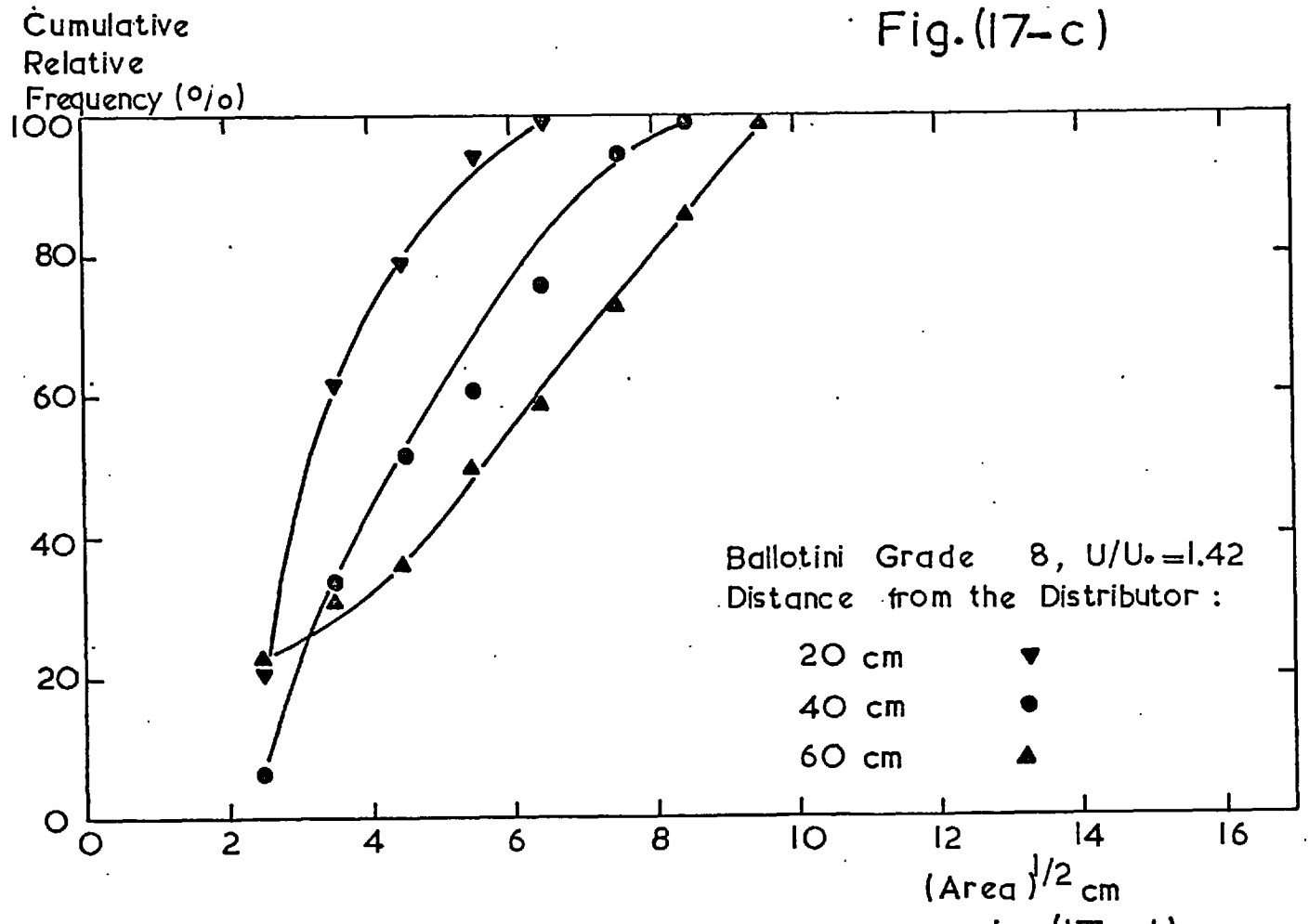

Fig.(17_d)

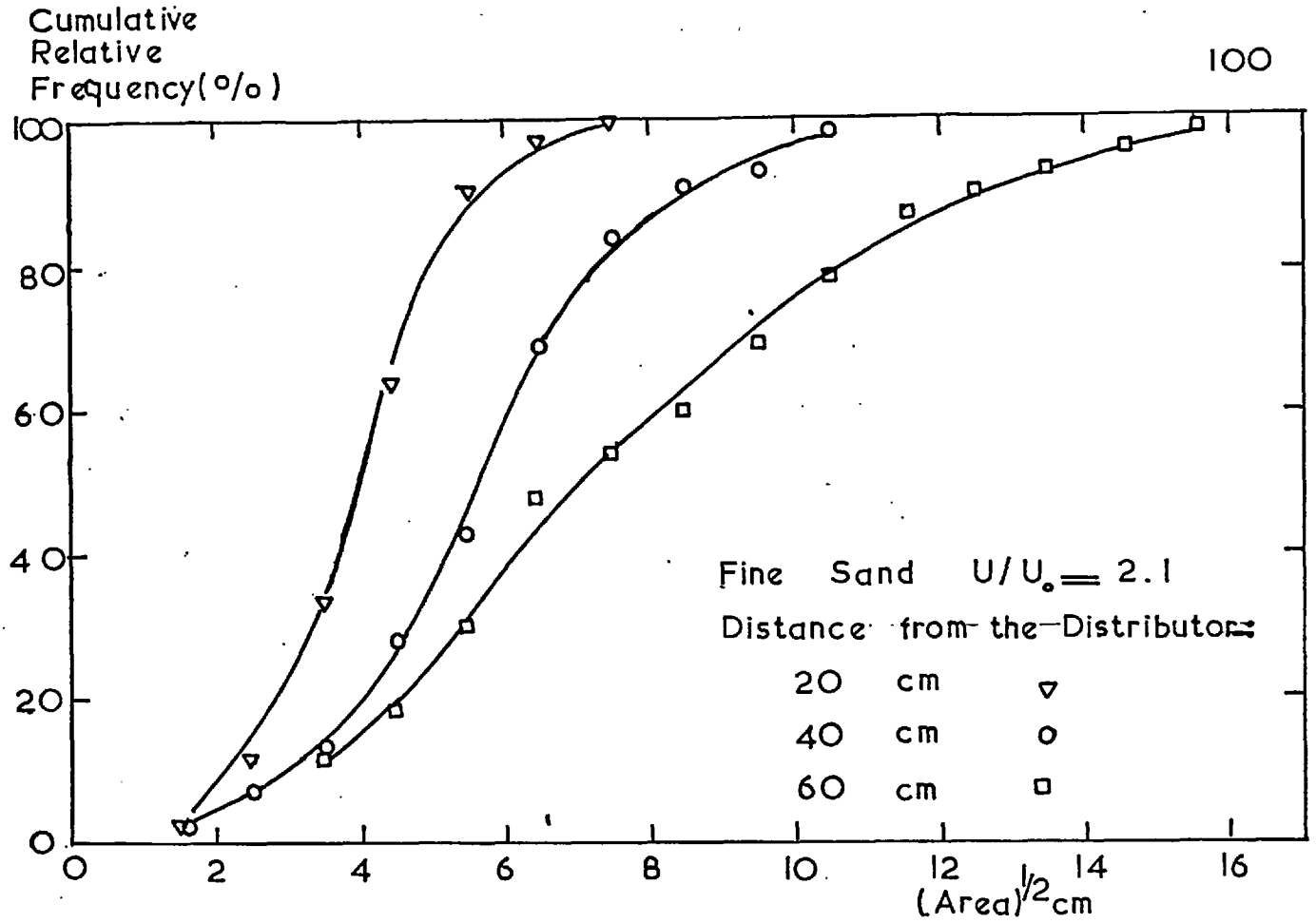

Fig(17-e)

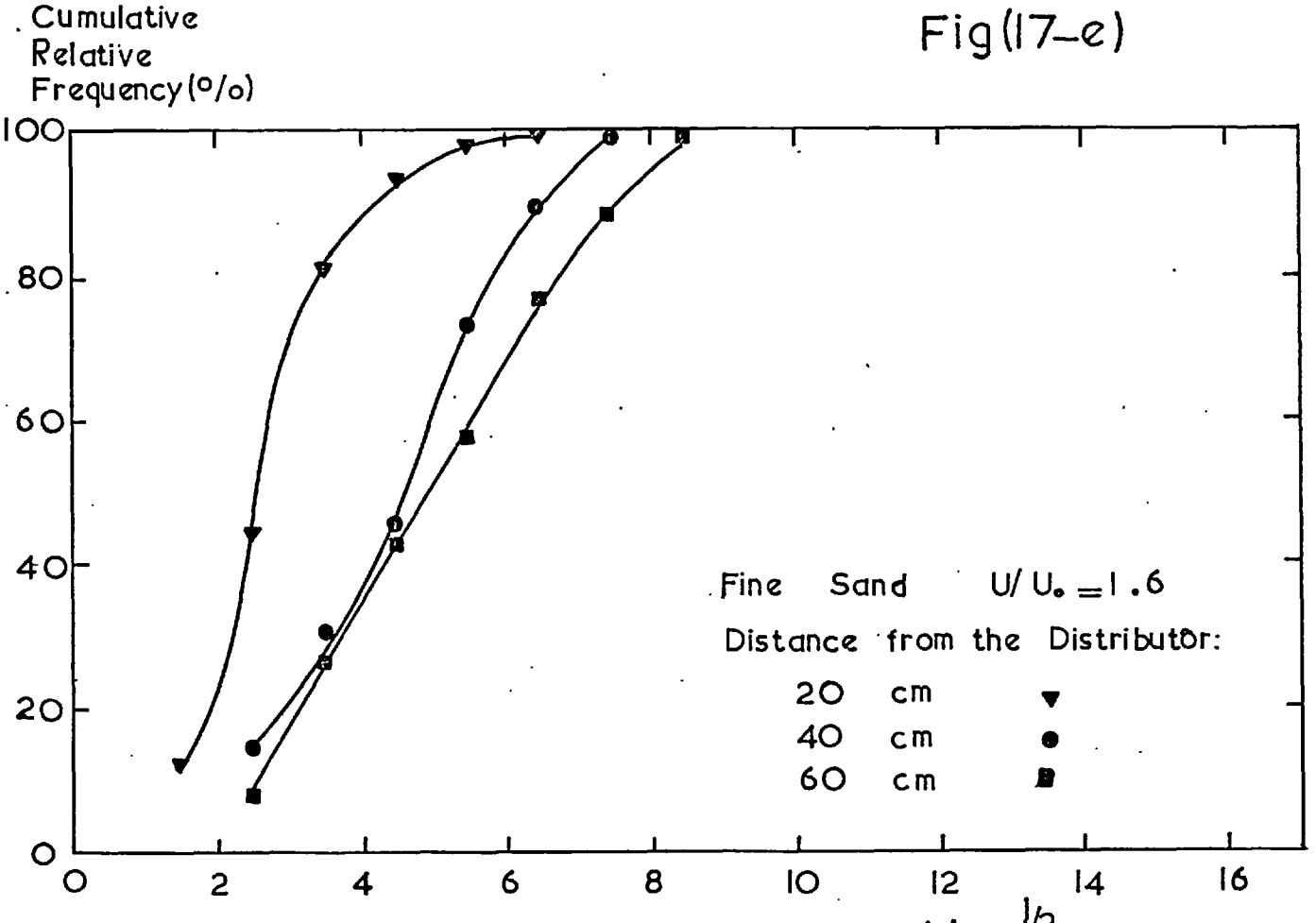

Fig(17-f)

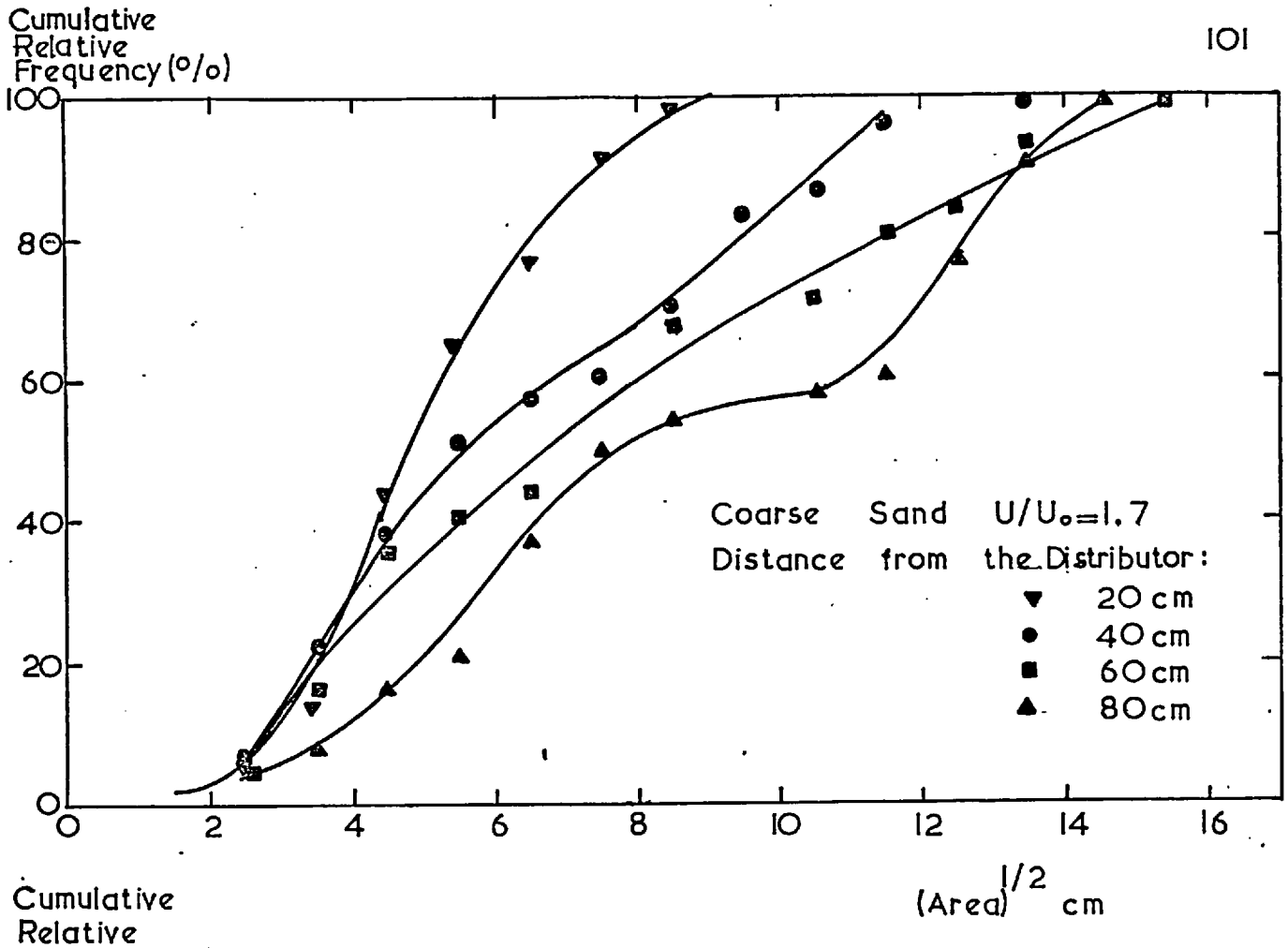

Fig(17_g)

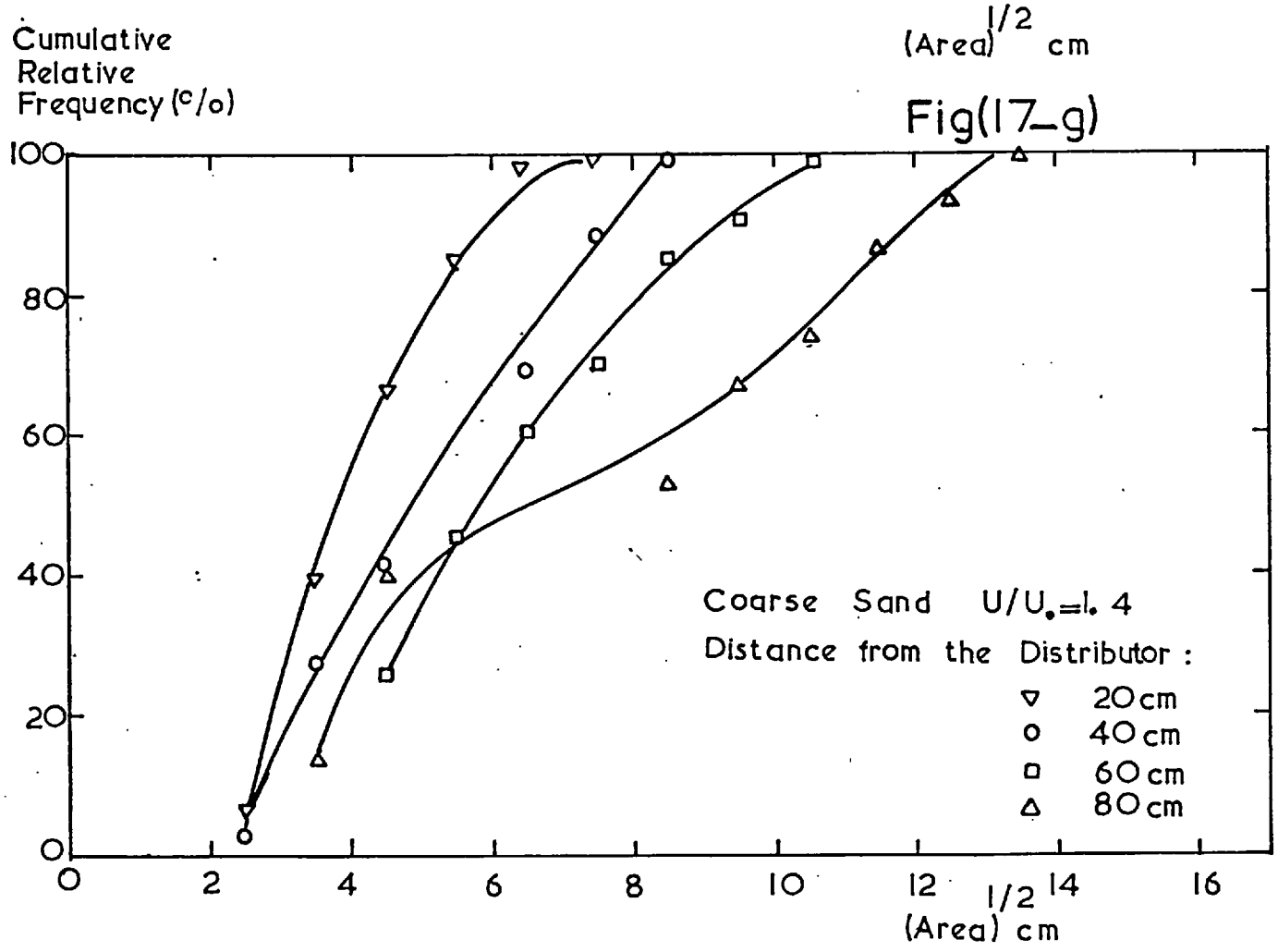

Fig.(17_h)

separately. The corresponding area was determined by comparing the weight with that of a piece of paper, of the same type, and of known area.

The general features of all the graphs are as follows:

(i) At each height there are a relatively large number of medium size bubbles and fewer number of small and large bubbles. As the height is increased the position of the most frequent bubble size is shifted towards the larger bubble sizes.

(ii) At higher heights the relative frequency of the most frequent bubble size is relatively smaller.

(iii) The range of size covered by the histograms is wider for higher levels. This is more pronounced when U/Uo is bigger.

(iv) The mean value of the range covered by the histogram is not necessarily the most frequently occurring size. Some of these features are more easily seen from Fig.(18) where the histograms of different heights are superimposed on each other.

(v) At higher levels a discontinuity in the bubble size distribution is observable.

Point (i) is in general agreement with the available information in the literature. Point (ii) suggests that at higher levels above the distributor the distribution of the bubble size is more uniform. Point (iii) is a consequence of (ii) and together with point (v) suggest that a wide range of size distribution is observed in fluidized beds. In particular the discontinuity in the size distribution could be attributed to bubble-splitting, when a bubble splits into several bubbles and also the presence of spontaneous bubbles.

Point (iv) is clearly noticeable from the present histograms as

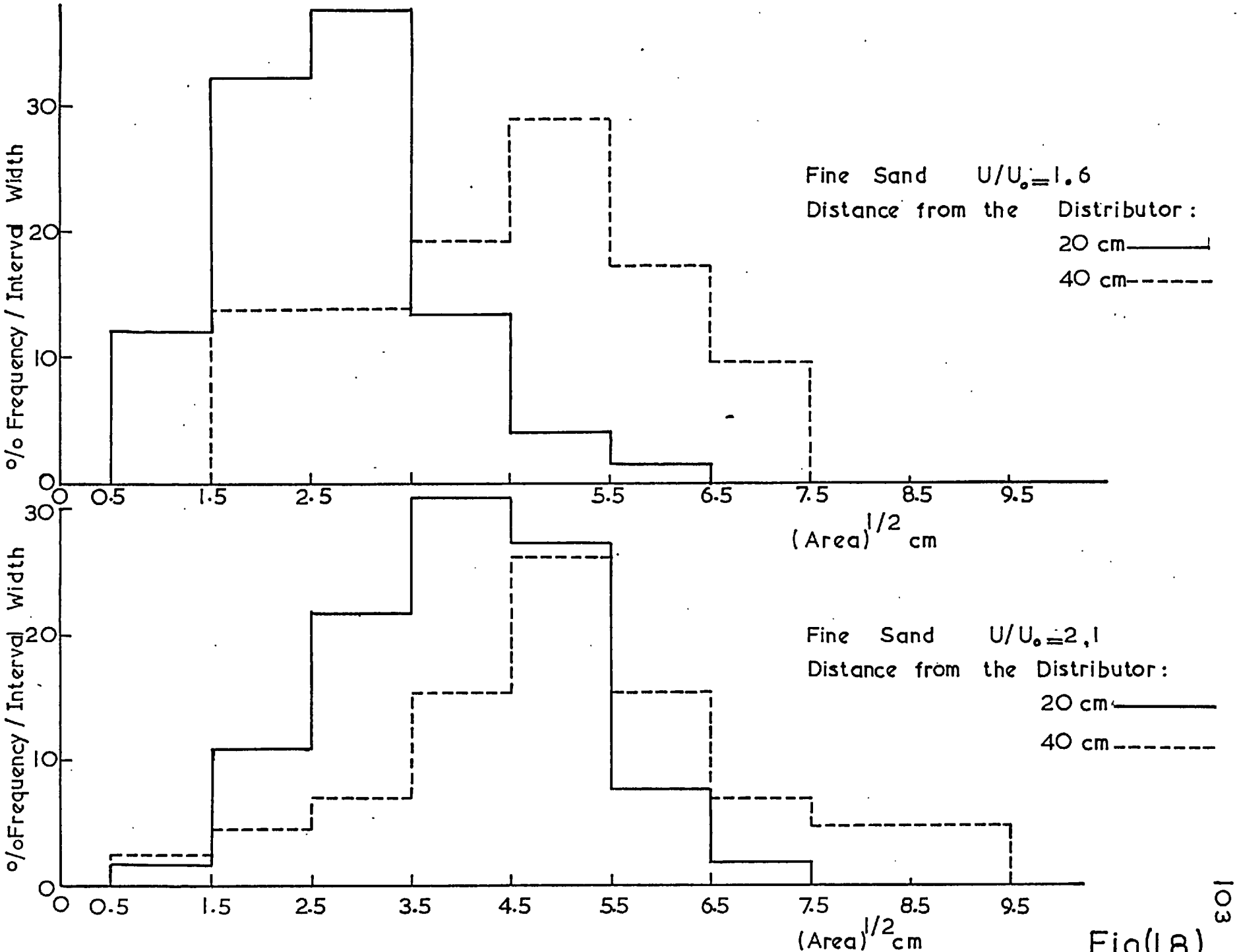
Fine Sand U/U₀=1.6
Distance from the Distributor:
20 cm
40 cm
% Frequency / Interval Width
(Area)^1/2 cm
Fine Sand U/U₀=2.1
Distance from the Distributor:
20 cm
40 cm
% Frequency / Interval Width
(Area)^1/2 cm

Fig.(18)

well as those reported by WHITEHEAD & YOUNG. In an attempt to obtain a more symmetrical distribution instead of $(\text{Area})^{\frac{1}{2}}$ the log $(\text{Area})^{\frac{1}{2}}$ was plotted on the horizontal axis. This did not improve the situation very much for those distributions which were very unsymmetrical. The shape of some of the distributions suggested that the gamma distribution might be a good description of the distribution of bubble size. This was tried for the case of coarse sand at different values of U/Uo. The result is presented in Fig.(19). It was necessary to improve the shape of the distribution by changing the cell interval. This of course is permissible in this case because the vertical axis is graduated in % relative frequency/interval. From the superimposition of the fitted gamma distribution it is seen that at the same distance from the distributor there is more symmetry for the higher value of U/Uo. The equation of the fitted curve is:

$$f(x) = \frac{1}{\alpha!\ \beta^{(\alpha+1)}}\ x^{\alpha}\ e^{-x/\beta}$$

When this function is drawn the effect of the parameter β is on the scale of the axis. For the present case, the magnitude of β was chosen to be 0.7. The magnitude of α was larger for the greater ratio of U/Uo (i.e. $\alpha = 6$ & 4 for $\frac{U}{Uo} = 1.8$ & 1.4 respectively).

From the above treatment it is seen that the mean value of the range of the bubble size is not necessarily the best parameter to characterize the bubble size distribution. Indeed, it depends very much on the type of the distribution. If the data had a Poisson distribution then the mean value was the most likelyhood estimate. Clearly here this is not the case because the Poisson distribution is applicable to discreet data and therefore it cannot be used in this case. As was shown above, the gamma distribution is a good represen-

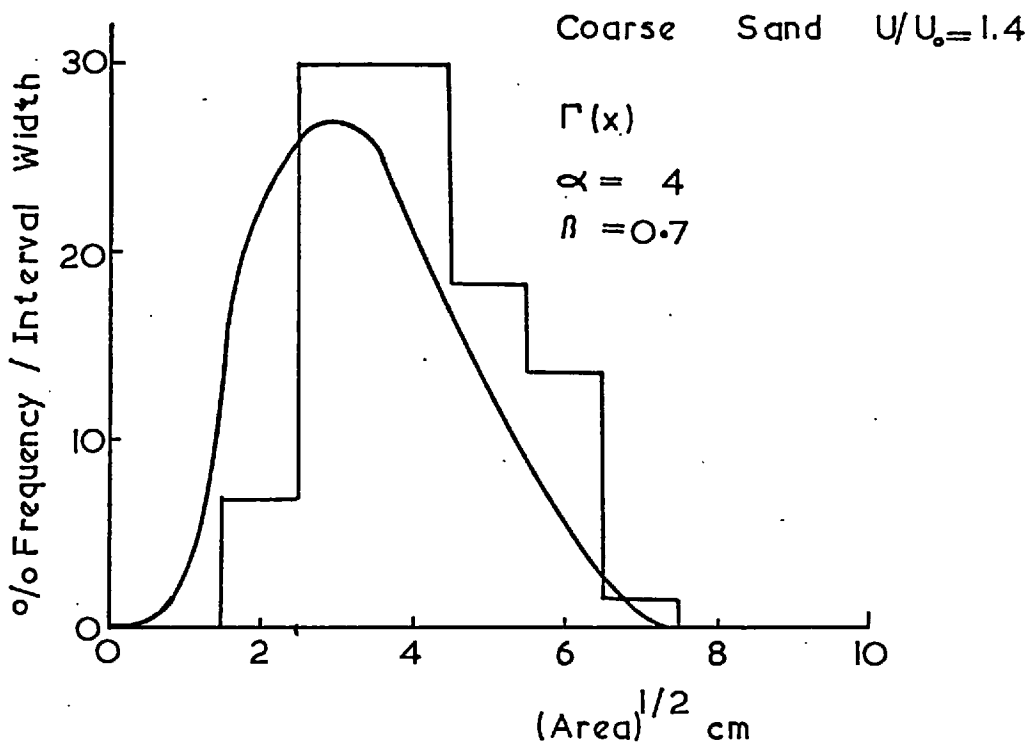
Coarse Sand U/U₀=1.4
Γ(x)
α = 4
ß = 0·7
% Frequency / Interval Width
30
20
10
0
0
2
4
6
8
10
(Area)^1/2 cm

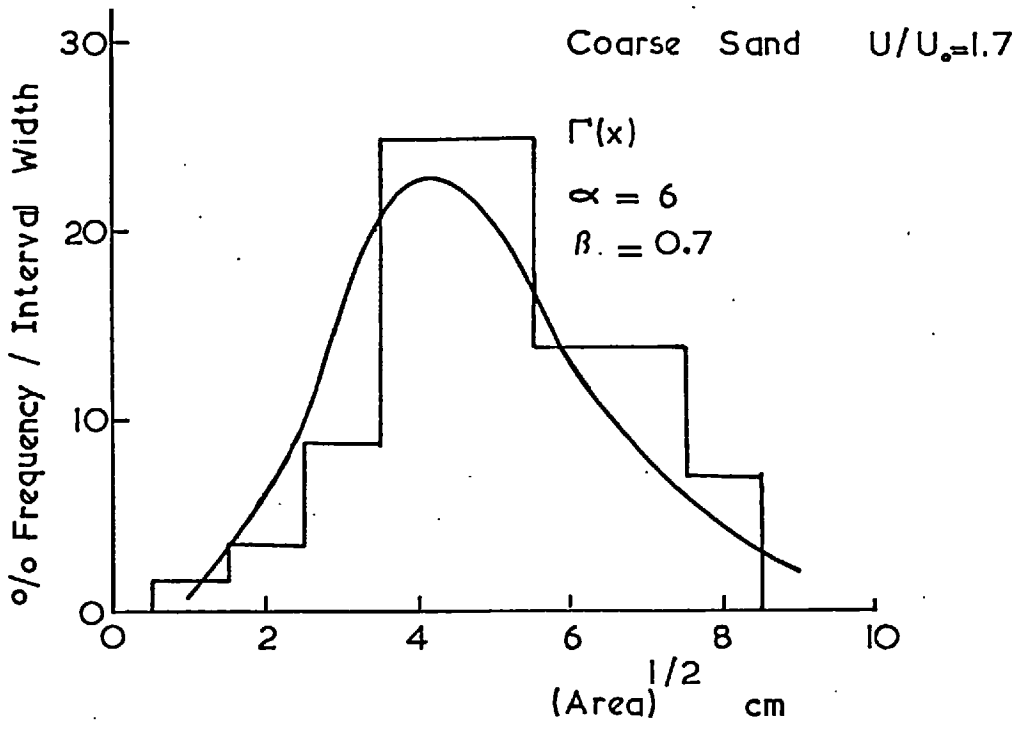
Coarse Sand U/U₀=1.7
Γ(x)
α = 6
ß = 0.7
% Frequency / Interval Width
30
20
10
0
0
2
4
6
8
10
(Area)^1/2 cm

Fig (19)

tative of the bubble size distribution. It can be applied to most of the cases considered here. However, the treatment is tedious and the maximum likelihood estimate is not very easily obtainable. In the light of the fact that the number of observations is not very large it does not seem to be justified to work at such level of refinement because the conclusions would suffer from the smallness of the number of observations anyway. Instead, we try to apply the normal distribution to those cases which could be approximated by this distribution. The advantage of this is that the calculation of the mean and variance are very easy and in particular the interval of $(\mu \mp 1.96\sigma)$ is the 95% of the area under the normal distribution curve.

The normal or Gaussian distribution is given by:

$$f(x) = \frac{1}{\sigma\sqrt{2\pi}} e^{-(x-\mu)^2/2\sigma^2} \qquad \text{Eq.(33)}$$

where μ and σ^2 are the mean and variance of the population respectively. When this function is drawn the effect of the parameter μ is such that a change in its value shifts the curve to left or right. The effect of σ is such that a change in its value changes the flatness or sharpness of the curve.

The values of μ and σ^2 are obtained from Eq.(34 a,b) as follows:

$$\mu = \frac{\sum_{i=1}^{n} Xi}{n} \qquad \text{Eq.(34a)}$$

$$\sigma^2 = \frac{1}{n-1} \sum_{i=1}^{n} X_i^2 - \frac{(\sum X_i)^2}{n} \qquad \text{Eq.(34b)}$$

It is possible to have many normal distributions with the same value of μ and different variances. It is clearly seen that the parameter μ alone does not describe completely the shape and properties of a

distribution, and it is of primary importance to know the magnitude of the variance when we are dealing with normally distributed populations.

Before applying the above expressions to calculate the values of σ and μ for the bubble size distribution we have to make sure that the population is normally, or approximately normally, distributed. One of the simplest ways of getting a rough check is to plot the data on probability paper. If such a plot seems to be fairly close to a straight line, it is reasonable to assume that we have approximately a normal distribution. In Fig.(20) a plot of a random sample of size 50 drawn from an artificially constructed normal population with mean zero and deviation one is given (23). This graph gives an idea of how a normal sample should look.

In Figs.(21a-e) we have plotted (on normal probability-linear graph paper) percentages of the relative cumulative frequency of the bubble size distribution as a function of (bubble area)$^{\frac{1}{2}}$ for most of the present data. By comparison with Fig.(20) it is clearly seen that the distributions presented could be well approximated by a normal distribution. For the [illegible] data which did not give a fairly straight line, Fig.(22), a plot on normal probability-logarithm graph paper was tried. This produced a better approximation to normality. Fig.(22). In the light of the evidence presented above it was concluded that a normal distribution would be a good representation for the bubble size distribution.

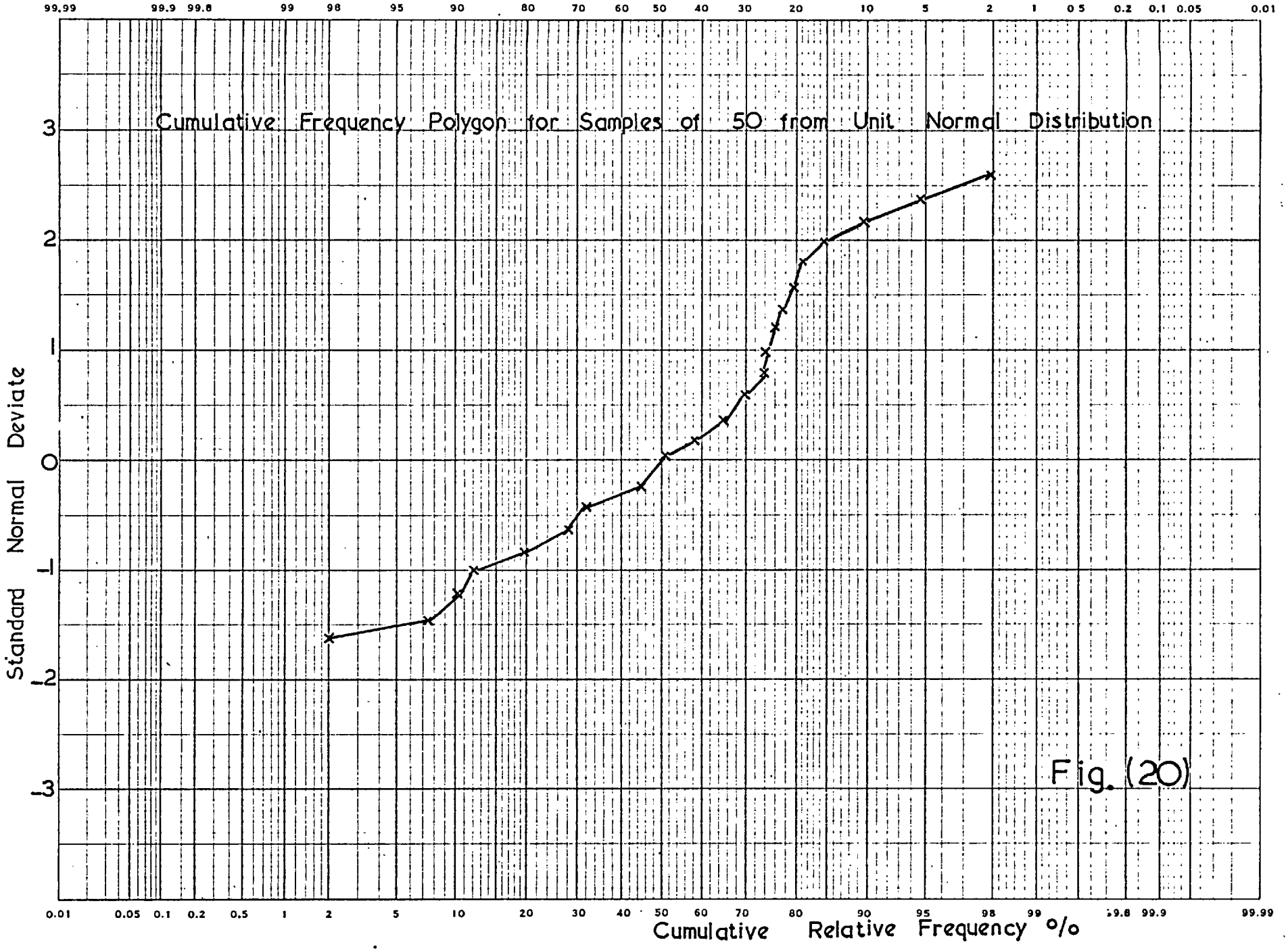
Cumulative Frequency Polygon for Samples of 50 from Unit Normal Distribution
Standard Normal Deviate
3
2
1
0
-1
-2
-3
99.99 99.9 99.8 99 98 95 90 80 70 60 50 40 30 20 10 5 2 1 0.5 0.2 0.1 0.05 0.01
0.01 0.05 0.1 0.2 0.5 1 2 5 10 20 30 40 50 60 70 80 90 95 98 99 99.8 99.9 99.99
Cumulative Relative Frequency %

Fig. (20)

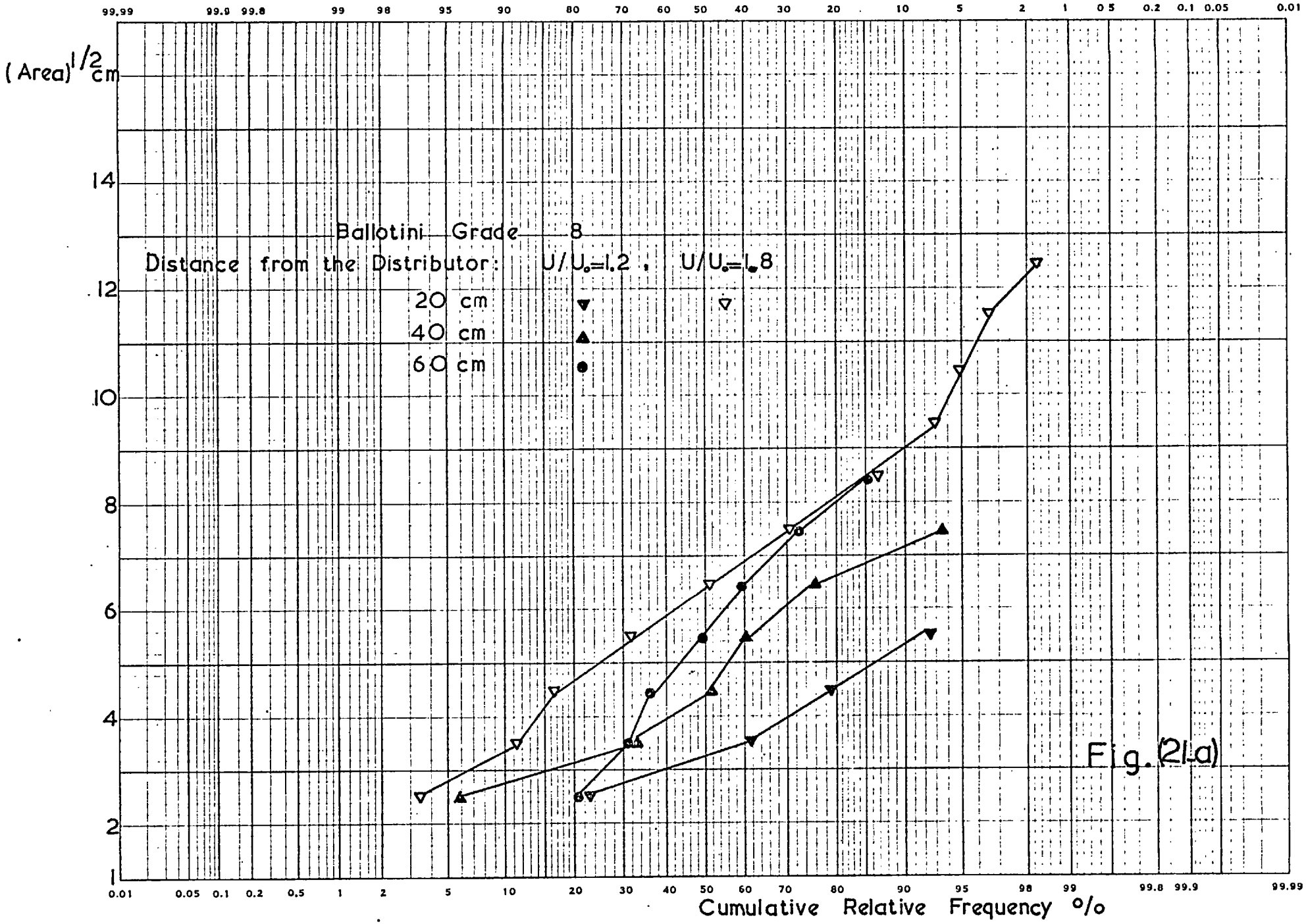
(Area)^1/2 cm
Ballotini Grade 8
Distance from the Distributor: U/U₀=1.2 , U/U₀=1.8
20 cm
40 cm
60 cm
Cumulative Relative Frequency %

Fig. (21-a)

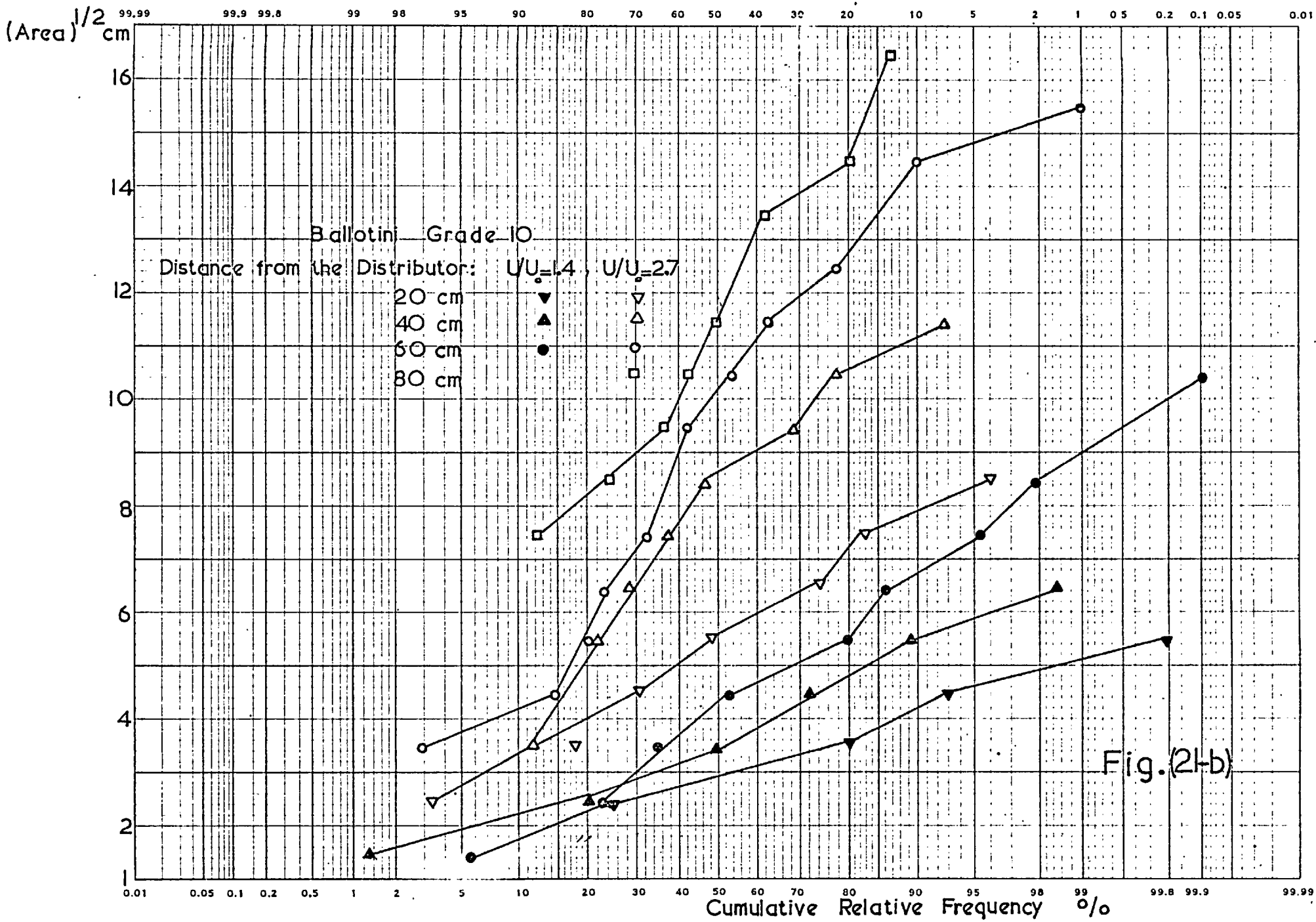
(Area)^1/2 cm
Ballotini Grade 10
Distance from the Distributor: U/U₀=1.4 , U/U₀=2.7
20 cm
40 cm
60 cm
80 cm
Cumulative Relative Frequency %

Fig. (2-b)

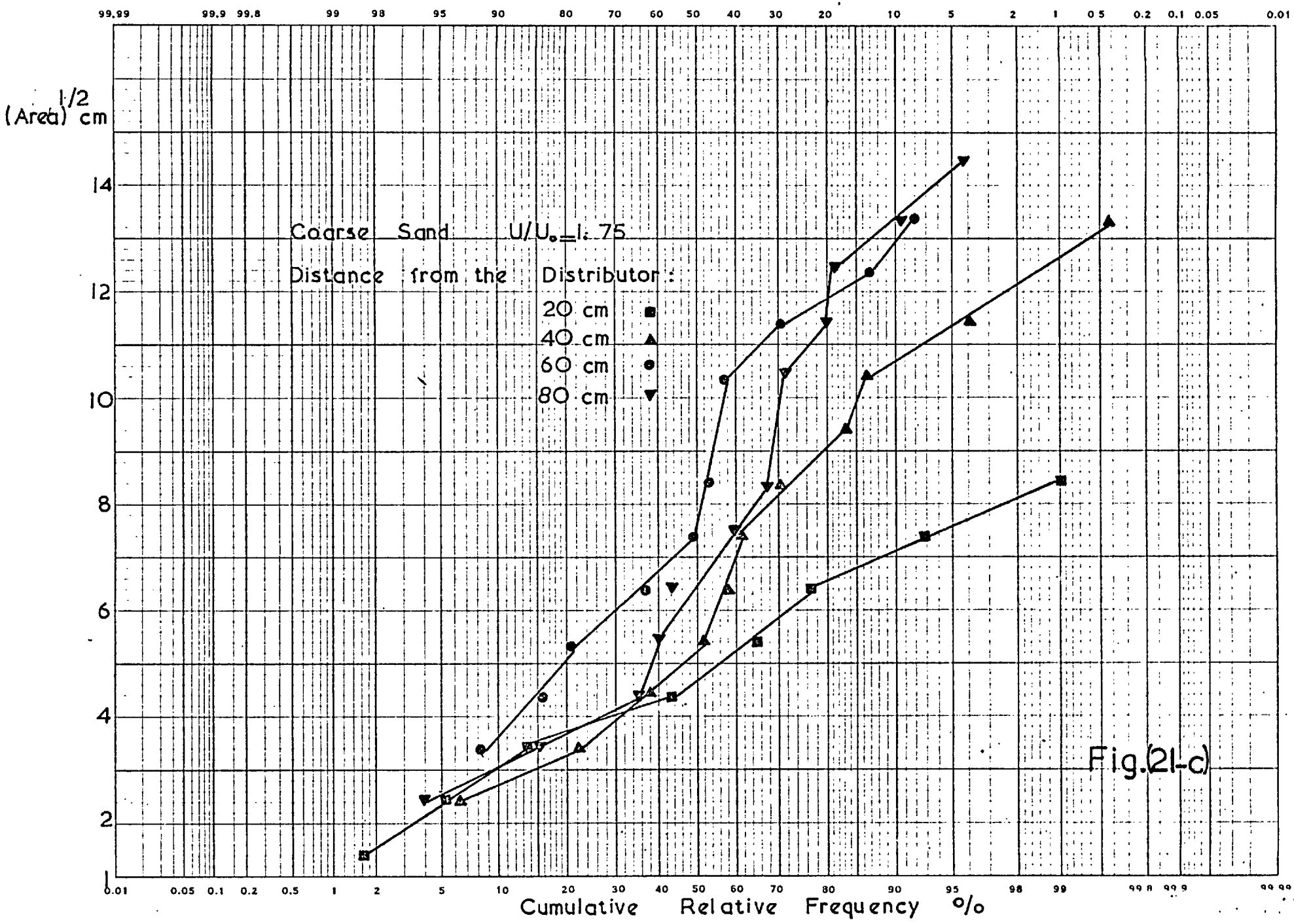
(Area)^1/2 cm
Coarse Sand U/U₀=1.75
Distance from the Distributor :
20 cm
40 cm
60 cm
80 cm
Cumulative Relative Frequency %
99.99 99.9 99.8 99 98 95 90 80 70 60 50 40 30 20 10 5 2 1 0.5 0.2 0.1 0.05 0.01
0.01 0.05 0.1 0.2 0.5 1 2 5 10 20 30 40 50 60 70 80 90 95 98 99 99.8 99.9 99.99
1 2 4 6 8 10 12 14

Fig.(21-c)

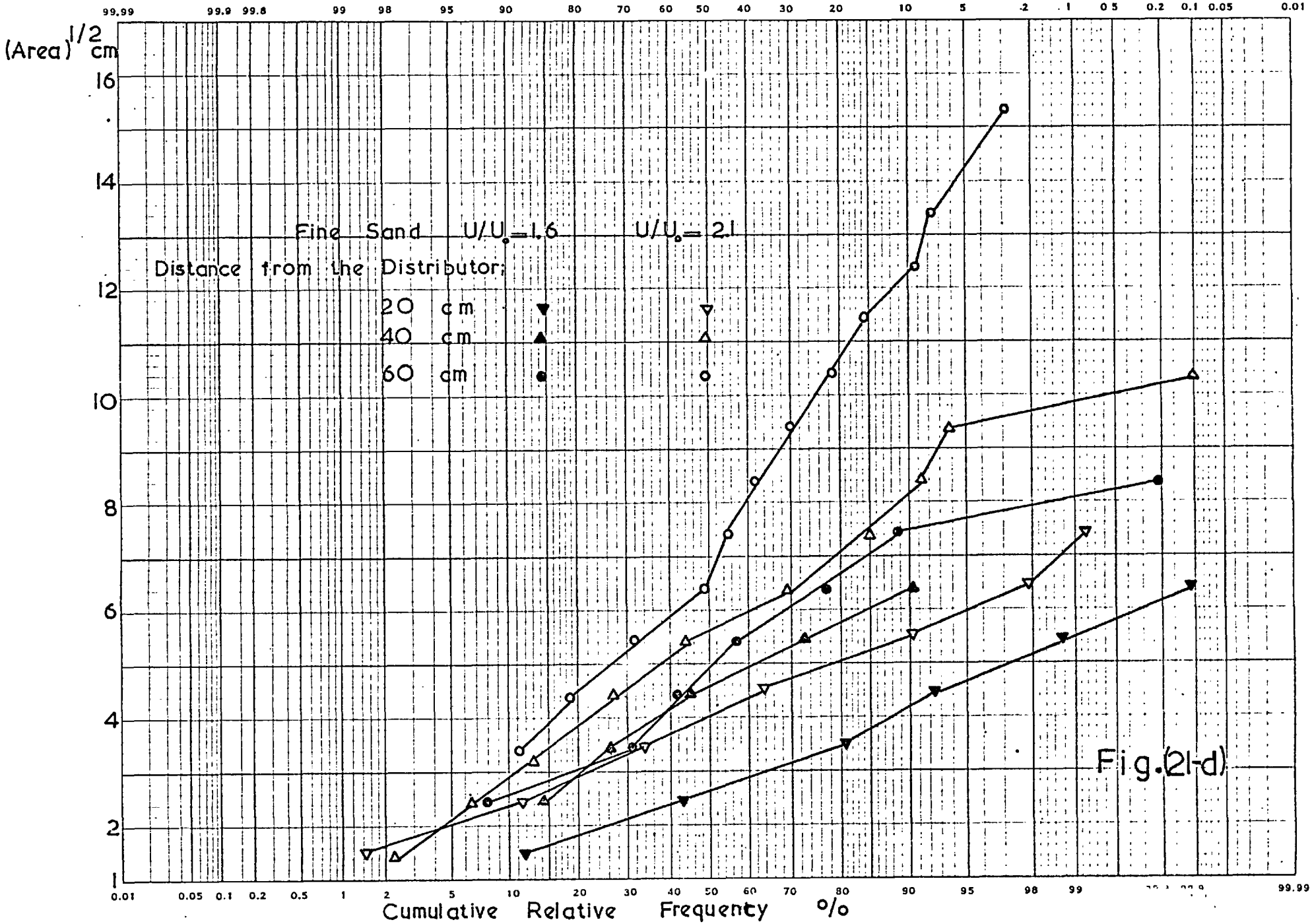
(Area)^1/2 cm
Fine Sand U/U₀=1.6 U/U₀=2.1
Distance from the Distributor;
20 cm
40 cm
60 cm
Cumulative Relative Frequency %

Fig.(21-d)

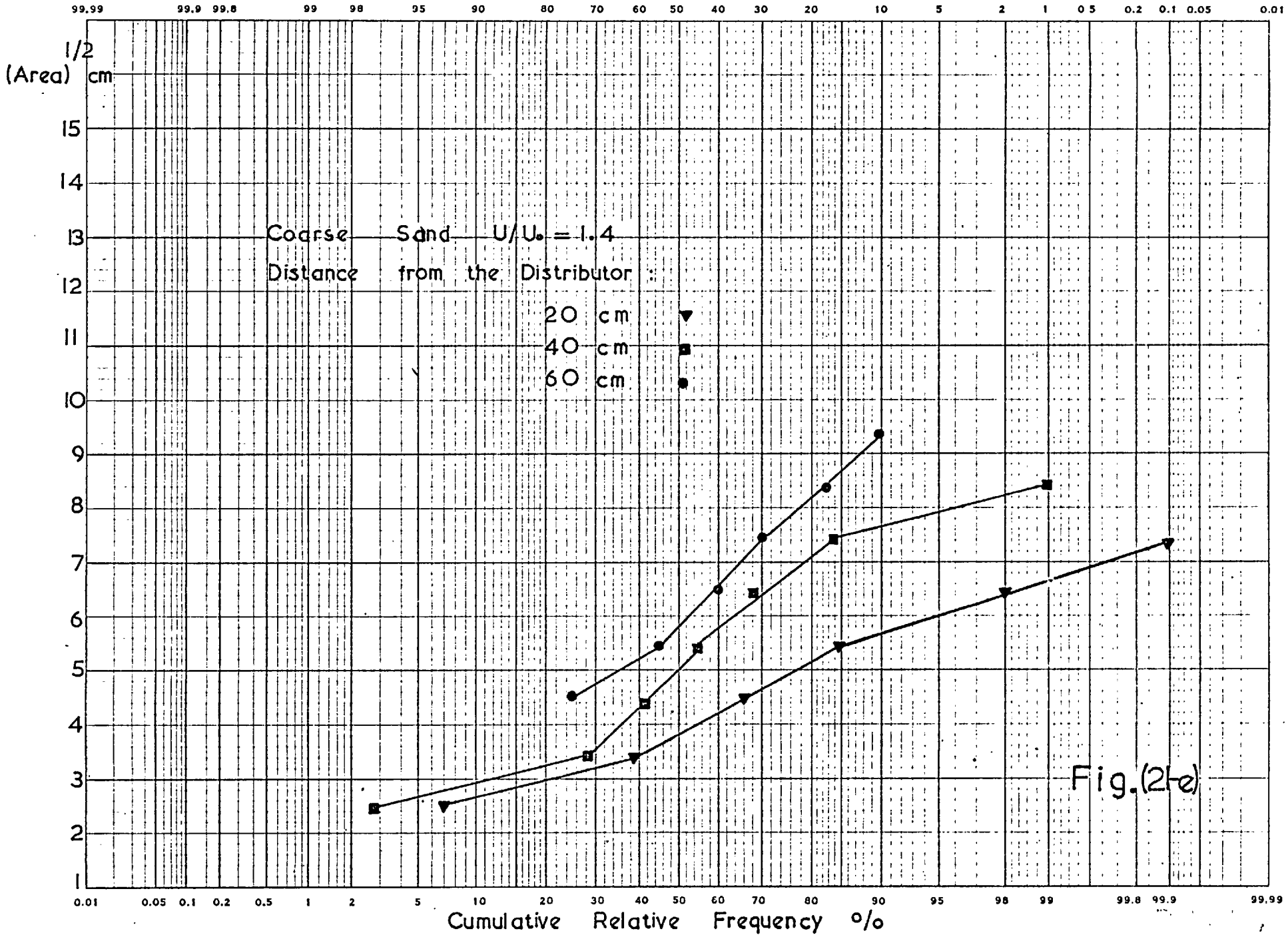
Coarse Sand U/Uo = 1.4
Distance from the Distributor :
20 cm
40 cm
60 cm
(Area)^1/2 cm
Cumulative Relative Frequency %
99.99 99.9 99.8 99 98 95 90 80 70 60 50 40 30 20 10 5 2 1 0.5 0.2 0.1 0.05 0.01
0.01 0.05 0.1 0.2 0.5 1 2 5 10 20 30 40 50 60 70 80 90 95 98 99 99.8 99.9 99.99
1 2 3 4 5 6 7 8 9 10 11 12 13 14 15

Fig.(2-e)

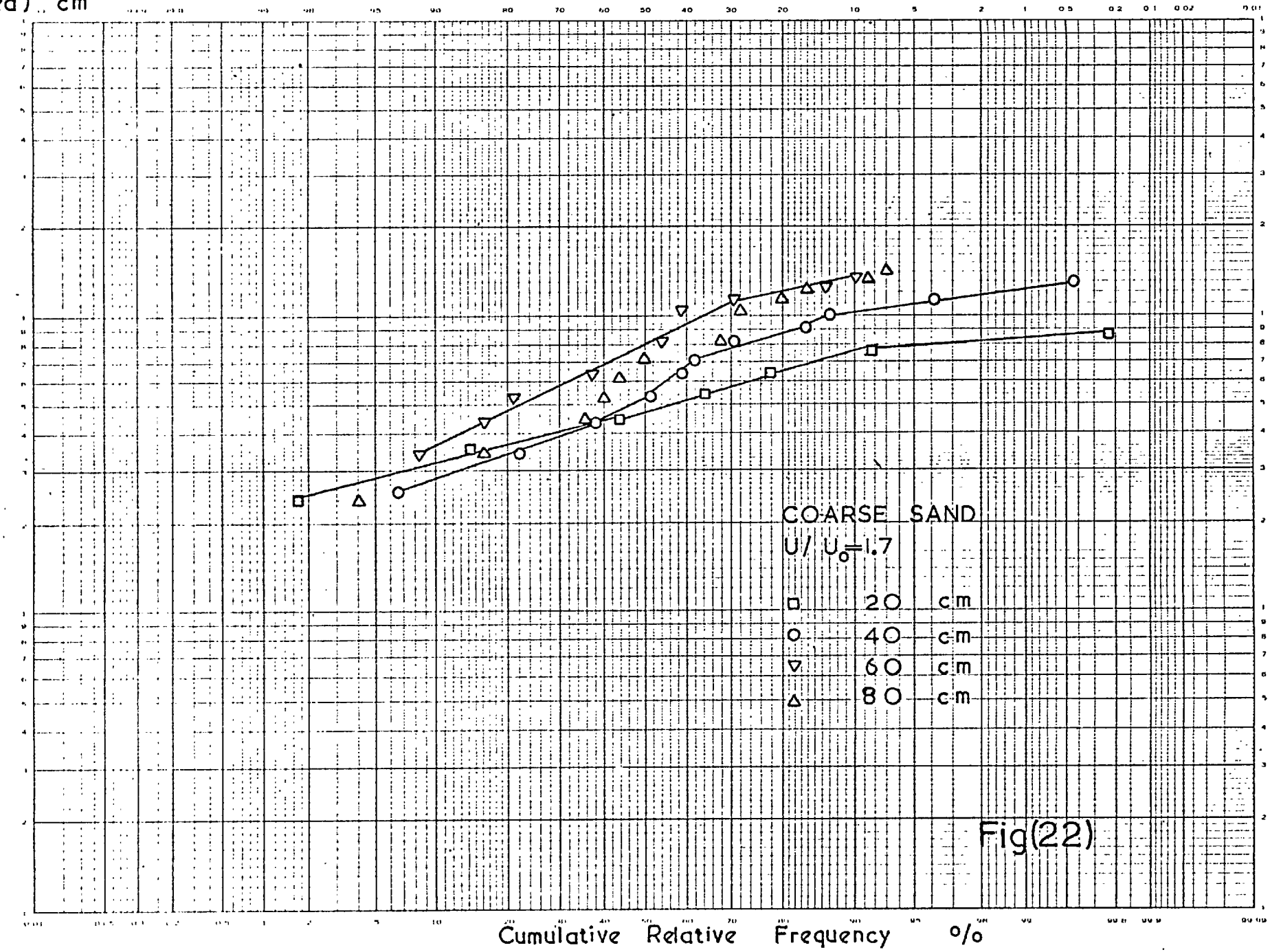
(Area)$^{1/2}$ cm
COARSE SAND
U/ U_o=1.7
□ 20 cm
○ 40 cm
▽ 60 cm
△ 80 cm
Cumulative Relative Frequency %

Fig(22)

TABLE (4)

Cell Boundary cm	B A L L O T I N I Grade 8								
	U/Uo = 1.2 , No. of Frames Analysed = 51								
	h* = 20 cm			h = 20 cm			h = 20 cm		
	N*	R.F.*	C.R.F.*	N	R.F.	C.R.F.	N	R.F.	C.R.F.
0.5 - 1.5	-								
1.5 - 2.5	13	22.8	22.8	2	6.0	6.0	5	22.8	22.8
2.5 - 3.5	22	38.8	61.6	9	27.3	33.3	2	9.2	32.0
3.5 - 4.5	10	17.4	79.0	6	18.2	51.5	1	4.5	36.5
4.5 - 5.5	9	15.8	94.8	3	9.1	60.6	3	13.6	50.1
5.5 - 6.5	3	5.2	100.0	5	15.2	75.8	2	9.1	59.2
6.5 - 7.5				6	18.2	94.0	3	13.6	72.8
7.5 - 8.5				2	6.0	100.0	3	13.6	86.4
8.5 - 9.5							3	13.6	100.0
TOTAL	57	100		33	100		22	100	

* N = Number of bubbles

R.F. = Relative frequency

C.R.F. = Cumulative relative frequency

h = Height above the distributor

TABLE (4) cont'd

Cell Boundary cm	B A L L O T I N I Grade 8								
	U/Uo = 1.8 , No. of Frames Analysed = 70								
	h = 20 cm			h = 40 cm			h = 60 cm		
	N	R.F.	C.R.F.	N	R.F.	C.R.F.	N	R.F.	C.R.F.
0.5 - 1.5									
1.5 - 2.5	2	3.3	3.3	1	3.0	3.0			
2.5 - 3.5	5	8.2	11.5	1	3.0	6.0			
3.5 - 4.5	3	4.9	16.4	5	15.2	21.2			
4.5 - 5.5	9	14.7	31.1	2	6.15	27.35	1	7.1	7.1
5.5 - 6.5	12	19.7	50.8	4	12.0	39.35			
6.5 - 7.5	13	21.3	72.1	3	9.1	48.45			
7.5 - 8.5	8	13.1	85.2	1	3.0	51.45			
8.5 - 9.5	5	8.2	93.4	5	15.2	66.65			
9.5 -10.5	1	1.6	95.0	5	15.2	81.85			
10.5 -11.5	1	1.7	96.7	4	12.0	93.85	3	21.4	28.5
11.5 -12.5	1	1.6	98.3	2	6.15	100.0	1	7.1	35.6
12.5 -13.5	1	1.7	100.0				1	7.1	42.7
13.5 -14.5							3	21.4	64.1
14.5 -15.5							3	21.4	85.5
15.5 -16.5							0		85.5
16.5 -17.5							0		85.5
17.5 -18.5							2	14.5	100.0
TOTAL	61	100		33	100		14	100	

TABLE (4) cont'd

Cell Boundary cm	B A L L O T I N I Grade 10											
	U/Uo = 1.4 , No. of Frames = 70											
	h = 20 cm			h = 40 cm			h = 60 cm			h = 80 cm		
	N	R.F.	C.R.F.	N	R.F.	C.R.F.	N	R.F.	C.R.F.	N	R.F.	C.R.F.
0.5 - 1.5				1	1.5	1.5	3	5.9	5.9			
1.5 - 2.5	25	26	26	13	19.7	21.2	9	17.6	23.5	4	13.8	13.8
2.5 - 3.5	52	54	80	19	28.8	50.0	6	11.7	35.2	6	20.7	34.5
3.5 - 4.5	16	16.7	96.7	15	22.7	72.7	9	17.6	52.8	5	17.2	51.7
4.5 - 5.5	3	3.3	100.0	11	16.7	89.4	14	27.5	80.3	5	17.2	68.9
5.5 - 6.5				6	9.1	98.5	3	5.9	86.2	1	3.5	72.4
6.5 - 7.5				1	1.5	100.0	5	9.8	96.0	2	6.8	79.2
7.5 - 8.5							1	2.0	98.0	1	3.5	82.7
8.5 - 9.5							0	0	98.0	3	10.3	93.0
9.5 -10.5							1	2.0	100.0	1	3.5	96.5
10.5 -11.5										1	3.5	100.0
TOTAL	96	100		66	100		51	100		29	100	

TABLE (4) cont'd

Cell Boundary cm	B A L L O T I N I Grade 10											
	U/Uo = 2.7 , No. of Frames = 70											
	h = 20 cm			h = 40 cm			h = 60 cm			h = 80 cm		
	N	R.F.	C.R.F.	N	R.F.	C.R.F.	N	R.F.	C.R.F.	N	R.F.	C.R.F.
0.5 - 1.5												
1.5 - 2.5	3	3.4	3.4									
2.5 - 3.5	13	14.6	18.0	5	11.9	11.9	1	3.0	3.0			
3.5 - 4.5	12	13.5	31.5	0	0	11.9	4	12.1	15.1			
4.5 - 5.5	16	18.0	49.5	4	9.5	21.4	2	6.1	21.2			
5.5 - 6.5	23	25.8	75.3	3	7.1	28.5	1	3.0	24.2			
6.5 - 7.5	10	11.2	86.5	4	9.6	38.1	3	9.1	33.3	2	12.5	12.5
7.5 - 8.5	9	10.1	96.6	4	9.6	47.7	0	0	33.3	2	12.5	25.0
8.5 - 9.5	3	3.4	100.0	9	21.3	69.0	3	9.1	42.4	2	12.5	37.5
9.5 -10.5				4	9.6	78.6	4	12.1	54.5	1	6.2	43.7
10.5 -11.5				6	14.3	92.9	3	9.1	63.6	0	0	43.7
11.5 -12.5				3	7.1	100.0	5	15.2	78.8	1	6.3	50.0
12.5 -13.5							0	0	78.8	2	12.5	62.5
13.5 -14.5							4	12.1	90.9	3	18.7	81.2
14.5 -15.5							3	9.1	100.0	0	0	81.2
15.5 -16.5										1	6.3	87.5
16.5 -17.5										0	0	87.5
17.5 -18.5										2	12.5	100.0
TOTAL	89	100		42	100		33	100		16	100	

TABLE (4) cont'd

Cell Boundary cm	FINE SAND								
	U/Uo = 1.6 , No. of Frames Analysed = 51								
	h = 20 cm			h = 20 cm			h = 20 cm		
	N	R.F.	C.R.F.	N	R.F.	C.R.F.	N	R.F.	C.R.F.
0.5 - 1.5	9	12	12						
1.5 - 2.5	24	32.0	44	6	14.3	14.3	2	7.7	7.7
2.5 - 3.5	28	37.4	81.4	5	11.9	26.2	6	23	30.7
3.5 - 4.5	10	13.3	94.7	8	19.0	45.2	3	11.5	42.2
4.5 - 5.5	3	4.0	98.7	12	28.6	73.8	4	15.4	57.6
5.5 - 6.5	1	1.3	100.0	7	16.7	90.5	5	19.4	77.0
6.5 - 7.5				4	9.5	100.0	3	11.5	88.5
7.5 - 8.5							3	11.5	100.0
TOTAL	75	100		42	100		26	100	

TABLE (4) cont'd

Cell Boundary cm	FINE SAND								
	U/Uo = 2.1 , No. Frames Analysed = 69								
	h = 20 cm			h = 40 cm			h = 60 cm		
	N	R.F.	C.R.F.	N	R.F.	C.R.F.	N	R.F.	C.R.F.
0.5 - 1.5	1	1.5	1.5	1	2.2	2.2			
1.5 - 2.5	9	10.5	12.0	2	4.3	6.5			
2.5 - 3.5	19	21.6	33.6	3	6.5	13.0	4	12.1	12.1
3.5 - 4.5	27	30.6	64.2	7	15.2	28.2	2	6.1	18.2
4.5 - 5.5	24	27.4	91.6	7	15.2	43.4	4	12.1	30.3
5.5 - 6.5	7	7.9	99.5	12	26.2	69.6	6	18.2	48.5
6.5 - 7.5	1	1.5	100.0	7	15.2	84.8	2	6.1	54.6
7.5 - 8.5				3	6.5	91.3	2	6.1	60.7
8.5 - 9.5				1	2.2	93.5	3	9.1	69.8
9.5 -10.5				3	6.5	100.0	3	9.1	78.9
10.5 -11.5							3	9.1	88.0
11.5 -12.5							1	3	91.0
12.5 -13.5							1	3	94.0
13.5 -14.5							0	0	94.0
14.5 -15.5							1	3	97.0
15.5 -16.5							1	3	100.0
TOTAL	88	100		46	100		33	100	

TABLE (4) cont'd

Cell Boundary cm	COARSE SAND											
	U/Uo = 1.7 , No. Frames Analysed = 69											
	h = 20 cm			h = 40 cm			h = 60 cm			h = 80 cm		
	N	R.F.	C.R.F.	N	R.F.	C.R.F.	N	R.F.	C.R.F.	N	R.F.	C.R.F.
0.5 - 1.5	1	1.76	1.76									
1.5 - 2.5	2	3.52	5.28	2	6.5	6.5				1	4	4
2.5 - 3.5	5	8.76	14.04	5	16.0	22.5	2	8.3	8.3	3	12	16
3.5 - 4.5	17	29.76	43.80	5	16.0	38.5	2	8.3	16.6	5	20	36
4.5 - 5.5	12	21.12	64.92	4	12.9	51.4	1	4.2	20.8	1	4	40
5.5 - 6.5	7	12.26	77.18	2	6.5	57.9	4	16.7	37.5	1	4	44
6.5 - 7.5	9	15.76	92.94	1	3.3	61.2	3	12.5	50.0	4	16	60
7.5 - 8.5	4	7.06	100.0	3	9.7	70.9	1	4.2	54.2	2	8	68
8.5 - 9.5				4	12.9	83.8	-	-	54.2	-	-	68
9.5 -10.5				1	3.3	87.1	1	4.2	58.4	1	4	72
10.5 -11.5				3	9.7	96.8	3	12.5	70.9	2	8	80
11.5 -12.5				-			4	16.7	87.6	1	4	84
12.5 -13.5				1	3.3	100.0	1	4.2	81.7	2	8	92
13.5 -14.5							2	8.3	100.0	1	4	96
14.5 -15.5										1	4	100
TOTAL	57	100		31	100		24	100		25	100	

TABLE (4) cont'd

Cell Boundary cm	COARSE SAND											
	U/Uo = 1.4 , No. Frames Analysed = 70											
	h = 20 cm			h = 40 cm			h = 60 cm			h = 80 cm		
	N	R.F.	C.R.F.	N	R.F.	C.R.F.	N	R.F.	C.R.F.	N	R.F.	C.R.F.
1.5 - 2.5	4	6.78	6.78	1	2.77	2.77						
2.5 - 3.5	19	32.2	38.98	9	24.93	27.70				2	13.34	13.34
3.5 - 4.5	16	27.12	66.10	5	13.93	41.63	5	25	25	4	26.66	40.00
4.5 - 5.5	11	18.64	84.74	1	2.77	44.40	4	20	45	-	-	40.00
5.5 - 6.5	8	13.56	98.30	9	24.93	69.33	3	15	60	-	-	40.00
6.5 - 7.5	1	1.7	100.0	7	19.39	88.72	2	10	70	-	-	40.00
7.5 - 8.5				4	11.28	100.0	3	15	85	2	13.34	53.34
8.5 - 9.5							1	5	90	2	13.34	66.68
9.5 -10.5							2	10	100	1	6.66	73.34
10.5 -11.5										2	13.34	86.68
11.5 -12.5										1	6.66	93.34
12.5 -13.5										1	6.66	100.0
TOTAL	59	100	-	36	100	-	20	100	-	15	100	-

TABLE (5)

STATISTICAL PROPERTIES OF BUBBLE SIZE DISTRIBUTION

Type of particle	U/U_o	h* = 20cm		h* = 40cm		h* = 60cm		h* = 80cm	
		σ^2	μ	σ^2	μ	σ^2	μ		μ
Ballotini	1.24	1.58	4.0	2.16	4.0	2.45	5.5	-	-
Grade 8	1.82	3.7	7.5	3.4	7.0	-	-	-	-
Ballotini	1.4	1.3	3.5	4.66	4.0	3.03	0.55	-	-
Grade 10	2.7	2.46	5.5	3.03	7.5	3.9	9.0	3.6	12.5
Fine	1.6	1.87	3.5	1.87	4.5	2.16	5.0	-	-
Sand	2.1	2.16	4.0	3.0	5.5	4.18	9.5	-	-
Coarse Sand	1.4	1.87	5.0	-	-	2.16	7.0	-	-

h* = height above the distributor.

In TABLE (5) the values of mean and variance of the bubble size distribution of various cases are given. A plot of mean values of bubble size distribution as a function of height and/or U/Uo gives the only obvious information that at longer distances from the distributor in a fluidized bed and also at higher values of U/Uo the bubble size is larger. It has been already established that the mean value of a normal population gives no information about the form of the distribution and therefore such a representation, often observed in the literature, does not carry all the desired information. Such graphs are more informative when they also contain some knowledge about the type of the distribution, e.g. variance of the distribution. Another efficient method of representation is to plot the values of the distribution function for various values of the independent variables. Here we plot the values of the probability density function given as Eq.(33), i.e.

$$f(x) = \frac{1}{\sigma\sqrt{2\pi}} e^{-(x-\mu)^2/2\sigma^2}$$

for various cases.

The plot of f(x) as a function of x at various heights, various values of U/Uo and for different particles are given in Figs.(23 a-d). All the information mentioned in the beginning of the chapter could be obtained quantitatively from the examination of TABLE (5) and Figs.(23a-d), i.e.,

(a) for a given particle size, at one value of U/Uo the mean value and the variance of the bubble size population is greater for higher levels above the distributor, but the relative frequency of the most probable size is smaller, i.e. bubbles are more uniformly distributed in size at higher levels.

(b) for one type of particle, at the same height the mean value and the variance of the population is greater for the higher value of U/Uo, but the frequency is smaller (which is as expected).

The effect of the particle size and shape on the distribution of the bubble size can be studied by interpolation of the data given in TABLE (5). The general conclusion is that at the same value of U/Uo and at the same distance from the distributor the variance and mean of the bubble size distribution is bigger for bigger particles. This conclusion is of course in agreement with the results of the bubble hold up experiment discussed previously.

$$f(x)=\frac{1}{\sqrt{2\pi}\,\sigma}\,e^{-(x-\mu\ 2}$$

Ballotini Grade 10 $U/U_o = 2.7$

Distance from the Distributor :

20 cm Curve (a)
40 cm Curve (b)
60 cm Curve (c)
80 cm Curve (d)

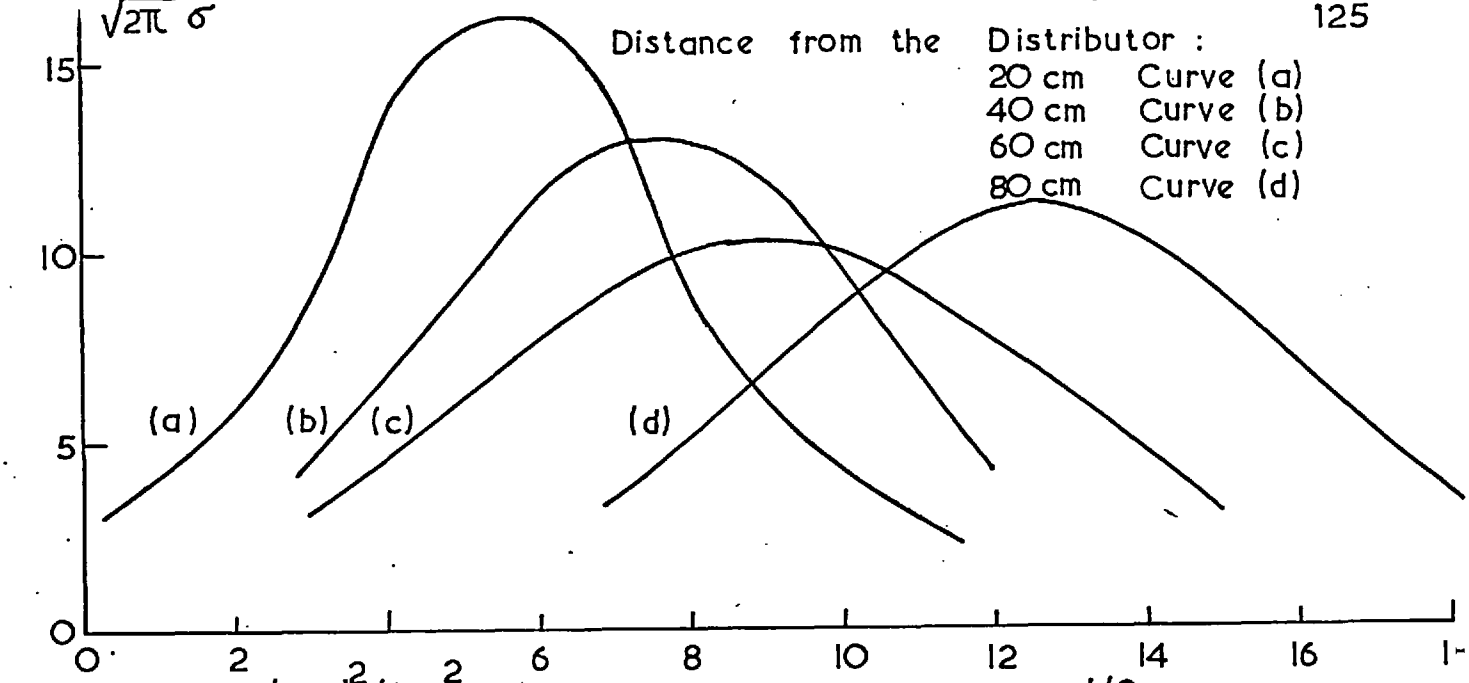

$$f(x)=\frac{1}{\sqrt{2\pi}\,\sigma}\,e^{-(x-\mu)^2/2\sigma^2}$$

Ballotini Grade 10 $U/U_o = 1.4$

Distance from the Distributor :

20cm Curve (a)
40cm Curve (b)
60cm Curve (c)
80cm Curve (d)

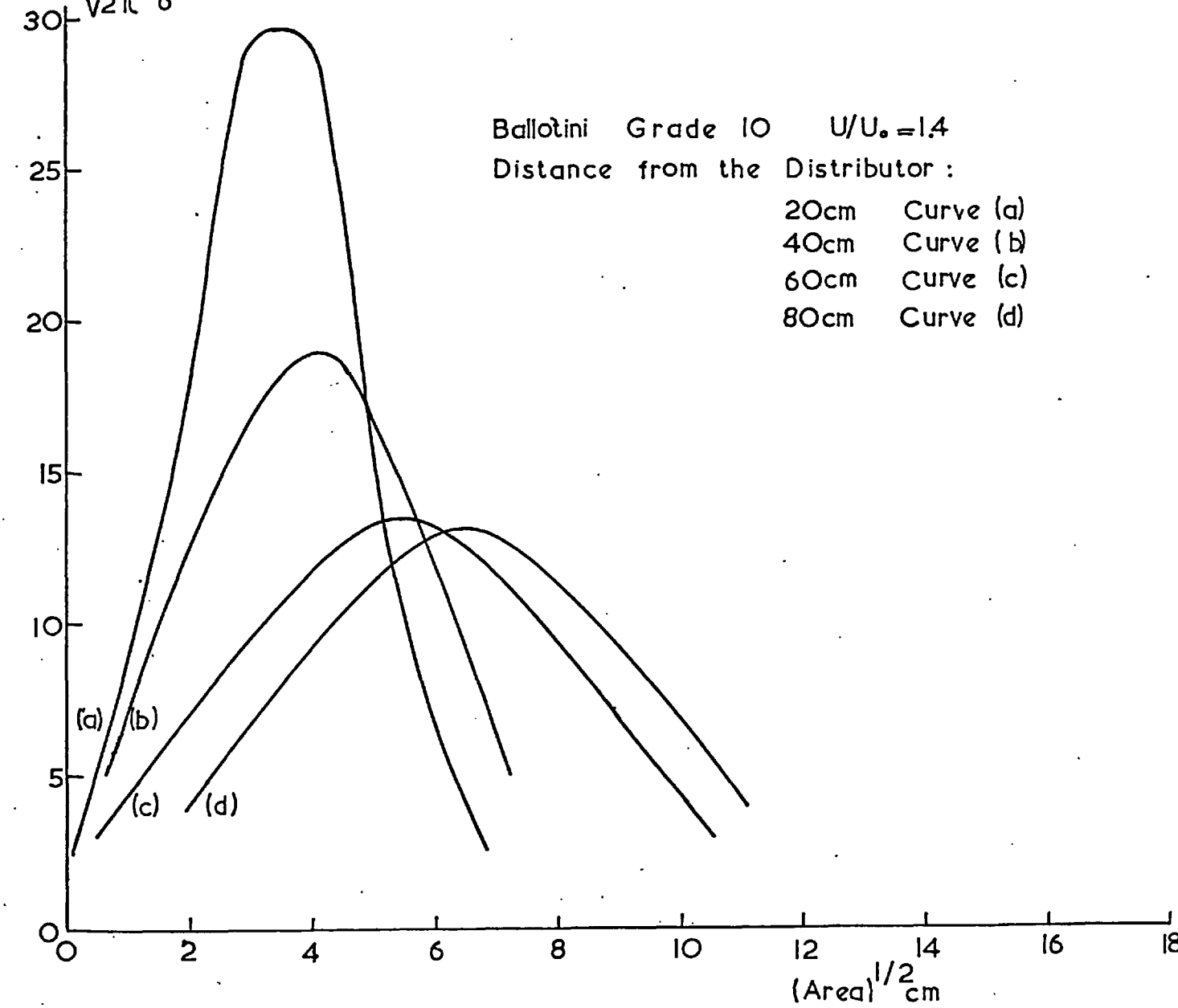

Fig.(23_a)

$$f(x)=\frac{1}{\sqrt{2\pi}\,\sigma}\,e^{-(x-\mu)^2/2\sigma^2}$$

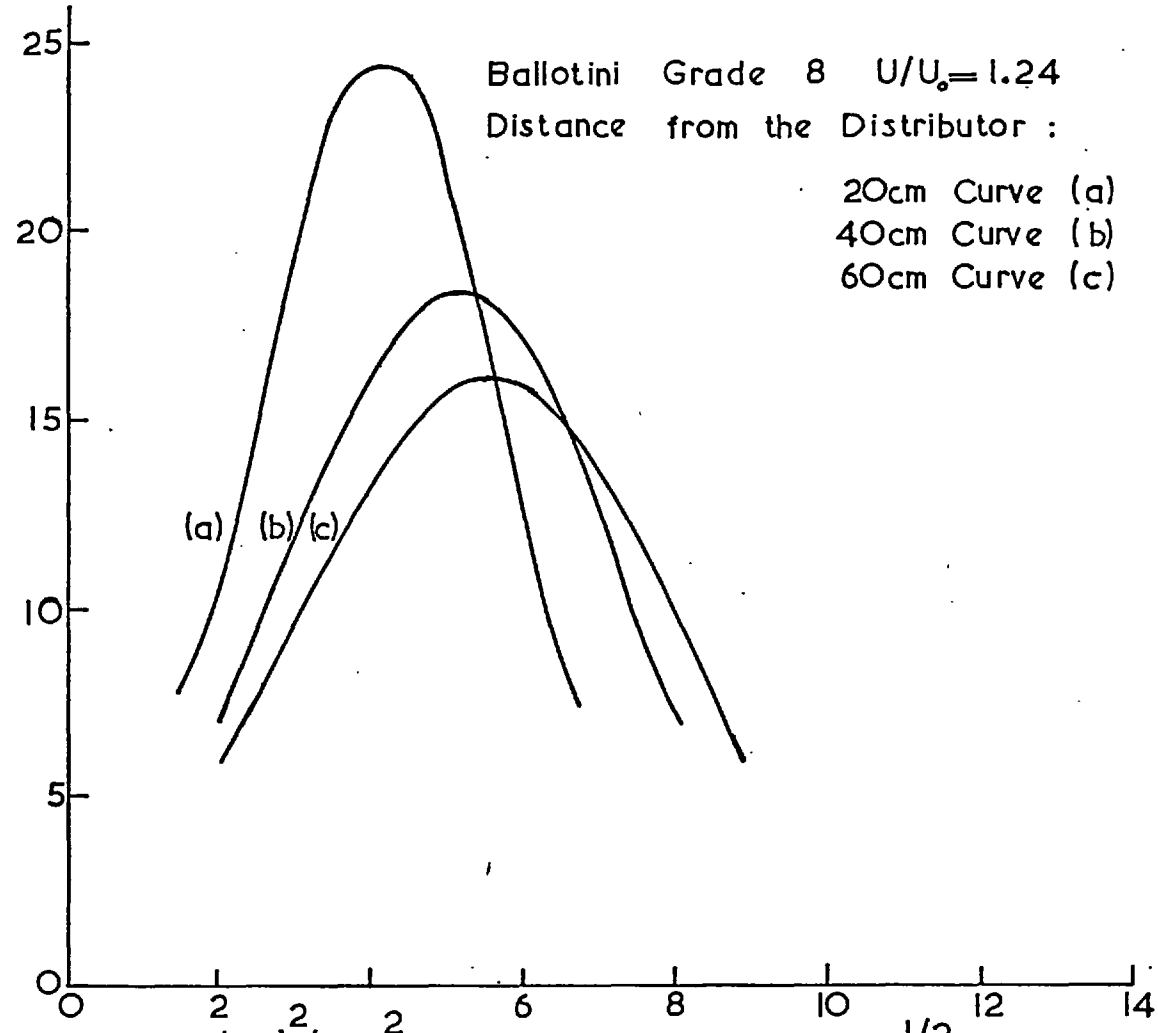

$$f(x)=\frac{1}{\sqrt{2\pi}\,\sigma}\,e^{-(x-\mu)^2/2\sigma^2}$$

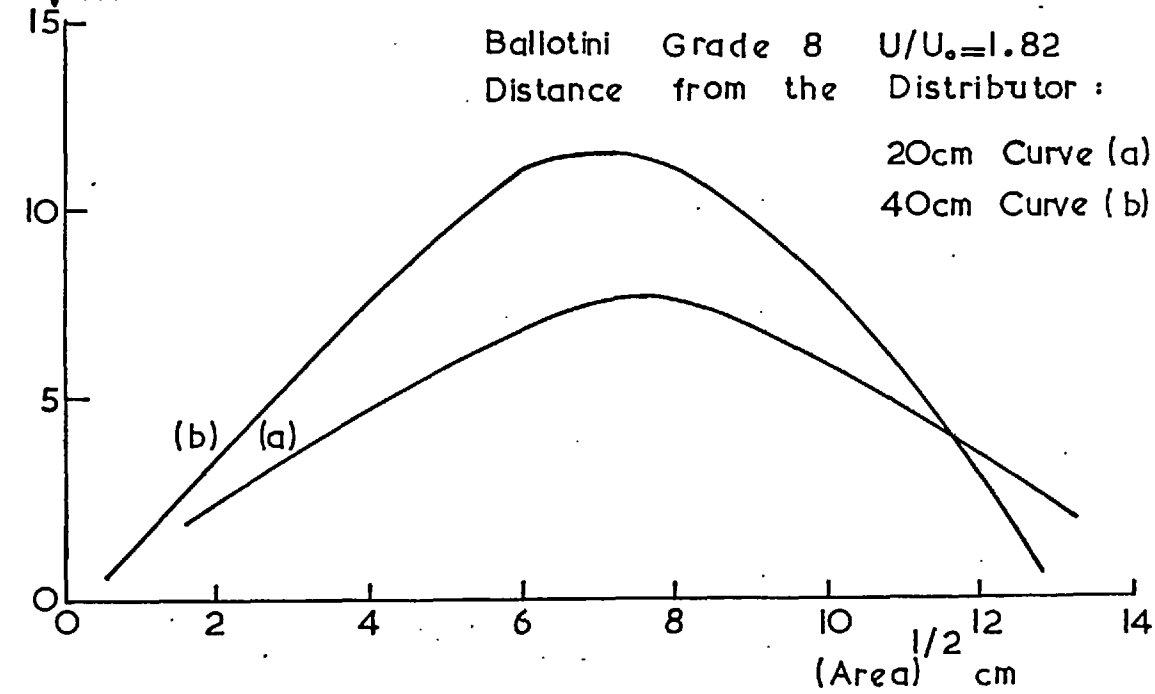

Fig.(23-b)

$$f(x)=\frac{1}{\sqrt{2\pi}\sigma}\,e^{-(x-\mu)^2/2\sigma^2}$$

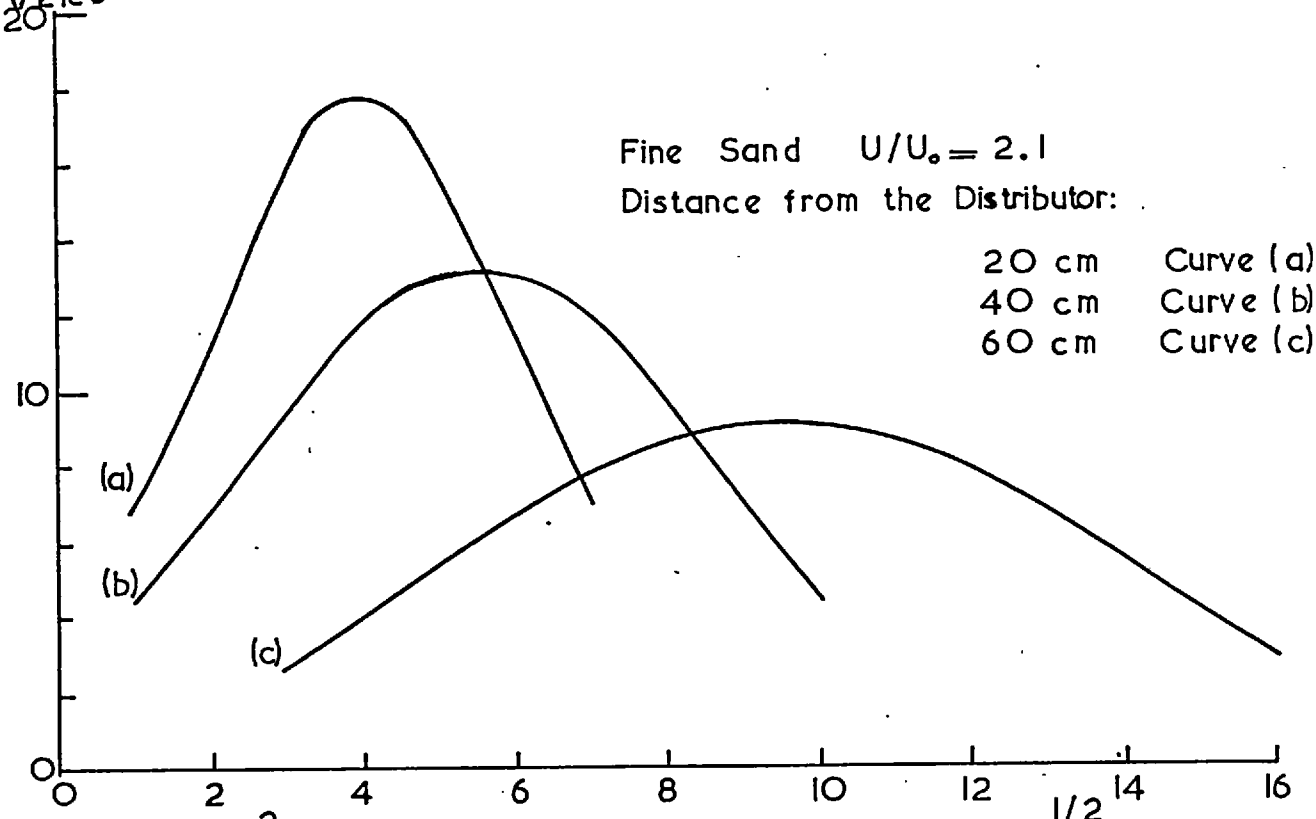

Fine Sand $U/U_o = 2.1$

Distance from the Distributor:

20 cm Curve (a)
40 cm Curve (b)
60 cm Curve (c)

$$f(x)=\frac{1}{\sqrt{2\pi}\sigma}\,e^{-(x-\mu)^2/2\sigma^2}$$

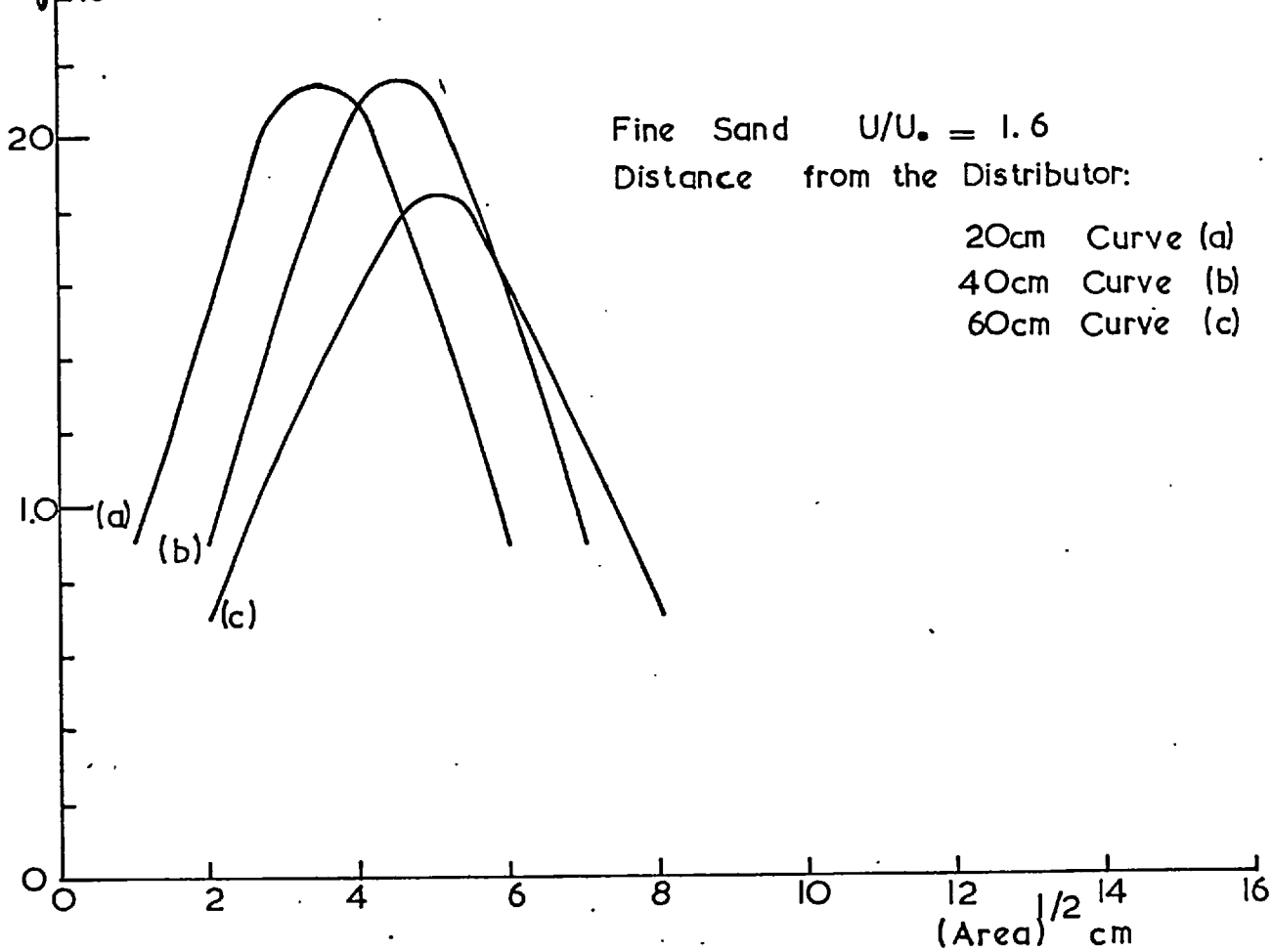

Fine Sand $U/U_o = 1.6$

Distance from the Distributor:

20cm Curve (a)
40cm Curve (b)
60cm Curve (c)

Fig.(23-c)

$$f(x)=\frac{1}{\sqrt{2\pi}\,\sigma}\,e^{-(x-\mu)^2/2\sigma^2}$$

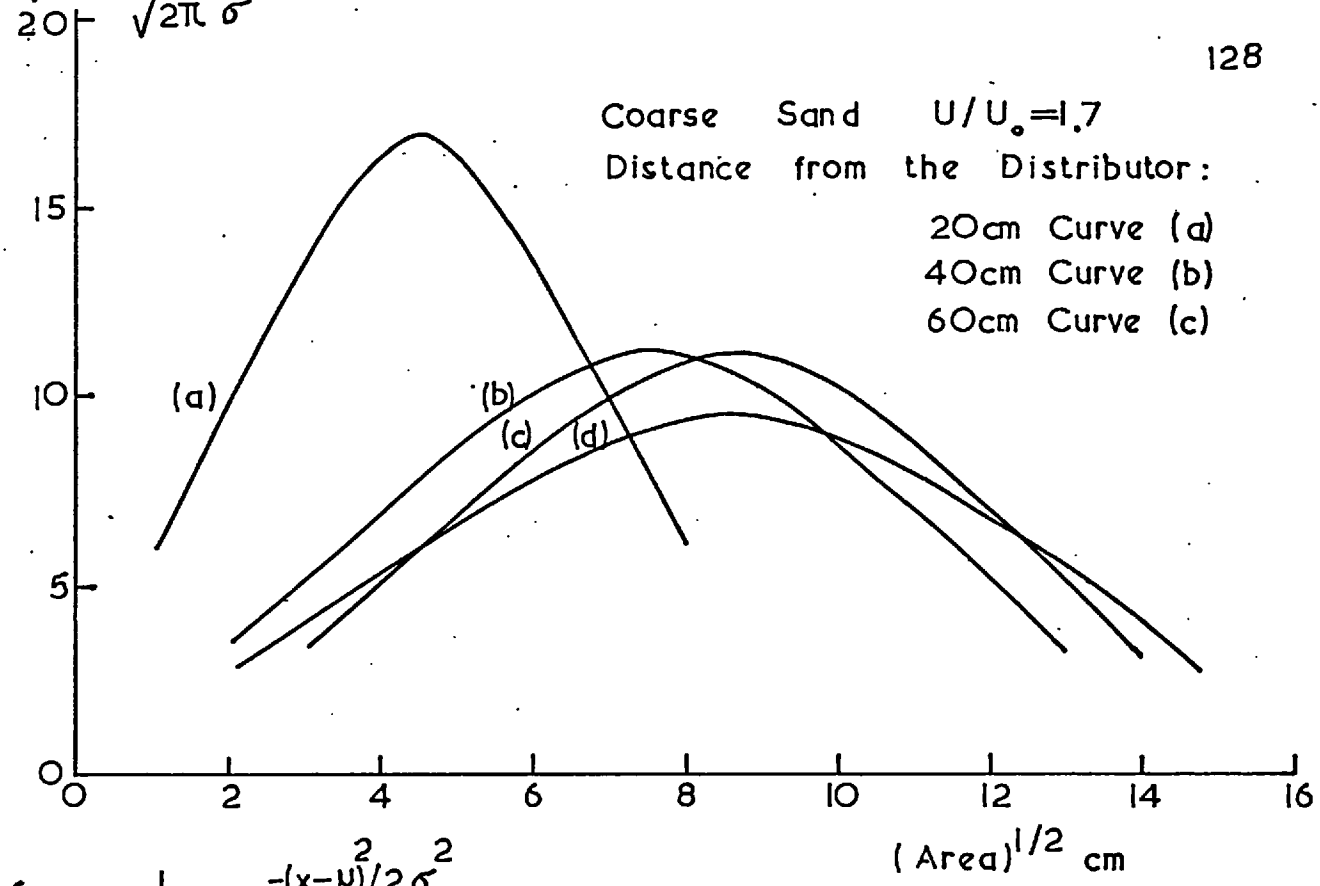

$$f(x)=\frac{1}{\sqrt{2\pi}\,\sigma}\,e^{-(x-\mu)^2/2\sigma^2}$$

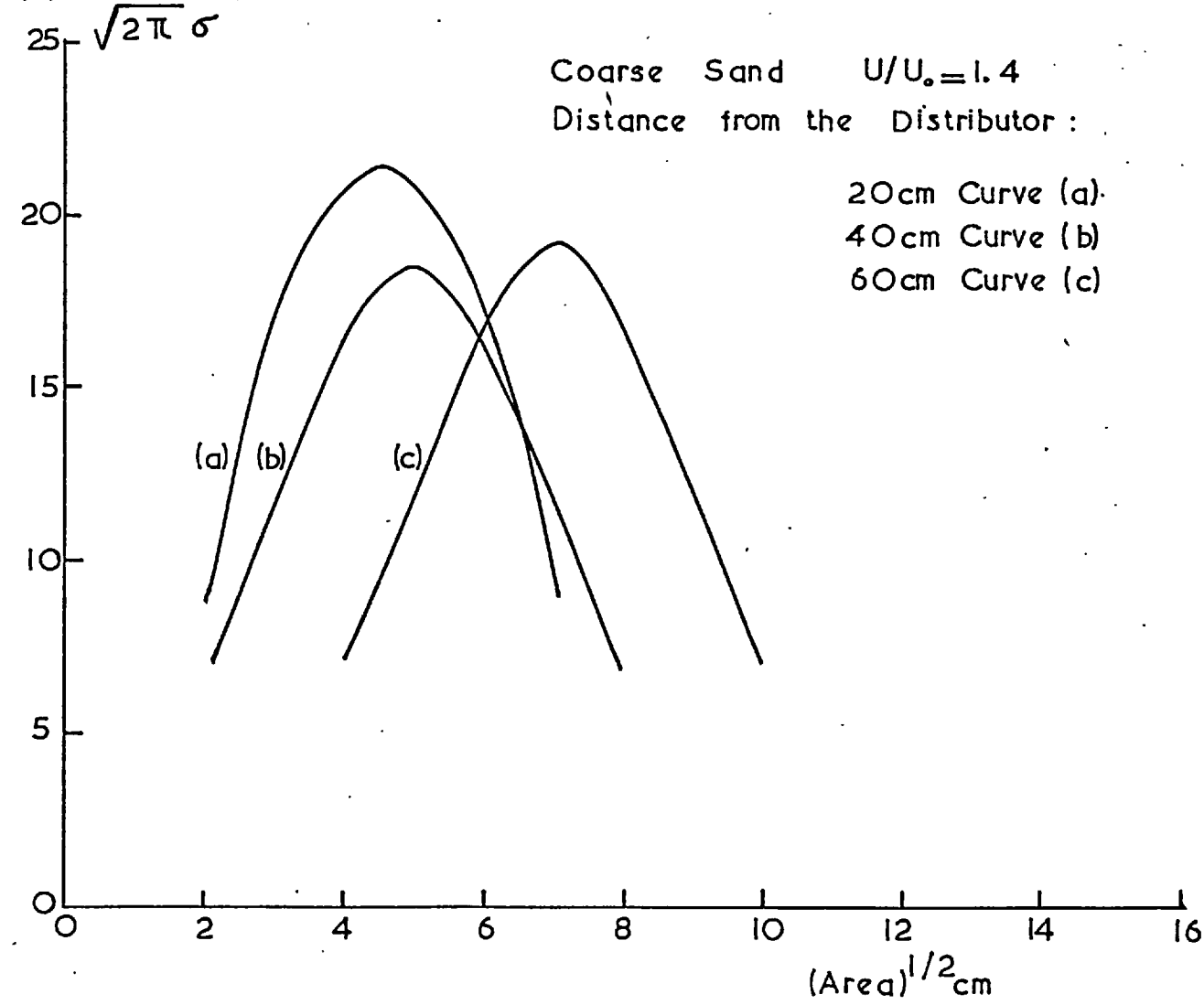

Fig.(23-d)

5.3 BUBBLE SIZE AT VARIOUS HEIGHTS

As was pointed out there are at least three reasons for the growth of bubbles in a fluidized bed, namely i) decrease in the effective hydrostatic pressure, ii) vertical coalescence and iii) horizontal coalescence. The mechanism (i) can be studied when (ii) and (iii) are not possible. This is when a single bubble is injected in an incipiently fluidized bed. However, it is very easy to show that for such a case the effect of reduction in the hydrostatic pressure produces negligible expansion in the volume of the bubble (HARRISON & LEUNG).

DAVIES & RICHARDSON (8) determined the growth of a single bubble in a three-dimensional fluidized bed from the contraction of the bed following the passage of the bubble. They correlated their data by the following empirical equation:

$$\ln \frac{VB_2}{VB_1} = \frac{\Delta H}{K}$$

When VB_1 and VB_2 are the volume of a bubble at injection and after moving through height ΔH, and K represents the distance the bubble must travel for its volume to increase by a factor of "e", and is a function of U-Uo and also the properties of the particles. Their observation took place at velocities well above the incipient value. The bed was reported to be non-bubbling.

In a two-dimensional fluidized bed, it is possible to make sure visually that no bubble exists and in particular if coarse particles are used the bed expansion is not so pronounced at incipient fluidization. The expansion of an injected gas bubble can be studied by cine photography of the bed with back illumination. Results of such an experiment are given in Fig.(24) where the area of an injected bubble is plotted at various heights from the point of injection. Ballotini grade 10

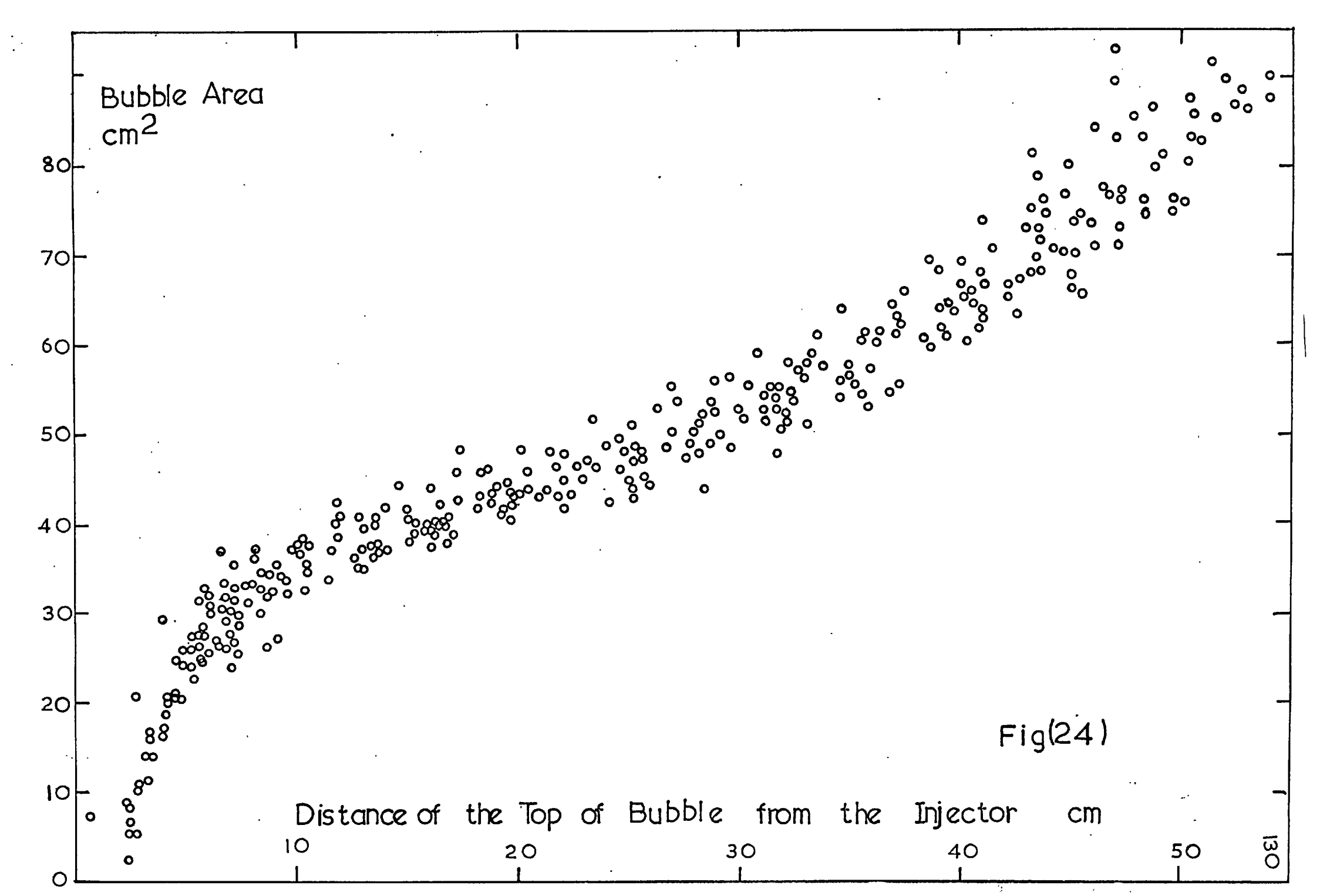
Bubble Area
cm2
80
70
60
50
40
30
20
10
0
10
20
30
40
50
Distance of the Top of Bubble from the Injector cm
Fig(24)

were fluidized at a velocity very close to Uo. The cine film (32 frames/sec) taken from the bed, was projected on a screen and the boundary of the injected bubble was traced at each frame and the area was measured by planimeter. The measurement was carried out for up to 5 injected bubbles. The best line, judged by eye, was drawn through the points and the values taken from that line were used to calculate the volume of the bubble which is plotted in Fig.(25) for various heights from the distributor. It was observed that for almost all the bubbles (all the same size of approximately 6 cm in diameter) the bottom of the bubble was attached to the injector until the roof of the bubble reached a distance of 32 cm from the distributor (6 cm from the injector). So on the graph from point "O" to point "A", the bubble was still growing. There is a significant change in the slope of the curve at point B about 40 cm from the distributor. This is perhaps due to the initial inertia motion of the bubble. Bubbles were injected at a pressure about five times the maximum pressure in the bed. This also may explain the sharp initial expansion of a bubble until it comes into equilibrium with the bed. From point B the volume of the bubble increases at a more or less constant rate. Near the surface, the rate of expansion is larger.

From Fig.(25) it is seen that from point B the volume of a bubble changes about 30% for an increase in height of 26 cm, which corresponds to a reduction in hydrostatic pressure of about 4%. Clearly such an expansion in volume cannot be only due to this reduction in the pressure. A partial explanation can be presented as follows.

In a bed of particles fluidized by a flow of gas close to the value of incipient fluidization, the gas expands due to the change in hydrostatic pressure as it rises up through the bed. Consequently, the

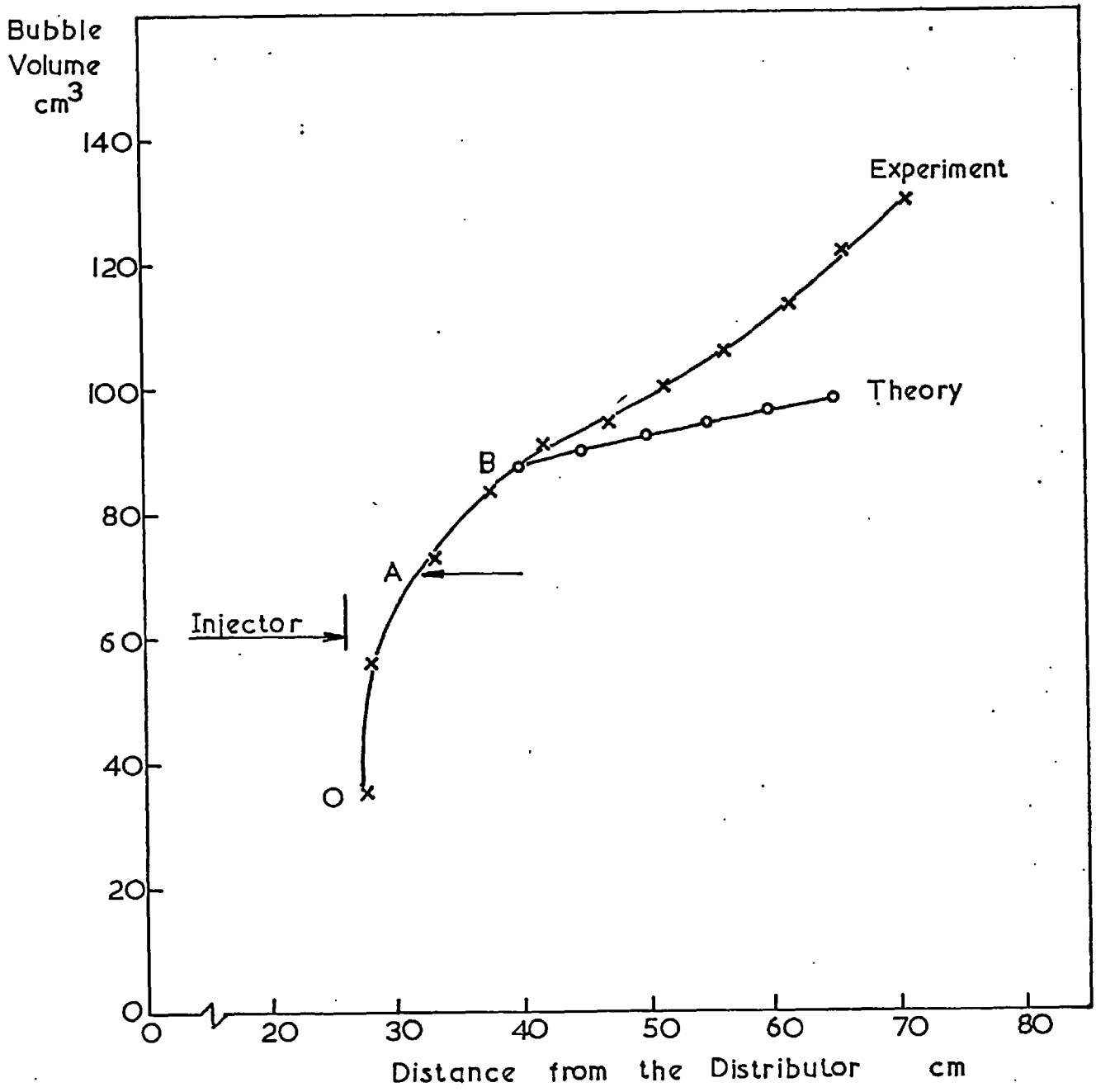
Bubble Volume cm3
140
120
100
80
60
40
20
0
0
20
30
40
50
60
70
80
Distance from the Distributor cm
Experiment
Theory
Injector
A
B
O

Fig. (25)

velocity of the gas increases with height. The effect is that for each flow rate, close to the incipient value, there exists a level in the bed, above which the bed is fluidized and below which the bed is still not fluidized. The same thing was observed by ROWE & SUTHERLAND (7) who noticed that when a bed was caused to operate at some fraction of U_{mf}, the upper part of the bed might nevertheless be fluidized and vigorously bubbling. They also attributed the reported slow mixing in the bottom of the fluidized bed to the fact that bubbles originate only above the bubbling level, i.e. not necessarily at the distributor (LITTMAN (38)).

The following point was also noticed during the course of experiments. The bed was operated at some velocity very close to the incipient value and hence some degree of natural bubbling occurred at the top of the bed. A bubble was injected into the bed, 26 cm above the distributor, and as this bubble rose up through the bed, all natural bubbles below and up to the level of the instantaneous position of the injected bubble disappeared. As long as the injected bubble was in the bed the presence of any other bubble below it in the bed was not detectable. At a short interval after the bubble burst at the surface, natural bubbling slowly and gradually started from the same level as before.(Plate (1)). Qualitatively this could be explained as follows:

Since a bubble is a region of higher permeability it is likely that the gas in all the small bubbles and bubble nuclei tend to converge towards a bigger bubble which is moving faster. In addition as the injected bubble moves faster than the other bubbles, (because of the larger size) then it is likely that many small bubbles ahead of it would be overtaken. For those bubbles which might nucleate at a level just after the injected bubble has passed, the effect of

FRAME

1	0.5	Sec. before injection
2		Injection
		Secs. after injection
3		0.06
4		0.25
5		0.50
6		0.75
7		1.00
8		1.25
9		1.38
10		1.44
11		1.50
12		1.56
13		1.62
14		1.88
15		2.13
16		2.38

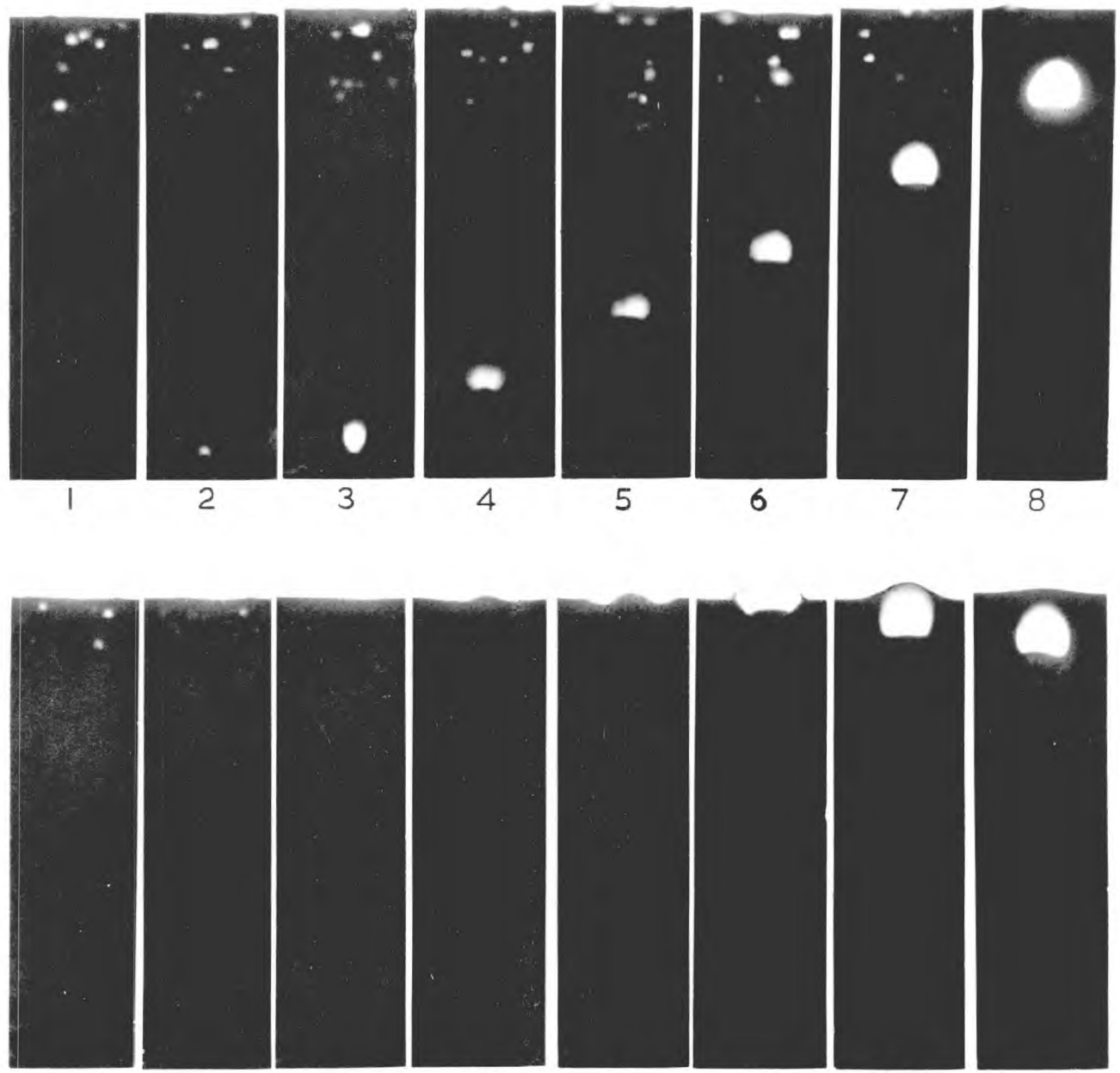

PLATE (1)

the wake of the latter could be such that the former are absorbed.

Now in the light of these observations and the corresponding explanation it is reasonable to attribute the expansion of a single bubble injected into an incipiently fluidized bed, partly to the sweeping action of the bubble on all or some of the natural bubbles present. In Appendix (3) a theoretical model based on the observational facts just mentioned is presented which enables us to calculate the volume of a bubble in a two-dimensional fluidized bed at various heights. To compare the theoretical predictions with the experimental facts, the volume of a bubble with an initial volume the same as those in Fig.(25) was calculated at various heights. Point B on Fig.(25) is taken to be the representation of the initial position and the volume of the bubble when at equilibrium with the bed. This point is taken to be the initial point for the calculation of the bubble size at various heights. Theoretical predictions for the bubble size are given on the same graph in Fig.(25). The justification for the rather arbitrary selection of point B as the initial point is that it is most likely to be the first point where the injected bubble comes into equilibrium with the surrounding particulate phase and then starts to expand uniformly as it rises. The agreement between the experiment and the theory does not seem to be very good. However, this is not surprising in view of several points. First, the theoretical consideration is not rigorous and is only supposed to provide some partial explanation for the observed facts presented previously. Indeed the treatment is fairly successful in showing the existing trend. Secondly, the experimental difficulties, as discussed previously, might be partly responsible for the discrepancy between the theory and experiment. Thirdly the treatment is applicable most when the condition is exactly at incipient situation. Any departure from this

state would shift the observed value of the bubble volume towards the higher magnitude. The discrepancy is more at higher levels above the distributor. (This is likely to be due to the extra expansion near the surface). Considering all these points it is seen that the theoretical model provides a reasonably good insight into the problem of bubble expansion in the absence of other bubbles of comparable size. In other words the treatment shows the influence of the small air bubbles indigenous to gas-solid beds on the larger injected bubbles. This is satisfactory in view of the fact that DAVIDSON & HARRISON (4) noticed that this influence was probably the main source of uncertainty giving rise to some of the scatter in the experimental results on coalescence in the vertical direction. This information is also very desirable as was pointed out by RIETEMA (35). However, the treatment is by no means complete and a more realistic model is necessary for the complete explanation of the situation.

Returning to the other possible mechanism of bubble growth, i.e. vertical and horizontal coalescence HARRISON & LEUNG(31) found that when a lower bubble enters the wake of the upper bubble coalescence occurs. During this process the lower bubble gradually becomes elongated and the upper bubble flattened. They calculated the growth by coalescence of a stream of bubbles assuming that the width and wake of the elongated bubble are both one-half of the spherical bubble. The work of TOEI & MATSUNO(30) was in agreement with HARRISON & LEUNG. They also studied the coalescence of two bubbles for the case where they were not on the vertical line. They found that when one bubble was obliquely below the other bubble coalescence occurred, but the required time for coalescence was longer than that for the vertical case. A theoretical model for the coalescence was given which enabled them to explain fairly well their experimental results.

Plate (2) shows a sequence of motion of two bubbles leading to coalescence. For the case of two bubbles on a horizontal line, TOEI & MATSUNO found that coalescence did not occur frequently. MUCHI et al (39) examined the streamlines of gas in the vicinity of two large coalescing bubbles and found that a single gas cloud can encompass both. WHITEHEAD & YOUNG (32) found that bubble coalescence occurs by both collision and gas transfer without apparent collision. Plate (3) provides further evidence for bubble coalescence without apparent collision which was observed very frequently in the course of the present experimental work. It is believed that horizontal coalescence, i.e. mechanism (iii) for bubble growth takes place mainly without collision and one bubble grows and the other diminishes in size as a result of gas transfer from the latter to the former which may also result in the complete elimination of the latter. The gas transfer may also take place from a bigger bubble to a smaller one.

COALESCENCE WITH COLLISION
(16 frames/sec.)

PLATE (2)

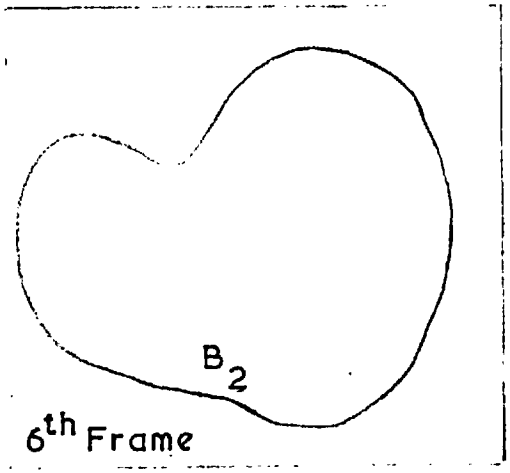

6th Frame

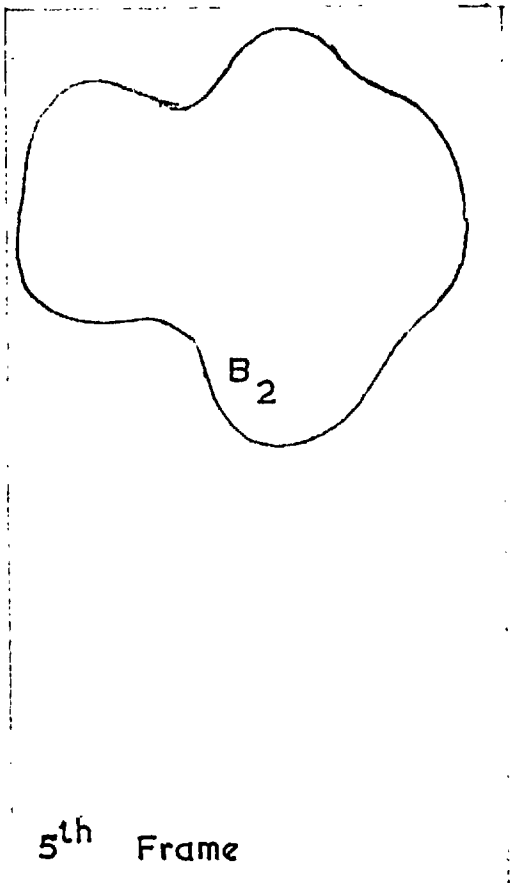

5th Frame

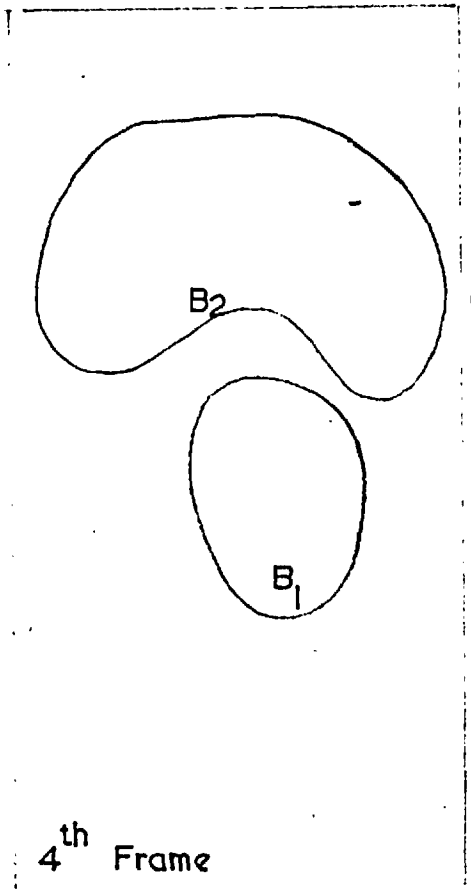

4th Frame

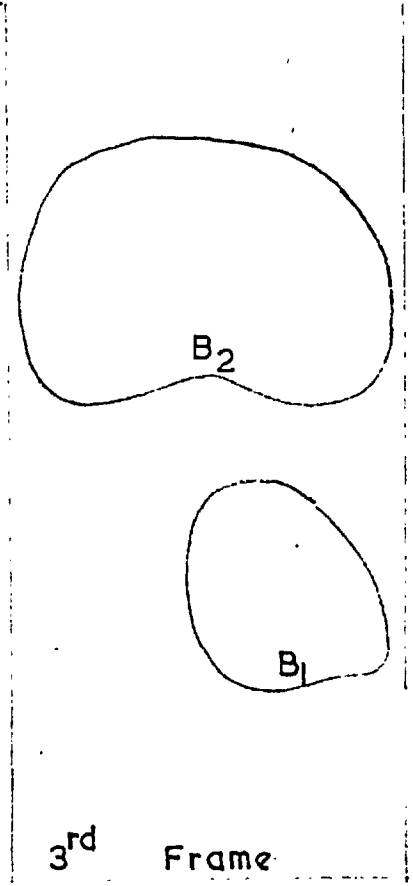

3rd Frame

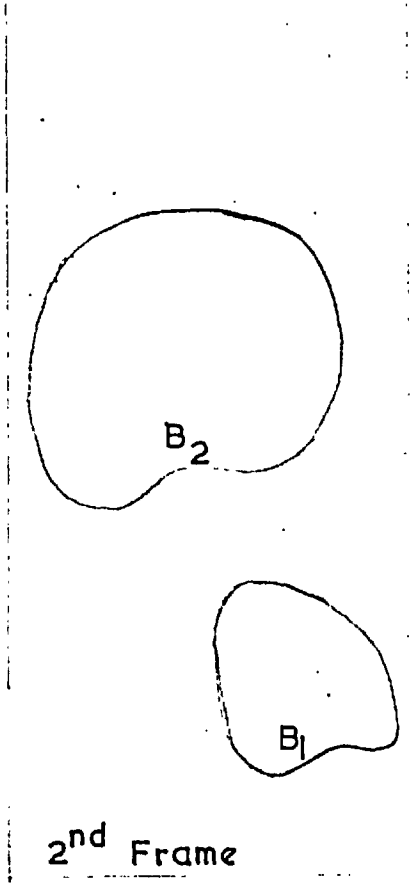

2nd Frame

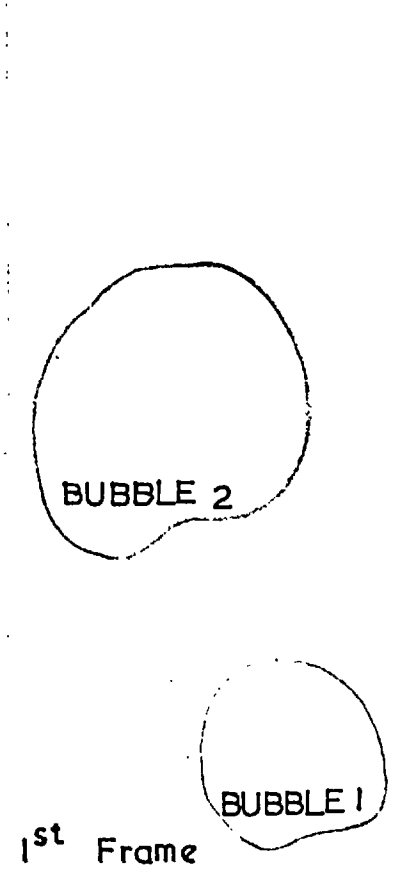

1st Frame

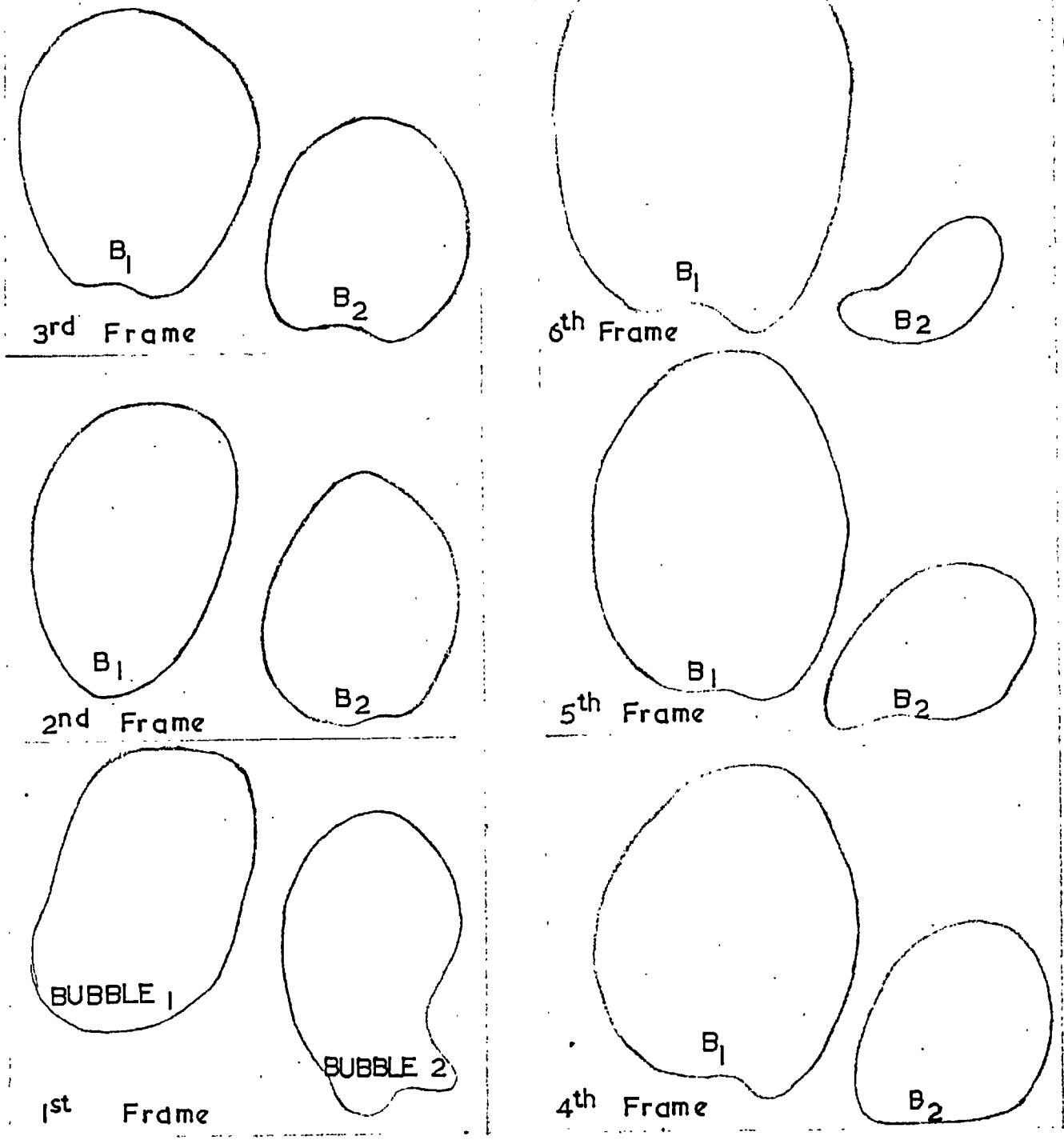
COALESCENCE WITHOUT COLLISION
(16 frames / sec)
B1
B2
3rd Frame
6th Frame
2nd Frame
5th Frame
8th Frame
BUBBLE 1
BUBBLE 2
1st Frame
4th Frame
7th Frame

PLATE (3)

5.4 DISTRIBUTION OF "α"

It was shown that the bubble size has a particular distribution in a gas fluidized bed which is governed by the properties of the system Since bubble size and velocity are related, there is a range of bubble velocity and also "α" in freely bubbling gas fluidized systems. A knowledge of the distribution of α is of primary importance in the design of gas fluidized reactors. (PARTRIDGE & ROWE (34)).

For the assessment of the α-distribution, precise knowledge of the bubble velocity and the incipient fluidization velocity of the system are needed. These have been obtained in the present work and the corresponding results for the distribution of "α" are presented. Examination of the data shows that the distribution is normal. A plot of the cumulative relative frequency on probability graph paper produces a fairly straight line which suggests an approximately normal distribution, Fig.(26). This is in agreement with the results obtained by WHITEHEAD et al (40) that the bubble velocity distribution is normal.

It is important to know the proportion of the bubbles with corresponding α greater and smaller than unity since this defines the behaviour of the system. In Fig.(27) the cumulative proportion of bubbles with α less than a specified value are given as function of $\frac{\alpha}{\varepsilon_{mf}}$. It is noticed that here the magnitude of $\frac{\alpha}{\varepsilon_{mf}} = 2$ is the criterion for the cloud formation. For the purpose of comparison the distribution at various heights and under various overall flow rates are presented. At a specific flow rate the proportion of bubbles with "α" greater than a certain value is bigger at greater distances from the distributor. This effect is more pronounced near the distributor and also close to the surface. The effect of the overall flow rate is such that the whole curve is shifted towards larger

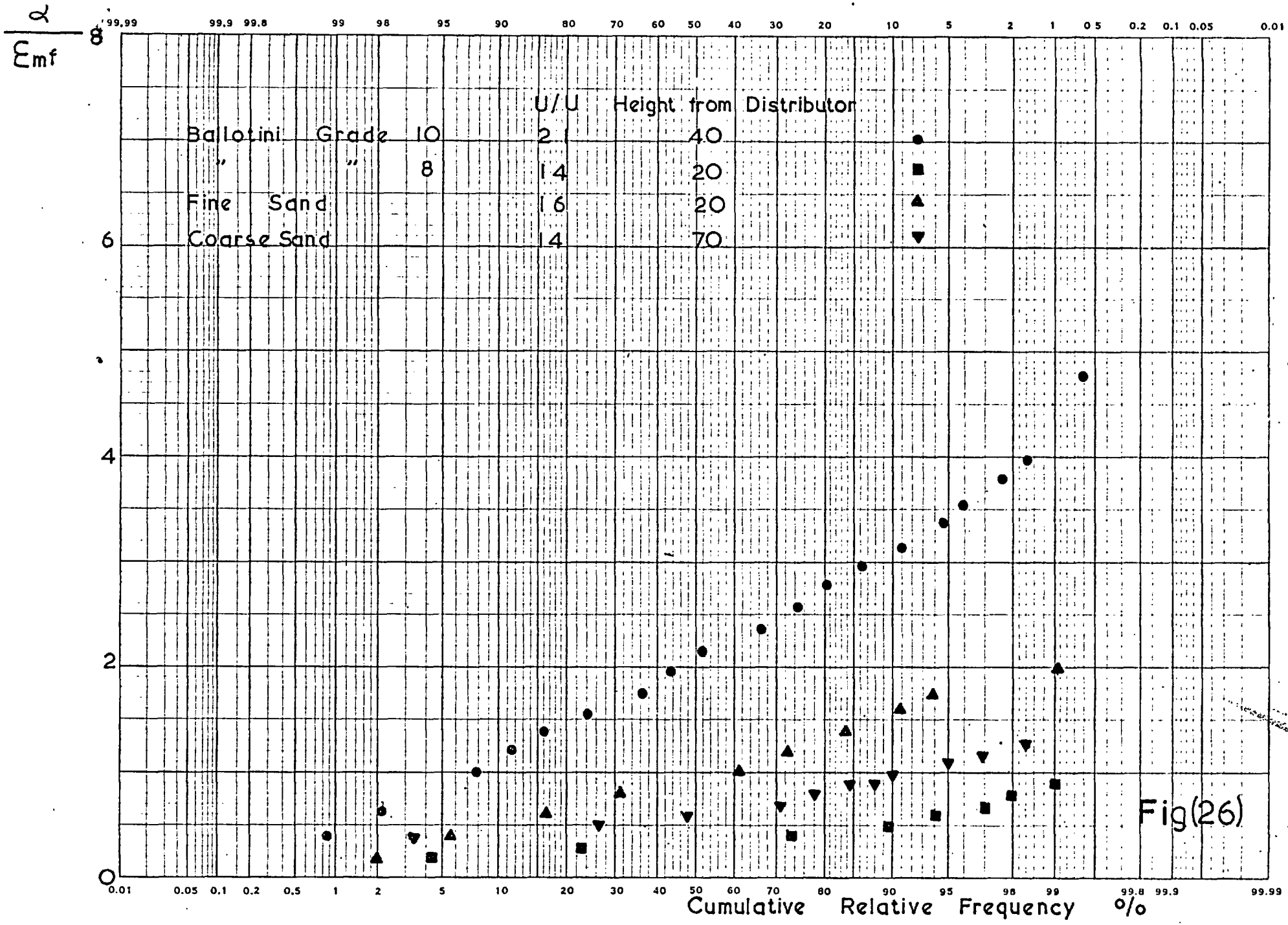
α / εmf
99.99 99.9 99.8 99 98 95 90 80 70 60 50 40 30 20 10 5 2 1 0.5 0.2 0.1 0.05 0.01
8
6
4
2
0
U/U Height from Distributor
Ballotini Grade 10 2.1 40
" " 8 1.4 20
Fine Sand 1.6 20
Coarse Sand 1.4 70
0.01 0.05 0.1 0.2 0.5 1 2 5 10 20 30 40 50 60 70 80 90 95 98 99 99.8 99.9 99.99
Cumulative Relative Frequency %

Fig(26)

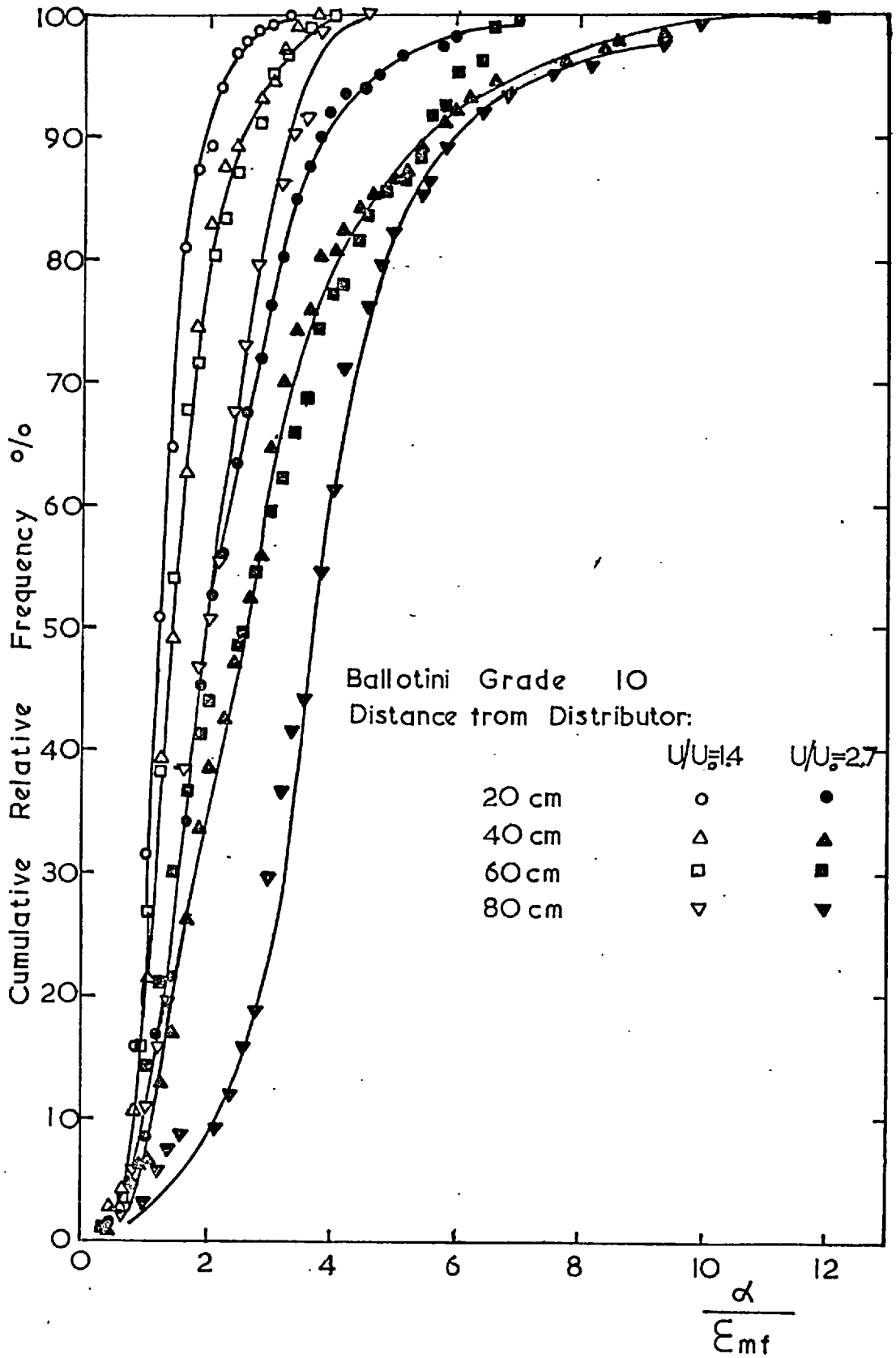
Cumulative Relative Frequency %
100
90
80
70
60
50
40
30
20
10
0
0
2
4
6
8
10
12
α / εmf
Ballotini Grade 10
Distance from Distributor:
U/Uo=1.4
U/Uo=2.7
20 cm
40 cm
60 cm
80 cm

Fig.(27)

values of $\frac{\alpha}{\varepsilon_{mf}}$. This means that at identical heights but at higher U/Uo a certain proportion of all the bubbles have "α" up to a greater value. The effect of particle size and shape can be seen from Fig.(28). At identical heights and identical flow rates a proportion of bubbles have greater α values for smaller particles. The effect of particle shape is not very significant. Graphs corresponding to sand particles fall close to that of the spherical particles with more or less identical incipient fluidization velocity.

As is seen, the particle size is the most influential factor in the distribution of α. This conclusion is very important with regard to the design of gas fluidized reactors. When the particle size is large proportionally more gas would pass through the particles (emulsion phase) and hence a higher overall degree of conversion is achieved. When a large proportion of bubbles move with a velocity much greater than that of the interstitial gas, i.e. $\alpha \gg 1$ most of the gas in those bubbles do not come into contact with particles and hence there would be a serious degree of by-passing. When the bubble velocity approaches that of the interstitial gas, some of the gas in the bubble come into contact with the surrounding particles in the cloud region, and hence there would be some degree of conversion. The greater the size of the cloud the higher the degree of conversion of the reactant. It has been shown (PARTRIDGE & ROWE) that the size of the region around a bubble in which the gas inside the cloud comes into contact with the particles can be represented by the empirical expression

$$\frac{V_{Cp}}{V_B} = \frac{1.17}{\alpha - 1}$$

where V_B = bubble volume, V_{Cp} = volume of the cloud space within the dense phase around the bubble, and $\alpha = U_B/U_i$. Assuming that the whole

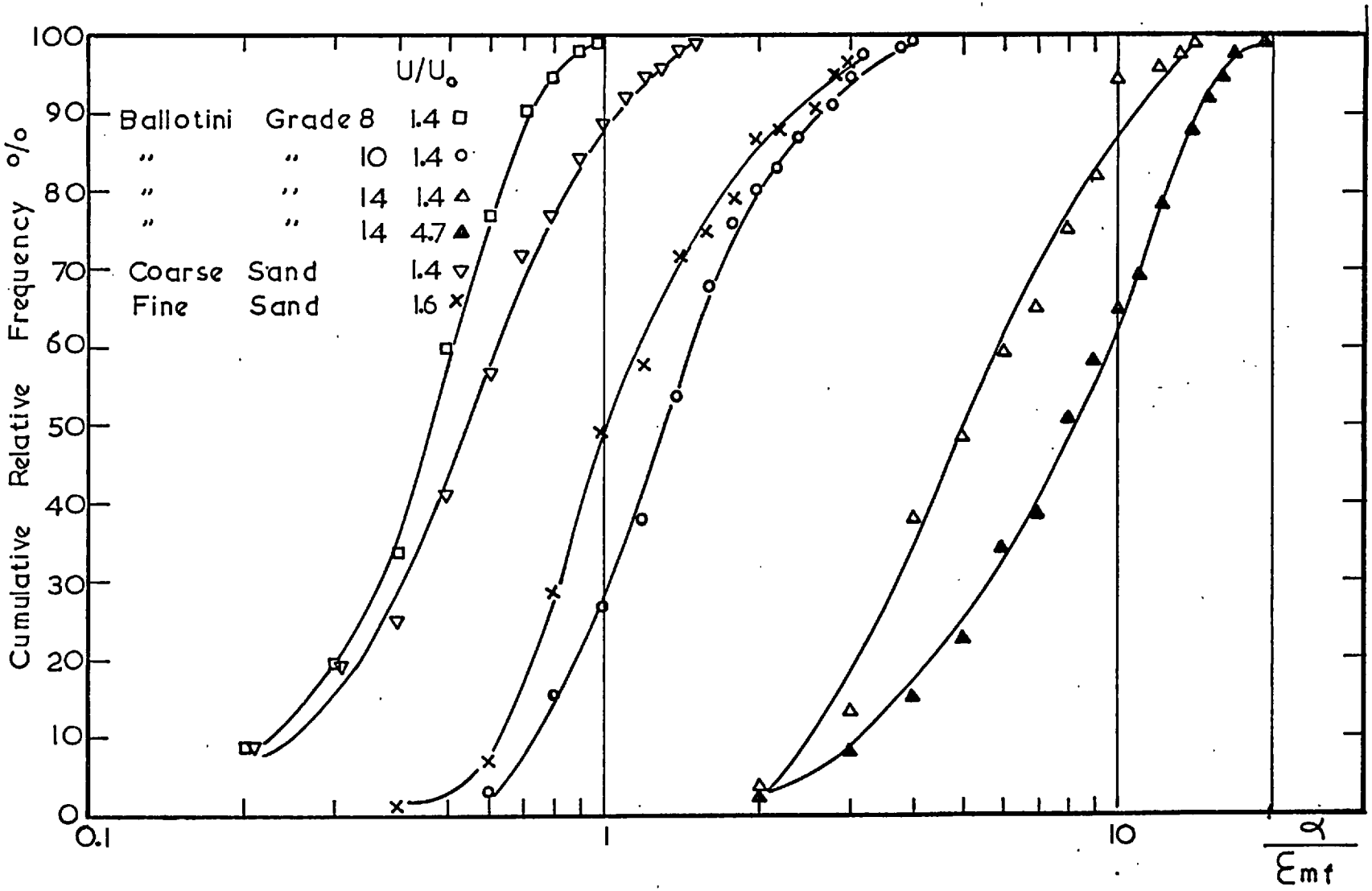
Cumulative Relative Frequency %
100
90
80
70
60
50
40
30
20
10
0
0.1
1
10
$\frac{d}{\varepsilon_{mf}}$
U/U$_o$
Ballotini Grade 8 1.4
" " 10 1.4
" " 14 1.4
" " 14 4.7
Coarse Sand 1.4
Fine Sand 1.6

Fig (28)

cloud is completely mixed and therefore has a uniform reactant concentration then for a slow reaction (in which the overall rate is determined largely by the fraction of gas in contact with solids) the rate of formation of the desired product is directly proportional to V_{Cp}. For values of $1 < \alpha < 2$, the contacting region is reasonably large. This range corresponds to a value of approximately $2 < \frac{\alpha}{\varepsilon_{mf}} < 4$. Now compare two particle sizes, i.e. ballotini grades 10 and 14 at a flow rate about 50 litre per minute. This flow rate corresponds to a value of $\frac{U}{U_o}$ of about 1.4 and 4.7 for ballotini grades 10 and 14 respectively. From the corresponding curves in Fig.(28) it is seen that for particle grade 10 (coarser) about 20% of all the bubbles have a reasonably large contacting region, while in the case of finer particles, grade 14, only about 15% of them have appreciably large contacting region. There is a slight improvement in the conversion taking place in the cloud region for larger particles. However, about 80% of the bubbles in larger particles have no cloud and most of the gas in the bubble comes into contact with particles, while 80% of all the bubbles in finer particles have negligibly small clouds and move much faster than the interstitial gas. The gas inside these bubbles remains completely isolated and makes practically no contact with particles. The overall conversion is seen to be much less than the case of coarse particles.

It is a well established fact that the parameter α is one of the most important factors which govern the behaviour and hence the design of the gas fluidized reactors. However, it is common practice to take an average value of α at a height and use this value as the true representative magnitude. It is clearly seen from the graphs that the average α is not necessarily the best representative of the situation. For a freely bubbling bed an overall statistical model in

which the behaviour of each bubble is taken into the account, perhaps, would be the most suitable model and the predicted behaviour would be more close to the reality. The statistical treatment of some of the most important features of gas fluidized systems considered in the present work shows that those features, i.e. bubble size distribution, α distribution etc. have familiar statistical properties. This suggests that the treatment of gas fluidized systems through a statistical model is justifiable. In building up such a model, these findings would be of indispensable necessity.

In the following tables the data of the distribution of $\frac{\alpha}{\varepsilon_{mf}}$. are represented.

BALLOTINI GRADE 8

Cell Interval	U/Uo = 1.4 Height Above the Distributor Cm				U/Uo = 1.8 Height Above the Distributor Cm				U/Uo = 2.9 Height Above the Distributor Cm			
	20	40	60	80	20	40	60	80	20	40	60	80
0.0 - 0.1	-	-	-	-	-	-	-	-	-	-	-	-
0.1 - 0.2	5	4	5	1	2	-	1	-	9	-	2	-
0.2 - 0.3	21	8	7	1	3	3	4	-	4	-	1	-
0.3 - 0.4	57	23	9	10	26	11	5	-	24	14	14	-
0.4 - 0.5	17	19	16	2	21	5	2	-	26	16	11	6
0.5 - 0.6	5	9	11	5	13	6	2	-	24	21	14	8
0.6 - 0.7	4	7	8	8	20	7	4	1	15	14	12	11
0.7 - 0.8	1	-	3	7	17	3	2	2	7	4	2	1
0.8 - 0.9	1	1	2	1	19	10	9	3	7	6	8	6
0.9 - 1.0	-	1	1	3	9	6	7	3	4	5	6	6
1.0 - 1.1	1	-	-	1	4	2	1	-	1	2	-	3
1.1 - 1.2	-	1	-	-	4	6	2	3	3	2	-	4
1.2 - 1.3	-	1	-	-	3	2	2	5	-	1	1	4
1.3 - 1.4	-	-	-	-	3	4	4	1	-	1	-	-
1.4 - 1.5	-	-	-	-	-	4	4	3	-	1	-	1
1.5 - 1.6	-	-	-	-	-	4	3	1	-	-	-	-
1.6 - 1.7	-	-	-	-	-	1	3	2	-	1	-	1
1.7 - 1.8	-	-	-	-	-	1	2	2	-	-	-	-
1.8 - 1.9	-	-	-	-	-	2	2	4	-	-	-	-
1.9 - 2.0	-	-	-	-	-	1	1	-	-	-	-	-
2.0 - 2.1	-	-	-	-	-	2	-	1	-	-	-	-
2.1 - 2.2	-	-	-	-	-	-	-	4	-	-	-	-
2.2 - 2.3	-	-	-	-	-	-	-	-	-	-	-	-
2.3 - 2.4	-	-	-	-	-	-	-	-	-	-	-	-
2.4 - 2.5	-	-	-	-	-	-	-	3	-	-	-	-
2.5 - 2.6	-	-	-	-	-	-	-	-	-	-	-	-
2.6 - 2.7	-	-	-	-	-	-	-	4				

DISTRIBUTION OF α/ε_{mf}

BALLOTINI GRADE 10

Cell	U/Uo = 1.4				U/Uo = 1.8				U/Uo = 2.9			
	Height Above the Distributor Cm											
Interval	20	40	60	80	20	40	60	80	20	40	60	80
0.0 - 0.2	-	-	-	-	-	-	-	-	-	-	-	-
0.2 - 0.4	-	3	-	-	3	1	1	-	2	1	1	1
0.4 - 0.6	4	1	3	1	2	2	1	-	-	3	1	-
0.6 - 0.8	20	7	13	2	8	5	1	4	7	3	6	-
0.8 - 1.0	24	12	11	3	7	1	1	3	6	1	8	1
1.0 - 1.2	29	18	12	3	21	4	7	1	16	7	7	2
1.2 - 1.4	22	11	16	2	24	5	5	1	8	5	10	1
1.4 - 1.6	25	14	14	11	32	11	10	-	24	11	7	1
1.6 - 1.8	10	13	9	5	17	14	10	3	20	9	5	-
1.8 - 2.0	3	9	4	2	7	9	7	1	13	6	3	-
2.0 - 2.2	7	5	3	3	10	10	6	-	5	5	-	;
2.2 - 2.4	5	2	4	7	12	16	8	6	16	5	5	2
2.4 - 2.6	1	4	-	3	4	9	7	8	7	6	1	2
2.6 - 2.8	1	1	4	4	4	8	8	6	8	4	6	2
2.8 - 3.0	1	3	4	-	10	5	13	5	8	11	5	8
3.0 - 3.2	-	2	3	4	4	7	7	-	7	6	3	5
3.2 - 3.4	1	-	-	2	9	3	4	6	9	5	4	3
3.4 - 3.6	-	1	-	1	1	2	-	3	5	2	3	2
3.6 - 3.8	-	-	1	4	6	2	4	2	4	5	6	11
3.8 - 4.0	-	-	1	-	-	1	-	1	4	1	3	1
4.0 - 4.2	-	-	-	-	4	-	2	1	3	2	1	7
4.2 - 4.4	-	-	-	-	-	-	1	1	-	2	4	-
4.4 - 4.6	-	-	-	1	-	-	-	1	1	1	2	4
4.6 - 4.8	-	-	-	-	1	1	1	-	2	1	2	2
4.8 - 5.0	-	-	-	-	-	-	-	2	-	1	-	2

.....over

/continued

Cell Interval	U/Uo = 1.4				U/Uo = 1.8				U/Uo = 2.9			
	Height Above the Distributor Cm											
	20	40	60	80	20	40	60	80	20	40	60	80
5.0 - 5.2	-	-	-	-	-	-	-	-	1	1	1	-
5.2 - 5.4	-	-	-	-	2	1	1	2	-	2	3	2
5.4 - 5.6	-	-	-	-	-	-	2	-	-	-	3	1
5.6 - 5.8	-	-	-	-	-	-	-	-	3	3	1	2
5.8 - 6.0	-	-	-	-	-	-	-	-	4	1	3	-
6.0	-	-	-	-	-	-	-	-	-	8	4	7

DISTRIBUTION OF $\alpha / \varepsilon_{mf}$

BALLOTINI GRADE 14

Cell	U/Uo = 2.9				U/Uo = 4.7			
	Height Above the Distributor Cm							
Interval	20	40	60	80	20	40	60	80
0 - 1	-	-	-	-	10	-	-	-
1 - 2	12	3	3	3	10	6	2	1
2 - 3	12	6	7	3	14	4	6	1
3 - 4	51	16	20	15	24	10	6	8
4 - 5	23	9	8	6	18	14	8	14
5 - 6	27	16	9	10	40	9	12	8
6 - 7	20	7	5	4	23	14	4	3
7 - 8	13	10	8	9	22	15	12	11
8 - 9	2	4	5	3	7	3	6	4
9 - 10	1	2	10	6	7	12	7	6
10 - 11	2	1	-	-	8	2	4	4
11 - 12	4	3	1	1	7	9	9	7
12 - 13	1	2	1	-	2	3	-	1
13 - 14	-	2	2	4	4	5	9	6
14 - 15	-	-	-	-	1	1	4	4
15 - 16	1	-	-	1	2	1	3	1
16 - 17	-	1	-	2	2	-	2	1
17 - 18	-	1	-	-	-	-	-	1
18 - 19	-	-	-	-	-	2	2	1
19 - 20	-	1	-	-	2	1	-	1
20 - 21	-	-	-	1	-	1	-	1
21 - 22	-	-	-	-	-	-	-	-
22 - 23	-	-	-	2	-	-	-	1
23 - 24	-	-	-	-	-	-	-	-
25	-	-	-	-	-	-	-	3

DISTRIBUTION OF α/ε_{mf}

FINE SAND

Cell Interval		U/Uo = 1.6				U/Uo = 2.1			
		Height Above the Distributor Cm							
		20	40	60	80	20	40	60	80
0.0	0.2	2	-	-	-	1	-	-	1
0.2	0.4	4	-	1	-	4	2	1	1
0.4	0.6	10	2	4	-	16	11	5	1
0.6	0.8	16	7	14	1	18	6	5	2
0.8	1.0	33	11	14	-	23	23	12	5
1.0	1.2	12	6	6	2	9	6	7	4
1.2	1.4	16	15	9	1	27	13	13	2
1.4	1.6	4	3	2	-	13	4	5	1
1.6	1.8	3	9	3	1	10	7	8	3
1.8	2.0	5	7	5	-	14	4	4	1
2.0	2.2	1	2	1	-	3	6	6	2
2.2	2.4	-	1	-	-	3	4	10	6
2.4	2.6	-	1	2	-	1	5	-	1
2.6	2.8	1	-	3	1	5	1	3	6
2.8	3.0	1	-	1	-	1	1	3	1
3.0	3.2	-	-	-	-	1	2	1	3
3.2	3.4	-	-	-	-	-	2	1	4
3.4	3.6	-	-	-	-	3	1	-	1
3.6	3.8	-	-	-	2	1	2	2	0
3.8	4.0	-	-	-	1	1	3	1	1
4.0	4.2	-	-	-	-	-	1	-	2
4.2	-	-	1	1	-	1	-	-	1

DISTRIBUTION OF $\alpha / \varepsilon_{mf}$

COARSE SAND

Cell Interval		U/Uo = 1.4 Height Above the Distributor Cm				U/Uo = 1.7 Height Above the Distributor Cm			
		20	40	60	80	20	40	60	80
0.0	0.1	-	-	1	-	-	-	-	-
0.1	0.2	8	4	5	-	7	1	1	1
0.2	0.3	24	8	8	-	19	3	2	1
0.3	0.4	25	8	4	2	17	6	2	3
0.4	0.5	44	11	1	10	41	12	11	9
0.5	0.6	6	9	11	5	15	14	14	-
0.6	0.7	19	12	11	15	26	19	8	4
0.7	0.8	2	5	2	1	5	4	2	5
0.8	0.9	1	5	7	6	5	18	6	5
0.9	1.0	1	4	3	1	2	4	5	4
1.0	1.1	2	1	3	4	2	4	6	4
1.1	1.2	1	-	1	-	-	2	7	3
1.2	1.3	1	1	1	-	3	1	8	3
1.3	1.4	-	-	2	-	2	2	-	4
1.4	1.5	-	2	1	1	3	2	1	4
1.5	1.6	-	1	-	-	1	1	-	-
1.6	1.7	1	-	-	-	-	-	-	1
1.7	1.8	-	1	-	-	-	1	-	-
1.8	1.9	-	-	-	-	-	1	-	2
1.9	2.0	-	-	-	-	-	-	-	-
2.0		-	-	-	-	-	1	1	2

CHAPTER 6

CONCLUSION

FLOW IN VARIOUS PHASES

(i) BUBBLE THROUGH FLOW

The percentage of the cross-section taken by bubbles and hence the total bubble through flow rate at a given level are decreasing functions of height. The relationship has been confirmed to be statistically significant. At identical values of the total flow rate, when expressed as multiples of the incipient value, i.e. U/Uo, the percentage of the cross-section taken by bubbles and the fraction of the flow carried as bubble through flow are greater for larger particles. The average value of the percentage cross-section taken by bubbles, i.e. the bubble hold up and the average value of the fraction of the total flow carried as bubble through flow, are greater at higher magnitudes of U/Uo for each particle size. For small values of U/Uo, the bubble hold up changes linearly with U/Uo, and at higher values it approaches the final limiting value assymptotically. There is excellent agreement between the magnitudes of bubble hold up obtained by different methods. This is an indication of the suitability of the method of the analysis.

(ii) VISIBLE BUBBLE FLOW

The visible bubble flow rate is an increasing function of height. The existence of the relationship is statistically confirmed. The average visible bubble flow increases with increasing U/Uo for each particle size and decreases with increasing particle size at each value of U/Uo. These conclusions are consistent with the previous

ones concerning the bubble through flow, although the quantities are independently measured. This again is another indication of the justifiability of the method of assessment of the various quantities.

(iii) TOTAL FLOW ASSOCIATED WITH BUBBLES

Total flow associated with bubbles, (i.e. visible + through bubble flow) is strictly a decreasing function of height. The relationship is statistically confirmed to exist. However, it can be assumed with small error, that the total flow associated with bubbles is constant at various heights. This conclusion has been shown not to be in serious conflict with the previous one. At a given value of U/Uo this flow generally decreases with increasing particle size. (Only one exception has been observed at low value of U/Uo for very fine particles). For each particle size, the total flow associated with bubbles increases with increasing U/Uo.

(iv) EMULSION FLOW

The average emulsion flow decreases with increasing U/Uo for each particle size. It generally increases at a given U/Uo with increasing particle size. (With only one exception, for very fine particles). These conclusions could have been drawn directly from the conclusions given in (iii).

TWO-PHASE THEORY

There is a very good agreement between the sum of the different contributions to flow in a fluidized bed, i.e. visible, through bubble flow, and emulsion flow on one hand, and the actual feed on the other hand. The observed discrepancies in some of the cases are not evidence for the inapplicability of the two-phase model. These discrepancies are very likely to be due to error in the measurement of various quantities at high U/Uo for small and irregular particles.

The value of k obtained in the experiments are scattered around

the theoretical line predicted by LOCKETT et al. They fall mostly above the line, however the agreement is satisfactory. All the values of k experimentally obtained, except for two of them where the experimental error is important, are less than 1.4. There is one value of k less than unity. This is in agreement with the theoretical findings reported in the literature and at any rate cannot be rejected as being a statistically extreme value. The theoretical line obtained from the analysis of GRACE & HARRISON overestimates all the experimental results.

BUBBLE SIZE DISTRIBUTION

The mean value of the range of the bubble size observed is not necessarily the best parameter to characterise the bubble size distribution.

The bubble size distribution appears to follow a normal distribution curve.

For a given particle size, at one value of U/Uo the mean value and variance of the bubble size population is greater for higher levels above the distributor but the relative frequency of the most probable size is smaller, i.e. bubbles are more uniformly distributed in size at higher levels.

For a given particle size, at the same height the mean value and the variance of the population is greater for the higher value of U/Uo, but the frequency is smaller.

At same value of U/Uo and at the same distance from the distributor the variance and the mean of the bubble size distribution is bigger for bigger particles. This conclusion is in agreement with bubble hold up results.

BUBBLE EXPANSION

The expansion of a bubble due to factors other than coalescence can be most suitably studied in a transparent two-dimensional bed of coarse particles.

The expansion of a single bubble under such conditions cannot be totally due to the reduction in the hydrostatic pressure.

The expansion of a single bubble injected into an incipiently fluidized bed, is due to the sweeping action of the bubble on all or some of the natural bubbles present. A theoretical model has been presented which provides insight into the problem of bubble expansion in the absence of other bubbles of comparable size.

Bubble coalescence without apparent collision takes place quite frequently in a vigorously bubbling bed. Bubble coalescence in horizontal direction takes place very often through this mechanism. One bubble grows and the other diminishes in size as a result of gas transfer from the latter to the former which may also result in the complete elimination of the latter. The gas transfer may also take place from a bigger bubble to a smaller one.

APPENDIX (I)

REGRESSION ANALYSIS

1. PERCENTAGE OF THE CROSS-SECTION TAKEN BY BUBBLES AT VARIOUS HEIGHTS

TABLE (A.I.1)

PERCENTAGE OF THE CROSS-SECTION TAKEN BY BUBBLES EXPRESSED AS THE PERCENTAGE OF THE MEAN VALUE OF THE SET OF THE OBSERVATION

X	BALLOTINI								SAND				Y
	Grade 8			Grade 10			Grade 14		Fine		Coarse		
	U/Uo			U/Uo			U/Uo		U/Uo		U/Uo		
cm	1.24	1.46	1.82	1.43	2.08	2.69	2.9	4.7	1.6	2.1	1.4	1.8	
20	110.3	115.9	146.1	119.9	121.6	118	139.2	130.8	126.1	97.2	140.0	131.3	124.7
30	127.4	110.0	131.5	121.7	97.7	112.8	108.9	117.5	99.3	125.9	114.9	108.3	114.7
40	98.9	95.3	91.8	93.5	105.1	102.4	86.7	89.8	102.5	95	90.0	96.7	95.6
50	78.0	112.2	87.6	93.5	91.8	99.8	82.7	95.1	96.2	97.2	75	92.4	91.8
60	98.9	95.3	92.8	104.0	107.3	102.4	92.8	85.8	105.6	103.8	108.7	92.4	99.2
70	102.7	90.5	73.0	97.0	96.2	88.5	96.8	102	96.2	95	87.8	93.8	93.8
80	83.7	79.7	77.2	70.5	74.1	76.3	92.8	79.2	70.9	86.2	83.6	85.1	79.9

X = distance of the cross-section from the distributor.

Y = average value of the fraction of the cross-section taken by bubbles. (Expressed as the percentage of the mean value of the set of the observation).

The necessary information for the statistical treatment, obtained from Table (A.I.1) is as follows:

$$\sum Xi = 350$$

$$(\sum (Xi))^2 = 1.225 \times 10^5$$

$$\sum (Xi)^2 = 2.03 \times 10^4$$

$$\sum Xi \sum Yi = 244825$$

$$\sum Xi\ Yi = 33245$$

If we express the relationship between Y and X (i.e. the percentage of the cross-section taken by bubbles at a level, and the height of the level) as

$$Y = \beta X + \alpha \qquad \text{Eq.(A.I.1)}$$

then, application of the method of least squares to the data gives:

$$\beta = -0.618,$$

and $$\alpha = 130.83$$

where β and α are calculated as follows:

$$\beta = \frac{\sum X_i\ Y_i - \frac{(\sum X_i)(\sum Y_i)}{n}}{\sum X_i^2 - \frac{(\sum X_i)^2}{n}} \qquad \text{Eq.(A.I.2)}$$

$$\alpha = \overline{Y} - \beta\ \overline{X} \qquad \text{Eq.(A.I.3)}$$

where n = size of the sample

$\overline{Y}$ and $\overline{X}$ are the mean value of the Y and X respectively.

We can estimate the variance of the deviation about the regression line from the Eq.(A.I.4) below:

$$s_{res}^2 = \frac{1}{n-2} \sum \left[Y_i - (\alpha + \beta X_i) \right]^2$$

$$= \frac{1}{n-2} \left[\sum (Y - \overline{Y})^2 - \beta \sum (X - \overline{X})(Y - \overline{Y}) \right] \qquad \text{Eq.(A.I.4)}$$

For this case we get $s_{res}^2 = 58$ and the standard error $s.e. = \frac{s_{res}}{\sqrt{n}}$.

We also carry on the significant test for the regression coefficient β as follows:

$$t = \frac{\beta - \beta_o}{\sqrt{s_{res} / \sum (X-\bar{X})}} \qquad \text{Eq.(A.I.5)}$$

where t = test statistic,

β_o = zero (This is the Null Hypothesis and we want to investigate whether or not the relationship exists, i.e. we want to see if β is significantly different from zero.) We get the value of t = -4.29 for this case. Referring to the Table of the t-Distribution (23,24), with the degree of freedom df = 5 we get that:

$$0.2\% < Pr(\beta=o) < 1\%$$

Therefore the hypothesis of β=o is rejected, i.e. β is significantly different from zero at 99% level, i.e. the relationship between Y and X exists. The confidence limits for $Y = \bar{y} + \beta (X-\bar{X})$ can be calculated from Eq.(A.I.6) below:

$$\bar{Y} + \beta (X-\bar{X}) \pm t_{(n-2)} s_{res} \sqrt{\frac{1}{n} + \frac{(X-\bar{X})^2}{\sum (X-\bar{X})^2}} \qquad \text{Eq.(A.I.6)}$$

The 99% confidence limits are given when the proper t is used.

The assumptions implied in the treatment given above are:

i) relationship is linear.

ii) variation about the line drawn through the data is constant.

iii) different observations are independent.

iv) deviations have a normal distribution.

Justification for assumptions (i), (ii), and (iii) are taken from the examination of the Fig. (5a - c). For assumption (iv) (necessary for the test of significant of β) Fig (6) show that the ratio of the variances at different values of the sample size is approximately the same, for $40 < m < 60$, as the ratio of the respective values of $\frac{1}{\sqrt{m}}$.

2. FRACTION OF THE FLOW CARRIED BY THE VISIBLE BUBBLE FLOW AT VARIOUS HEIGHTS

TABLE (A.I.2)

FRACTION OF THE FLOW CARRIED BY VISIBLE BUBBLE FLOW (EXPRESSED AS THE PERCENTAGE OF THE MEAN VALUE OF THE SET)

X	BALLOTINI								SAND				Y
	Grade 8			Grade 10			Grade 14		Fine		Coarse		
	U/Uo			U/Uo			U/Uo		U/Uo		U/Uo		
cm	1.28	1.46	1.82	1.43	2.08	2.69	2.9	4.7	1.6	2.1	1.4	1.8	
20	86.5	100	91.5	91.2	95.6	95	105	100	82	97	96	89.5	94.1
30	111	101	100	100.3	97.5	98	102	99	107	100	107	94	101.4
40	94.5	103	90.5	96	100	100.5	94	96.5	99	95.5	89.6	95.8	96.5
50	81	108	98	97.5	97	99	94	99.5	100	96.6	90.5	99.5	96.7
60	101	94	103	100.5	105.5	102.5	95.5	100	109	105	103	100.5	101.6
70	118	96	98.5	108.5	102	101	101.5	103	104	102.5	96	110.5	103.4
80	108	95.5	117.5	93.2	100	104	106	101	100.5	103	92	113	102.6

X = height of a level above the distributor.

Y = fraction of the flow carried by bubbles. (Expressed as the percentage of the mean value of the set of the observations).

(ABOVE DATA ARE ALSO GIVEN IN FIG.(9)).

The necessary information for the statistical treatment, obtained from Table (A.I.2) is as follows:

$$\sum X_i = 350$$

$$(\sum X_i)^2 = 122500$$

$$\sum (X_i)^2 = 20300$$

$$\sum X_i \sum Y_i = 243705$$

$$\sum X_i Y_i = 35161$$

The model for the regression line is taken to be $Y = \beta X + \alpha$. Applying the method of the least squares, from Eqs.(A.I.2) and (A.I. 3) we get:

$$\beta = 0.123$$

$$\alpha = 93.32$$

The variance of the deviations about the regression line is calculated from Eq.(A.I.4), and from Eq.(A.I.5) the test statistic is calculated to give:

$$t = 2.4$$

Referring to the Tables of t-Distribution (23, 24) with degree of freedom df = 5 we conclude that the probability of the Null Hypothesis being true, i.e. $\beta = \beta_o = o$ is about 5%. So the hypothesis of $\beta = o$ is rejected and therefore we conclude that the relationship between Y and X, i.e. ($\sum d_i U_{Bi}$) and height exists with a 95% probability. The confidence intervals for $Y = \overline{y} + \beta (X-\overline{X})$ can be calculated from Eq.(A.I.6). The 95% confidence limits are plotted in Fig.(9).

3. FRACTION OF THE FLOW ASSOCIATED WITH BUBBLES

TABLE (A.I.3)

FRACTION OF THE FLOW ASSOCIATED WITH BUBBLES
(EXPRESSED AS THE PERCENTAGE OF THE MEAN VALUE OF THE SET)

X	BALLOTINI								SAND				Y
	grade 8			grade 10			grade 14		Fine		Coarse		
	U/Uo			U/Uo			U/Uo		U/Uo		U/Uo		
cm	1.24	1.46	1.82	1.43	2.08	2.69	2.9	4.7	1.6	2.1	1.4	1.8	
20	101	107	113	102	102	101	107	102	89	105	119	108	108
30	119	106	111	108	99	101	102	100	112	100	112	101	106
40	98	99	93	95	101	101	95	97	98	98	92	97	97
50	81	109	95	98	97	100	94	99	99	97	85	96	98
60	100	96	99	102	103	102	96	98	105	104	107	97	101
70	108	94	90	105	101	99	101	102	100	100	94	102	100
80	94	89	99	88	94	98	104	99	96	94	90	99	95

X = height of a level above the distributor.

Y = fraction of the flow associated with bubble (averaged).

The necessary information for the statistical treatment, obtained from TABLE (A.I.3) is as follows:

$$\sum X_i = 350$$

$$\sum (X_i)^2 = 20300$$

$$(\sum X_i)^2 = 122500$$

$$\sum X_i Y_i = 34780$$

$$(\sum X_i)(\sum Y_i) = 246750$$

The model for the regression line is taken to be

$$Y = \beta X + \alpha$$

Applying the method of the least squares, from Eq.(A.I.2) and (A.I.3) we get:

$$\beta = -0.17 \ , \ \alpha = 109.1$$

The variance of the deviations about the regression line is calculated from Eq.(A.I.4) and from Eq.(A.I.5) the test statistic is calculated to give:

$$t = -2.6$$

Referring to the Tables of t-distribution (23) with degree of freedom df = 5, it is concluded that the probability of the Null hypothesis being true, i.e. $\beta = \beta_o = o$ is less than 5%. Therefore the relationship between X and Y exists with a probability of 95%. The confidence intervals for $Y = \overline{y} + \beta (X - \overline{X})$ can be calculated from Eq.(A.I.6)The 95% confidence limits are plotted in Fig.($_{12}$).

APPENDIX (II)

DETERMINATION OF U_{mf}

The incipient flow rate can either be predicted theoretically or measured experimentally. There are a number of correlations available. It has been shown (41) that the predicted results from various correlations are not in general of high accuracy and differ by as much as an order of magnitude for large particles. This confirms the conclusion that the only way to assess the incipient velocity is to measure it. (DAVIDSON & HARRISON (4)).

The experimental method generally used is to measure the pressure drop in the bed as a function of the flow rate of the fluidizing fluid. Measurements are taken with both increasing and decreasing flow rate and the incipient velocity is determined as the velocity at which the pressure drop curve changes its slope due to transition from fixed to fluidized behaviour. Methods based on the measurements of the heat transfer coefficient at the wall of the containing vessel have also been used (42). The drawbacks of all these methods have been discussed elsewhere (43). The main criticism is that the transition from fixed to fluidized situation takes place over a range of flow rates, and when this range is wide, the assessment of the true magnitude of the incipient velocity is not possible. A different experimental method was proposed (43) which appeared to be of greater accuracy than the pressure drop flow rate method. This method leaned heavily on the basic assumption that the two-phase theory of fluidization was applicable. In the present work since we actually

are concerned with the validity of the two-phase model, this method cannot be utilized for the assessment of the incipient fluidizing velocity. Hence the only way is to use the pressure drop method. We are going to discuss the uncertainty in the results obtained by this method and try to reduce this to a minimum. Finally, the confidence intervals for the experimentally determined magnitude of incipient velocity will be given.

A bed of particles is said to be fluidized when the drag imposed by the flowing fluid through the particles equals the weight of them. It has been observed by many investigators, that fluidization starts first near the surface. ROWE & SUTHERLAND (7), for instance, noticed that when the bottom of the bed was just fluidized the top was bubbling strongly. This can be easily explained by the fact that the fluidizing fluid expands as it rises through the bed because of the reduction in pressure with height. The present observations also confirm that the top of the bed becomes fluidized sooner than the bottom when the flow rate is increased.

Two probes 10" apart with the lower one 6" above the distributor were located at the wall of the bed and connected to the branches of a "U" manometer. The pressure difference for increasing and decreasing flow was determined. The pressure drop between another pair of probes 10" apart with the lower one 46" above the distributor was determined in another experiment. The results of both experiments are presented in Fig.(A.1). As it is noticed, the data for both cases coincides up to a point from where they deviate from each other. It is noticed that when the upper pair of probes show a constant pressure drop with increasing flow rate, the lower one shows increasing pressure drop. The percentage difference between the pressure at the top and the bottom of the bed is comparable to the percentage change

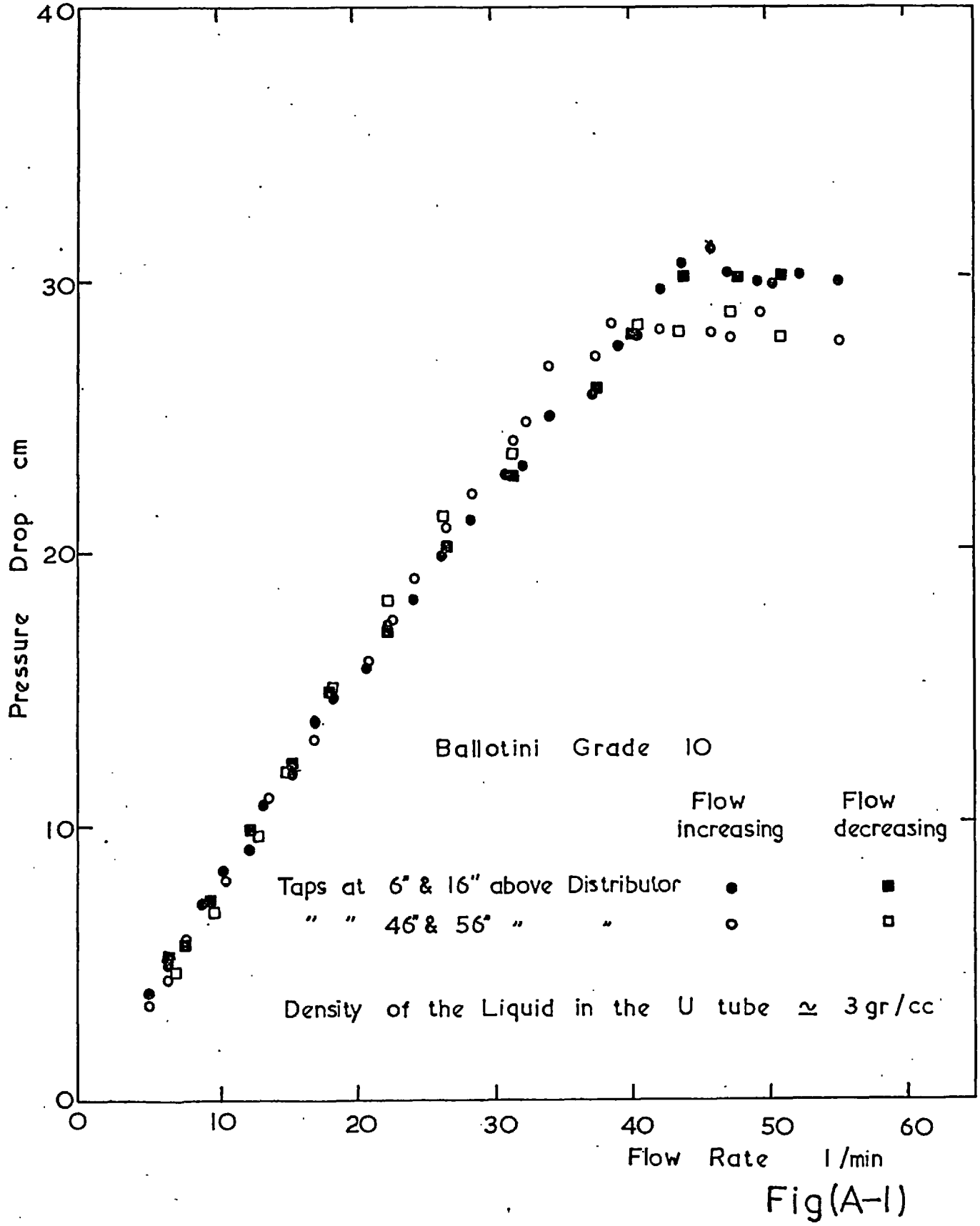
40
30
20
10
0
0
10
20
30
40
50
60
Pressure Drop cm
Flow Rate l/min
Ballotini Grade 10
Flow increasing
Flow decreasing
Taps at 6" & 16" above Distributor
" " 46" & 56" " "
Density of the Liquid in the U tube ≃ 3 gr/cc

Fig(A-1)

in the required flow for incipient fluidization. Ideally, if there was no expansion in the fluid, these two curves would have been completely identical. Here we see that transition of the whole bed from fixed to fluidized behaviour takes place over a rather wide range of the flow rate. Now when only one probe is used for the measurement of the pressure and the other branch of the U manometer is opened to atmosphere, the data so obtained are representative of the average situation (over the whole length of the bed). This is the reason why a wide range in the transition velocity is observed. Here in order to get a fairly sharp transition from fixed to fluidized bed and hence an unambiguous value for the incipient velocity, the pressure drop is measured between two probes some distance apart. Then a probe closer to the one at the foot was selected and the pressure drop was determined. The distance between the probes was reduced until there was no appreciable improvement in the quality of the pressure curve at the transition region. Results for ballotini grade 10 are presented in Fig.(A2). The transition is very much sharper when the probes are closer together than when away from each other. There is no marked change in the quality of the curve when the distance between the probes is reduced to less than 10". Similar curves for irregular sand (large particles) are presented in Fig.(A3). The same trends are noticeable in this case too. However, the quality is not as good as in the case of spherical particles. This of course is expected because of the shape irregularity and wide size distribution.

In the light of the above considerations it was concluded that a separation distance of about 10" between two probes, one directly above the other in the measurement of incipient velocity by pressure drop method was necessary. The data obtained in this way have a very

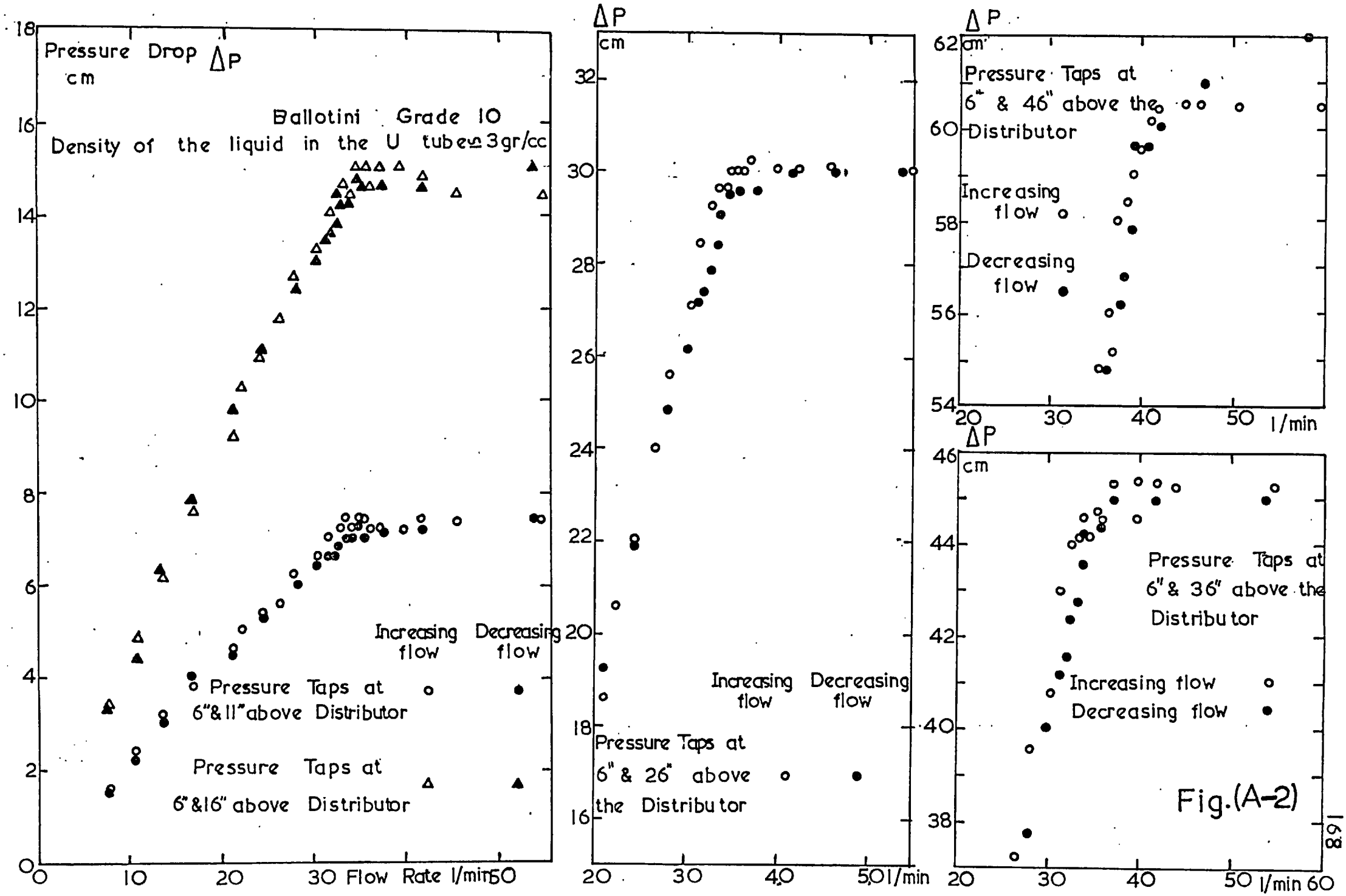
Pressure Drop ΔP
cm
Ballotini Grade 10
Density of the liquid in the U tube ≃ 3gr/cc
Increasing flow
Decreasing flow
Pressure Taps at
6"&11" above Distributor
Pressure Taps at
6"&16" above Distributor
Flow Rate l/min
ΔP
cm
Increasing flow
Decreasing flow
Pressure Taps at
6" & 26" above the Distributor
l/min
ΔP
cm
Pressure Taps at
6" & 46" above the Distributor
Increasing flow
Decreasing flow
l/min
ΔP
cm
Pressure Taps at
6" & 36" above the Distributor
Increasing flow
Decreasing flow
l/min

Fig.(A-2)

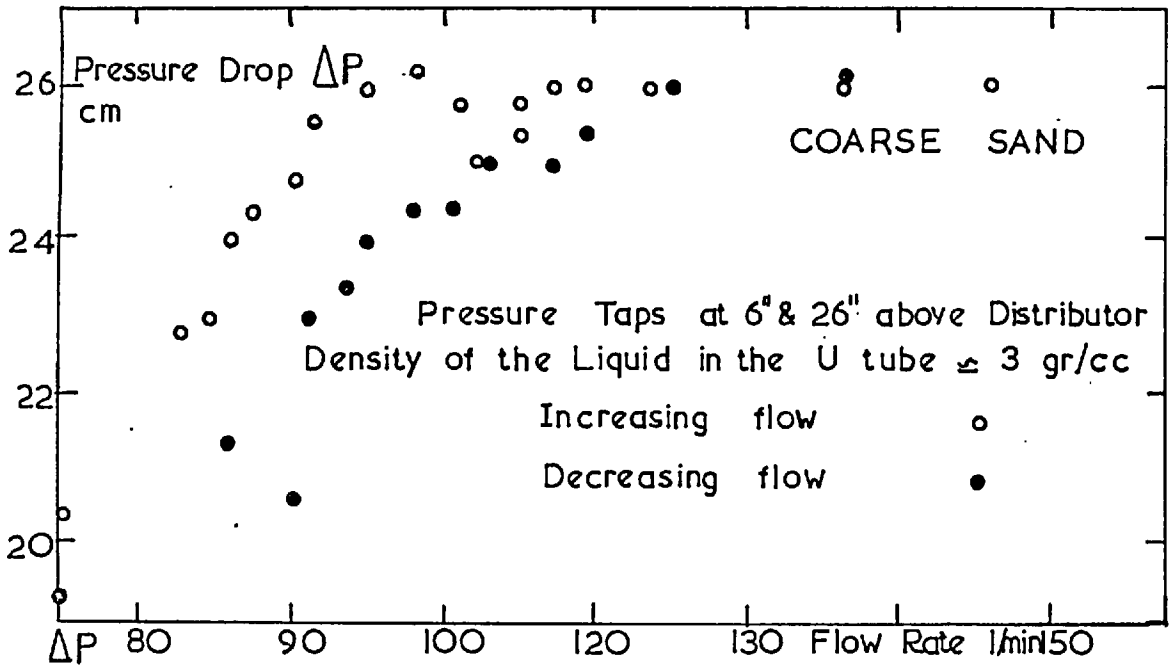
Pressure Drop ΔP
cm
COARSE SAND
Pressure Taps at 6" & 26" above Distributor
Density of the Liquid in the U tube ≃ 3 gr/cc
Increasing flow
Decreasing flow
ΔP
Flow Rate l/min

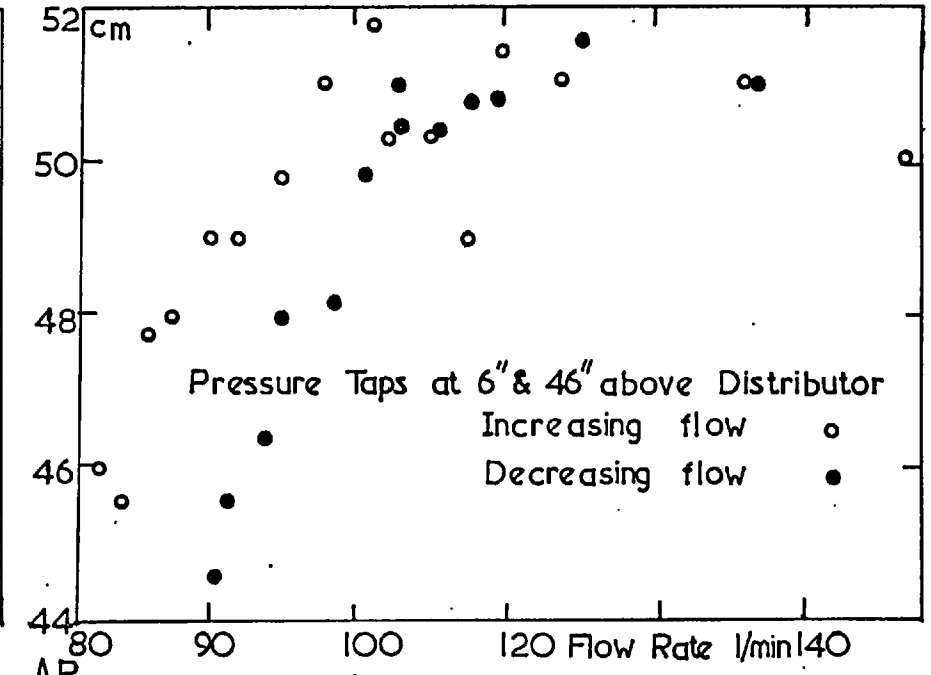
cm
Pressure Taps at 6" & 46" above Distributor
Increasing flow
Decreasing flow
Flow Rate l/min

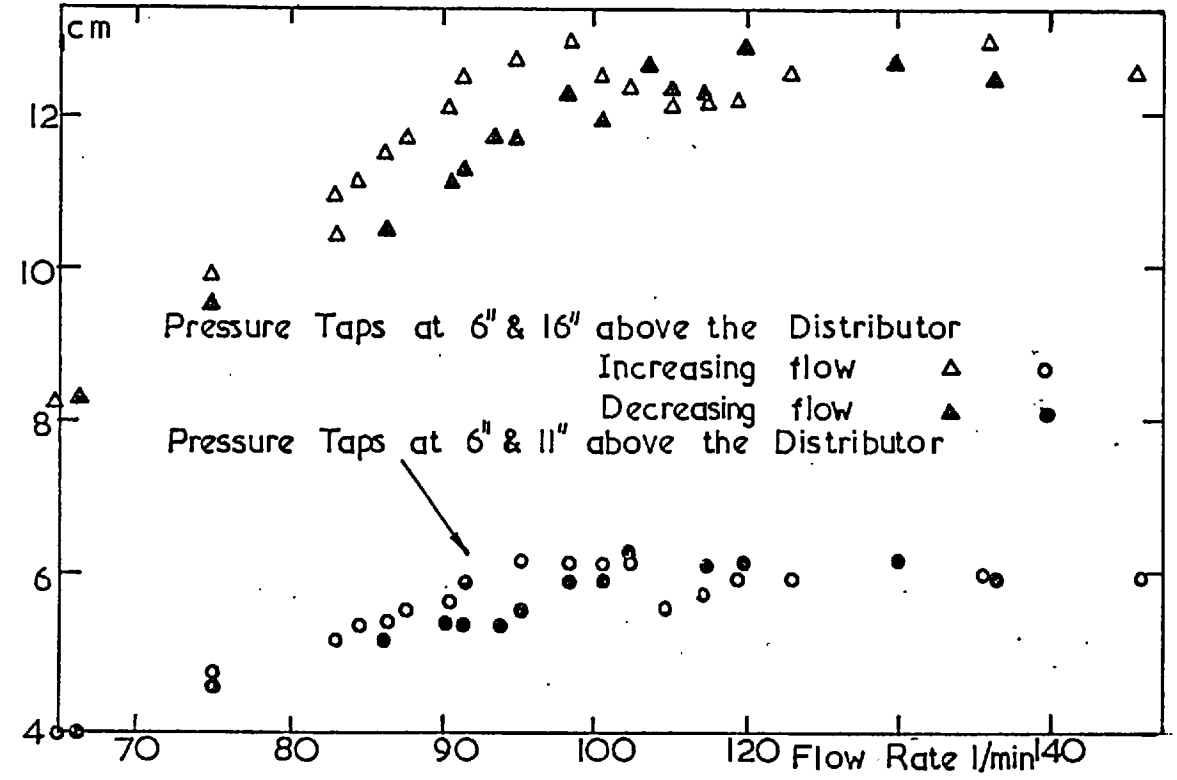
cm
Pressure Taps at 6" & 16" above the Distributor
Increasing flow
Decreasing flow
Pressure Taps at 6" & 11" above the Distributor
Flow Rate l/min

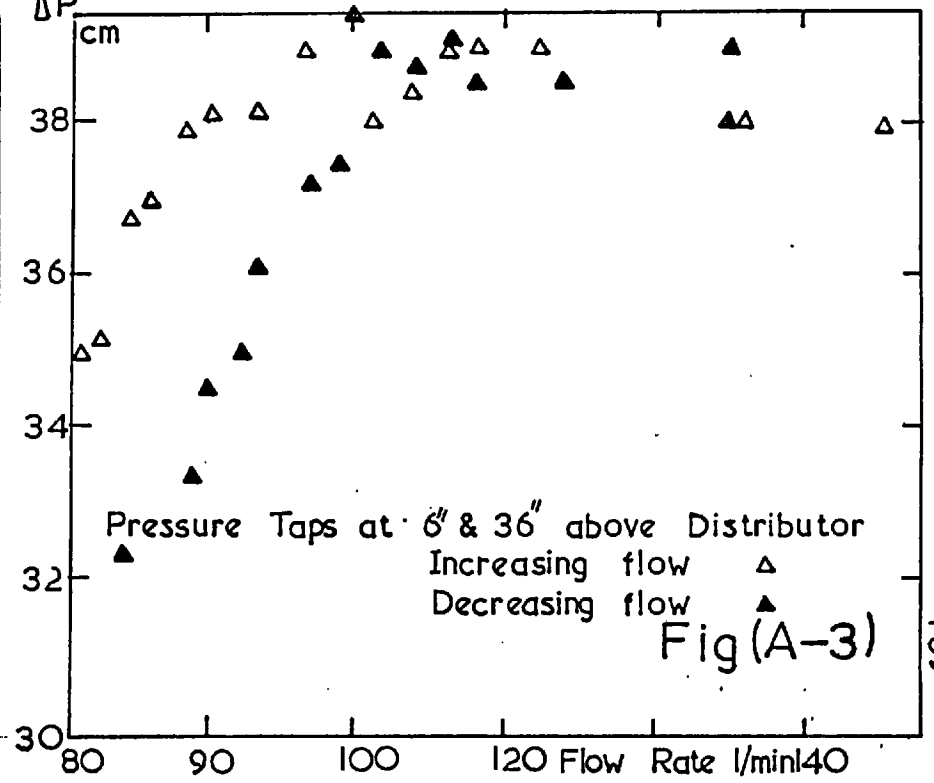
ΔP
cm
Pressure Taps at 6" & 36" above Distributor
Increasing flow
Decreasing flow
Flow Rate l/min

Fig (A-3)

small variance. In order to get an idea about the quantitative magnitude of the variance some experiments were performed with ballotini grade 10. The magnitude of the incipient flow rate Q_{mf} is given in the following table and the corresponding pressure drop curves are presented in Fig.(A2) and Fig.(A4). The pressure drop was determined as a function of increasing and decreasing flow rate. The distance between the probes in all these experiments was 5" except in two cases in which it was 10". The lower probe was always 6" above the distributor. The liquid in the manometer tube was either water or TETRABROMETHANE with a density of 2.97 g./cc. No significant difference between the quality of these curves obtained under various conditions was noticeable.

Run	1	2	3	4	5	6
Q_{mf} l./min	35	35	36	35	37	35.5

From these data the variance was calculated and has a value of

Var $(Q_{mf}) = 0.5$. This corresponds to a standard deviation of about 0.7 which is seen to be negligibly small.

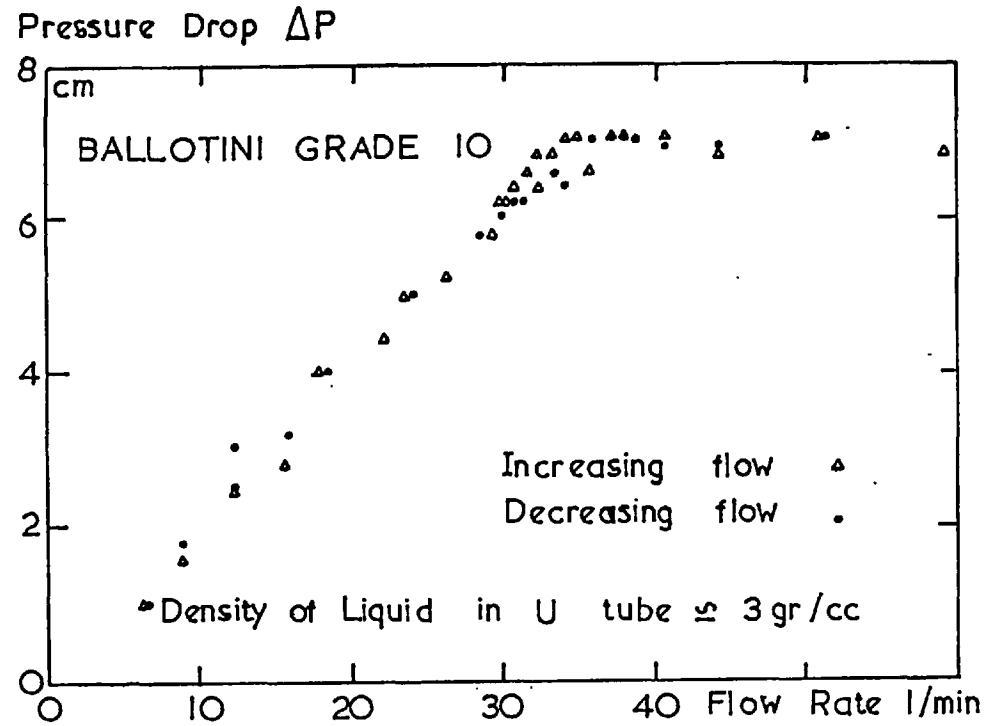
Pressure Drop ΔP
cm
BALLOTINI GRADE 10
Increasing flow
Decreasing flow
Density of Liquid in U tube ≤ 3 gr/cc
0
2
4
6
8
10
20
30
40
Flow Rate l/min

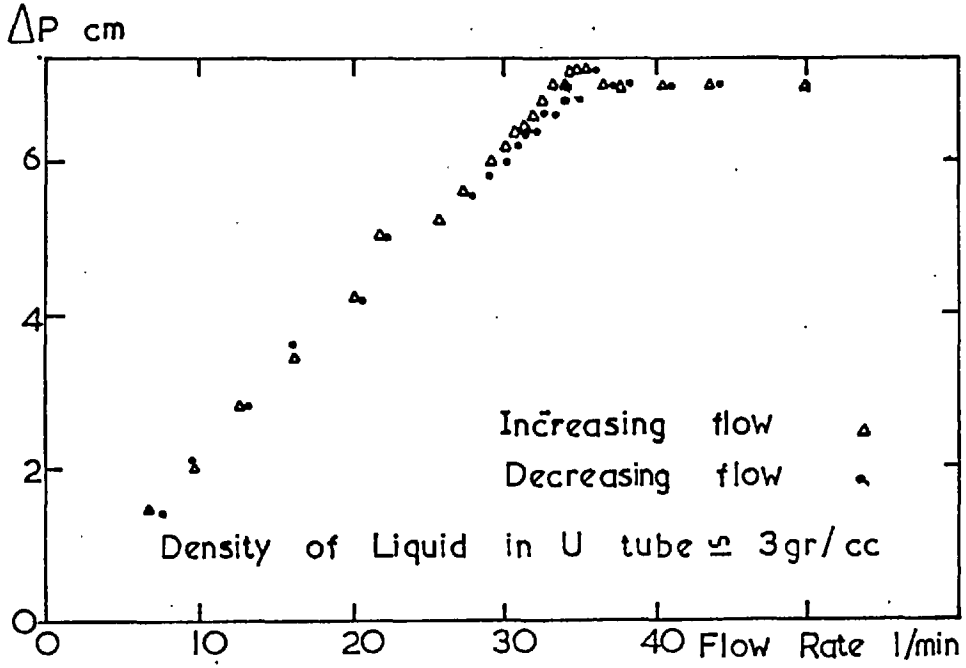
ΔP cm
Increasing flow
Decreasing flow
Density of Liquid in U tube ≤ 3gr/cc
0
2
4
6
10
20
30
40
Flow Rate l/min

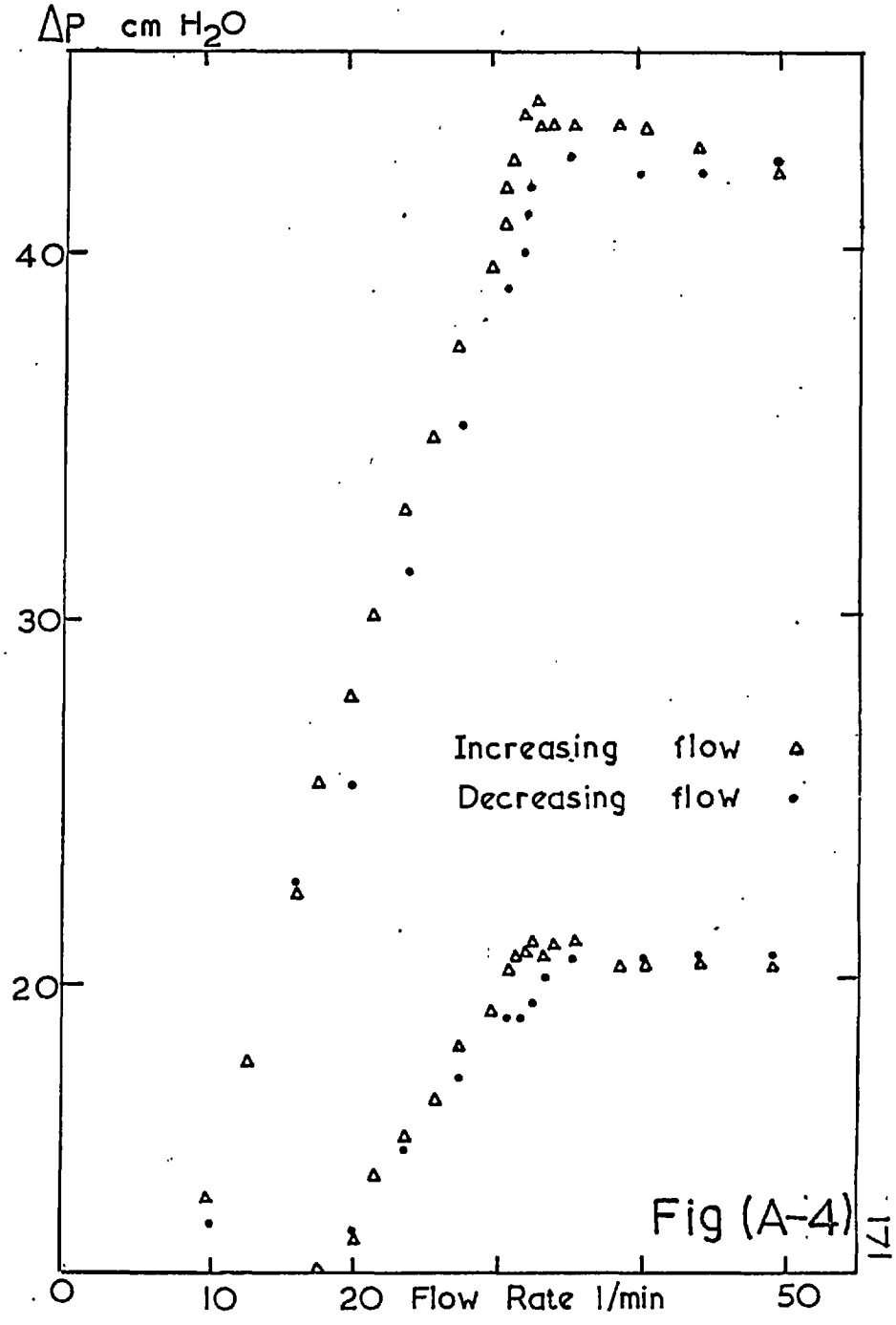
ΔP cm H2O
Increasing flow
Decreasing flow
0
20
30
40
10
20
50
Flow Rate l/min

Fig (A-4)

APPENDIX (III)

GROWTH OF A SINGLE BUBBLE

As was discussed previously when a bed is operated at some fraction of the incipient velocity Uo the top of the bed might be bubbling due to the gas expansion. Now in order to have the bed fluidized at some given level, a specific rate of flow must be maintained at the foot of the bed. The magnitude of this flow rate at atmospheric pressure would be smaller for higher levels. In other words for a given flow rate at the foot of the bed, there would be an excess flow V_E above what is necessary for incipient fluid rate at each level. The magnitude of this excess flow would be greater for higher levels. It is possible to show on theoretical grounds that the volume flow rate of the gas necessary for incipient fluidization is inversely proportional to the height above the distributor. However, such a relationship would contain parameters the determination of which are not straightforward. Instead let us assume that the necessary flow for incipient fluidization Vx (cm^3/sec) at a height X (cm) could be approximated by a polynomial like:

$$V_x = A + BX + CX^2 + DX^3 \text{ etc.}$$

where A, B, C and D are to be evaluated experimentally. If the bed is operated at some flow rate V_F, the excess flow at each level is given by:

$$V_E = V_F - V_X = V_F - (A + BX + CX^2 + DX^3 \text{ etc.}) \qquad \text{Eq.(A.III.1)}$$

Suppose we have a two-dimensional bed of particles which is

fluidized by some flow rate V_F, and also suppose that we have a bubble of diameter D_B, constant velocity U_B and volume V_B in the bed. We impose a velocity U_B in the reverse direction of the motion of the bubble on the whole system. Now the bubble is stationary and the particulate phase is moving downwards with a velocity U_B with respect to the bubble. A layer of emulsion phase with a thickness dx takes a time interval dt to cross the boundary of bubble. We have then $dt = \frac{dx}{U_B}$. During this period of time there is an excess flow equal to $(V_E\ dt)$ available. We assume that a fraction C_{RT} of this excess flow is captured by the bubble. As a result of this the volume of the bubble is increased by an amount equal to dV_T given by

$$d\,V_T = (C_R)_T\ (V_E)_T\ \frac{dx}{(U_B)} \qquad \text{Eq.(A.III.2)}$$

Now consider the situation at the lower boundary of the bubble. It takes a time interval dt for a fresh layer of emulsion phase with thickness dx to be formed next to the lower boundary and just outside the bubble (i.e. it takes a time dt for a hypothetical layer of emulsion phase of thickness dx to get out of the bubble). During this time interval $dt = \frac{dx}{U_B}$ there is an excess flow $(V_E)_B dt$ supplied by this layer. It is assumed that the fraction of this layer which is influenced by the presence of the bubble is exhausted from excess flow, then the flow absorbed by the bubble and hence the increase in its volume would be given by:

$$d\,V_B = (C_R)_B\ (V_E)\ \frac{dx}{U_B} \qquad \text{Eq.(A.III.3)}$$

where C_{R_B} is the fraction captured by the bubble. Adding Eq.(A.III.2) and (A.III.3) we get the total increase in the volume of the bubble during a time interval dt:

$$dV = \frac{(C_R)_B\ (V_E)_B}{(U_B)_B} + \frac{(C_R)_T\ (V_E)_T}{(U_B)_T}\ dx \qquad \text{Eq.(A.III.4)}$$

We further assume that $(V_E)_B = (V_E)_T = (V_E)_C$ (where C denotes the position of the centre of the bubble). This is justified because V_E is a weak function of the height. We also assume that $C_{R_T} = \frac{D_B}{L}$ where L is the width of the bed, and $C_{R_B} = \frac{1.5\ D_B}{L}$. The factor 1.5 is because it is believed that the effect of the presence of the bubble extends down to 1.5 D_B below the bubble (cf.TOEI & MATSUNO). For the volume of the bubble we have:

$$V_B = \frac{\pi\ s\ D_B^{\,2}}{4}$$

where V_B and D_B are the volume and diameter of the bubble and s is the bed thickness. For the velocity of the bubble, U_B, we have:

$$U_B = \tfrac{1}{2}\sqrt{g\ R_B}\ ,\ R_B \text{ being } \frac{D_B}{2}$$

It follows that:

$$U_B^{\,4} = \frac{g^2}{16\ \pi\ s}\ V_B \text{ or } U_B = \frac{g^{\frac{1}{2}}}{(16\ \pi\ s)^{\frac{1}{4}}}\ V_B^{\frac{1}{4}}$$

and also

$$C_{R_T} = \frac{2}{L\sqrt{\pi\ s}}\ V_B^{\frac{1}{2}}$$

$$C_{R_B} = \frac{3}{L\sqrt{\pi\ s}}\ V_B^{\frac{1}{2}}$$

Substitution into Eq.(A.III.4) gives:

$$V_B^{-\frac{1}{4}}\ d\ V_B = \frac{5(16\ \pi\ s)^{\frac{1}{4}}}{L\sqrt{\pi\ s\ g}}\ V_E\ dx$$

Integration between V_{B_1} and V_{B_2}, and X_1, X_2 gives:

$$4/3\left[V_B^{\,3/4}\right]_{V_{B_2}}^{V_{B_1}} = \frac{5(16\ \pi\ s)^{\frac{1}{4}}}{L\sqrt{\pi\ s\ g}} \int_{X_1}^{X_2} V_E\ dx \qquad \text{Eq.(A.III.5)}$$

For V_E we have:

$$V_E = V_F - (A + BX + CX^2 + DX^3 + \ldots\ldots)$$

where V_F is the operating flow rate and A, B, C and D are constants.

The magnitude of these constants for ballotini grade 10 was found experimentally and are as follows:

$$A = 619.85 \text{ cm}^3/\text{sec} \qquad B = -0.73 \text{ cm}^2/\text{sec}$$

$$C = 0.93 \times 10^{-3} \text{ cm/sec} \qquad D = -0.34 \times 10^{-5} \frac{1}{\text{sec}}$$

V_F was measured in the usual way. With these information the left hand side of the Eq.(A.III.5) was integrated and then the volume of a given bubble was calculated at various heights. These results are presented in Fig.(25).

P A R T T W O

CHAPTER 1

INTRODUCTION

That an exact knowledge of the pressure distribution in a gas fluidized bed is of utmost importance in the understanding of the gas fluidized systems, cannot be over emphasized. The formulation of the gas and solid flow patterns in the neighbourhood of a rising bubble as given by the elegant model proposed by DAVIDSON (44) is a striking example where the explanation of the behaviour of these systems leans heavily on this requisite knowledge. Pressure, velocity, voidage and interparticle force distribution in a gas solid system are interrelated. The remarkable stability of the roof and floor (i.e. top of the wake) of a rising bubble has very much to do with the velocity distribution of the percolating gas through the boundary of the bubble. Hence, a knowledge of the pressure distribution around a rising bubble, being the related variable, becomes very desirable. Pressure distribution, when measured experimentally also provides a means for the comparison of various analysis proposed for the description of the behaviour of bubbles in terms of the fluid and particle mechanics.

There is no doubt in the light of the above statement, that a study of pressure distribution is highly desirable. Any attempt at studying this problem would be highly rewarding in that the results of such study would greatly benefit the advancement of the understanding of some of the most important aspects of bubbles in gas

fluidized systems which is the aim of the present work. Therefore the following part of this work is going to be devoted to the study of the above mentioned problem.

CHAPTER 2

LITERATURE SURVEY

WACE & BURNETT (45) investigated the pressure distribution around a stationary bubble model consisting of a gauze sphere. The sphere was suspended in a bed and the adjacent pressures were picked up by a moveable probe. The sphere suspension, a $\frac{3}{16}$ in. diameter brass tube, was soldered to the bubble at the top and the bottom of the latter. The pressure-tapping was drilled through the tube in the centre of the bubble. The pressure isobar prepared had a curvature close to the bubble. Particles above the roof of the bubble were observed to be loosely packed and this was a disadvantage for the model. The fact that the bubble-model was stationary also made the situation unrealistic. However, the general conclusion is seen not to be in conflict with the results obtained in more realistic situations to be mentioned later. The authors also reported in their paper a preliminary record provided by G.A. HENWOOD of the pressure change round a moving gauze sphere picked up by a probe fixed at distance of almost one bubble diameter from the model bubble. The result is seen to be in broad agreement with later works. DAVIDSON & HARRISON (4) defined that the necessary pressure to bring about the particle motion was the sum of the pressure within the fluidizing fluid and the interparticle force, i.e.

$$P = p_f + p_p \qquad \text{Eq.(1)}$$

where P = overall pressure calculable from Bernoullie.

p_f = pressure within the fluidizing fluid.

p_p = pressure due to the interparticle forces.

They suggested that if p_p was large and positive, then it was unlikely that the particulate phase would behave as fluid of zero viscosity. The negative value was suggested to be impossible because it would imply tensile forces between particles. Therefore, the only possible situation fully consistent with the assumption of zero viscosity of the particulate phase would be $p_p = 0$. The pressure within the fluid p_f was shown to be the solution of the Laplace's equation for p_f with the proper boundary conditions. They derived an expression for P along the vertical axis of a bubble which was suggested to be incorrect because it did not satisfy the condition of constancy of the pressure in the bubble. For this expression to be correct, it was necessary that the velocity of the bubble be given by:

$$U_b = (2\ g\ a)^{\frac{1}{2}} \qquad \text{Eq.(2)}$$

for the three-dimensional case where U_b and a are the bubble velocity and radius and g is the acceleration of gravity. It was shown that Eq.(2) was justified. They argued that P and p_f could then be compared and the difference would be an indication of the interparticle forces. The comparison showed that interparticle pressure p_p was small at all points on the vertical axis of the bubble.

REUTER (46) was the first one to investigate experimentally the problem of the pressure distribution around a real rising bubble in a gas fluidized system. He employed a rectangular fluidized bed. The bubbles were formed so that they crawled up one of the wider faces of the bed; the motion was consequently three-dimensional, the bubble being effectively halved by the wall. A miniaturized inductive pressure transducer was used to pick up the pressure change as a

bubble passed the pressure-tapping located at the mid-line of the wall of the bed. The electronic equipment consisted of a carrier frequency measuring bridge in conjunction with a cathode ray oscillograph, the screen of which was photographed by a cine camera. The movement of the bubble was simultaneously photographed together with a watch for the purpose of synchronization of the pressure recordings and the photographs. The experimental results were reported in the form of graphs of the pressure distribution along the axis of symmetry and along lines parallel to the axis, and also in form of pressure isobars. In REUTER'S opinion the measured pressure gradient above and below the bubble was associated with the formation of compact layers of particles (reduced voidage) around the bubble which, it was concluded, accounted for the structural stability of the bubble.

ANGELINO et al (47) reported a decrease in voidage around the nose of the rising bubble. PYLE & STEWART (48) suggest that their flowrate, perhaps, was not adequate to prevent the formation of defluidized regions within the bed.

STEWART (49) compared the theoretical and experimental results of the pressure distribution around a bubble and concluded that many of the features of REUTER'S results (three-dimensional) were exhibited by the pressures from COLLINS' (50) analysis for two dimensions. This last comparison, though in principle questionable, showed that for example the centre of pressure was above the geometrical centre of the bubble; the magnitude of the pressure differences was less than those given by DAVIDSON'S analysis. It was also shown that the expression derived from the JACKSON (28) and MURRAY (21) analyses in all cases gave values of pressure much less than those experimentally observed. The latter analysis was invalid below the bubble because the

sign of the pressure difference expression was positive in that region. When REUTER'S experimental bubble velocity was used in JACKSON'S analysis instead of the theoretical one, the corresponding curve resembled more closely the curve defined by REUTER'S experimental results. The agreement of the results in this case was attributed to the fact that JACKSON'S expression for the pressure was derived from a particle momentum equation, including allowance for porosity changes, and hence the development of the fluid pressure approaching the bubble was controlled by the rate of change of particle momentum. It was then concluded that there was good reason to expect that porosity change of the type predicted by JACKSON existed.

LOCKETT & HARRISON (51) measured the voidage variations around a rising bubble using a capacitance probe technique. Their results were in qualitative agreement with those predicted by JACKSON'S analysis. However, they found that the voidage around a bubble was dependent on the particle size distribution. Smaller changes of voidage from the incipient value occurred near a bubble in a system of particles of uniform size than in a system with a wide size distribution. They also found that the region of increased porosity is of much greater thickness than the theory predicts. STEWART (52) showed that selection of a more appropriate bubble velocity in the theoretical analysis in the work of LOCKETT & HARRISON (51) could have given satisfactory agreement with the experimental results obtained in the case of particles of narrow size distribution and improved the prediction of the results in the case of particles with large size distribution. This was justified because the coefficient of the velocity of rise was a function of particle size and shape as shown by ROWE & PARTRIDGE (53). These findings were in strong conflict

with the hypothesis of the formation of compact layers of particles put forward by REUTER (54).

RIETEMA (55) applied soil-mechanical theory to fluidized beds. Much emphasis was laid on solid-solid interaction. Evidence for this was derived from various observations and in particular from electrical conductivity measurements in beds of charcoal particles. It was concluded that solid interaction was a normal phenomena which should be taken into account for the theoretical treatment of gas fluidized systems. This was clearly not in agreement with the findings of DAVIDSON & HARRISON (4), considered previously, that the inter-particle pressure was small. However, the model of the gas and solid flow around a bubble proposed by DAVIDSON(44), was not invalidated by this conflict. This was proposed by HIMSWORTH (56) who noticed that the particles in the dense phase of a gas fluidized bed, and in low voidage regions of a channelling liquid fluidized bed moved in a characteristically streamline fashion, whereas the particles in liquid fluidized beds at low voidage moved in a noticeably more random manner. It was suggested that the particles in low voidage regions were in almost continuous contact with one another, whereas this was not the case at high voidages. In a low voidage region each individual particle would be constrained to move at roughly the same speed and roughly the same directions as the particle with which it was in contact. It followed that a group of adjacent particles would tend to remain together, and would move in the orderly fashions that were required by DAVIDSON'S (44) equations. It was concluded that the demonstrable success of those equations was a consequence of the physical contact between particles.

BYSMAN & PEARSMAN (57) investigated the problem of the stability of the ceiling of an upside down fixed bed pressed against an upper

supporting plate by the flow of a fluid. The pressure drop at raining point was measured first when water was the flowing medium (where interparticle forces could be neglected) and then when air was the flowing fluid. From the comparison of the data it was possible to calculate some type of interparticle force which was defined by the authors. The method employed seems to be questionable. However, if the proposed model is considered to be correct, the examination of the data shows that the maximum observed interparticle force is about 20% of the weight of the particle. Also it is noticeable that at low humidity negative interparticle force could exist. This was suggested to be explained by the electrostatic forces being active at low humidity.

In this chapter the conflict between points of view concerning voidage variation around the bubble and effect of interparticle forces is given. The conflict in the case of interparticle forces has been discussed by HIMSWORTH (56). The conflict which is totally unexplained is the case of voidage variations. This is one of the main problems that we are concerned with in the present work.

CHAPTER 3

SCOPE OF THE INVESTIGATION

We are going to discuss why the present work was undertaken and what problems were planned to be investigated. We also want to see in what way the results of this investigation could help the understanding of the behaviour of bubbles in fluidized beds.

As was mentioned in the previous chapter JACKSON (28) showed on theoretical grounds that the voidage in front of a rising bubble in a gas fluidized bed is greater than the incipient value. Following JACKSON'S work, LOCKETT & HARRISON (51) measured the voidage in front of a rising bubble and found that it was greater than the incipient value. Although there was some difference in details between theory and experiment, the experimental results and the theoretical predictions were in absolute agreement in that the voidage in front of a rising bubble is greater than far away from it.

REUTER (46) recorded the pressure variation picked up by a probe fixed to the wall of the apparatus as a three-dimensional bubble was forced to crawl along the wall. Although his experimental method is questionable, because of the effect of the wall, he was able to pick up pressure variations which agreed qualitatively with the theoretical pressure curve given by DAVIDSON & HARRISON (4). STEWART (49 has compared the findings of REUTER with the theoretical predictions of DAVIDSON (44), JACKSON (28) and MURRAY (21). We will discuss the merits of this comparison later on. At the moment we concentrate on the argument put forward by REUTER (54) regarding

the voidage variation.

REUTER, on the basis of the pressure distribution, found experimentally, argues that voidage in front and behind a bubble has to be smaller than the incipient value. LOCKETT & HARRISON (51) following the work of REUTER measured the pressure distribution around a two-dimensional bubble. They obtain results in reasonable agreement with REUTER, however they conclude that the pressure distribution should be interpreted in terms of increased voidage near the bubble.

Now as was stated just above, the fact that voidage in front of a rising bubble is greater than far away from it, has been shown theoretically and confirmed experimentally from direct measurement of the voidage and also indirectly from the interpretations of the pressure distribution. (LOCKETT & HARRISON) The question is why REUTER in his argument starting with a correct premiss, i.e. relatively higher pressure gradient above and below the bubble, arrived at a conclusion which is clearly contradictory to what the theory suggests and experiment confirms, i.e. increased porosity. This is one of the questions we are concerned with.

That this undertaking is important is very clear and can be stated as follows. REUTER, by hypothesising the formation of compact layer of high solid concentration around the bubble explains the structural stability of the bubble. If it is shown that REUTER'S hypothesis is not correct then how could this remarkable structural stability of a bubble be explained. This is another question which is planned to be answered.

In REUTER'S experiments bubbles were always in contact with the wall of the apparatus which was slightly inclined to make bubbles visible. The results obtained were in qualitative agreement with the DAVIDSON & HARRISON predictions. This was discussed at some length

by STEWART (49). In these experiments the direction of the rise of the bubbles was different from normal due to the contact of the bubbles with the wall. Clearly an external force completely irrelevant to the dynamics of the system was imposed on the bubble. Effectively the particle movement near the nose of the bubble was in two dimensions, at least for some small region near the wall. At the foot of the bubble the presence of the wall imposed some restriction on the gas and particle motion. Altogether the pressure distribution and flow pattern were different from those of a freely rising three-dimensional bubble and hence the results of the measurements on such bubbles, although maybe in qualitative agreement with idealized theoretical prediction, do not provide a test when different theoretical predictions are compared.

In the light of the above argument one comes to the conclusion that the only way to obtain unambiguous results for the pressure distribution around a bubble is to use a two-dimensional bed. Any such measurement when combined with a knowledge of the exact position of the bubble provides reliable information. This is also another task which was undertaken during the course of the present work.

The literature survey given in the previous chapter and definition of tasks to be undertaken and goals to be achieved discussed in this chapter brings us to the time when this part of the present work was started in 1968. Preliminary measurements were carried in a small two-dimensional gas-fluidized bed discussed elsewhere (41). The results obtained were in agreement with the present results. However, it was decided to perform the experiments on a larger apparatus to eliminate any possible dimensional limitations.

Similar experiment has been performed by LITTMAN & HOMOLKA (58). Their work was handicapped in several ways. First and the most

important one, as acknowledged by the authors themselves, was that a precise knowledge of the position of the bubble was lacking. The size of the apparatus used was also small. (The width was about three times the bubble diameter). Results of their investigation was in broad agreement with the already available information. However, there were some anomalies which were not fully understood and explained.

This chapter is concluded by giving once again the questions to be answered by the present work in a summarized form.

1) What is the pressure distribution around a rising bubble in a gas fluidized bed ?
2) How could the structural stability of a rising bubble be explained ?
3) How does the pressure gradient distribution around such a bubble come into agreement with the already established knowledge on voidage distribution.
4) How could the anomalies in the literature be explained ?

CHAPTER 4

EXPERIMENTS

4.1 APPARATUS

The apparatus, a two-dimensional fluidized bed, consisted of two sheets (31"x83"x$\frac{1}{2}$") of perspex held apart $\frac{1}{2}$" from each other. The full description of the apparatus was given in part one. Glass particles ballotini grade 8 and 10, and coarse and fine samples of sand particles were used. The specification of the particles were given in part one.

For the measurement of the pressure around bubbles, the appropriate pressure tappings were connected to a micromanometer (HILGER & WATTS, TYPE M.D.C.) head ($_p$) with proper range. The output from the micromanometer was connected to an ultra-violet recorder (q) and in some cases to a cathode ray oscilloscope (r). An injection unit (s) was employed which could be adjusted to give a pulse with a desirable interval to the solenoid valve (t) which would inject a bubble into the bed when supplied with air. The solenoid valve was supplied from a completely separate air source, i.e. a cylinder (u) of pressurized air, through a reducing valve. The solenoid output was very close to the bed. The connecting tube was about an inch in length. The injection unit was also connected to the U.V. recorder and when a pulse was produced a mark on the output of the recorder was made through an internal event marking unit. This mark showed when an injection occurred. A flash discharging unit (v) was connected to the injection unit which illuminated a small bulb (w) situated in the field of the camera (o), when a pulse was produced. This made an impression on the cine film. The synchronization of the recorder and the camera was possible in this way. Injection and the subsequent motion of the bubble was recorded by a cine camera (16 frames/sec.).

4.2 EXPERIMENTAL PROCEDURE

The pressure-tapping in the path of the bubble (i.e. middle of the bed) and also the reference pressure tapping which was situated at the same height but away from the latter were connected to the proper micromonometer head. The proper range of the micromanometer was selected. The resistance in the line of connections between the manometer and the ultra violet recorder was selected such that the tracings had the minimum amount of noise disturbances and at the same time were of a reasonable amplitude. Proper speed for the recorder output was selected. The bed flow rate was adjusted to be close to the incipient value in such a way that an injected bubble neither expanded nor contracted appreciably during the period of rise. This meant that in some cases there was some spontaneous bubbling very close to the bed surface. The effect of these natural bubbles on the quality of the records will be discussed later. The injection interval and pressure was selected such that a bubble of desirable size was obtainable. The bed was illuminated from the rear and a flash bulb was put in the field of view; the discharging unit was connected to the injection apparatus. The event marking circuit between the injector and the recorder was closed.

A few seconds before a bubble was to be injected, the camera was put into operation by one operator; the other operator put the recorder in operation and injected a bubble. The process of injection simultaneously discharged the flash which put an impression on the film, and at the same time an event mark was produced on the records through the working of the event marking mechanism. A few seconds after the injected bubble had completely left the bed the camera and recorder were stopped. These provisions made sure that the whole history of events in the bed at the point of pressure-tapping, from

before the injection of the bubble, during the period of presence and rise of the bubble and after the bubble has left the bed was recorded. Synchronization was very exact through the technique employed. The whole sequence took something about six to eight seconds during which the speed of camera was known, from previous experiments, to be constant. For reproduction of the recordings the bed flow rate was checked and the running mechanisms of the camera was set to the initial condition and then the whole sequence was repeated. When the effect of a variable such as injection pressure, and/or interval, bed height, and background flow rate etc. was to be studied that variable was changed and the rest kept constant and the experiment was exactly repeated up to a desirable number of times.

Between consecutive runs it was necessary to protect the rear wall of the bed from the intense radiative heat of the illuminating lamps by putting a sheet of asbestos between the light source and the bed. In order to produce bubbles which did not split during the period of rise it was necessary, in a few cases, to inject a bubble before the bubble which was to be photographed was injected. No significant difference between recordings of such a bubble and a bubble injected without prior injection was detectable. However, the prior injection did not take place commonly because the reproducibility of bubbles were generally very good anyway and in particular those bubbles which split or were somehow different were quite interesting for the purpose of the study of the resulting effects on the readings.

4.3 EXPERIMENTAL RESULTS

A typical record of the pressure picked up by the micromanometer when a bubble was injected into the bed and rose up the bed is given in Fig.(1). In order to increase the contrast in the representation, the actual records have been traced onto tracing paper. This has been done for all the recordings. The vertical axis is pressure and the horizontal one is time. We notice that on the foot of records there is a mark. This mark shows when the injection of the bubble occurred and it is produced by an event marking mechanism discussed previously. It does not give any information about the duration of the injection and therefore the size of this mark on the record is a function of the speed at which the recording paper moves.

Fig.(2) shows the record picked up when two bubbles of identical size and under identical situations, (but slightly different from the injection presented in Fig.(1)) were injected into the bed one after another. A reasonable time interval was allowed to make sure that the effect of the first bubble on the pressure had completely ceased before the second bubble was injected. As was previously mentioned, the reproducibility of the experiment was generally very good. This is quite apparent from th examination of Fig.(2). There is a remarkably good reproducibility for the magnitude of the pressure in similar parts of the two records. Reproducibility is also very good along the time axis. In some parts of the curve along the time axis there is a negligible difference between the two curves which could be due to many reasons one of the most important of them the difference between velocities of the rise of the bubbles.

As it is seen from the curves in Fig.(1) and Fig.(2) there is some disturbance superimposed on the tracings. There are two reasons for these disturbances. First is that even when there is no

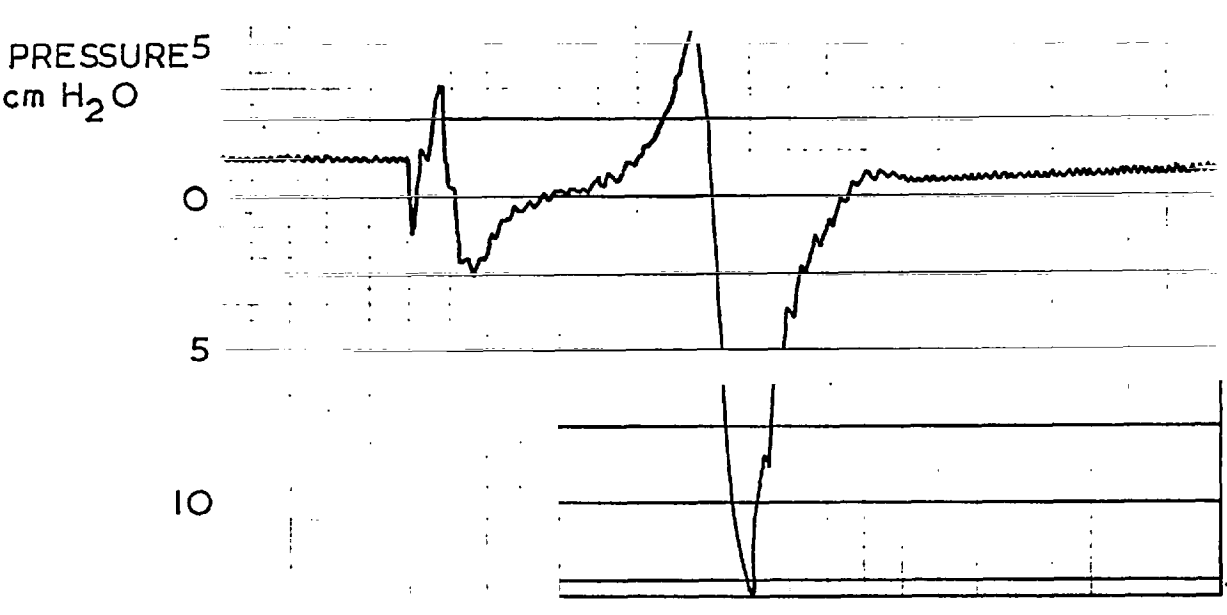

Typical Pressure Time curve for one Injected Bubble.

Fig (1)

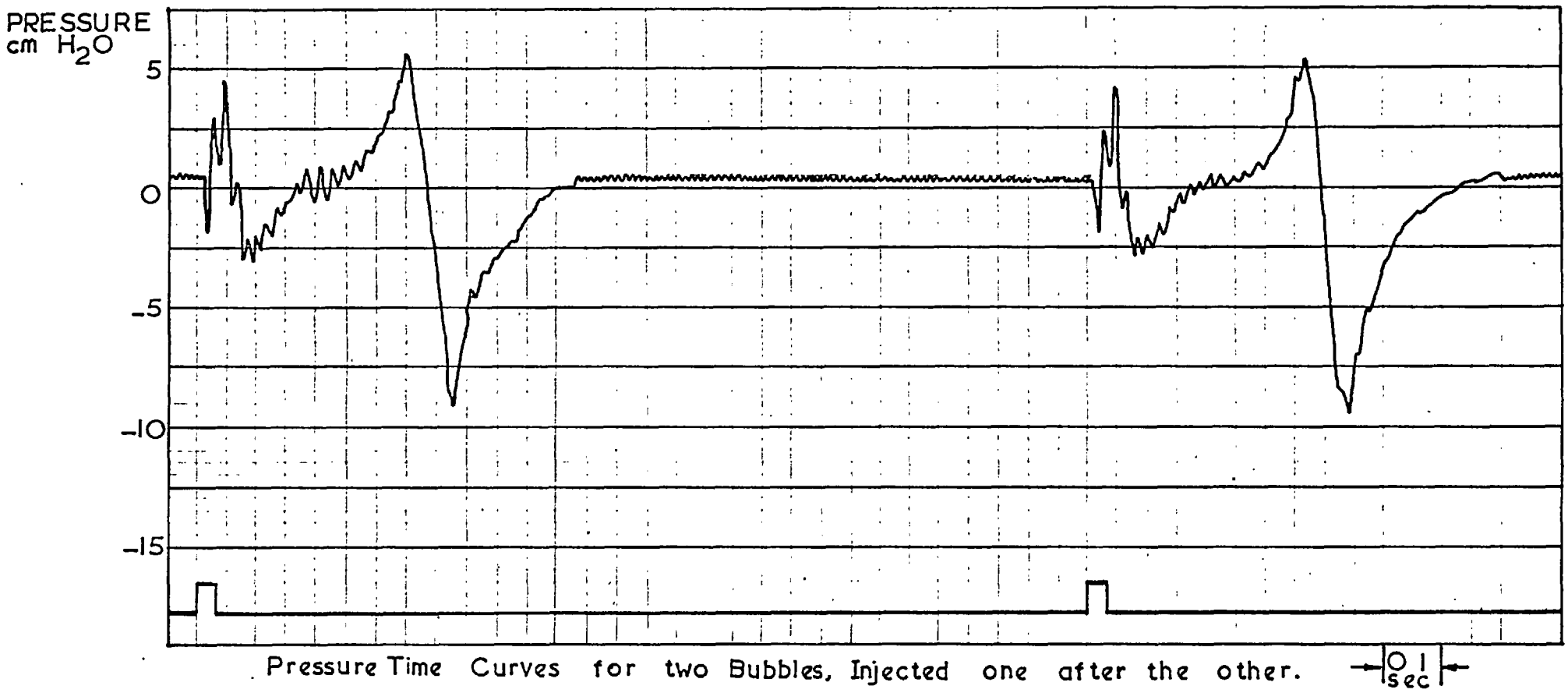

Pressure Time Curves for two Bubbles, Injected one after the other.

Fig(2)

connection between the micromanometer and the recorder, i.e., when the recorder is on its own, the output has a disturbance. Judging from the lines on the upper edge of the output and also the records obtained where there was no connection, this disturbance is the 50 cycle/sec. mains frequency. Therefore, this type of disturbance has no connection with the behaviour of the bed. The second reason is, however, due to the behaviour of the bed at various values of the flow rate of the fluidizing fluid. In Fig.(3) the pressure variation picked up by the probe at increasing flow rates are presented. Trace No.(1) is the mains 50 c/sec. No.(2) is when the bed is operating at a flow rate close to the incipient value. It is seen that there is not much difference between (1) and (2). The shape is still straight. At higher flow rates the shape deviates from straight and in addition to the 50 cycle/sec. mains frequency some sort of wave like disturbances are observed. This is believed to be due to spontaneous bubble nuclei which originate at higher levels in the bed when the whole bed is operated under incipient conditions. The type and orientation of the probe also has some influence on these disturbances. As the flow rate is increased at a value a few percent higher than incipient value, spontaneous bubbles become so large that their movement, if near the probe, cause pressure variations very similar to an injected bubble.

In order to make sure that the connection between the pressure tappings and micromanometer head were identical with respect to pressure drop inside the connecting tubes, and also other possible influential factors, the following experiment was performed. A few bubbles were injected into the bed under identical conditions. Then the connection between the pressure-tappings and the openings of the micromanometer head were reversed. Under the same conditions as the

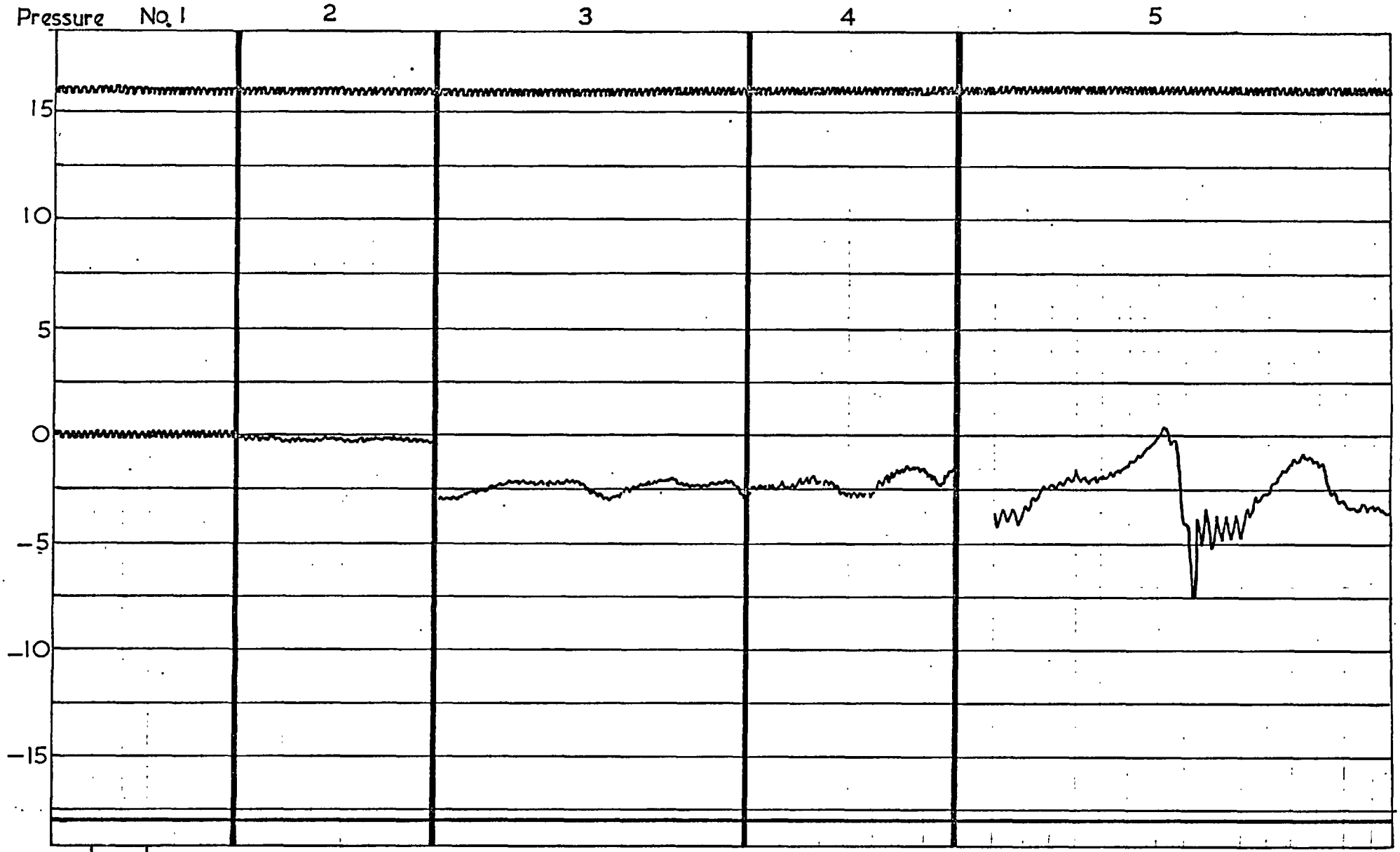

BEHAVIOUR OF BED AT VARIOUS FLOW-RATES

Fig (3)

previous injection a few bubbles were injected. The reproducibility of the obtained results was good with respect to the reproducibility of the injected bubbles. As is seen from Fig.(4) the effect is completely reversed. It was concluded that no significant difference between the lines of connection existed.

As is noticed the curves so far presented are pressure-time curves which are the direct output of the recorder. However, a precise knowledge of the position of the bubble with respect to the pressure probe is required if any conclusive inference is to be made from the pressure data. In other words, the pressure time-curves have to be converted to pressure-distance curves. To do this, as was mentioned previously, the motion of the injected bubble was recorded by a cine film at 16 frames/sec. A synchronization technique was employed to provide exact synchronization between the pressure-time curves obtained from the recorder and the distance-time data obtained from the analysis of the films. Thus it was possible to take recordings of the pressure picked up by the probe (recorded) and also of the distance of the bubble from the probe at identical moments of time. In this way pressure-distance curves were prepared. A typical pressure-distance curve constructed as explained above is given in Fig.(5). A typical record of the position of the injected bubble is also provided. This was obtained by tracing the boundary of the bubble at each frame when the film was projected onto a screen. Inclusion of this record is useful also when the effect of bubble deformation, splitting etc. on the pressure change at a point is being studied. On this curve the vertical axis is the pressure picked up by the probe. The probe is situated at origin (point "o") of the horizontal axis which gives the distance of the bubble from the probe. In other words for each point on the curve the ordinate of the point

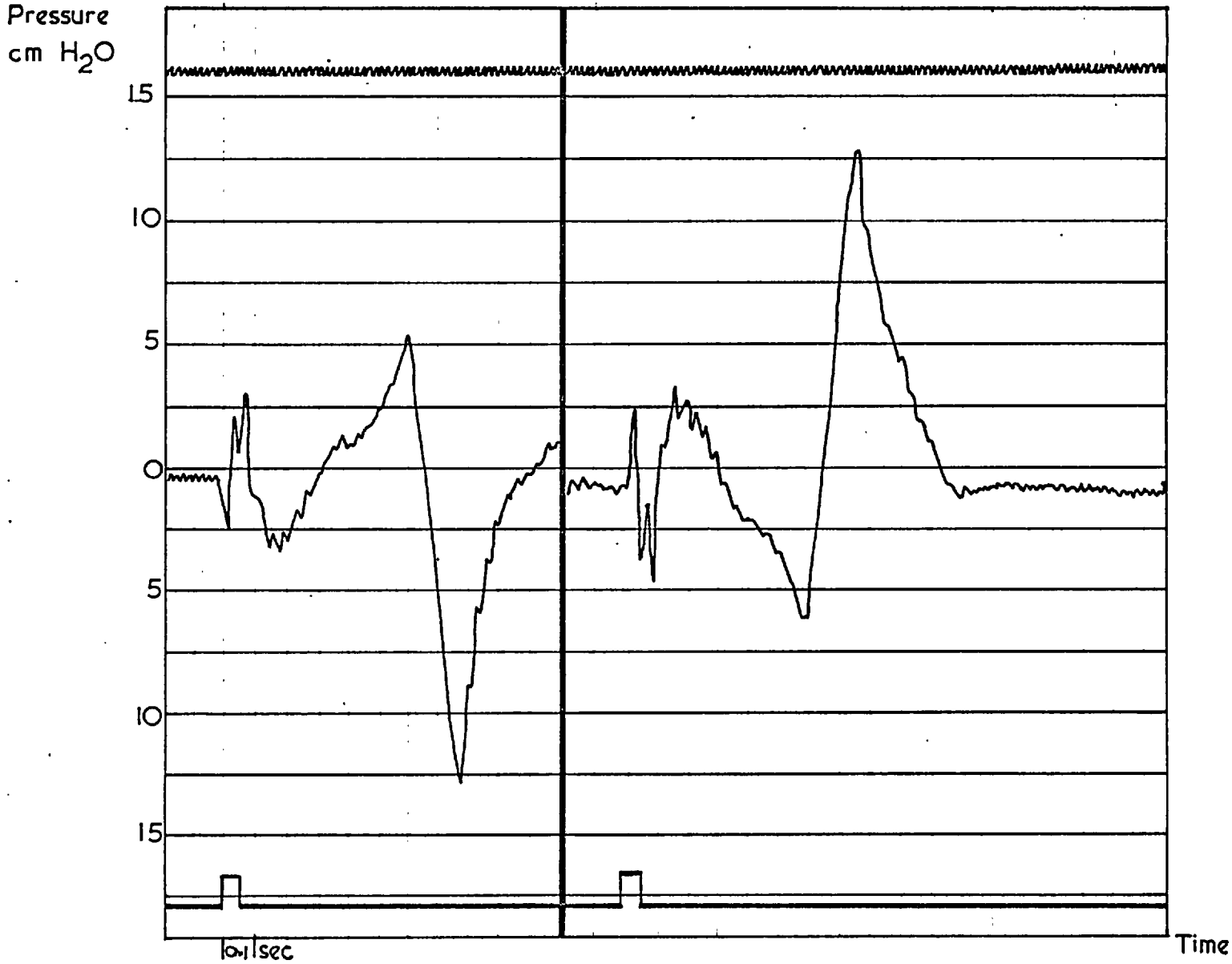

EFFECT OF REVERSING THE CONNECTION BETWEEN PRESSURE PROBES AND MICROMANOMETER

Fig(4)

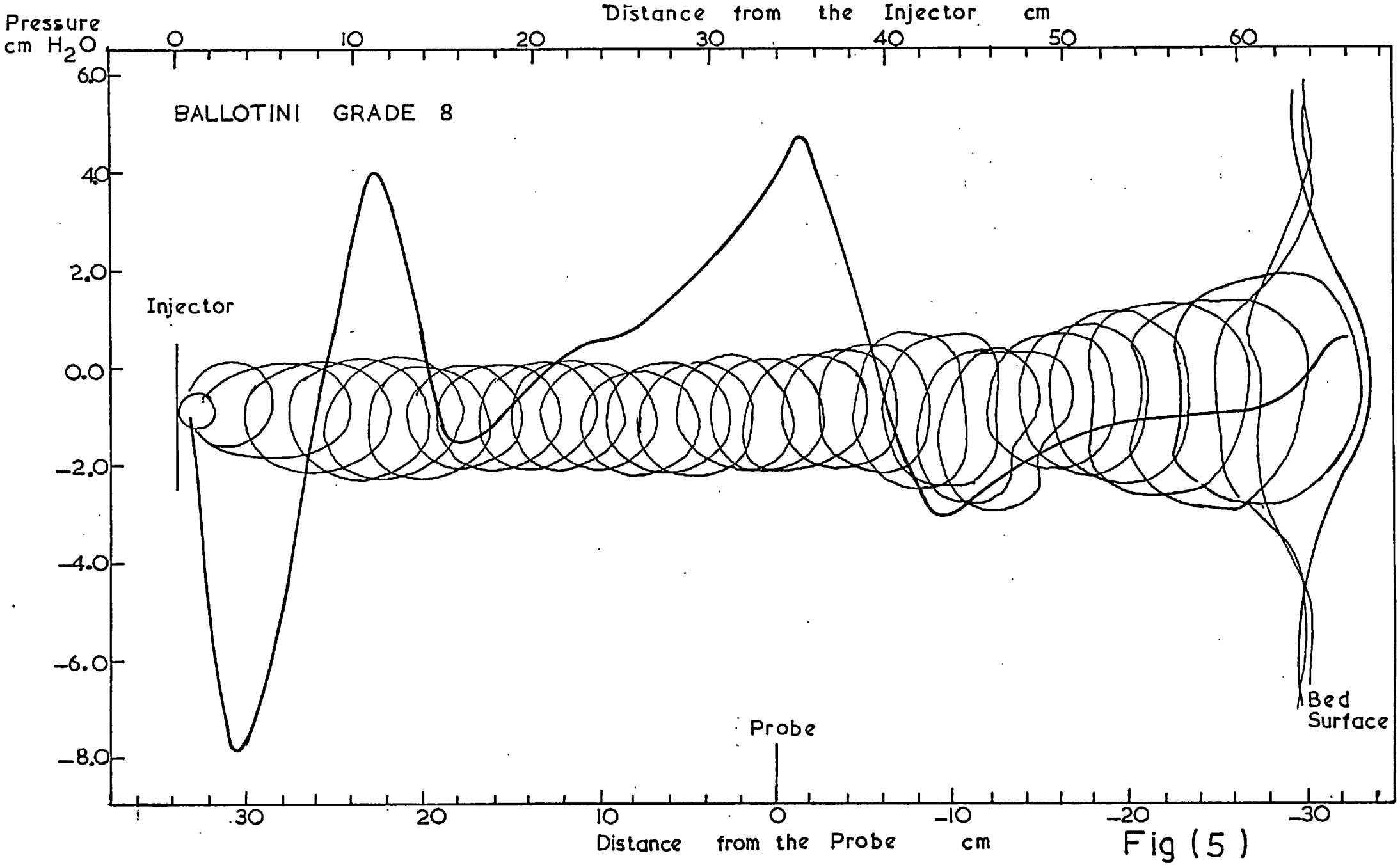
Pressure
cm H_2O
Distance from the Injector cm
0
10
20
30
40
50
60
6.0
4.0
2.0
0.0
-2.0
-4.0
-6.0
-8.0
BALLOTINI GRADE 8
Injector
Bed
Surface
Probe
30
20
10
0
-10
-20
-30
Distance from the Probe cm

Fig (5)

gives the pressure picked up by the probe when the distance of the tip of the bubble from the probe is given by the abscisa.

A more useful way of representation of the same data given in Fig.(5) is as follows: Consider when a bubble is injected in the bed and the pressure is picked up by two probes, one in the path of the bubble and the other far away from the bubble but at the same horizontal line. As was mentioned this is the pressure due to the presence of the bubble at various distances, i.e. the graphs show how pressure at a point is affected when a bubble approaches, embraces and passes the probe. Now consider the hypothetical situation where the bubble is held stationary and the set of the two probes are approaching the bubble, i.e. downwards with a velocity U_B. At each moment, and here at each distance from the bubble, the pressure difference between the probes is the absolute pressure on the axis of symmetry of the bubble at that point minus the hydrostatic pressure at a point far away from the bubble but on the same horizontal line. We notice that the situation is exactly the same as the previous case when the probes were stationary and the bubble was approaching with a velocity of U_B towards the probes. The analogy is exact for all the different situations. This means that we can transform Fig.(5) as follows:

We take point O, the origin on the distance axis, to represent the tip of the stationary bubble. Now every point on the distance axis represents the distance of the hypothetical moving probe from the centre of the hypothetical stationary bubble. In particular for the purpose of visualization, we take the circle best fitted to the bubble at the moment when it touches the probe and superimpose this circle on the so obtained diagram in such a way that the nose of the bubble rests at point O on the graph presented in Fig.(5). We further grade

the distance axis in multiples of the bubble radius. Bubble radius is taken to be unity which makes all the distances dimensionless. Such a curve is presented in Fig.(5a) which gives a very clear picture of the instantaneous distribution of pressure in front, below and also inside a rising bubble. For a point with some distance from the probe the instantaneous pressure can easily be read off from the graph.

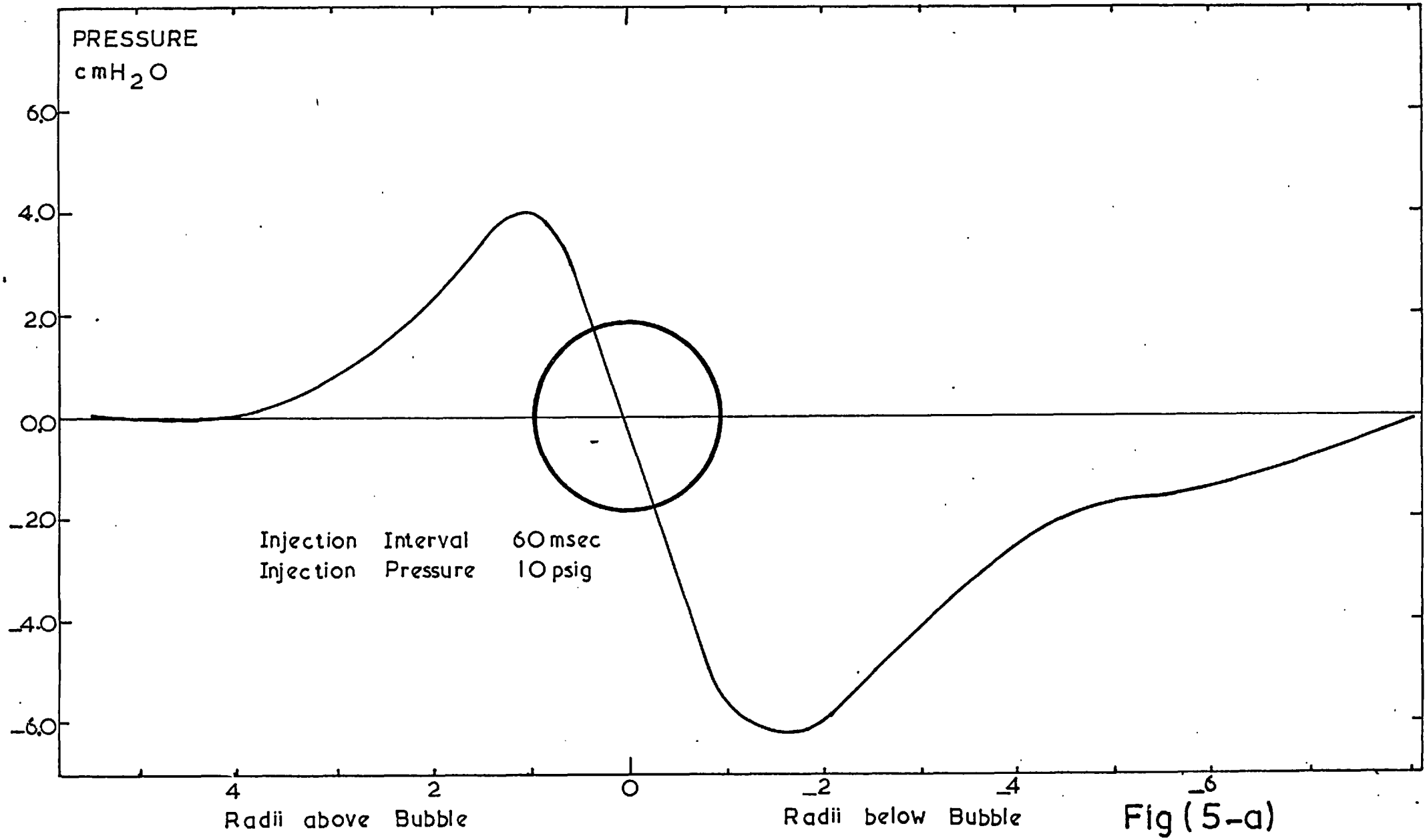
PRESSURE
cmH2O
6.0
4.0
2.0
0.0
-2.0
-4.0
-6.0
Injection Interval 60 msec
Injection Pressure 10 psig
4
2
0
-2
-4
-6
Radii above Bubble
Radii below Bubble

Fig (5-a)

4.4 DESCRIPTION OF VARIOUS PARTS OF THE PRESSURE CURVE

Fig.(6) is another way of representation of the data. The left-hand side vertical axis is the height above the injection point. The horizontal axis is the time from the moment of the injection of a bubble. The curve designated by (Height) is a plot of the distance of the tip of a bubble from the point of injection as a function of time. The position of the pressure probe is shown by a horizontal line. The shape of the bubble when it is near the injector, probe and at the time when it is just about to burst at the surface is given. This curve, apart from the initial and the tail portion where the injection effect and surface effects persist respectively, is reasonably straight, suggesting a uniform velocity of rise.

The left-hand side vertical axis is the pressure in cm of water. The curve designated by "Pressure" is the curve which was obtained as the bubble, discussed above, was injected and rose past the pressure probe. This curve was transformed from the recorder output and is represented here on a rather different scale.

The pressure curve given in Fig.(6) can be considered as the general form of the pressure-time curves. All various effects, not necessarily present in every one of the pressure curves, are present here. Such a curve can be divided into three basically different regions, each representing a particular effect. These regions are roughly shown on the curve by AB, BC, CD. Region AB corresponds to the effect of injection. There are some sharp and fast variations in the pressure. The shape of the curve in this region is very sensitive to the overall conditions such as the type of the probe, injection pressure, and background flow rate. We need not be concerned about the actual shape, which in this graph is different from the previous graphs at the moment. This will be discussed in more detail later on.

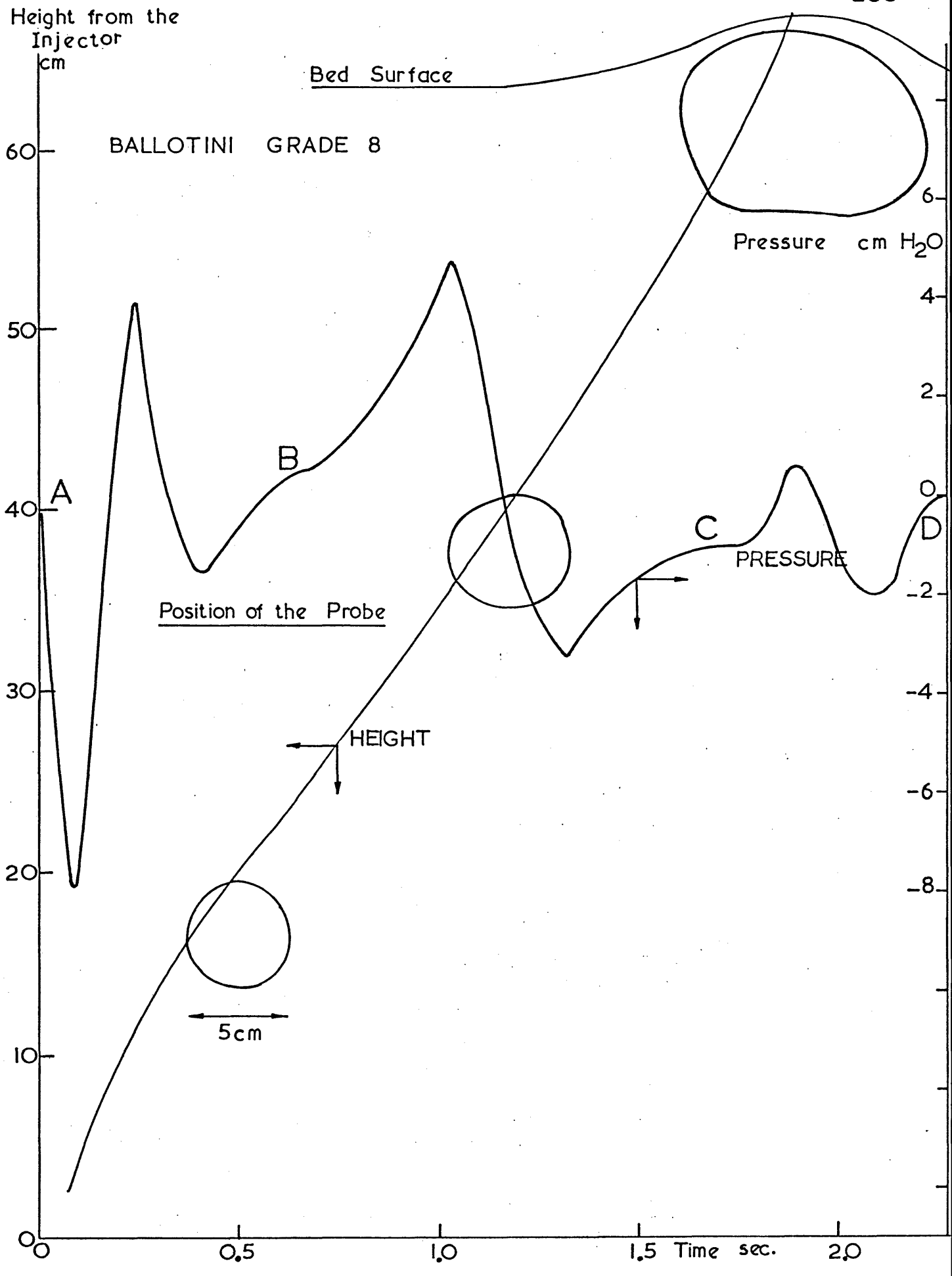
Height from the Injector cm
Bed Surface
BALLOTINI GRADE 8
Pressure cm H_2O
A
B
C
D
PRESSURE
Position of the Probe
HEIGHT
5cm
60
50
40
30
20
10
0
6
4
2
0
-2
-4
-6
-8
0.5
1.0
1.5
Time sec.
2.0

Fig.(6)

The next region which is the most important part of the curve is BC. This region which starts with a normal bed pressure (set at zero) corresponds to the pressure variation as the bubble approaches, embraces and leaves the pressure probe. This part of the curve will be discussed in full detail. Region CD is the effect observed when the bubble has produced a hump at the surface and is just about to leave the bed. This region was not observed unless the probe was situated fairly close to the surface. When this effect was present the previous region, i.e. BC was somewhat affected by the closeness of the bed surface and the probe. Therefore, when this region, i.e. BC was to be studied the height was increased so that no surface effect was observable. However, region CD also shows an interesting effect and was studied at some length to be discussed later. We notice that the free-hand continuation of the curve in region BC, from C, connects point C to D in such a way that the resultant curve resembles very much the curves presented in the previous figures. From point D, the pressure is more or less the same as the normal bed pressure and the condition is the same as prior to bubble injection.

The Initial Part of the Pressure Curves

It is seen from Fig.($_2$) that this portion is quite reproducible under identical situations. When injection occurs after a very small period of time of about 0.04 seconds a reduction in pressure is picked up by the central probe. After that, pressure starts to increase and at approximately 0.1 sec. a peak in the pressure is recorded. Then it starts to fall to a local minimum at about 0.2 seconds after the injection. From there the pressure starts to rise and reaches the normal bed pressure at 0.4 seconds after the injection. From this point the next portion of the curve starts.

Now the injection takes place with a pressure which is higher

than the pressure inside the bed at the point of injection. Therefore, at the moment of injection there is an instantaneous step change in the pressure. Consequently some sort of pressure wave may be formed which travels with a particular velocity defined by the overall properties of the system. Neglecting the initial reduction in the pressure picked up by the central probe for the moment, it is reasonable to say that the rise in the pressure picked up by the probe is due to the pressure front moving from the injection point towards the probe. The peak corresponds to the moment that the pressure front meets the central probe. If this pressure variation in the initial portion of the curve is really due to the injection of the bubble at a relatively high pressure then we would anticipate that a higher injection pressure would result in a higher peak. On Fig.(7) recordings obtained at identical conditions are presented. The only variable was the injection pressure which was selected to be at 5, 10, 15 psig. In each case two or more bubbles were injected to eliminate any uncertainty due to possible random variation of any uncontrollable factor. The reproducibility was good and here only one recording for each case is presented. It is clearly seen that at higher injection pressure the observed peak is distinguishably higher. When the injection pressure is doubled or trebled the magnitude of the peak correspondingly is almost doubled or trebled. We clearly see that the results of this test is highly satisfactory and is as it was anticipated. We further notice that the magnitude of the local minimum observed changes with respect to changes in the injection pressure. This is important when the significance of this reduction in pressure is analysed. It was claimed that at the time of injection a pressure wave may develop and the front move with some specified velocity (defined by the overall properties of the situation) towards

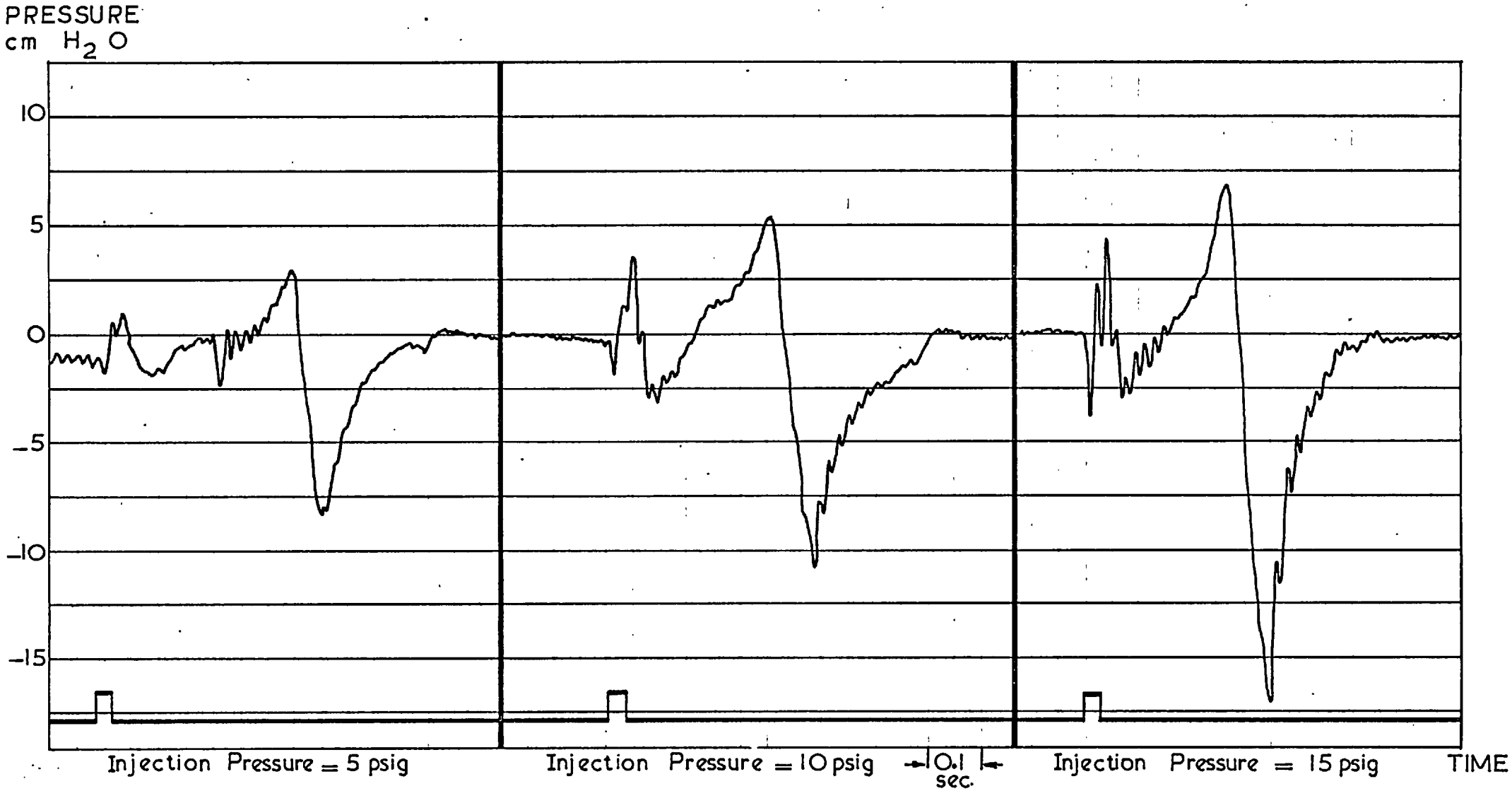

EFFECT OF THE INJECTION PRESSURE

Fig(7)

the central probe. We can design an experiment to check the validity of this proposal. Suppose that the distance between the injection point and the pressure probes was increased, then assuming that the pressure wave velocity is unaffected, then we would expect a corresponding time shift in the portion of the pressure peak recorded on the pressure-time curve. Fig.(8) shows the result of such an experiment. Identical bubbles were injected at two points. One was 41 cm and the other 51 cm below the pressure probes. Again more than one bubble were injected at each point to exclude the effects of random variations. Although small, there is indeed a clear time shift in the position of the pressure peak of the order of 0.01 second for a difference of 10 cm in the position of the injection point below the probes, giving a velocity of 10 m/sec for the wave front.

Another way to check whether part AB in Fig.(6) is really due to the effect of injection is as follows. We inject a few bubbles into the bed under identical conditions. Then keeping all the factors unchanged the injection interval (i.e. the time interval during which gas is fed into the bed) is changed and a few bubbles are injected. The same thing is repeated for various injection intervals. Then if part AB is really due to the injection we anticipate that this portion changes in a consistent way with respect to the change in injection interval. The results of such an experiment for injection intervals of 20, 60 and 100 m sec are given in Fig.(9). In each case more than one bubble was injected and the reproducibility of the effect was seen to be satisfactory. Now as it is quite clear from Fig.(9) as the injection interval is increased the duration of the observed peak is correspondingly increased. The result is seen to be highly satisfactory and again as anticipated.

It was claimed that the reproducibility of the initial portion

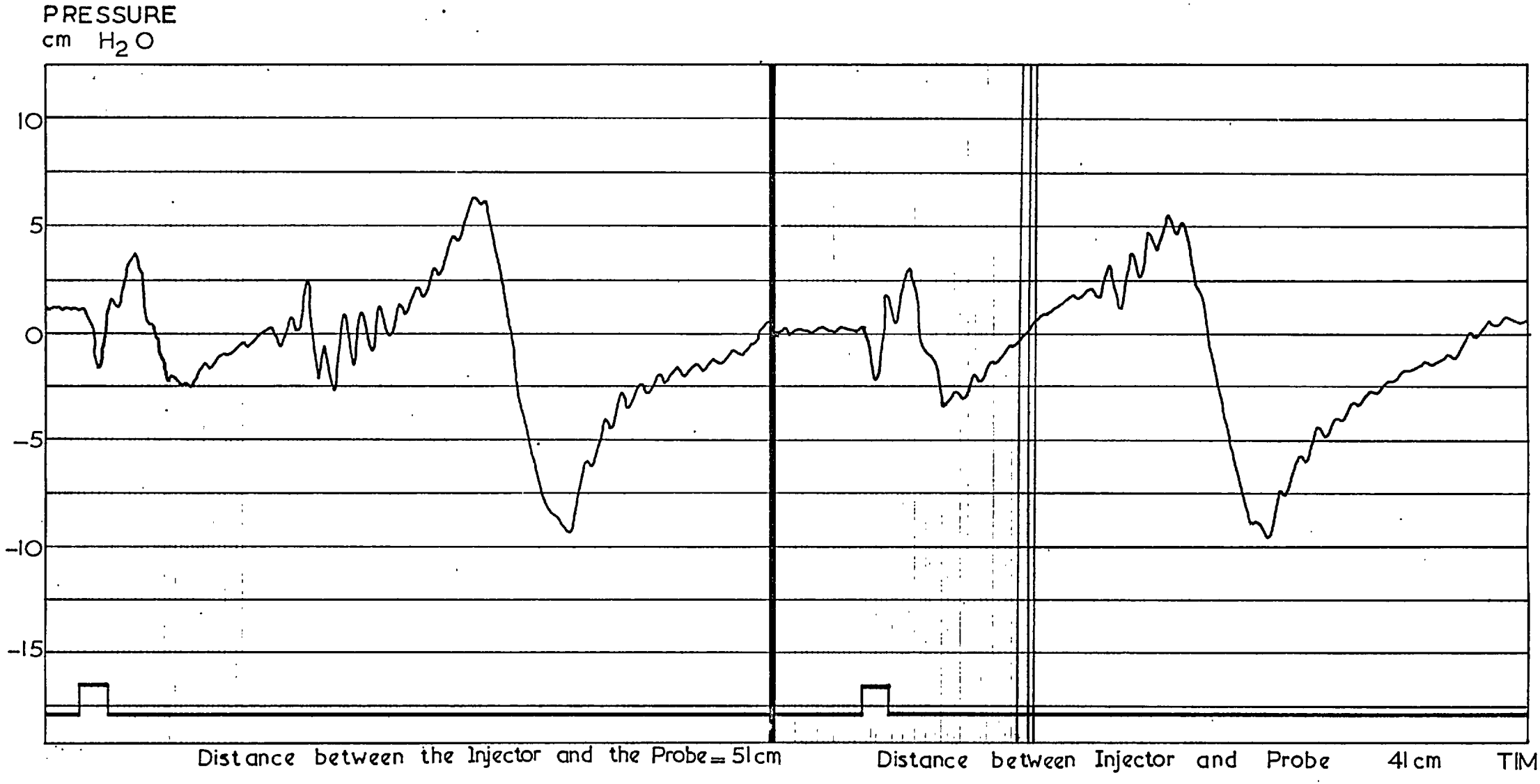

EFFECT OF THE DISTANCE BETWEEN THE INJECTOR AND THE PROBE

Fig(8)

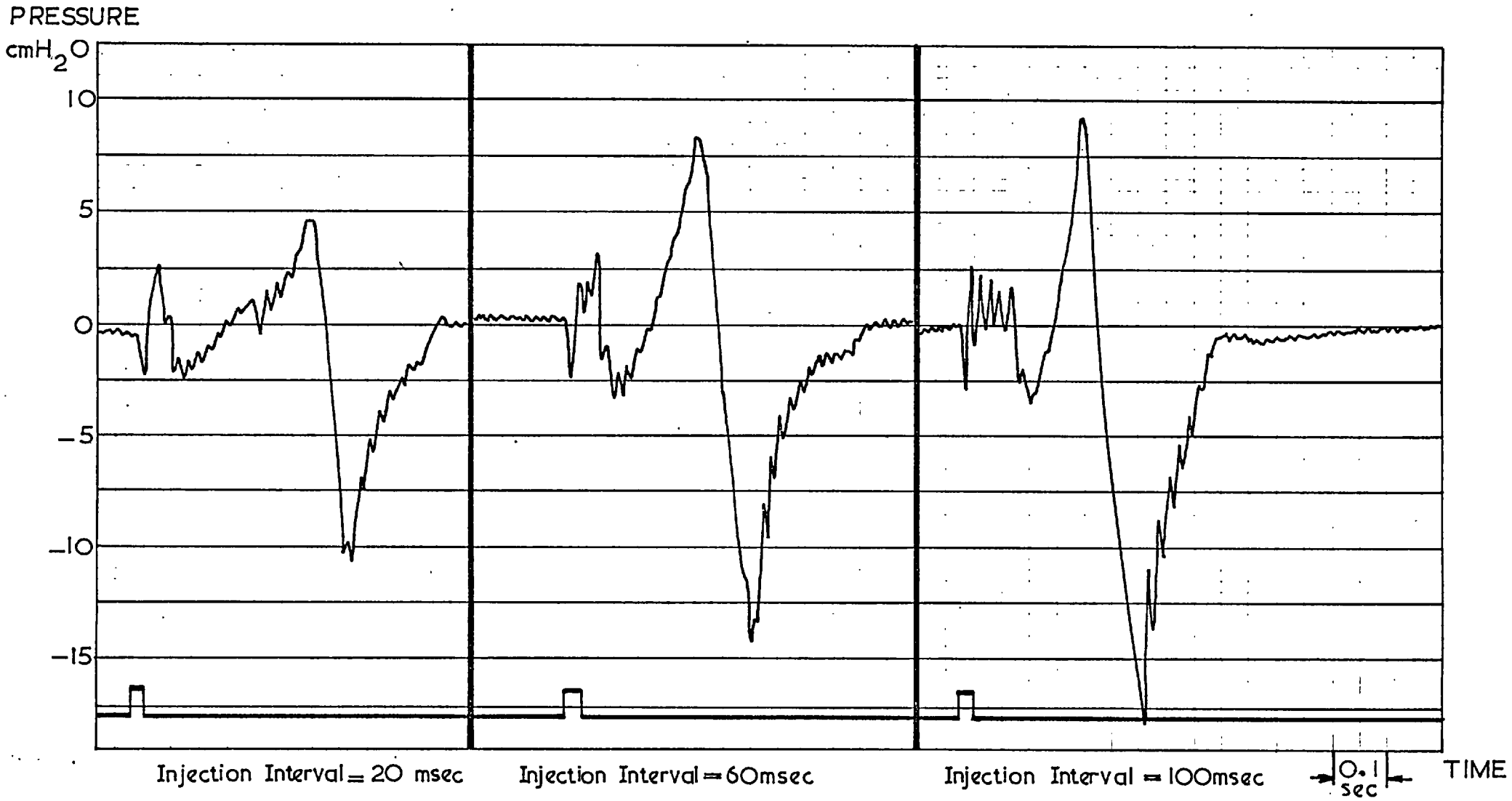

EFFECT OF THE INJECTION INTERVAL

Fig(9)

of the pressure curve was good. This statement is of course correct. However, the behaviour of the system in this part of the curve was very sensitive to the overall situation. A slight change of one factor resulted in some drastic change in this portion of the curve. Particle size, background flow rate, probe orientation are some of the influencing factors. One of the probes (which was used mainly for pressure gradient measurement, to be discussed later) had a marked effect on this part of the curves. The effect was such that the injection peak was not observed and instead the pressure started to decrease as a result of injection, cf. Fig.(5). A local minimum was picked up at almost the same time co-ordinate as the previously observed peak. The rest of the initial portion of the curve was, however, similar to what was observed when the other probe was employed. The reason for this change in the behaviour of the initial portion of the pressure curve was not fully understood. However, at each combination of the various factors the reproducibility of the initial portion was quite good and the position and magnitude of injection peaks were reasonably predictable. It is admitted that the overall picture in this portion of curve is still not very clear and in giving a general description, which embraces all variety of different combinations of various factors, attempts have not been very successful. This of course is not surprising in view of the large number of factors involved in gas fluidized systems, a few of which are known with reasonable certainty and even fewer being controllable. One has also to think of the fact that the instantaneous step change in the pressure due to injection makes the conditions even worse.

One of the factors contributing to the ambiguous respond of the bed with respect to the injection effect (i.e. initial portion of pressure curves) is the behaviour of the reference probe. Ideally,

one wishes that the reference probe (no matter where it be) remains neutral with respect to any occurring event in the bed; but this is not necessarily fulfilled. Of course it is possible to make sure that the reference probe has no response with respect to the movement of a bubble by selecting a proper size for the bubble and also locating the probe where no significant change results as the bubble passes up the bed. However, this does not necessarily mean that the probe has no response towards the actual injection of the bubble. Once the reference probe responds to the actual injection, there would be some interval of time over which the response persists. For instance, an increase in the pressure at a point caused by injection, at some other point, is followed by a decrease in the pressure when the cause is eliminated. The response is not necessarily instantaneous. Consequently even when the cause is eliminated the effect could be persistent. We have been thinking of some sort of wave generation and propagation when an injection occurs. However, response of the reference probe near the wall, with respect to an approaching wave, could be quite different from one in the same position but with no physical wall in its vicinity (i.e. in an infinite bed). The impact of the wave with the wall and its repercussions could very well result in a pressure variation at the reference probe long after the original cause (i.e. injection) has been completely eliminated. Thus the ambiguous behaviour and high sensitivity of the initial portion of the curve with respect to change in various properties of the system such as background velocity, etc. is not surprising. In view of these questions about the effectiveness of the reference probe, the use of static reference outside the bed was considered. However, we are primarily interested in the effect of the bubble only, and as we have seen, the process of injection causes

pressure waves in the bed, and events near the surface of the bed may also cause pressure waves. Accordingly it was decided that a reference within the bed, which would also be subjected to these extraneous disturbances, was the better choice.

Before we embark on the study of the other parts, there is one more point to be established regarding the initial portion of the pressure curves. Fig.(10a) shows a curve obtained when one of the openings of the pressure gradient probe was used in conjunction with the usual reference probe. We see that the pressure after a short interval following the injection decreases. There is a local minimum in the curve after which the pressure returns to the normal value of the system. When the height of the probe is changed by 41 cm the curve represented in Fig.(10b) is obtained. A shift of about 0.03 sec. time coordinate of the local minimum is noticeable. Now assuming a wave property for the factor which produces the pressure variation observed in the initial portion of the curve we can calculate the velocity with which this wave is moving. So far as the nature of this wave is concerned one can think of a perturbation in the velocity of the percolating gas as a result of the injection of a relatively high pressure puff of air. This velocity perturbation then would result in a porosity perturbation which would move with some specified velocity in all directions. This effect diminishes completely when it reaches the side walls of the bed where the reference probe is located. The central probe would pick up the effect of this perturbation as it moves towards and passes the probe. The calculated velocity of the propagation is about 13 m/sec.

Tail of the Pressure Curves

Part CD on Fig.(6) is believed to correspond to the moment when an injected bubble is about to leave the bed. This is apparent

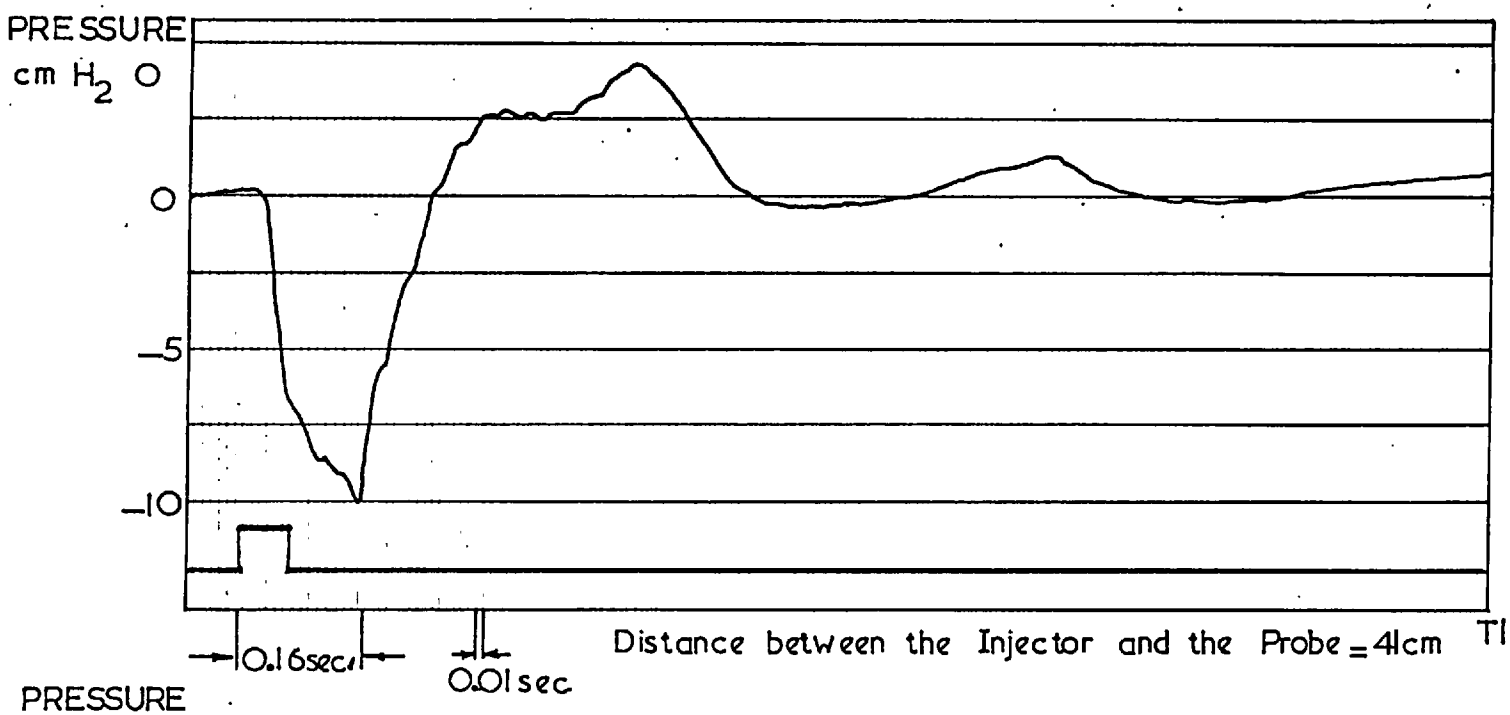

Fig. (10 a)

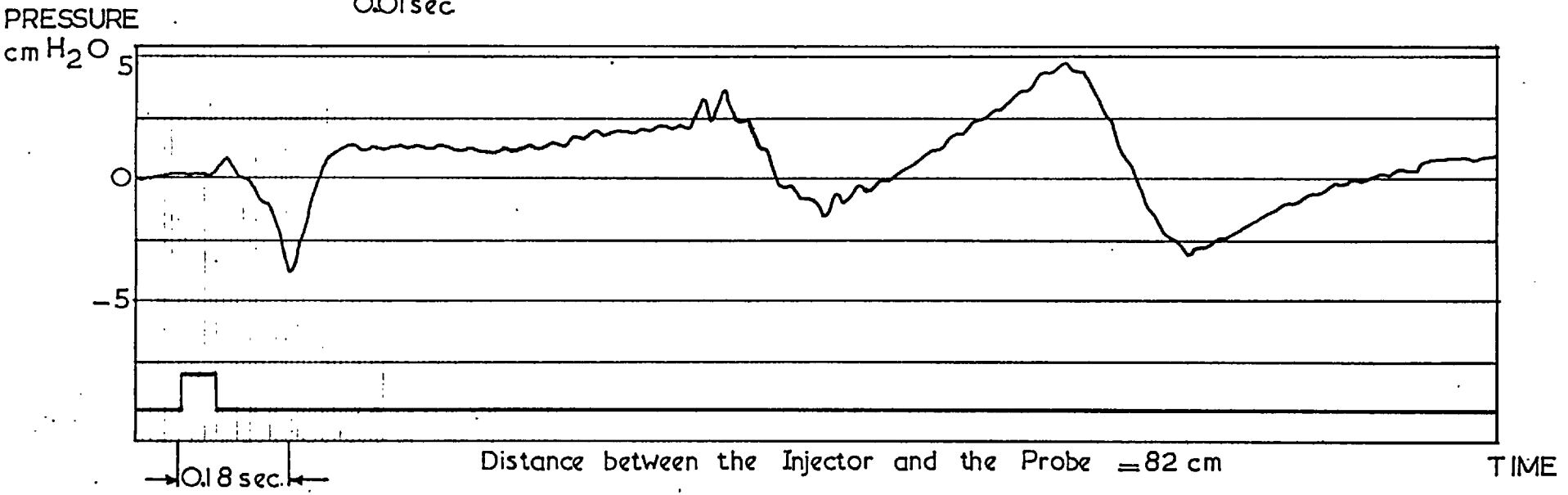

Fig.(10-b)

EFFECT OF THE DISTANCE BETWEEN THE INJECTOR AND THE PROBE

from the comparison of the position of the bubble and the pressure curve at the corresponding moment of time. Before point C the pressure curve slopes upward and provided the surface of the bed is away enough from the pressure probe the curve continues its upward movement until it reaches the normal bed pressure. However, when the bed height above the probe is not long enough portion CD is clearly distinguishable. As is seen from Fig.(6) the onset of this effect corresponds to the time when the bubble starts to produce a hump on the surface. A reduction in the pressure picked up by the probe follows. A local minimum is noticeable after which the pressure rises gradually to the normal bed pressure.

Now if the pressure variation in region C-D is indeed due to the interaction between the bubble and the surface of the bed then one would again anticipate a time shift in the position of this variation as the height of the bed is increased. Similar bubbles under identical conditions were injected into the bed, the height being the only variable. Resulting pressure-time curves are given in Fig.(11). It is seen that when the height of the bed is increased by 23 cm a time shift of about 0.2 second in the position of the kink on the tail of the pressure curve is noticeable. This suggests a velocity of about 115 cm/sec for the bubble near the surface. This indeed is a very high velocity. Now let us compare this velocity with the average velocity with which the bubble has moved from the injector towards the pressure probe. This distance is about 33.5 cm in this case and the bubble takes about 0.52 sec to travel this distance. The average velocity is about 64 cm/sec. Comparison with velocity of 115 cm/sec for the same bubble near the surface shows that the bubble is accelerated to at least twice its average velocity inside the bed. We notice that this twofold increase in the velocity is also notice-

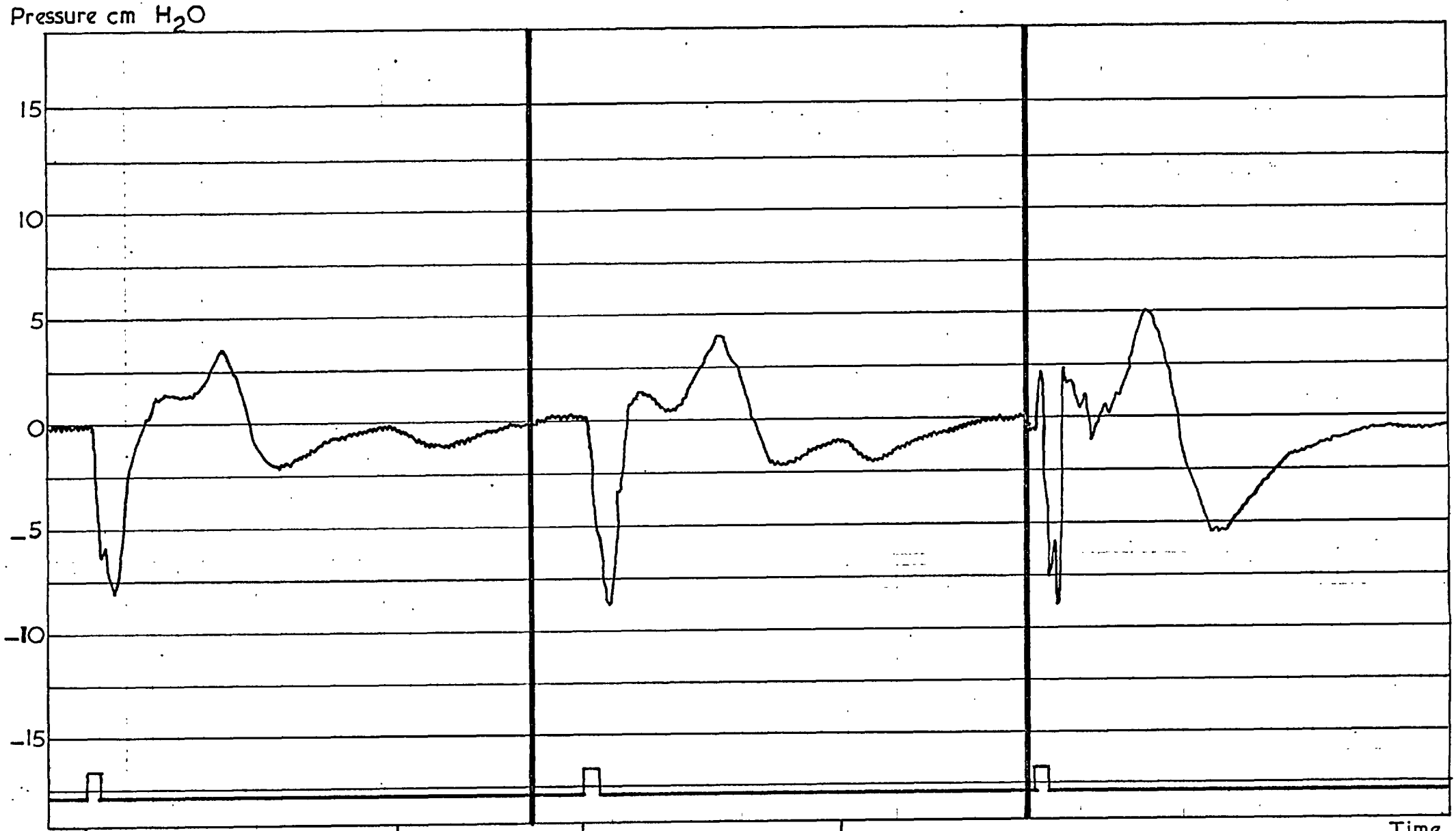

EFFECT OF THE BED HEIGHT ON THE SHAPE OF THE TAIL OF THE PRESSURE CURVE

Fig(11)

able from the example in Fig.(6). There the distance of the tip of the bubble from the injector is given at each moment of time from the injection. The examination of graph shows that the bubble velocity inside the bed is about 30 cm/sec and near the surface about 56 cm/sec. Although the actual magnitude of the velocity is smaller than the case in Fig.(11) (because the bubble was smaller), the two-fold increase in the velocity of bubble is apparent. Now a twofold increase in the velocity of a bubble during a relatively short interval of time (0.25 sec. from Fig.(6)) is quite a significant change and would result in a significant variation in the flow pattern and other associated problems. The resulting effect can very well extend down enough in the bed to be sensed by the probe. This two-fold increase in the velocity of the bubble may cause a rate of gas removal, which is more than can be supplied without some local de-fluidization of the particulate phase below the bubble. The result may be a partial defluidization below the bubble extending as low as, or even lower than, the position of the pressure probe. The result of this would be a decrease in the pressure picked up by the central probe. Such a defluidization causes the bed to contract, and this can be seen when the bubble has just left the bed. Plate (I) shows a few frames of the sequence of the behaviour of a bubble near the surface. The reduction of the height of a bed after a bubble or a train of bubbles have left the bed is a well-known fact in the literature. Attempts have gone as far as the assessment of the assumed uniform rate of bubble expansion, based on the experimental measurement of bed contraction following the passage of bubbles. (RICHARDSON & DAVIES (8)). Here it is clearly seen that the bubble velocity starts to change from when its tip is nearly one bubble diameter below the surface of the bed (cf. ROWE, PARTRIDGE & LYALL (59)).

The change in the size of the bubble near the surface of the bed is also noticeable from the examples of Figs.(5). As is seen a bubble has expanded rather drastically at the moment when it is about to burst at the surface.

Now examination of Plate (1) shows that as the bubble continues its travel out of the bed, the roof starts to get thinner gradually. The remarkable stability of the roof of the bubble, before it bursts, can be attributed to the high velocity of gas through it in that interval. If the theoretical velocity of a bubble inside a fluidized bed is U_B, then the velocity of the gas inside the bubble and through the roof is at least about $U_B + 2\ U_{mf}$ where U_{mf} is the incipient fluidization velocity on a superficial basis. Now we have just shown that the bubble velocity is roughly doubled near the surface. This means that the velocity of the gas inside and through the roof of the bubble is of the order of $2\ U_B + 2\ U_{mf}$. A velocity of this magnitude may very well explain the stability of the roof of the bubble near the surface. Another interesting feature of bubbles in fluidized beds is the remnant of what was considered to be the wake of a bubble when it was inside the bed. The behaviour of the wake has been studied by many investigators. ROWE & PARTRIDGE (60) gave an excellent account of formation, movement, and shedding details of wake. Now as is seen from Plate (1), a hump in the path of the bubble, after it has left the bed, is present for some fraction of second. One explanation for the presence of this residual hump may be that the high rate of gas removal exhausts the top layers of the surface from gas and therefore particles become defluidized. The characteristic shape of the wake is preserved by this defluidization until the redistribution of the flow evens the surface (Plate (1)).

Now going back to the description of the tail of the pressure

curve, it is noticed that after the onset of pressure variation near the surface, the pressure reduces down to a minimum. It is noticed that there is no time shift for this minimum, from the onset of the variation, as the bed height changes. This is, however, expected. Once the bubble's tip has reached the point where the variation in pressure starts, then the subsequent movement of the bubble is not related to the height of the bed over the probe. The pressure recovery is the next thing which follows after the bubble has completely left the bed. Then the distribution of the gas, and hence the surface, becomes uniform and level through the dynamics of the system. One more point to notice is that where the height of the bed is less than a certain level, defined by the overall situation, the portion C-D of the tail is no more noticeable. The reason for this may be that when a bubble is just about to pass the pressure probe, the closeness of the bed surface brings the tip of the bubble in almost direct contact with the outside of the bed. The situation is such that the onset of the pressure variation due to the surface effects, discussed earlier, coincides with the beginning of pressure variation due to the effect of the wake and results in a uniform pressure recovery profile, and in particular a low pressure to be picked up by the probe. It is realized that this latter effect could partly be due to the fact that the bubble in this situation is rather larger than that in a taller bed and therefore causesa pressure change of larger magnitude.

4.5 PRESSURE DISTRIBUTION AROUND A RISING BUBBLE

General Considerations

The pressure variation at a point inside a gas fluidized bed due to the injection of a high pressure puff of air, and also due to the approach of the bubble so formed towards the surface of the bed were studied in previous sections. In this part we are only concerned with the pressure variation at a point as a freely rising bubble approaches, embraces and leaves the point. In other words we are going to study the BC part of the pressure curve given in Fig.(6). As far as injection effect, i.e. part AB, is concerned it is possible, as it was pointed out, to locate the probe at a long enough distance from the injection point so that the effect diminishes far before the steady rise of bubble starts. Experiments which were performed on a small scale apparatus showed that 25 cm was the minimum distance between the probe and the injection, necessary to ensure that all injection effects cease before any effect of the movement of the bubble could be detected. In the present apparatus the minimum distance between the probe and the injector was about 33 cm. It is also necessary to select a height of the particulate phase above the probe in such a way that the surface effects, i.e. portion D-C in Fig.(6), are absent. In the course of the present experiments a distance of 33 to 41 cm between the probe and the injector, and a height of the particulate phase between 90 and 110 cm above the distributor gave satisfactory results. In the initial portion of the pressure curve there was always a constant pressure region of a reasonable length ensuring the equilibrium of the bubble with the particulate phase, before the onset of the pressure variation due to the approach of the bubble. Also no significant surface effects were detectable on the tail portion of the pressure curves.

Now we consider the following situation. If bubbles were produced without any injection effects, or if they were injected far below the pressure probe, then the constant-pressure region would have extended, as is shown in Fig.(12a, b), far below the position of the pressure probe on the pressure-distance curves, with absolutely no change in the subsequent pressure variations. So it is realised that one is justified to extend the constant-pressure region down to the initial position of the bubble, even if the injector is not very far from the probe. We are going to do this when considering the comparison between the theory and experiment.

Shape of the Curve and Effect of Various Factors

The typical shape of the curve is as given in Fig.(1). Neglecting the initial part, which was shown to be due to the effect of the injection, it is seen that the pressure is uniform and the same as the normal bed pressure for an interval of time during which because of the remoteness of the bubble from the probe, no effect is sensed by the probe. The length of this interval is a function of the distance between the injector and the probe as was shown earlier. After this the pressure starts to rise gradually as the bubble approaches the probe and reaches a maximum when the nose of the bubble is very close to it. Evidence given in Figs.(5,6) clearly supports the above statement. A more or less linear fall in the pressure follows which corresponds to the time interval the probe is inside the bubble. This again can be seen from Fig.(5,6). The pressure recovery follows next, when the bubble is getting away from the probe. When the distance between the probe and the bubble is long enough the pressure returns to the normal bed pressure. From Fig.(6) it is seen that the pressure drop between the observed maximum and minimum is about 9 cm of water. The diameter of the

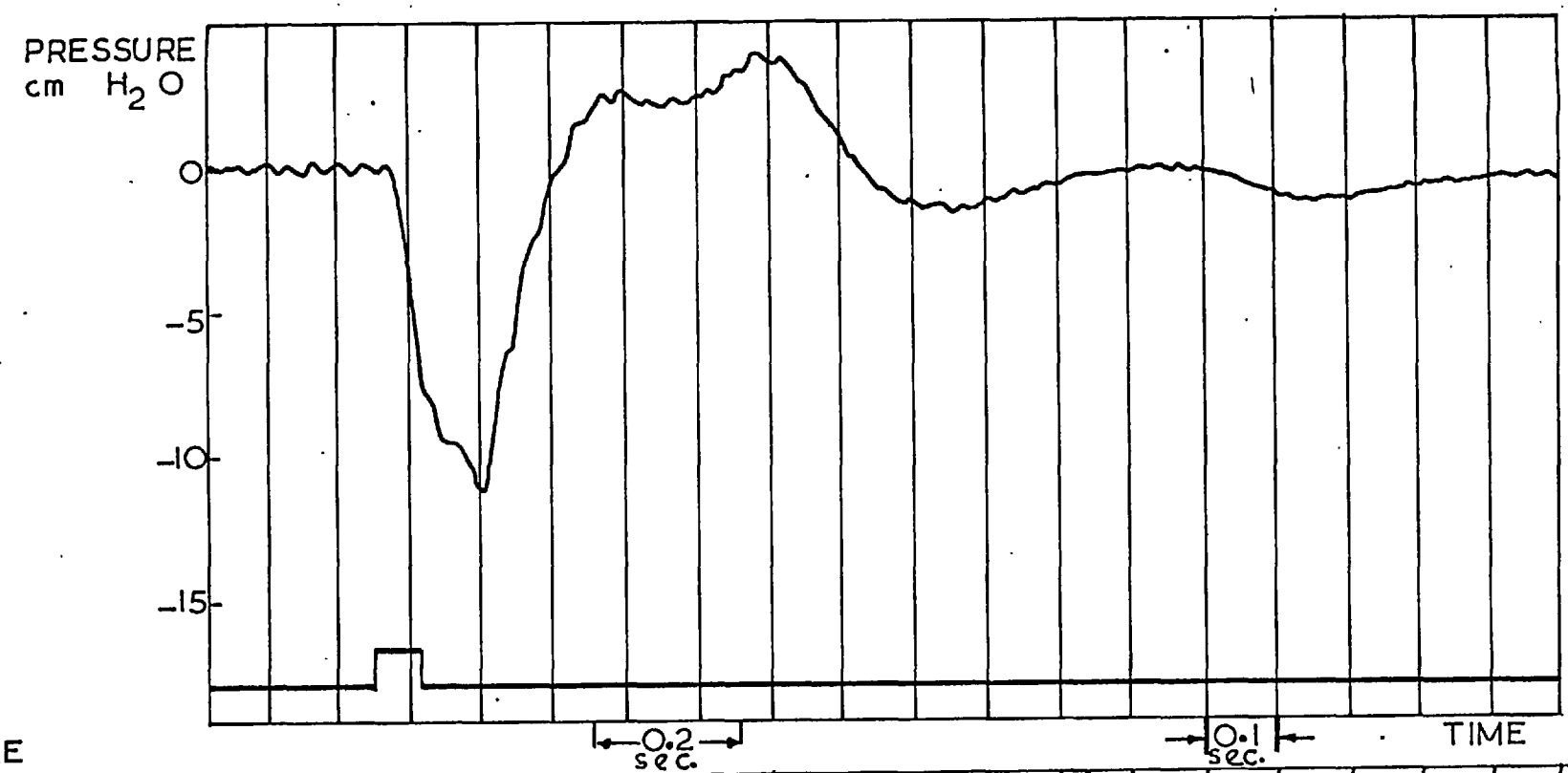

Fig (12-a)

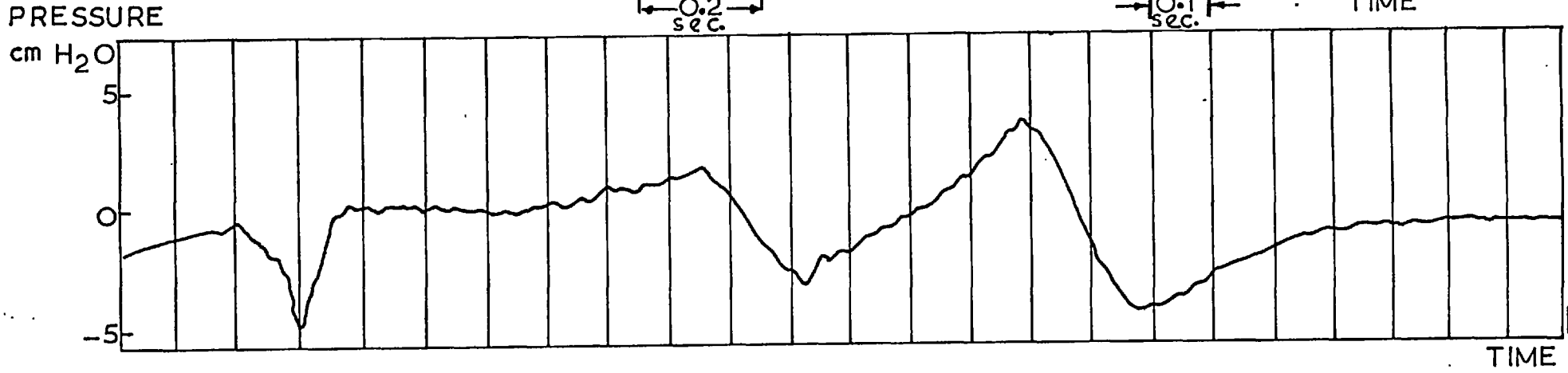

Fig(12-b)

Effect of the Distance between the Probe and the Injector on the Constant Pressure Region.

fitted circle to the bubble is approximately 6.5 cm., which, taking the density of the particulate phase (glass particles) 1.3 gr/cc, is equivalent to approximately 9.5 cm of water pressure head. So it is seen that the pressure difference when the top and bottom of the bubble are at the pressure probe is equal to the pressure drop across one bubble diameter of the incipiently fluidized particles. This pressure drop, however, is not equally divided in front and behind the bubble. The reproducibility is generally very good with respect to the reproducibility of the actual bubbles injected under identical conditions, Fig.(2). The background velocity, when changed moderately, had some effect on the quality of the tracings, Fig.(3). The effect of a longer injection interval or/and bigger injection pressure is a larger pressure drop between the top and bottom of the bubble. This is expected because a larger injection period or/and pressure results in a bigger bubble which would produce a larger pressure drop. The effect of the distance between the injector and the probe is a shift of the whole pressure curve along the time axis. This is shown in Fig.(8) and Figs.(10a,b).

4.5.1 DISCUSSION

Some of the experimental results are presented in Fig.(13 a - f). These are from a set of experiments performed under a variety of conditions. The theoretical curves obtained from various theories, and also Reuter's (three-dimensional) experimental results, have been included. The horizontal axis is distance. The bubble is assumed stationary with its nose at the origin of the co-ordinates. Points on the left and right of the origin represent points in the bed above and below the probe respectively, and here their distances from the centre of the bubble are considered positive and negative respectively. The probe is situated at the origin and the pressure curve is the pressures picked up by the probes when the bubble is at various distances from the central probe. However, as was discussed previously it is more informative to transform the pressure-distance curves into a form which gives the pressure distribution above and below the bubble. The vertical axis here is the pressure difference between the two probes one in the path of the bubble and one in the same horizontal level but away from the bubble. Effectively these curves give the difference between the absolute pressure at a point on the vertical axis of a bubble and the hydrostatic pressure at the same level. Thus it is presumed that the pressure at the reference point is not affected by the presence of the bubble. That this is justifiable was discussed previously and more justification will be presented later on.

The theoretical curves give also the difference between the absolute pressure and the hydrostatic pressure at each point. The curve attributed to DAVIDSON is obtained by solution of Laplace's equation for the pressure inside the fluidizing fluid giving:

$$p_f = -J(r - a^2/r) \cos \theta \qquad \text{Eq.(3)}$$

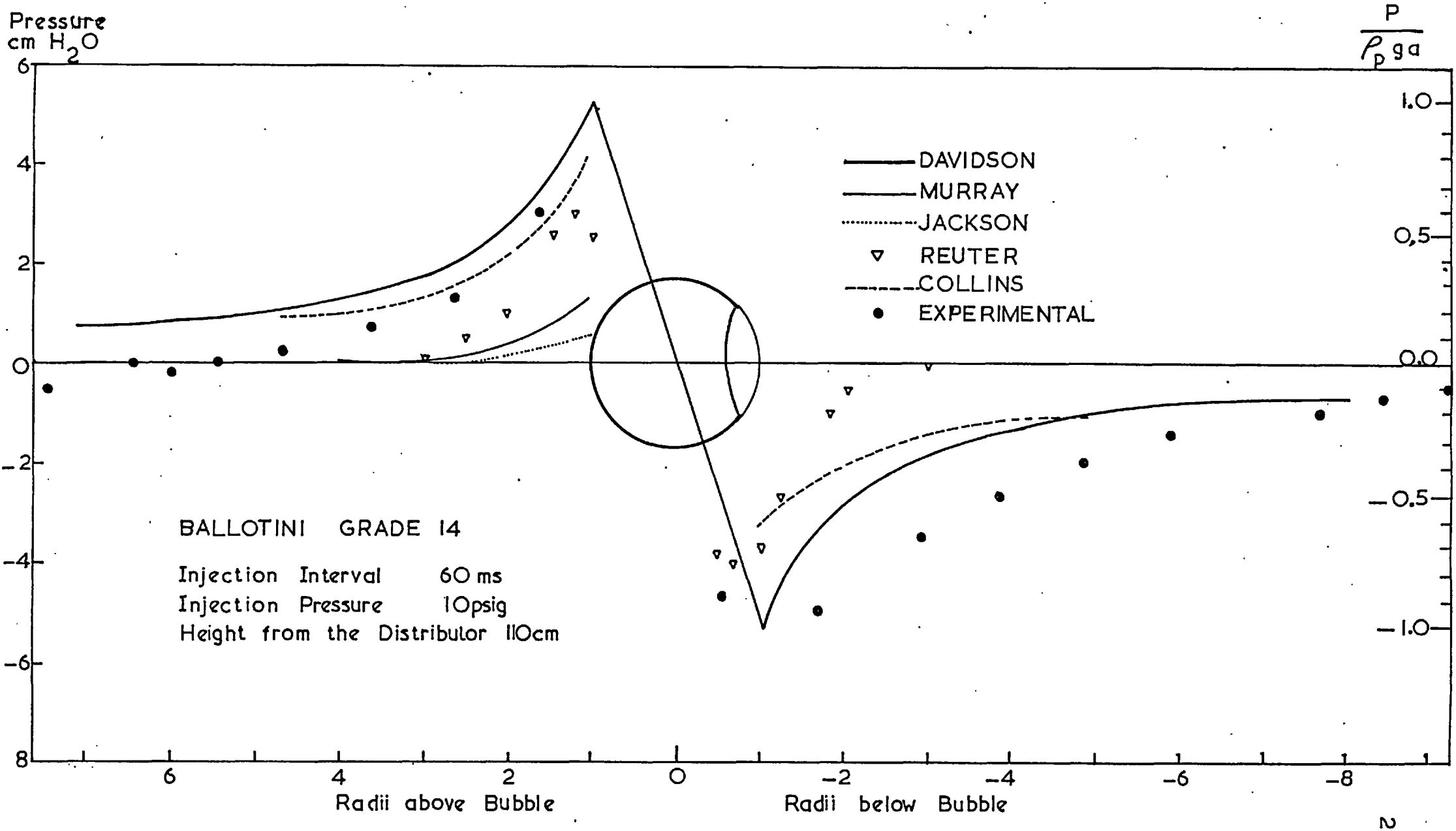
Pressure
cm H_2O
$\frac{P}{\rho_p g a}$
6
4
2
0
-2
-4
-6
8
1.0
0.5
0.0
-0.5
-1.0
DAVIDSON
MURRAY
JACKSON
REUTER
COLLINS
EXPERIMENTAL
BALLOTINI GRADE 14
Injection Interval 60 ms
Injection Pressure 10psig
Height from the Distributor 110cm
6
4
2
0
-2
-4
-6
-8
Radii above Bubble
Radii below Bubble

Fig. (13-a)

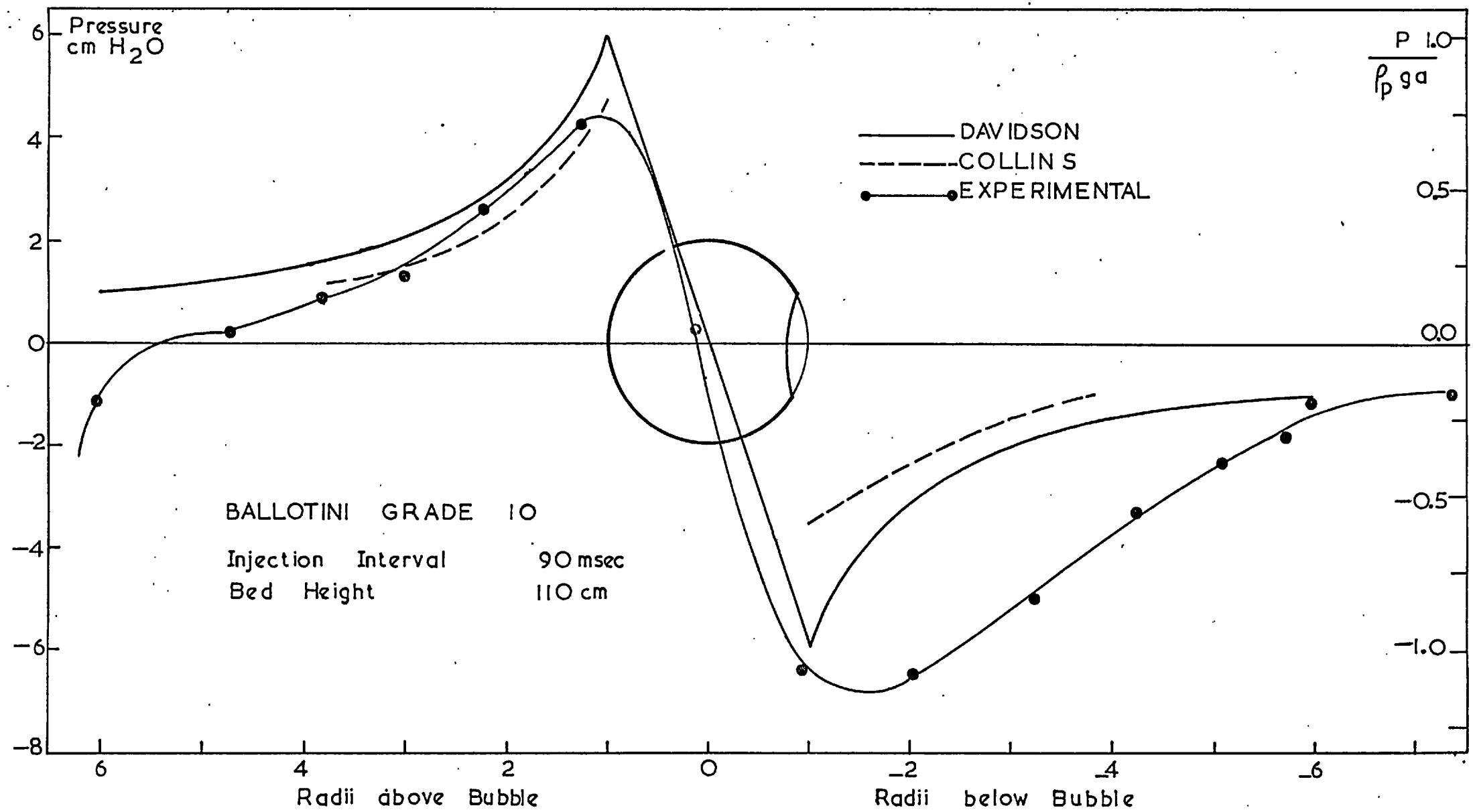
Pressure
cm H_2O
$\frac{P}{\rho_p g a}$ 1.0
DAVIDSON
COLLINS
EXPERIMENTAL
BALLOTINI GRADE 10
Injection Interval 90 msec
Bed Height 110 cm
6
4
2
0
−2
−4
−6
−8
0.5
0.0
−0.5
−1.0
6
4
2
0
−2
−4
−6
Radii above Bubble
Radii below Bubble

Fig (13-b)

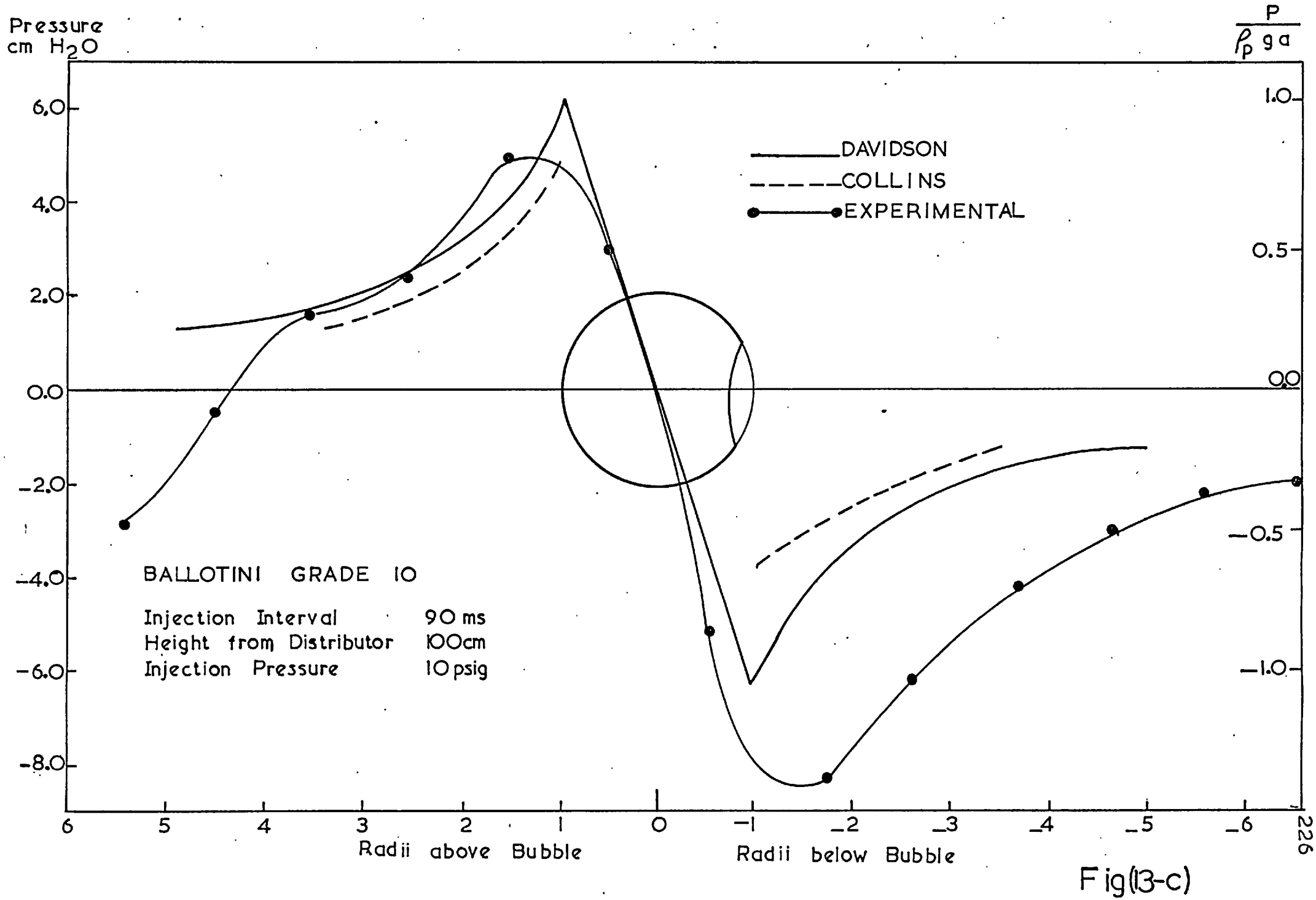
Pressure
cm H_2O
$\frac{P}{\rho_p g a}$
6.0
4.0
2.0
0.0
-2.0
-4.0
-6.0
-8.0
1.0
0.5
0.0
-0.5
-1.0
DAVIDSON
COLLINS
EXPERIMENTAL
BALLOTINI GRADE 10
Injection Interval 90 ms
Height from Distributor 100cm
Injection Pressure 10 psig
6 5 4 3 2 1 0 -1 -2 -3 -4 -5 -6
Radii above Bubble
Radii below Bubble
226

Fig(13-c)

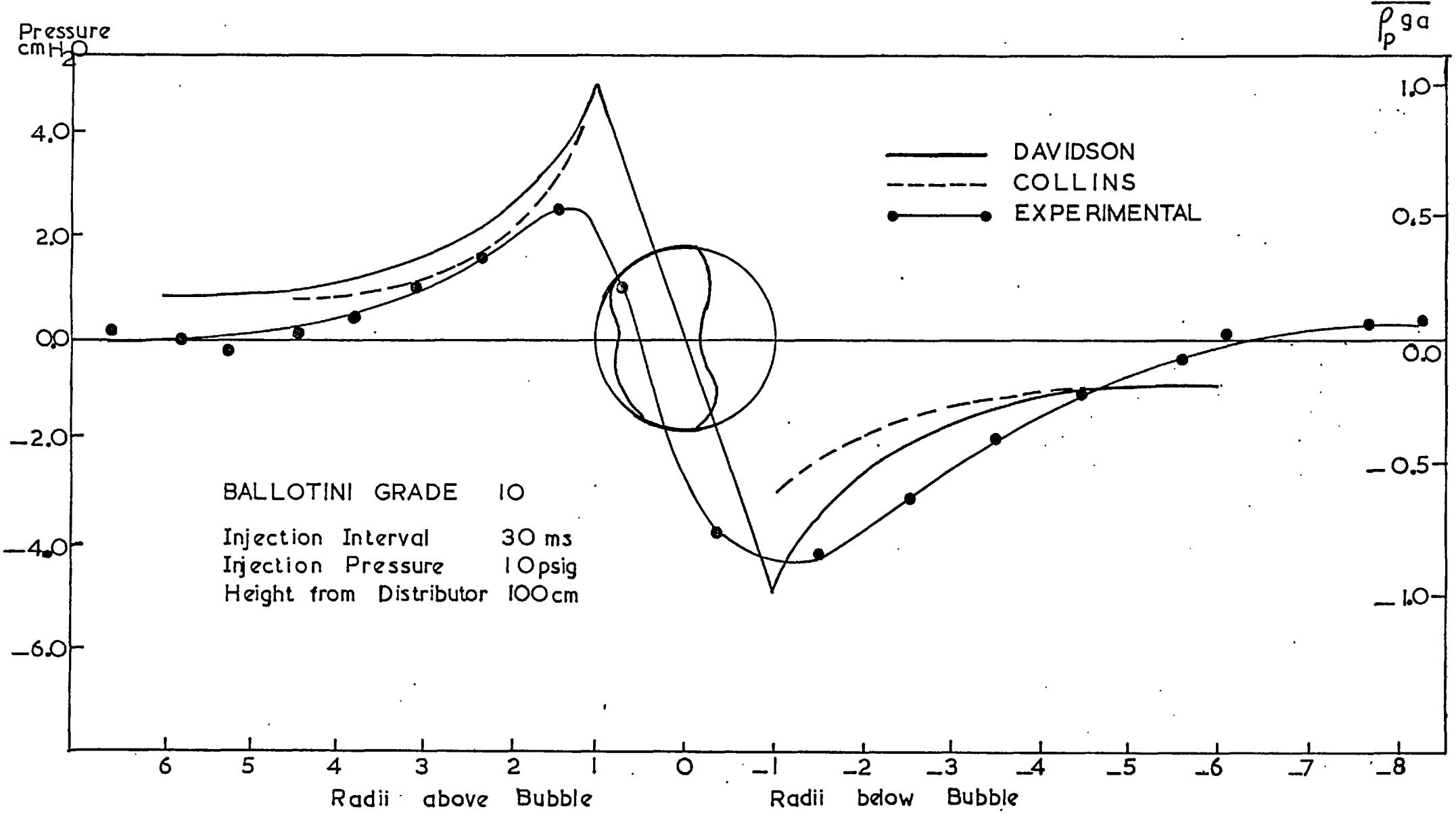
Pressure cm H2O
4.0
2.0
0.0
-2.0
-4.0
-6.0
1.0
0.5
0.0
-0.5
-1.0
DAVIDSON
COLLINS
EXPERIMENTAL
BALLOTINI GRADE 10
Injection Interval 30 ms
Injection Pressure 10psig
Height from Distributor 100cm
6 5 4 3 2 1 0 -1 -2 -3 -4 -5 -6 -7 -8
Radii above Bubble
Radii below Bubble

Fig (13-d)

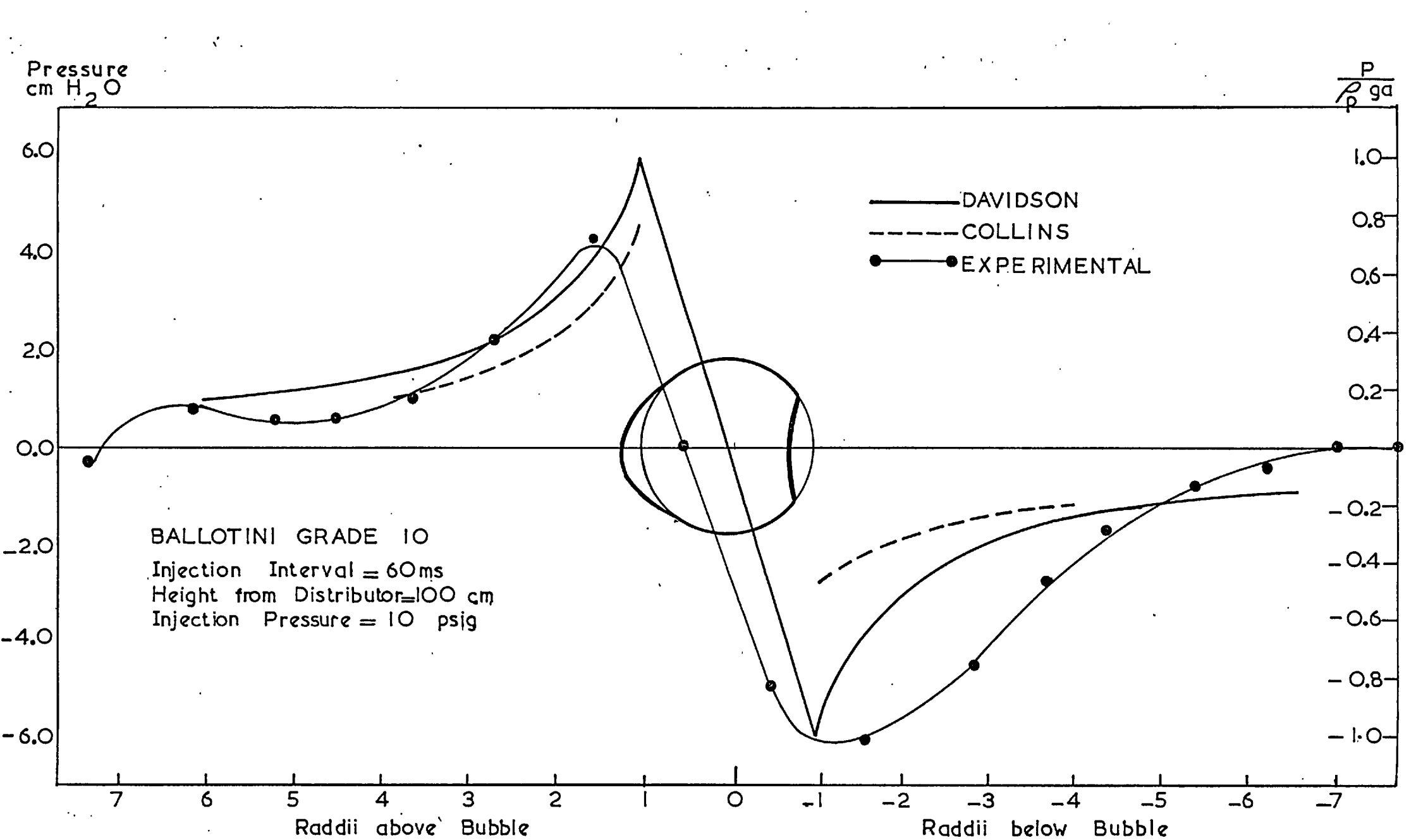
Pressure
cm H_2O
$\frac{P}{\rho_p ga}$
6.0
4.0
2.0
0.0
-2.0
-4.0
-6.0
1.0
0.8
0.6
0.4
0.2
-0.2
-0.4
-0.6
-0.8
-1.0
DAVIDSON
COLLINS
EXPERIMENTAL
BALLOTINI GRADE 10
Injection Interval = 60ms
Height from Distributor=100 cm
Injection Pressure = 10 psig
7 6 5 4 3 2 1 0 -1 -2 -3 -4 -5 -6 -7
Raddii above Bubble
Raddii below Bubble

Fig (13e)

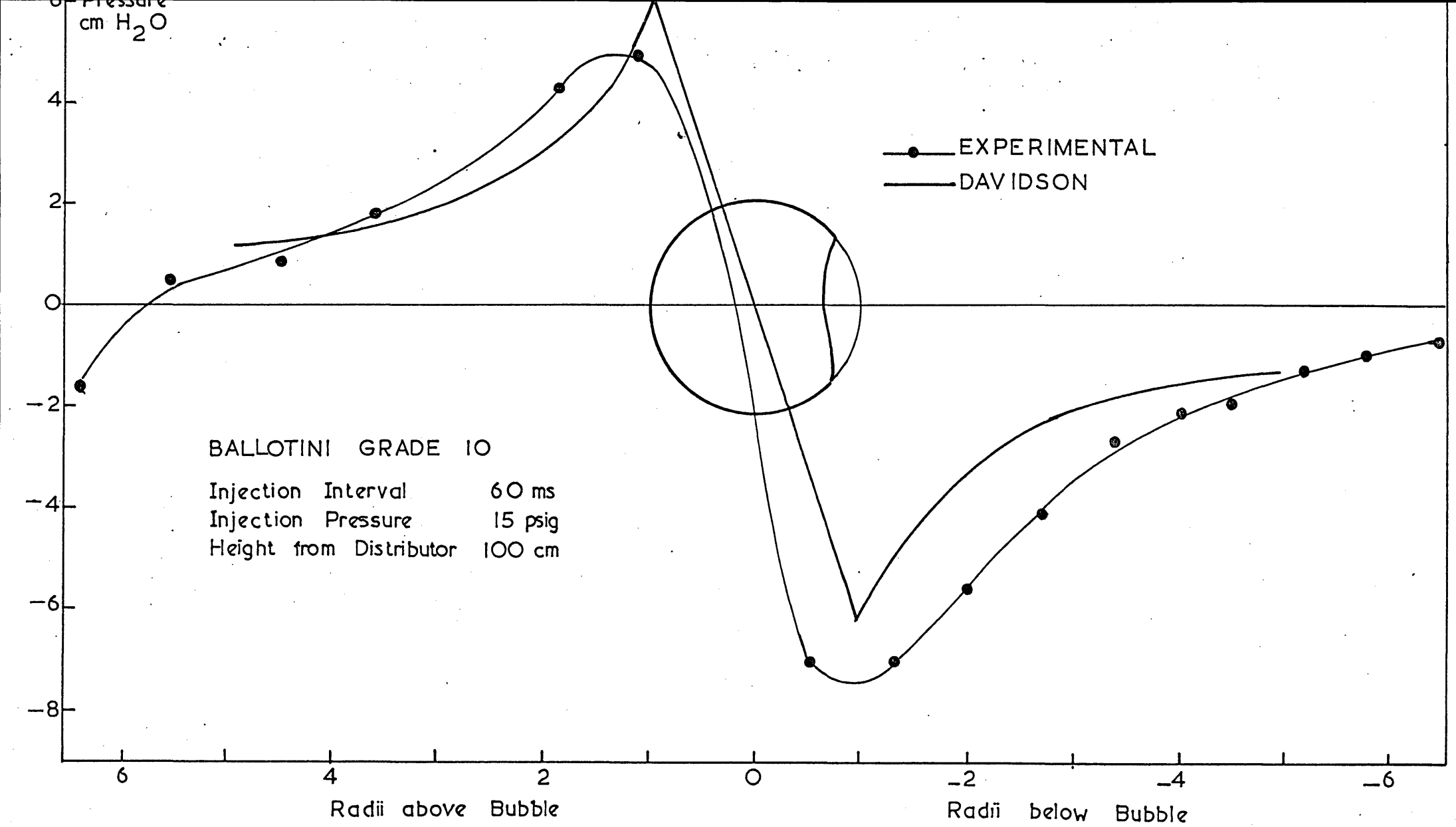
Pressure
cm H_2O
4
2
0
−2
−4
−6
−8
EXPERIMENTAL
DAVIDSON
BALLOTINI GRADE 10
Injection Interval 60 ms
Injection Pressure 15 psig
Height from Distributor 100 cm
6
4
2
0
−2
−4
−6
Radii above Bubble
Radii below Bubble

Fig.(13-f)

for the two-dimensional case, where r and θ are the polar co-ordinates, a is the bubble radius, and p_f the pressure in the fluidizing fluid. The boundary conditions see that the pressure inside the bubble must be constant, and at large distances from the bubble, the pressure gradient in the vertical direction in the fluid must provide the necessary flow for fluidization, i.e. balance of the weight of particles. The first boundary condition is satisfied since at r = a we have p_f = o everywhere. The second boundary condition necessitates that

$$\left(\frac{\partial p_f}{\partial r}\right)_{\theta=o} = J = \rho_p \, g \qquad \text{Eq.(4)}$$

where ρ_p = particulate phase density,

g = gravitational acceleration.

The proper sign must be used above and below the bubble. Putting Eq.(4) into Eq.(3) gives:

$$p_f = \mp \rho_p \, g \, (r - a^2/r) \cos\theta \qquad \text{Eq.(5)}$$

Now at each point the hydrostatic pressure with respect to the centre of the bubble is $-\rho_p \, g \, r \cos\theta$. Subtracting this from Eq.(5), and dividing both sides by $\rho_p \, g \, a$, the pressure drop across one bubble radius height of the particulate phase, we get:

$$\text{pressure difference} = \pm \frac{a}{r} \cos\theta$$

The positive and negative signs apply to above and below the bubble respectively. If we let "s" represent $\frac{r}{a}$, then for the pressure-difference between a point on the axis of the symmetry of a bubble and a point on the same level but far away from the bubble we get:

$$\text{pressure difference} = \pm \frac{1}{s} \qquad \text{Eq.(6)}$$

Eq.(6) represents the curve attributed to DAVIDSON in graphs presented here and is referred to frequently. In some of the graphs

presented other theoretical curves are also included. We will discuss the theoretical curve due to JACKSON (28) later on. Curves due to MURRAY (21) and COLLINS (50) are those derived by STEWART (49) from the respective stream functions. The expression for pressure difference attributed to MURRAY (21) is $\frac{1}{4s^2}$ Eq.(7) (two-dimensional) only for the region above the bubble, and the one due to COLLINS is:

$$\frac{1}{2}\left\{s + 0.54 - \sqrt{(s + 0.54)^2 + 0.32} + \frac{3.5}{s - 0.77 + \sqrt{(s - 0.54)^2 + 0.32}}\right\}$$

for above the bubble and,

$$-\frac{1}{2}\left\{s - 0.54 - \sqrt{(s - 0.54)^2 + 0.32} + \frac{3.5}{s + 0.77 + \sqrt{(s - 0.54)^2 + 0.32}}\right\}$$

Eq.(8)

for below the bubble.

As is seen from Fig.(13 a - f) the reproducibility of the experimental results are good with respect to the bubble shape reproducibility, however, when compared with theory, the shape of the curves drawn through the experimental points vary from one bubble to another. This of course is not unexpected, because besides the fact that the bubble shape and size varied slightly from one experiment to another one, the experimental error involved also contributed to the observed scatter of the results. Generally, one source of error is the transformation of the pressure-time curve to pressure-distance data. Another source of error is in the determination of the exact position of the boundary of bubble in each frame. The bubble boundary image was not always sharp, particularly near the top of the bubble. Now in order to reduce the effect of all experimental error one has to average the results obtained under

identical controllable conditions.

In this part of the experiment bubbles were injected under various injection conditions. An injection interval was selected and a few bubbles were injected. Then the injection interval was changed and a few more bubbles were injected. Altogether three injection intervals of 30, 60 and 90 m.sec. were employed in this part of the work. These were selected because it was known from previous experiments that this range of injection interval produced bubbles of favourable size and stability. The height of the bed was changed and the whole set of experiments were repeated. Then, the injection pressure was changed and other factors were kept constant. The pressure recordings and the bubble tracings for several individual bubbles are given in the APPENDIX (I). The results obtained under identical injection pressure and interval are summarized and given in Fig.(14 a - d). Now considering all various factors contributing to the scatter of the results, one can see from these figures that the scatter is reasonably small. As is noticed the change in the height of the particulate phase does not affect the results. This of course is expected provided the height does not change too drastically; here about 10%. The best circle fitted to the bubbles are also superimposed. This gives an idea of the size of the bubbles near the pressure probe. The size of bubbles changed with height slightly, but more significantly near the injector, due to the initial growth of the bubble, and near the surface because of the surface effects. Apart from these two extreme regions, the size of the circle superimposed is a fair representative of the bubble size at reasonable distances above and below the probe. In Fig.(14a,b), the bubbles are seen to be of approximately 4 cm in radius. In the case of Fig.(14c,d), the radius is about 4.5 cm. Bubble velocities for various cases are

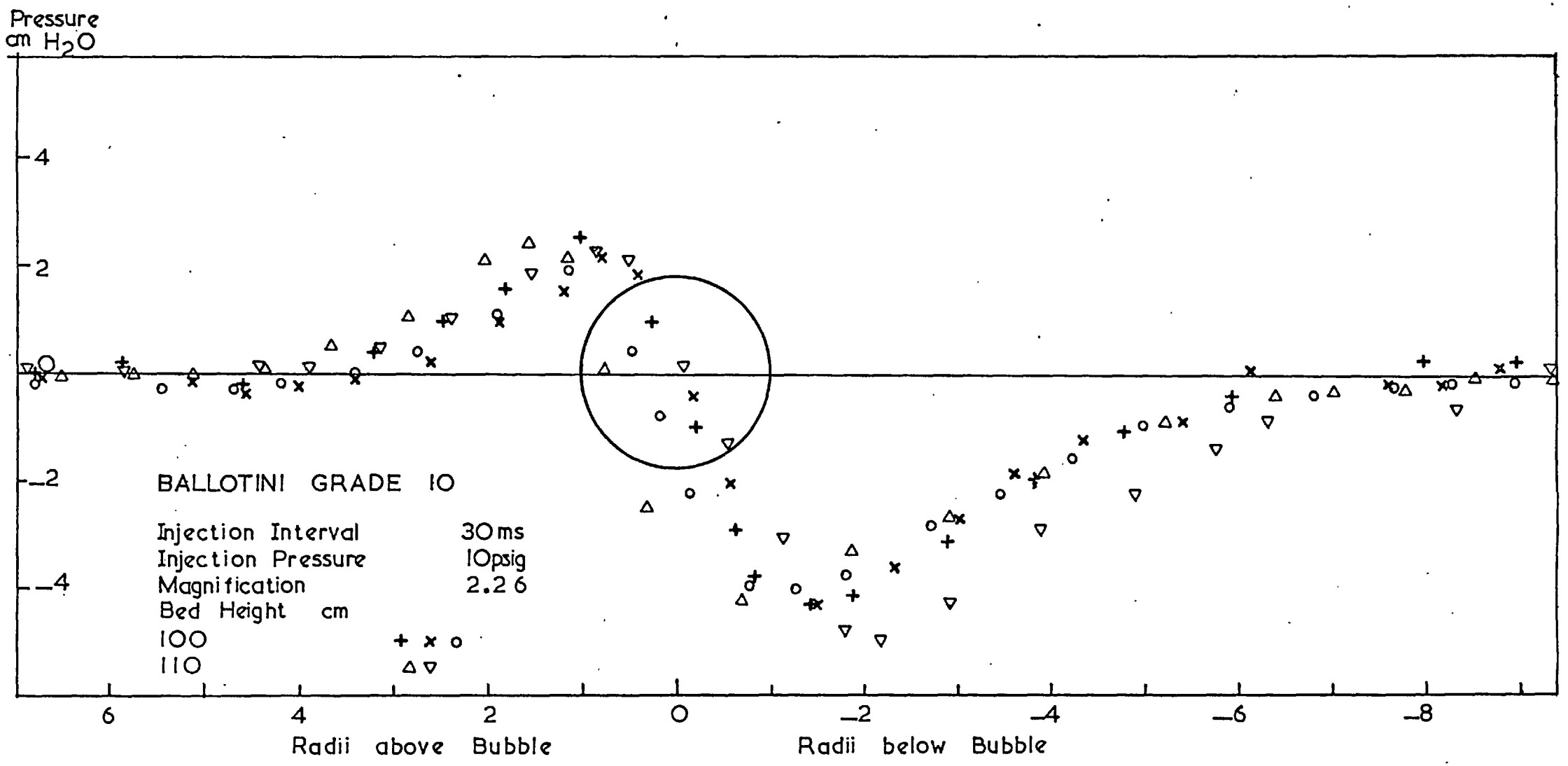
Pressure
cm H_2O
4
2
0
−2
−4
BALLOTINI GRADE 10
Injection Interval 30 ms
Injection Pressure 10 psig
Magnification 2.26
Bed Height cm
100
110
6
4
2
0
−2
−4
−6
−8
Radii above Bubble
Radii below Bubble

Fig. (14a)

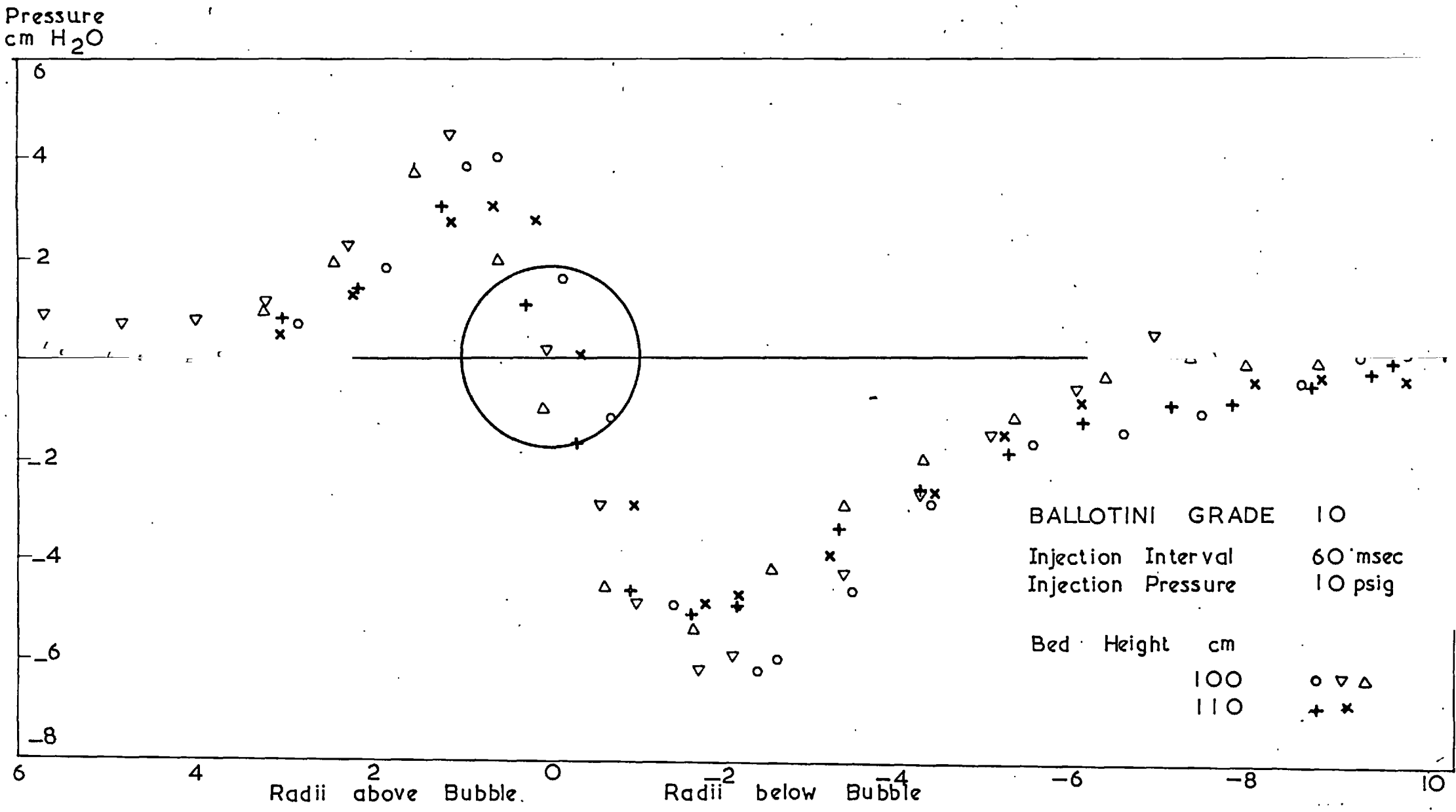
Pressure
cm H_2O
6
4
2
-2
-4
-6
-8
6
4
2
0
-2
-4
-6
-8
10
Radii above Bubble.
Radii below Bubble
BALLOTINI GRADE 10
Injection Interval 60 msec
Injection Pressure 10 psig
Bed Height cm
100
110

Fig.(14-b)

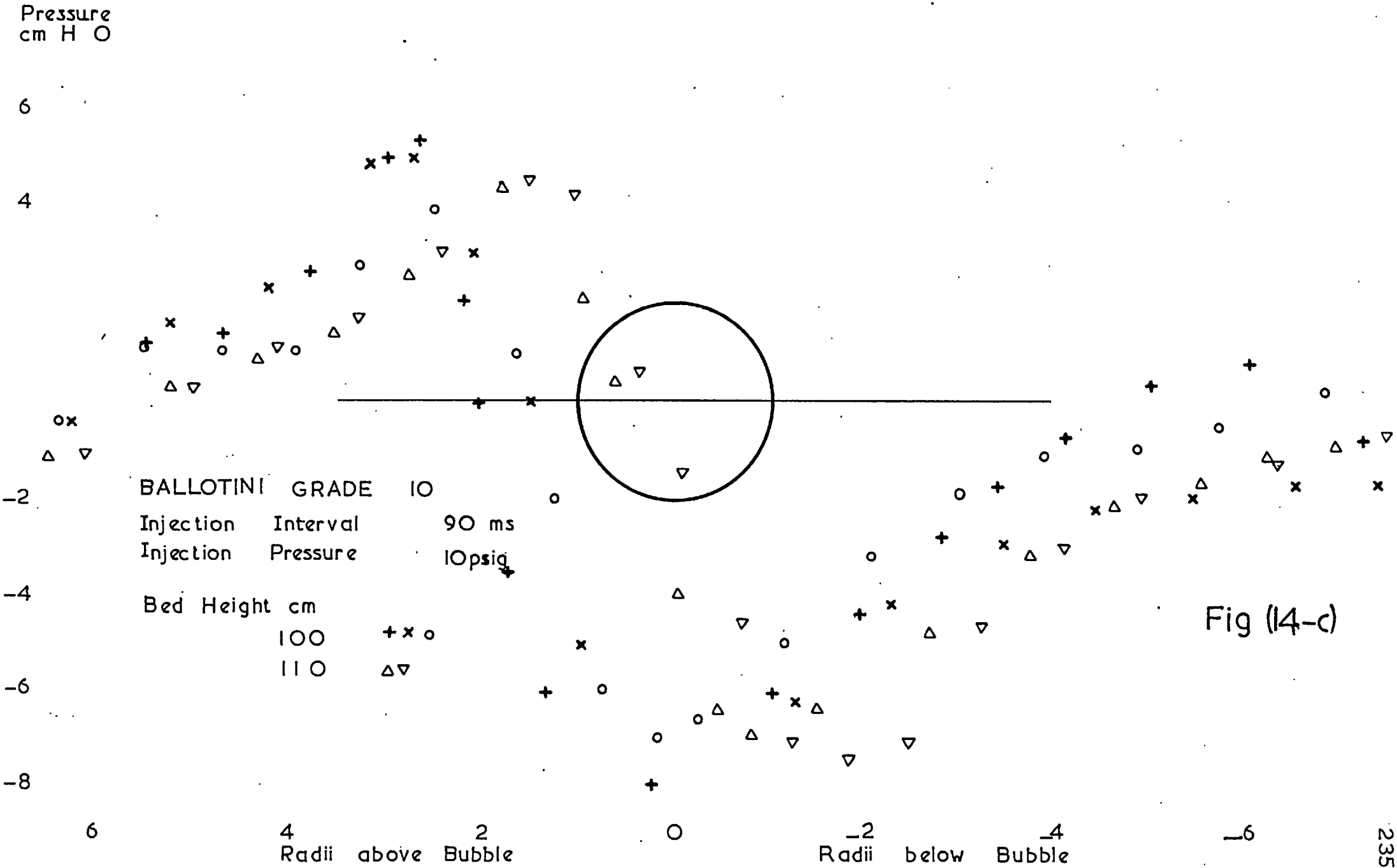
Pressure
cm H O
6
4
-2
-4
-6
-8
BALLOTINI GRADE 10
Injection Interval 90 ms
Injection Pressure 10psig
Bed Height cm
100
110
6
4
2
0
-2
-4
-6
Radii above Bubble
Radii below Bubble

Fig (14-c)

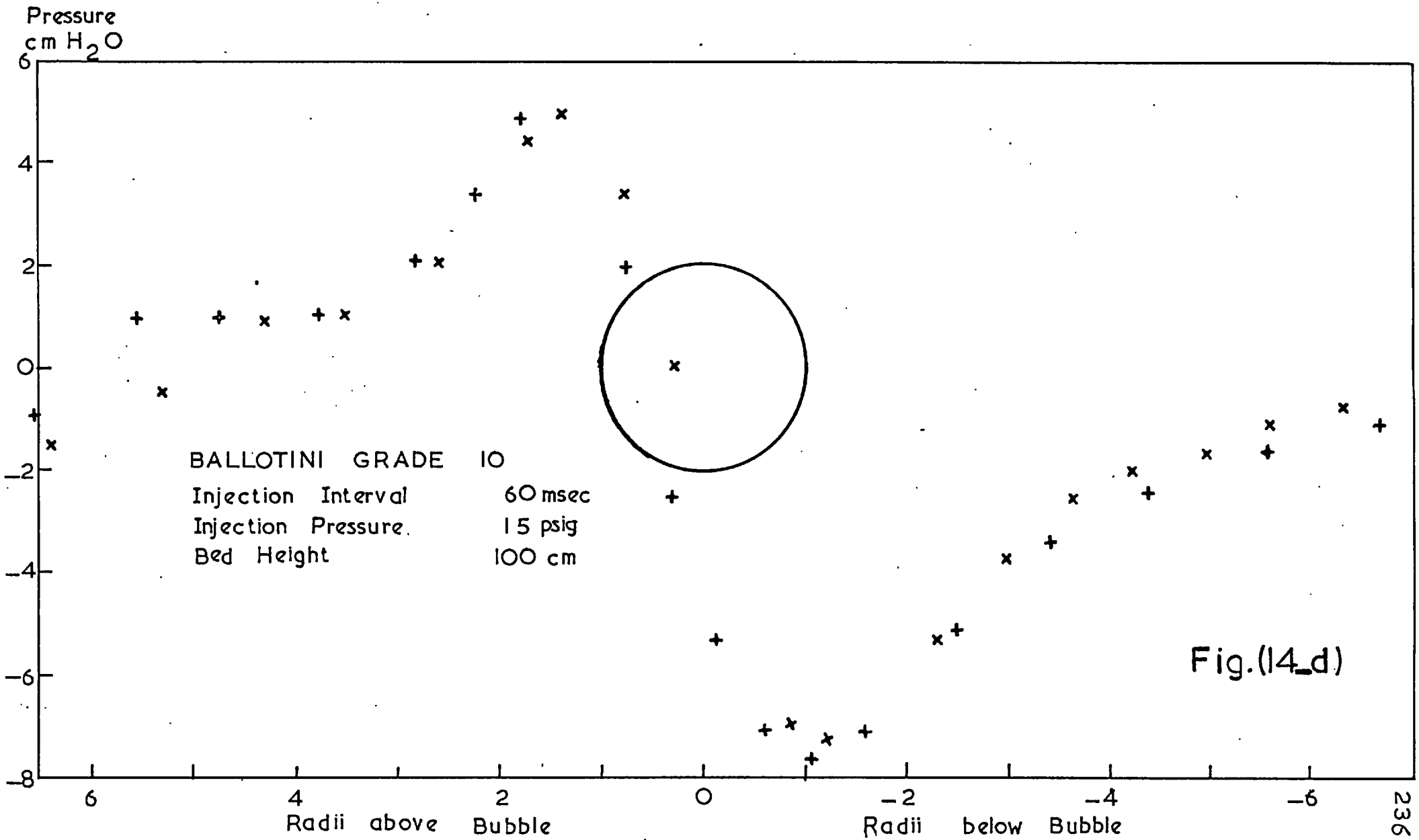
Pressure
cm H_2O
6
4
2
0
−2
−4
−6
−8
BALLOTINI GRADE 10
Injection Interval 60 msec
Injection Pressure 15 psig
Bed Height 100 cm
6
4
2
0
−2
−4
−6
Radii above Bubble
Radii below Bubble

Fig.(14_d)

given in the following Table:

TABLE (1)

PROPERTIES OF BUBBLES IN FIGS.(14 a - d),

DETERMINED EXPERIMENTALLY

BUBBLE IN	U_B cm/sec	RADIUS cm	$K = U_B / \sqrt{g R_B}$
Fig.(14a)	53.0	4.1	0.84
Fig.(14b)	63.0	4.1	0.99
Fig.(14c)	67.0	4.5	0.99
Fig.(14d)	70.5	4.5	1.05
AVERAGED	63.4	4.3	0.97

The experimentally determined constants of the bubble radius-velocity equation are also tabulated above. As it is noticed the magnitude of K is about twice the theoretical one, the average being 0.97.

Visual comparison of the points on Fig.(14a) and Fig.(14b) show that there is a slight but noticeable difference which reveals a particular trend. Although no significant difference in the size of the bubbles in Fig.(14a) and Fig.(14b) was noticeable, it seems reasonable to suggest that a longer injection interval, produces a bigger bubble. This would result in a pressure variation of higher absolute magnitude. This argument may explain the observed difference between the 30 m.sec. and 60 m.sec. injection intervals results. Now this argument must be equally applicable for other cases as well. However, the observed trend in the above case is not so clearly noticeable when the results of 60 m.sec. and 90 m.sec. injection intervals are compared. This is so in spite of the fact that the

bubble radius is distinguishably different in these last cases as it is seen from Fig.(14b) and Fig.(14c). These apparent anomalies are more clearly realized by the examination of Fig.(15) in which the curves drawn through the points in Figs.(14 a - d) are represented. As was pointed out there is an explainable trend for the case of results of 30 m.sec. and 60 m.sec. injections. This trend is not clearly observed for the 90 m.sec. injections. A shift of the curve towards the left is noticed. The reason for this is not completely known. It is noticed, however, that at injection intervals of 90 m.sec. when the injection pressure is increased, the obtained results are in agreement with the expected trend, i.e. higher magnitude for pressure variation. It is likely that at longer injection intervals if the pressure is not high enough, leaking of the gas from the growing bubble to the surrounding particulate phase becomes relatively more pronounced. It may also be that at relatively lower injection pressure (when the interval is long) the bubble detaches from the nozzle before the injection is complete. This is likely because the injection pressure is not necessarily constant during the whole period of injection, particularly when the interval is relatively longer and the initial pressure low. All these factors could cause the injected bubble, under these circumstances to be smaller than the expected size. This in turn would result in a pressure variation which would not show the expected trend. Suppose a small bubble detaches from the nozzle during the injection period, before the main bubble does and hence moves in front of the main bubble. This early detached bubble would not be observable, visually if its diameter is less than the bed thickness, i.e. 1.27 cm. Of course it is quite likely that the bigger bubble would overtake the smaller one. But provided the initial distance

between them is fairly large and also the size of the secondary bubble happens not to be as large as it should, due to extra leakage during the first detachment, it is quite likely that the primary bubble would continue its rise without being overtaken. The pressure variation due to the movement of this bubble would affect the overall pressure variation in that a pressure peak might be recorded, when the primary bubble is near the probe, while the main bubble has not reached the probe. The overall result would be something like the 90 m.sec. injection where a pressure peak happens at a distance from the probe. These explanations are not meant to be the description of what exactly has happened in this case but they could be considered as reasonable and likely explanation which could be applied.

Before going any further in the relative comparison of the pressure curves there are some points which are apparent at this stage. First of all, as was explained before a larger injection pressure or/and interval would result in a larger pressure variation. The observed trend as these variables change would be as expected. Another important point is that as is seen from Fig.(15), from about 1.5 bubble diameters below the centre of the bubble, the curve for all different cases more or less coincides. This suggests that the direct effect of the presence of a bubble is not sensed below 1.5 bubble diameter from its centre, i.e. the region in which the dynamics of the system could be affected by the presence of a bubble extends only down to 1.5 its diameter below the centre. This conclusion is very important in that it confirms the results obtained by different investigators about the minimum distance between two bubbles to affect each other, and hence coalesce. As was discussed in the first part of the present work, HARRISON & LEUNG (31) found a value of 1.1

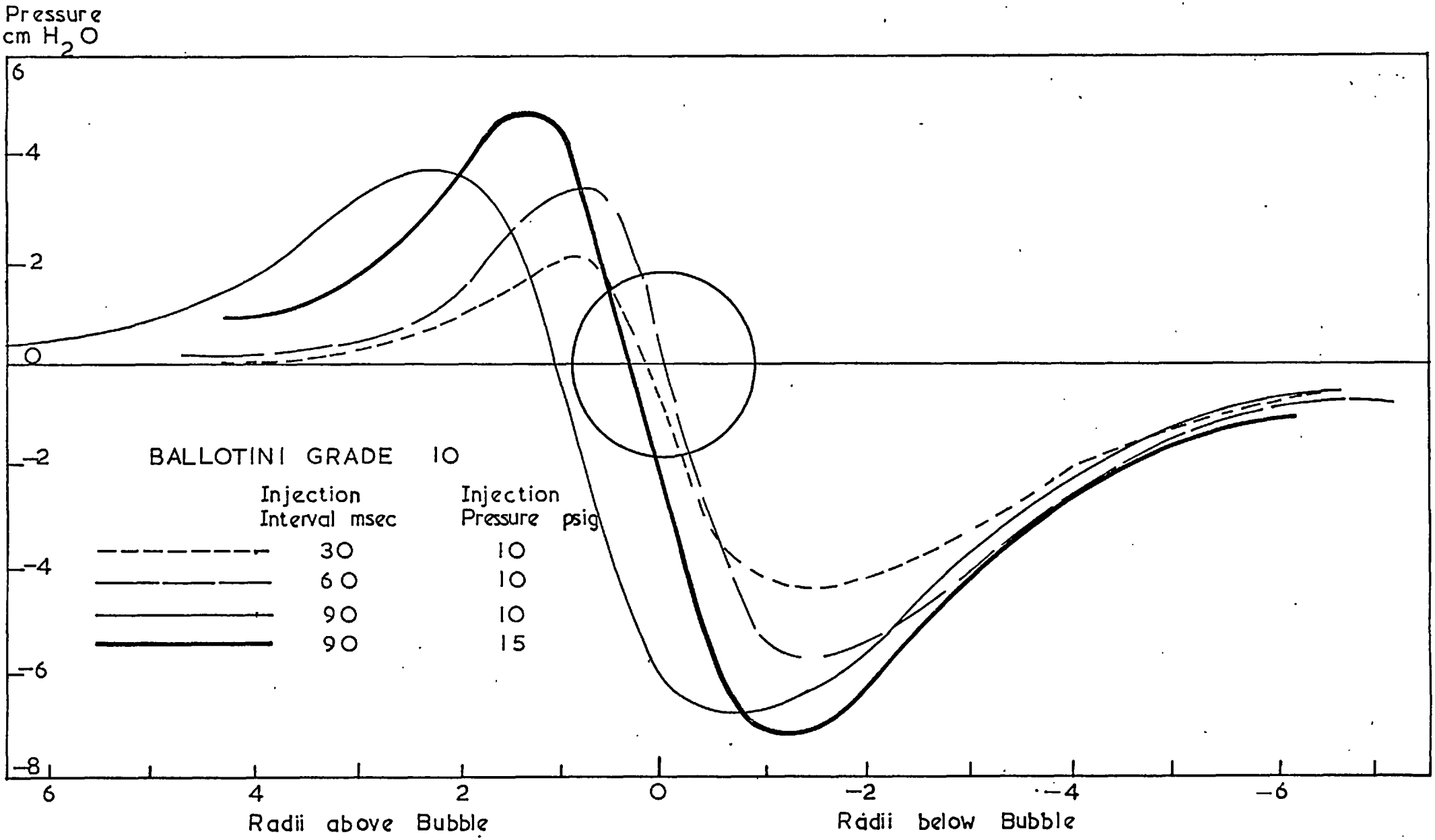
Pressure
cm H_2O
6
4
2
0
−2
−4
−6
−8
BALLOTINI GRADE 10
Injection Interval msec
Injection Pressure psig
30 10
60 10
90 10
90 15
6
4
2
0
−2
−4
−6
Radii above Bubble
Radii below Bubble

Fig (15)

bubble diameter and TOEI& MATSUNO (17) found that a distance of about the sum of the diameters of two bubbles between their centre, i.e. for equal size bubbles, 1.5 bubble diameters between the centre of the one above, and the tip of the one below, was the minimum distance necessary for coalescence to occur. This distance was considered to be the extent of a bubble's wake. The work of LOCKETT & HARRISON (51) also showed that the voidage variation from the incipient value below the bubble extends to about one bubble diameter below its centre. This also gives an indication of the extend of the region where the effect of a bubble's wake can be present. Here the experimental data on pressure distribution suggests a more or less same size for the extent of the wake, as concluded by voidage variation and coalescence experiments, behind a rising bubble. The conclusion drawn by LITTMAN & HOMALKA (58), that the effect of bubble wake is extended down to 5 to 6 bubble radii below the bubble does not seem to be correct. Perhaps the inappropriate interpretation of the pressure recovery curves in the above mentioned work is responsible for their conclusion. The work had some handicaps as acknowledged by the authors. Here the more refined experimental technique has provided evidence which is in full agreement with results obtained from completely different experiments.

Returning to the curves in Fig.(15), the data for bubbles of different size show a consistent and explainable trend, with the exception of the curve corresponding to 90 m.sec. injection interval at 10 psig, for the reasons discussed earlier. In order to compare the experimental data with theoretical prediction, it is desirable to have as many data as possible. In the present situation the data have been obtained from bubbles of different size. The change in the size was, however, small. The data can be brought together if we

represent the pressure in a dimensionless form by dividing by (ρ_p g a), which is the pressure drop across one bubble radius height of the particulate phase with density ρ_p and "g" and "a" being the acceleration of gravity and the respective bubble radius respectively. An advantage is that the comparison of data obtained from bubbles of different size is more meaningful in this way. Also as is noticed from Fig.(16), where the dimensionless pressure data are presented, apart from the curve obtained at 90 m.sec. injection at 10 psig, the data are symmetrically distributed with respect to the injection parameters. It can be seen, very easily, that the curve obtained by averaging all the data on Fig.(16) describes the average behaviour very well. It can also be seen that exclusion of the curve due to 90 m.sec. injection at 10 psig does not produce any significant change in the resulting average curve. It ought to be mentioned that data corresponding to the above mentioned curve cannot be considered extreme values and hence rejected. Comparison of the calculated test statistic from the data with the test criterion in tables of percentage points for ratios involving extreme values suggest that the above mentioned data are from the same population as the rest of the data.

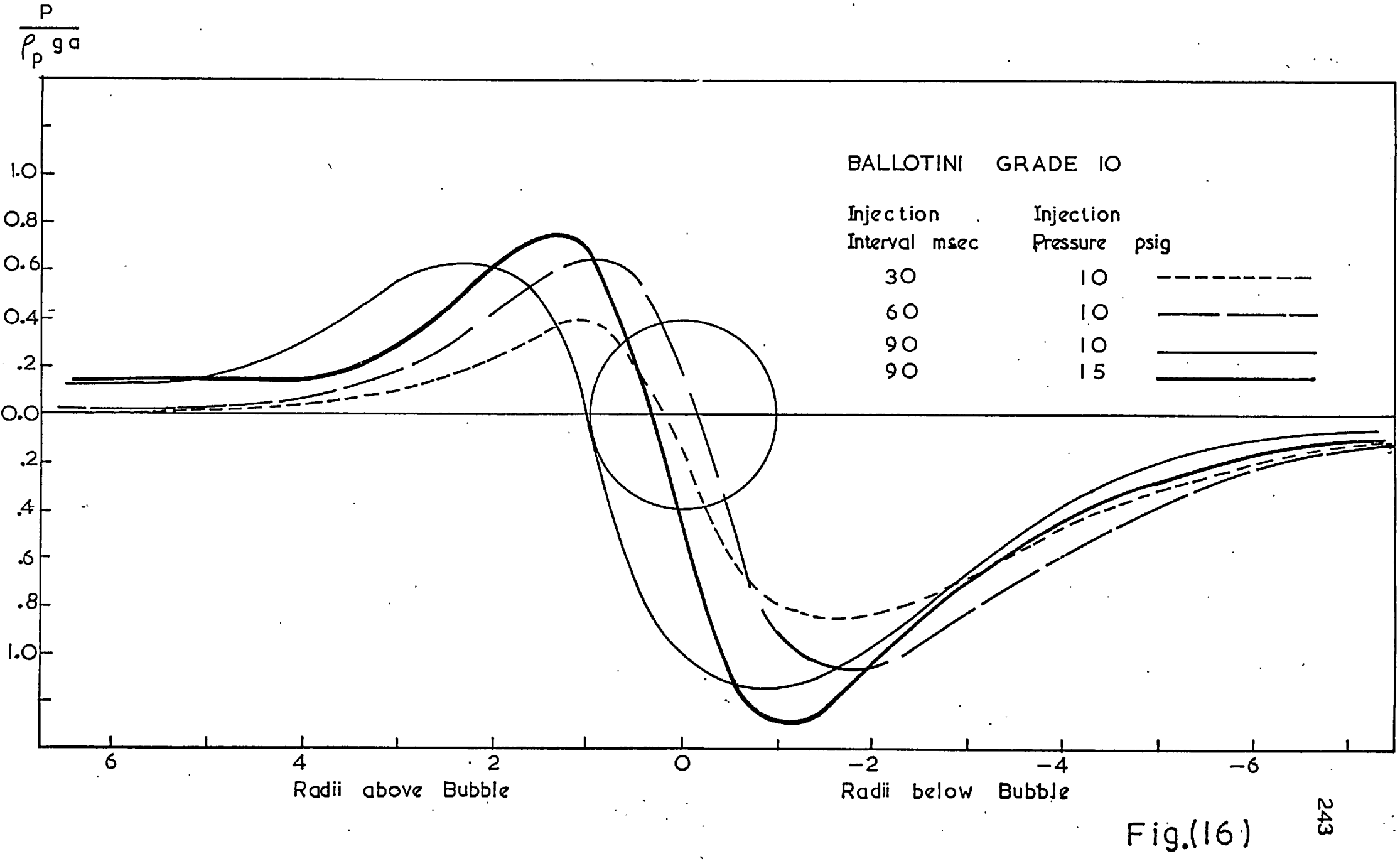
P / ρp g a
1.0
0.8
0.6
0.4
.2
0.0
.2
.4
.6
.8
1.0
BALLOTINI GRADE 10
Injection Interval msec
Injection Pressure psig
30 10
60 10
90 10
90 15
6
4
2
0
−2
−4
−6
Radii above Bubble
Radii below Bubble

Fig.(16)

4.5.2 COMPARISON WITH THEORY

Fig.(17) shows the experimental pressure data in dimensionless form, i.e. P/ρ_p g a as function of the dimensionless distance $\frac{r}{a}$ from the tip of the bubble. These data have been obtained by averaging all the data in Fig.(16) and hence are the overall average of data obtained from seventeen individual bubble pressure-distance curves. Theoretical curves due to various authors are also plotted. Curves 1 and 2 are due to DAVIDSON (44) and COLLINS (50) respectively, and are the only ones which provide values for pressure below the bubble as well as above it. Curve 5 due to JACKSON (28) is not applicable below the bubble as suggested by the author for the reasons discussed. Curve 4 due to MURRAY (21) is also not applicable below the bubble because of the improper sign in the corresponding expression. Curve 3 is obtained from JACKSON'S analysis (28) following the suggestion by STEWART (49) that the experimental bubble velocity should be used in the JACKSON'S analysis rather than the theoretical one.

It can be shown that the expression for the pressure distribution around a two-dimensional bubble, following JACKSON is:

$$\frac{P}{\rho_p g} = - U_B^2 \left[\frac{2a^2}{r^2} \sin^2\theta - \frac{a^2}{r^2} + \frac{a^4}{2r^4} \right] - g\, r \cos\theta \qquad \text{Eq.(9)}$$

For the pressure inside the bubble to be constant it is required that:

$$U_B^2 = \tfrac{1}{4}\, g\, a$$

Substitution in Eq.(9) and rearrangement gives:

$$\frac{P}{\rho_p\, g\, a} = - s \cos\theta - \frac{1}{4s^2} \left[\frac{1}{2s^2} + 1 - 2\cos^2\theta \right] \qquad \text{Eq.(10)}$$

Along the axis of the symmetry of the bubble $\theta = o$ and $\cos\theta = 1$. In order to obtain the pressure difference between a point on the axis of symmetry of the bubble and a point on the same level but away from the bubble, we subtract the hydrostatic pressure from

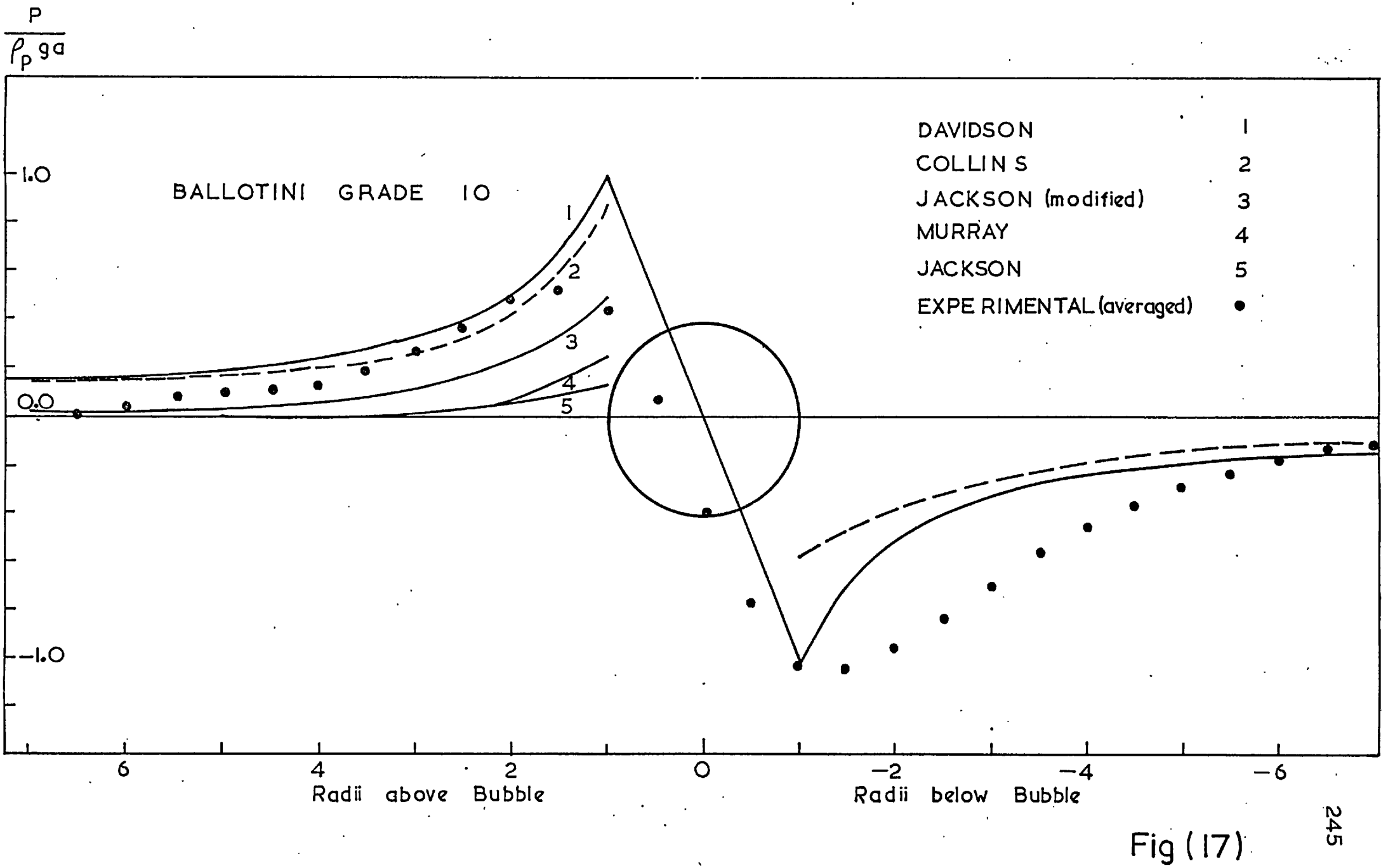
P / ρp g a
BALLOTINI GRADE 10
DAVIDSON 1
COLLINS 2
JACKSON (modified) 3
MURRAY 4
JACKSON 5
EXPERIMENTAL (averaged)
1.0
0.0
-1.0
1
2
3
4
5
6
4
2
0
-2
-4
-6
Radii above Bubble
Radii below Bubble

Fig (17)

Eq.(10). This would result in:

$$\text{Pressure difference} = \frac{1}{4s^2}\left(1 - \frac{1}{s^2}\right) \qquad \text{Eq.(11)}$$

along the vertical axis. The expression is plotted in Fig.(17) and is represented as curve (5).

As was presented previously the constant of the bubble velocity radius equation obtained from this set of experiments is about 0.97. The bubble experimental velocity could be written as $U_B = \sqrt{ga}$ (the K is taken to be 1.0 instead of 0.97). Now if this bubble velocity is employed in Eq.(9), the final expression for the pressure difference, equivalent to Eq.(11) would be given by

$$\text{Pressure difference} = \frac{1}{s^2}\left(1 - \frac{1}{2s^2}\right) \qquad \text{Eq.(12)}$$

Equation (12) is plotted in Fig.(17) and is represented by curve 3. Before making any statement concerning the comparison of the experiment and the theory, we have to see if this modification of JACKSON'S analysis in regard to the pressure expression is permissible. The justification is not straightforward, and the fact that bubble velocity in the experiments is different from theory does not provide enough, if not at all, ground for such a modification. The expression for the bubble velocity obtained from JACKSON'S analysis, i.e. $U_B = \frac{1}{2}\sqrt{ga}$ is a necessary condition for the constant pressure condition inside the bubble to be satisfied, and therefore the arbitrary selection of the experimental bubble velocity is inconsistent with respect to this condition. Strictly it is not justifiable to employ the experimental bubble velocity in the theoretical analysis. However, when the problem is considered in more detail, some partial justification becomes apparent. JACKSON analysis is for circular bubbles and its pressure equation provides values for the pressure which are supposed to be constant along the boundary of the bubble.

It is known that even when the theoretical bubble velocity is employed in the analysis the pressure does not remain truly constant along the bubble boundary. This suggests that the shape of the bubble has to be adjusted for the pressure condition to be satisfied. It is then quite reasonable that with another choice of the bubble shape, a different bubble velocity would meet the pressure boundary condition. In particular if the bubble is more pointed in the nose the velocity would be higher, as is frequently observed in practice. Examination of the bubble tracings given in the APPENDIX (^{I}) shows that in a number of cases in the present work elongated bubbles were observed. Such bubbles move with a higher velocity than circular ones with the same area. Thus there are good reasons to believe that a higher bubble velocity should be used in JACKSON'S pressure equation.

Returning to the problem of the comparison of experimental results and theoretical predictions, one notices that the curves 4 and 5 due to MURRAY and JACKSON predict values for pressure which are too low everywhere. Curve 2 due to COLLINS above the bubble is not significantly different from Curve 1 due to DAVIDSON. Below the bubble it predicts values which are of smaller absolute value than DAVIDSON. COLLINS analysis is for a circular bubble with a wake and is a transformation of the circular bubble considered by DAVIDSON. This transformation takes place in order to provide a bubble with wake, and when this is done the behaviour of the gas and particle movement around the bubble is considered. No assumption about the behaviour of the wake is made and the treatment is purely mathematical. It is unlikely that such a treatment would produce results in better agreement with experiment, than the DAVIDSON treatment, i.e. circular bubble model. In fact it is quite apparent from Fig.(17)

that deviation from experiment values is more for COLLINS expression. Bearing in mind that this part of the experimental data are the most reliable and reproducible, the considerable deviation of COLLINS prediction from the experimental results suggests that the model is less realistic than the DAVIDSON'S model, at least so far as the pressure distribution is considered. This conclusion is, however, incompatible with the conclusion drawn by STEWART (49) on the basis of similarity between REUTER'S three-dimensional experimental results and COLLINS two-dimensional predictions. Such a comparison is not strictly permissible and could be quite misleading, firstly because REUTER'S results are for a three-dimensional bubble, while COLLINS treatment is for a two-dimensional case, and secondly because REUTER'S results are not quantitatively reliable as was discussed previously.

As is seen the most successful theoretical curves are curve 1 due to DAVIDSON and curve 3 which is obtained by the modification of JACKSON'S analysis following the suggestion of STEWART. For up to four bubble radius the experimental results are in marginally better agreement with JACKSON'S modified curve. However, the agreement with DAVIDSON curve is fairly good. From this point down to 1.5 bubble radius the agreement with DAVIDSON is much better. Near the bubble, however, the agreement between the experimental results and JACKSON'S modified prediction is very good. Inside the bubble, pressure change is linear, which is as expected, and gives a pressure centre which is distinctly above the geometrical centre of the bubble. The slope of the pressure curve inside the bubble changes noticeably from half bubble radius below the geometrical centre. This coincides with the wake region inside the circular bubble. At the bottom of the wake there is a good agreement between the magnitudes of DAVIDSON'S prediction and the

experiment, however the slopes of the respective curves are quite different. This of course is not surprising in view of the fact that DAVIDSON model considers a completely circular bubble without wake. The agreement between the experimental results and COLLINS prediction is very poor, and this is in spite of the fact that in COLLINS model a wake is present. This again suggests that the artificial imposition of wake does not improve the situation. Down to half a bubble radius below the bottom of the circular bubble there is a region where the pressure distribution is almost the same as in the particulate phase far away from the bubble. After this region the pressure recovery starts and the curve slopes upward. An inflection point is noticeable about 3 bubble radii below the centre of the bubble. At about 6 bubble radii most of the pressure recovery has taken place and the pressure reaches that of the normal bed, a short while after.

Returning to the region above the bubble we see that DAVIDSON and also COLLINS curves are reasonably representative of the situation down to one bubble radius from the tip of the bubble. The reason perhaps is that the assumption of constancy of voidage in DAVIDSON model is justifiable in that region of the bed above the bubble. LOCKETT & HARRISON (51) showed that the extent of voidage variation is about one bubble radius above the bubble. From this region down to the bubble tip the voidage changes more and more from the incipient value. It is then expected that DAVIDSON'S predictions deviate more and more from the experimental results, (Fig.(17)). At the same time it is clearly noticed that in this region JACKSON'S modified expression for the pressure predicts results which are in satisfactory agreement with the experimental results. At the tip of the bubble this agreement is seen to be very good, (Fig.(17)). This is quite expected

because, as was pointed out by STEWART (49), JACKSON'S pressure expression is the only one which is obtained from a particle momentum equation with allowance for voidage variation. Inclusion of the voidage variation is important when the development of the fluid pressure, controlled by the rate of change of particle momentum is considered. Perhaps it should be mentioned here that the degree of agreement between JACKSON'S modified expression and the present experimental data is much better than that of JACKSON modified and REUTER'S experimental data, as discussed by STEWART (49). This is perhaps due to the fact that REUTER'S data, for the reasons previously discussed, are not accurate, at least for the purpose of comparison with theory. The declining agreement between DAVIDSON predictions and the experimental results from a region corresponding to the top of the wake inside the circular bubble (which is not considered in DAVIDSON model) down to a few bubble radii below the bubble suggest that the activity of the wake is more pronounced below the circular bubble rather than inside it. The fact that the expression due to COLLINS predicts results which are in much less agreement with experiment, in spite of the imposition of the wake in the model, supports this suggestion. From about three radii below the bubble where the influence of the bubble and the wake has vanished, the agreement between DAVIDSON'S predictions and the experiments improves. This also supports the above suggestion.

We notice that there is a region near the lower boundary of the bubble where the pressure gradient is the same as in the particulate phase far away from the bubble. This, however, does not mean that the gas and particle flow pattern is the same. In fact we know that voidage in this region is higher than the incipient value. So in order to have a pressure distribution the same as in the distant

particulate phase, there must be a higher velocity through the particles. More about this point will be said later on. We have also noticed that there is an inflection point in the pressure recovery part of the pressure curve about 1.5 bubble diameters below the centre of the bubble. This is consistent with the previous findings that the effect of wake is not sensed beyond 1.5 diameters below the centre. It is from this point where the dynamics of the system becomes the only controlling factor for the pressure. It is quite likely that this inflection point is due to this change in the mechanism by which pressure recovery and adjustment takes place.

4.5.3 EFFECT OF PARTICLE SHAPE AND SIZE ON THE PRESSURE VARIATION

In Fig.(18) and Fig.(19) the pressure distance data obtained when bubbles of almost identical size were injected in beds of glass particles of different size are presented. These figures correspond to cases where ballotini grades 10 and 8 respectively were used. The circles imposed on the graphs are the circles of best fit to the bubbles near the probe in each case. For ballotini grade 10 a significant part of the bubble is occupied by the wake. Such a wake is not observed for ballotini grade 8 as can be seen from Figs.(19a, b, c) where the pressure data and bubble tracings are presented for each injected bubble separately. The corresponding graph for ballotini grade 10 is presented in Fig.(18a) from which the presence of the wake is quite apparent. The bubble size however in both cases were the same (judged from the fitted circle) and about 6.5 cm in diameter. As is noticed from the information supplied on the graphs, the overall conditions for these cases were quite different, and were adjusted in such a way to produce bubbles of identical size. The data can directly be used for the purpose of comparison.

In Fig.(20) the lines of best fit through the points of Fig.(18) and Fig.(19) are together represented. Examination of Fig.(20) shows that there are three major differences between the curves corresponding to ballotini 8 and 10. The first difference is that the curve corresponding to ballotini grade 8 (larger particles) has a higher peak near the bubble nose. The reason for this can be presented as follows.

ROWE (61) has shown that in a gas fluidized system when a local change in the particle spacings occurs, there needs to be a considerable change in the velocity of the fluidizing fluid, if the particles

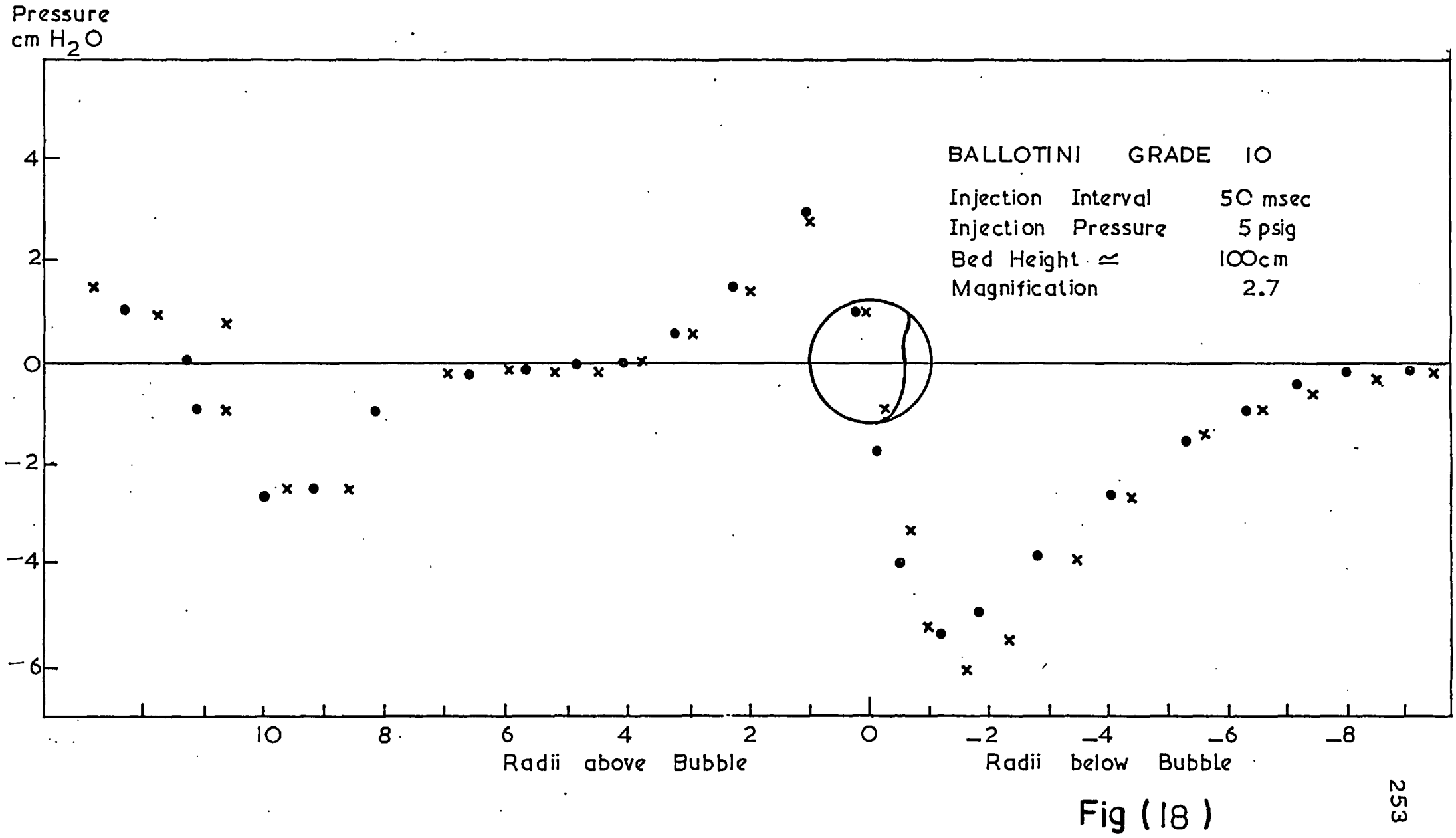
Pressure
cm H_2O
BALLOTINI GRADE 10
Injection Interval 50 msec
Injection Pressure 5 psig
Bed Height ≃ 100cm
Magnification 2.7
4
2
0
−2
−4
−6
10
8
6
4
2
0
−2
−4
−6
−8
Radii above Bubble
Radii below Bubble

Fig (18)

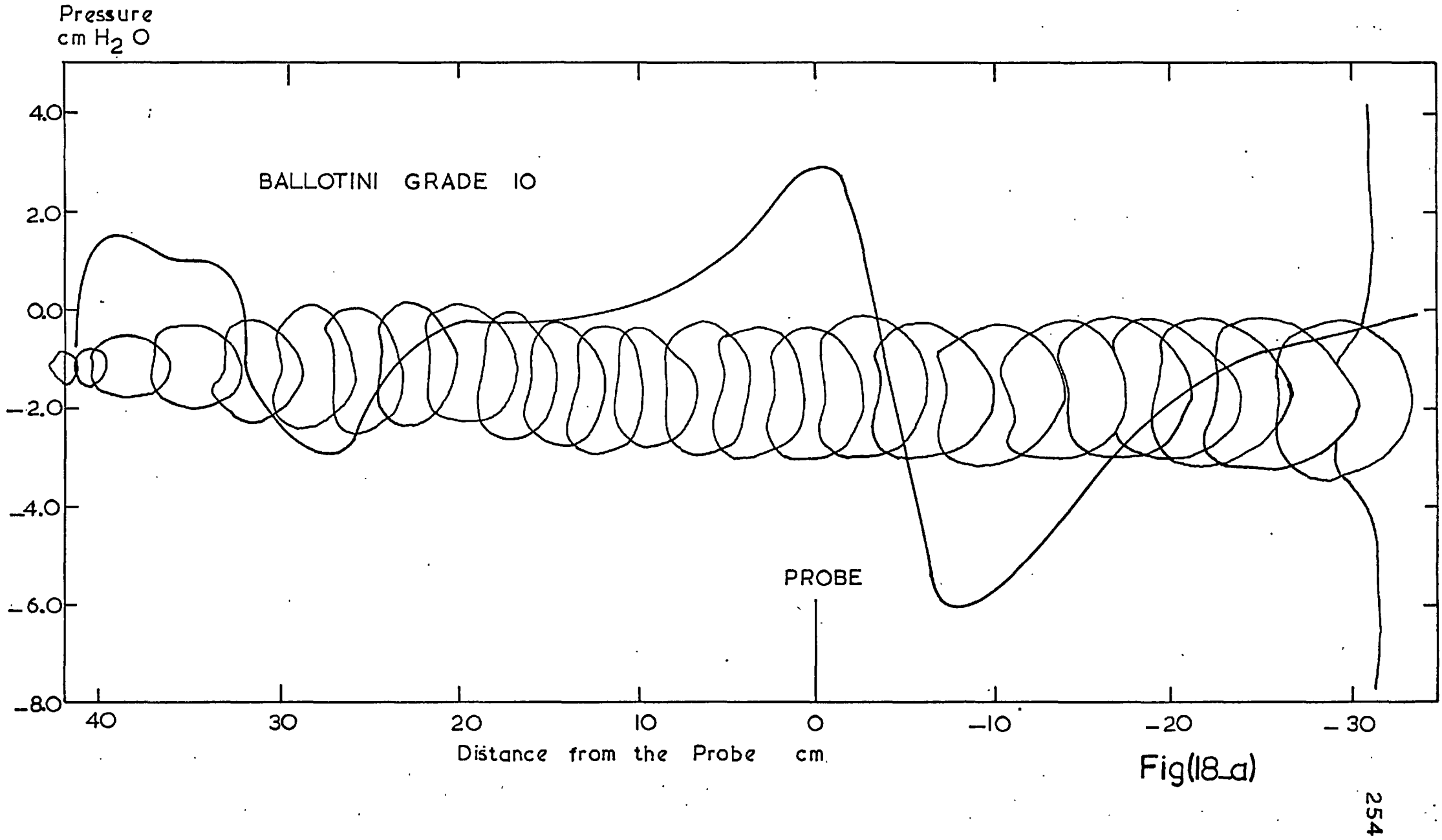
Pressure
cm H_2O
4.0
2.0
0.0
-2.0
-4.0
-6.0
-8.0
BALLOTINI GRADE 10
PROBE
40
30
20
10
0
-10
-20
-30
Distance from the Probe cm

Fig(18_a)

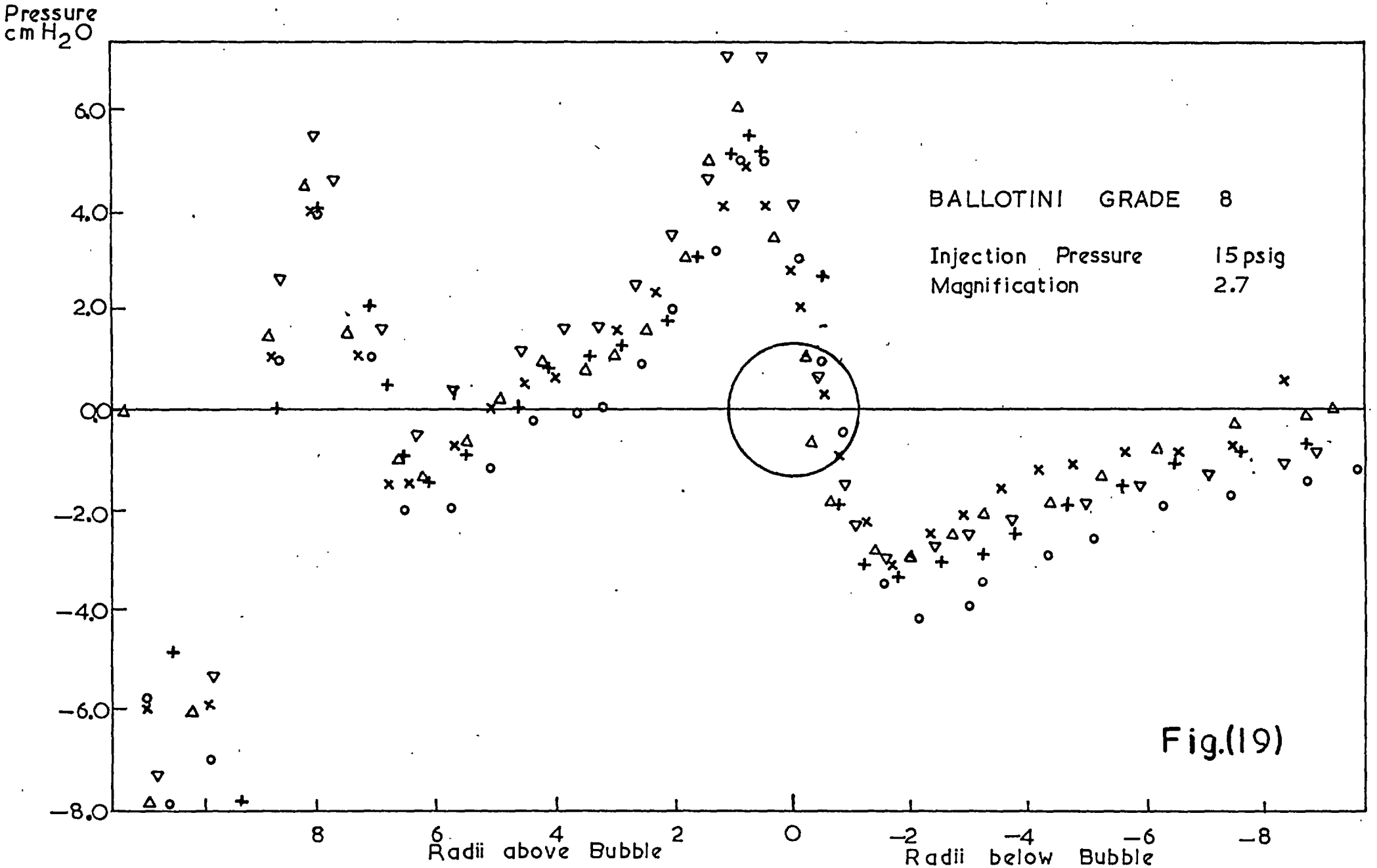
Pressure
cm H_2O
6.0
4.0
2.0
0.0
−2.0
−4.0
−6.0
−8.0
8
6
4
2
0
−2
−4
−6
−8
Radii above Bubble
Radii below Bubble
BALLOTINI GRADE 8
Injection Pressure 15 psig
Magnification 2.7

Fig.(19)

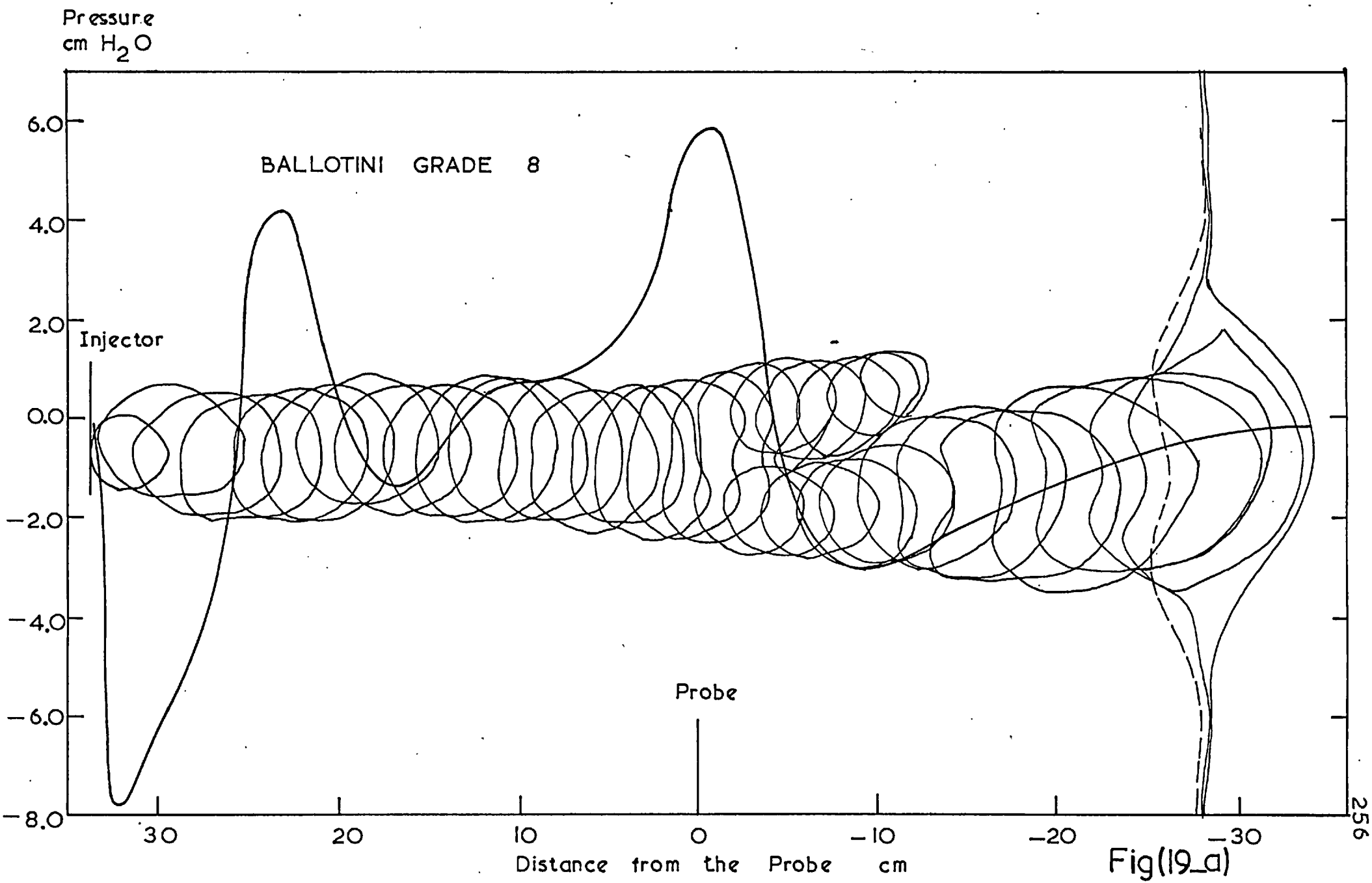
Pressure
cm H_2O
BALLOTINI GRADE 8
6.0
4.0
2.0
0.0
−2.0
−4.0
−6.0
−8.0
Injector
Probe
30
20
10
0
−10
−20
−30
Distance from the Probe cm
256

Fig(19_a)

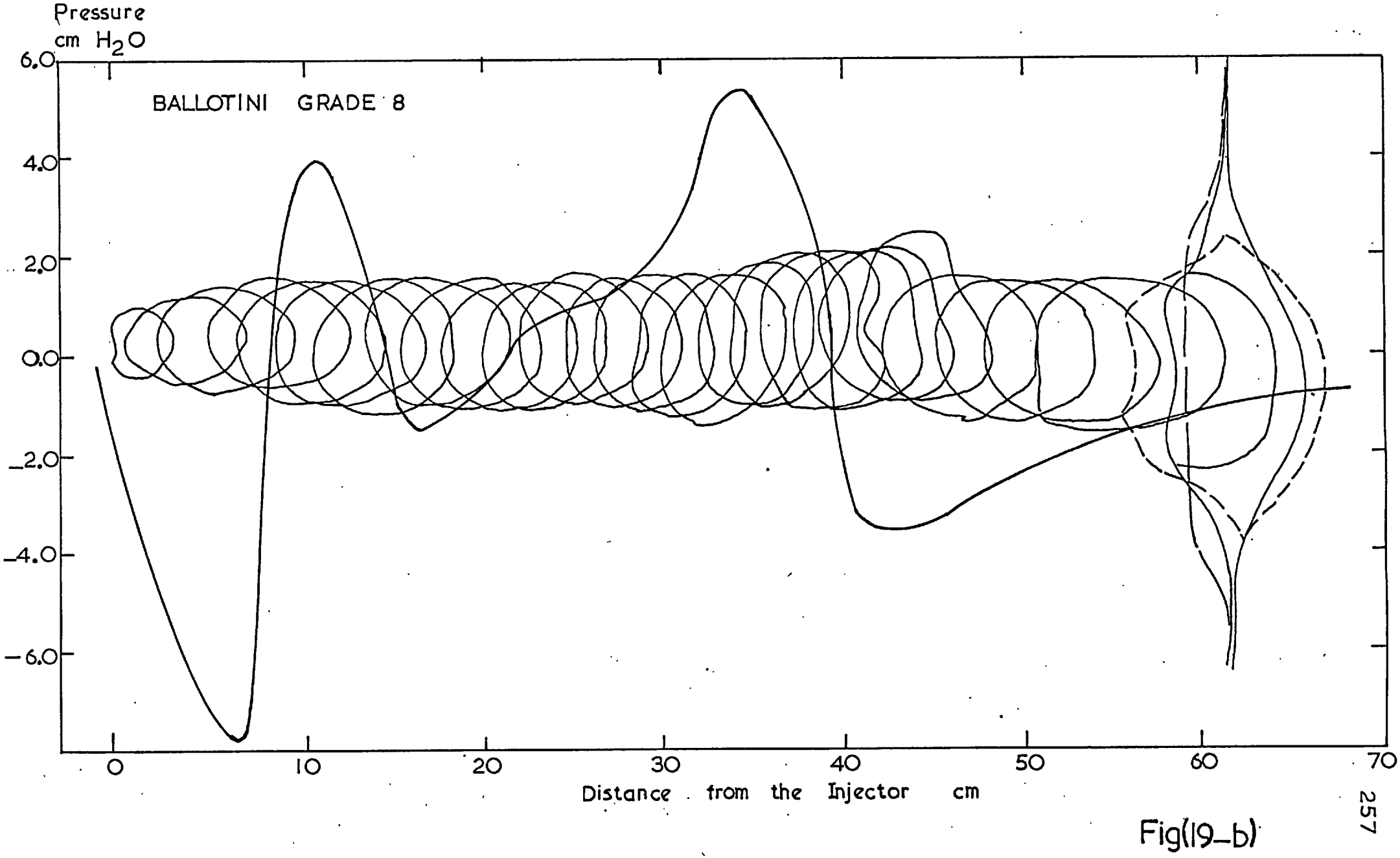
Pressure
cm H_2O
BALLOTINI GRADE 8
6.0
4.0
2.0
0.0
-2.0
-4.0
-6.0
0
10
20
30
40
50
60
70
Distance from the Injector cm

Fig(19-b)

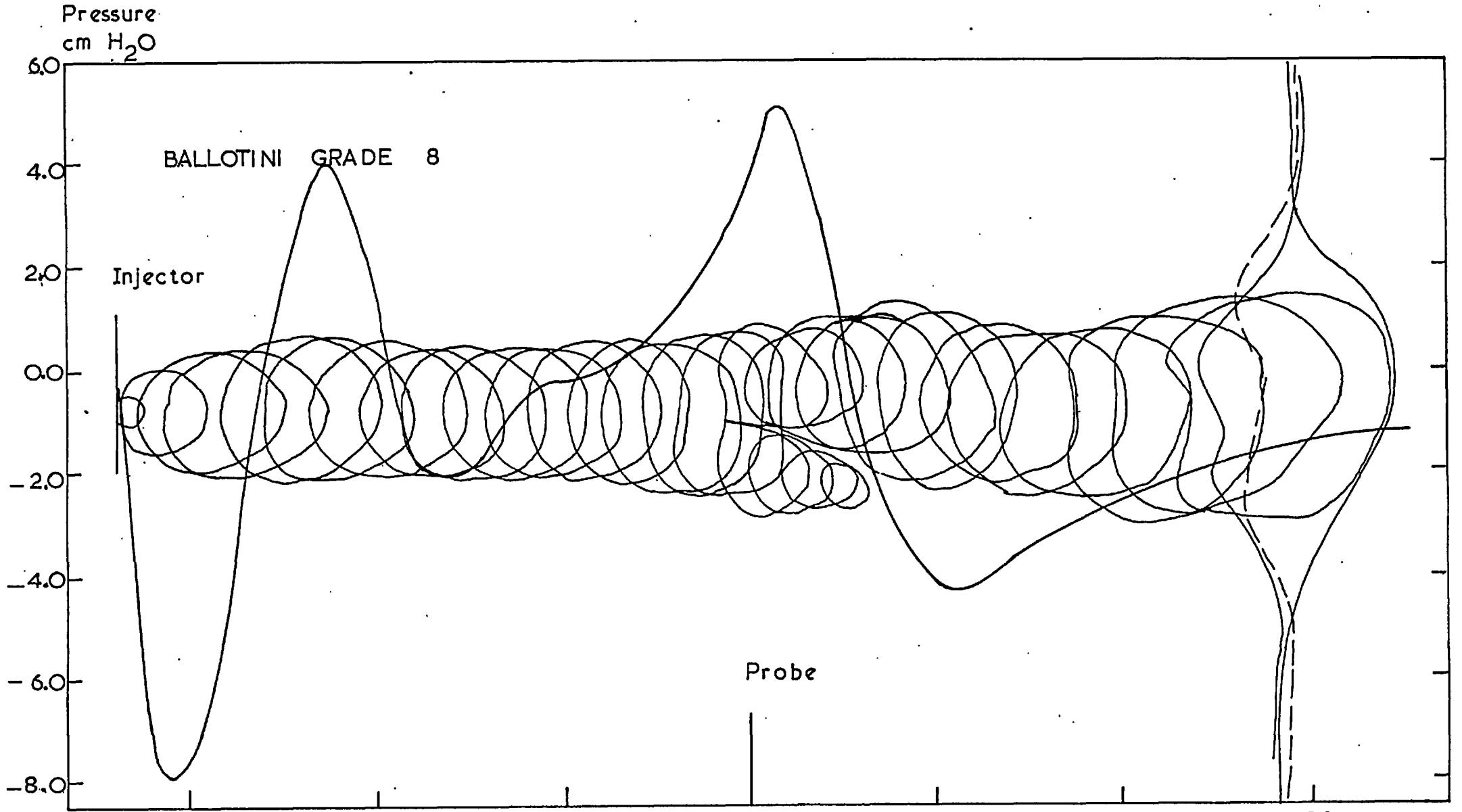
Pressure
cm H_2O
6.0
4.0
2.0
0.0
-2.0
-4.0
-6.0
-8.0
BALLOTINI GRADE 8
Injector
Probe
30
20
10
0
-10
-20
-30
Distance from the Probe cm

Fig (19_c)

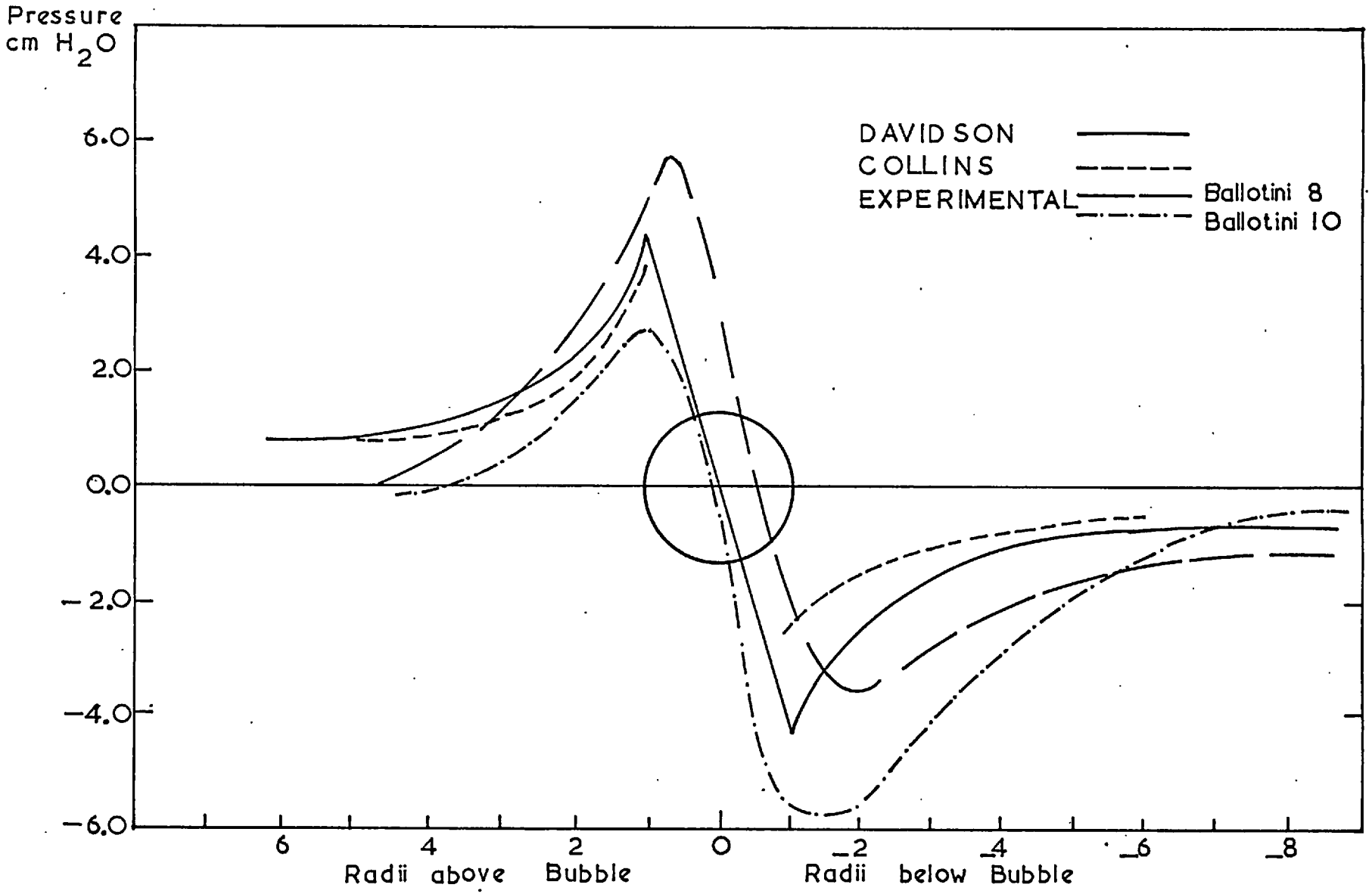
Pressure
cm H_2O
6.0
4.0
2.0
0.0
−2.0
−4.0
−6.0
DAVIDSON
COLLINS
EXPERIMENTAL
Ballotini 8
Ballotini 10
6
4
2
0
−2
−4
−6
−8
Radii above Bubble
Radii below Bubble

Fig.(20)

are to be supported. Starting from the equation for the prediction of required velocity change due to particle displacement, and a simple order of magnitude calculation, it can be shown that the ratio of the required velocity change due to identical displacement in systems of different particle size is proportional to the square of the ratio of particle diameters. Thus there needs to be a higher pressure gradient in the case of larger particles. Now clearly the downstream pressure is the same for systems of different particle size but identical material. This is because the pressure at a point far above the bubble is a function only of the depth below the surface. Therefore it follows that there must be a higher pressure near the nose of the bubble in a system of larger particles. We see that the observed difference between the pressure data for ballotini grade 8 and 10 are expected. Of course we have assumed the same displacement and hence voidage at the nose of bubbles in the different cases. This is justifiable in view of the fact that JACKSON'S analysis for voidage around a bubble is independent of the particle size. The slight dependence of the voidage distribution on the size range distribution of particles, reported by LOCKETT & HARRISON is not very significant. Their experimental results for the narrow size range sample of particles could be very well fitted by theory. The anomolous behaviour of the wide size range sample could have been due to several experimental difficulties and therefore is not in serious conflict with respect to the theory. The above argument is due to STEWART (52) and will be referred to again. For the present we notice that in the absence of any conflicting evidence the assumption of identical voidage for different particle sizes is justifiable.

The next difference to be considered is that as is clearly seen from Fig.(20) for the region behind the bubble values of pressure

obtained for larger particles fall above those for smaller ones. As was pointed out earlier the bubbles in the case of ballotini grade 8 did not have a wake as pronounced as in the case of grade 10. Experimental work of ROWE & PARTRIDGE (53) on X-ray studies of bubbles in three-dimensional fluidized beds of spherical glass particles showed that the wake fraction of bubbles decreased as the particle size increased. It may be that the absence of wake in the case of ballotini grade 8 is responsible for the observed difference.

The next and the last difference between the results corresponding to ballotini grades 8 and 10 is that for the former case the pressure centre falls below the geometrical centre of the bubble. It is noticed that the whole of the pressure curve in Fig.(19) and Fig.(20) for ballotini grade 8 is slightly shifted towards the right. This may be due to some inaccuracy in the determination of the exact position of the bubble. However, this is not very likely because all the results in Fig.(19) stay very close together and therefore the shift cannot be due to accidental error. There might have been some bias in this particular set of experiments the source of which is not known however. At any rate this uncertainty about the exact position of the bubble is not very serious and does not affect the conclusions concerning the previous arguments. As far as the position of the pressure centre is concerned, it can be said that for larger particles this point falls below that of the smaller particles.

In addition to glass ballotini, coarse and fine sand were also employed in these experiments. The pressure data obtained when bubbles of identical size of about 10 cm diameter were injected are represented in Fig.(21) and Fig.(22) respectively. The best curves drawn through these points for both cases are given in Fig.(23). It is noticed that all major differences as observed in the case of

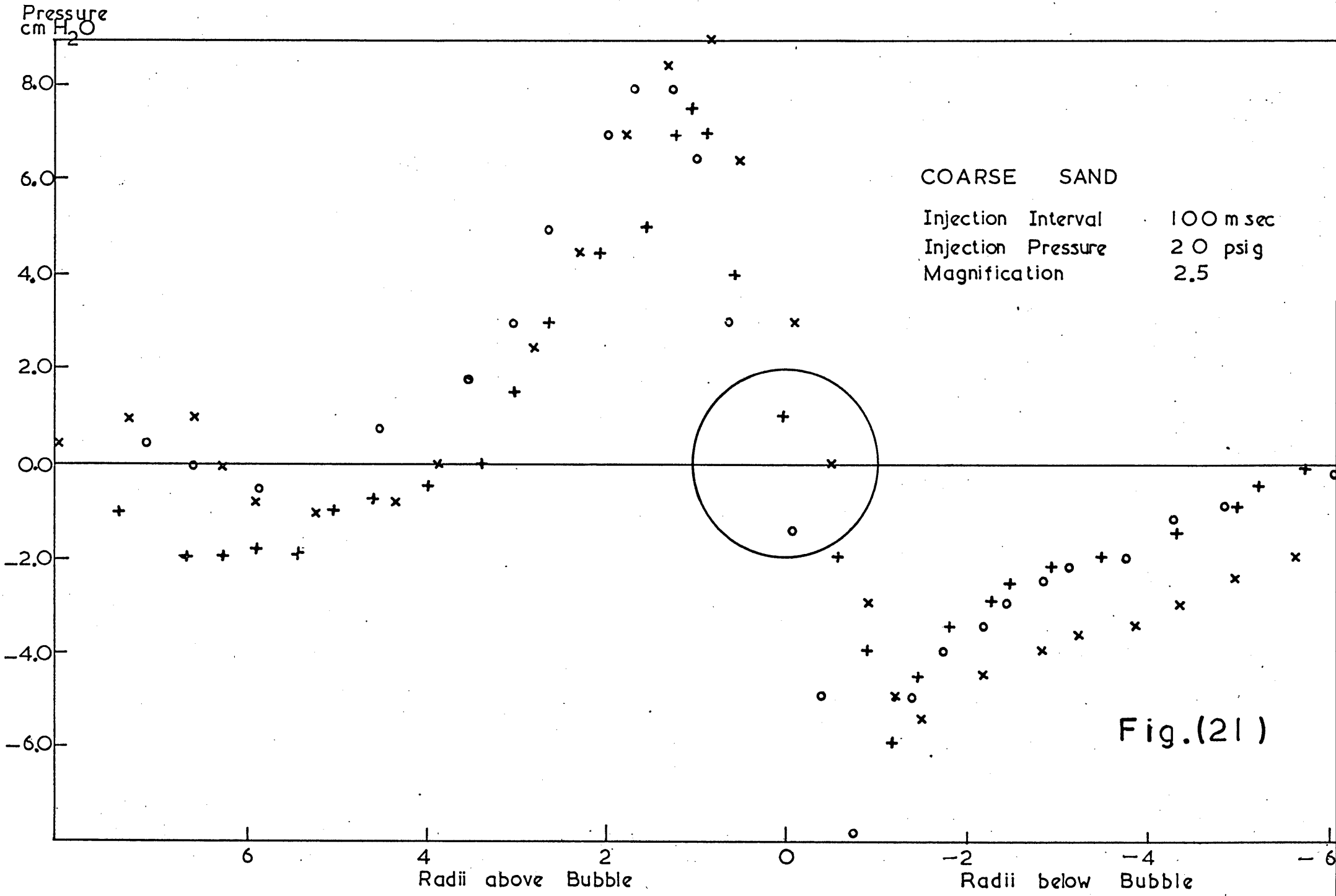
Pressure
cm H_2O
8.0
6.0
4.0
2.0
0.0
-2.0
-4.0
-6.0
COARSE SAND
Injection Interval 100 m sec
Injection Pressure 20 psig
Magnification 2.5
6
4
2
0
-2
-4
-6
Radii above Bubble
Radii below Bubble

Fig.(21)

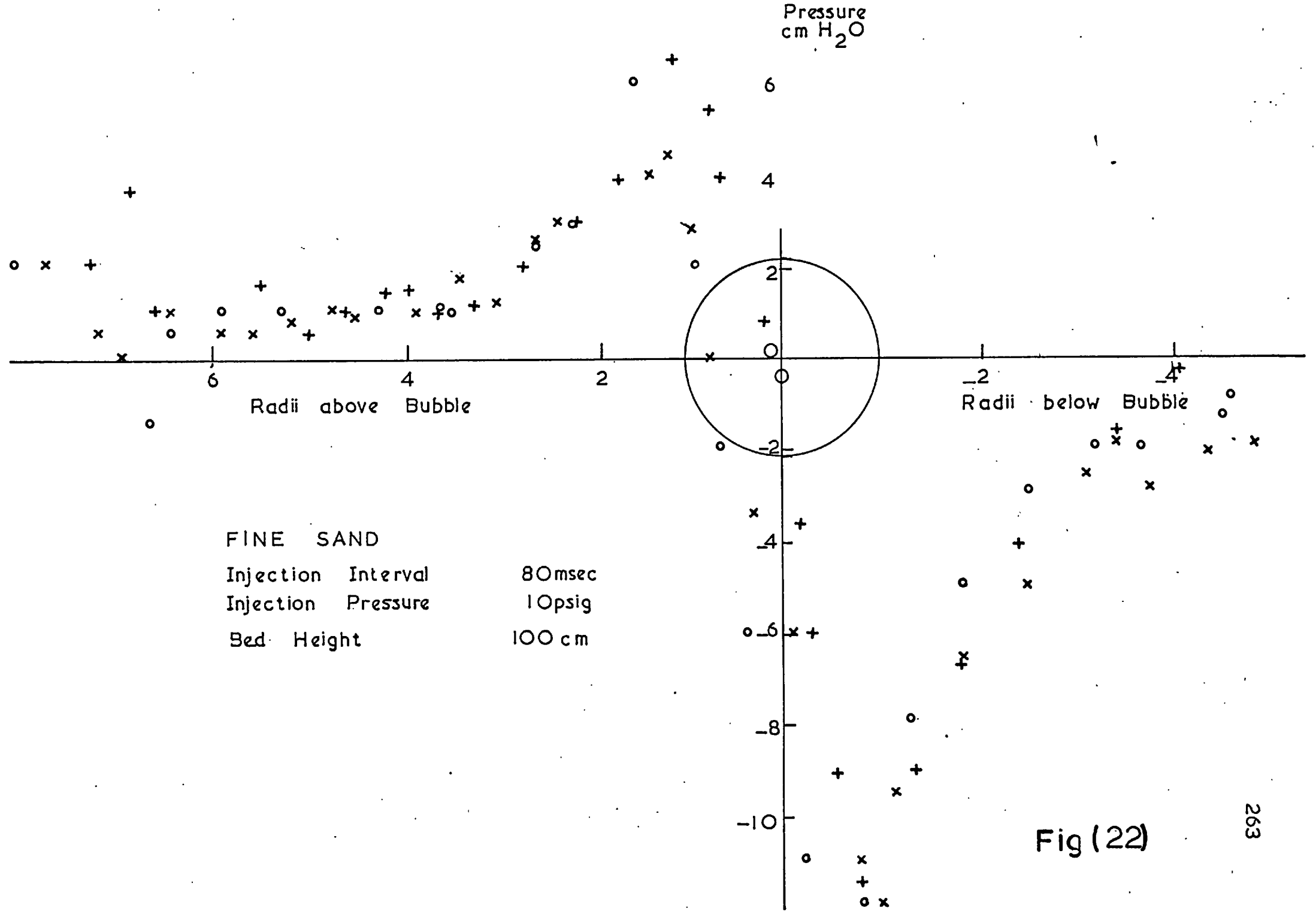
Pressure
cm H_2O
6
4
2
0
-2
-4
-6
-8
-10
6
4
2
0
-2
-4
Radii above Bubble
Radii below Bubble
FINE SAND
Injection Interval 80msec
Injection Pressure 10psig
Bed Height 100 cm

Fig (22)

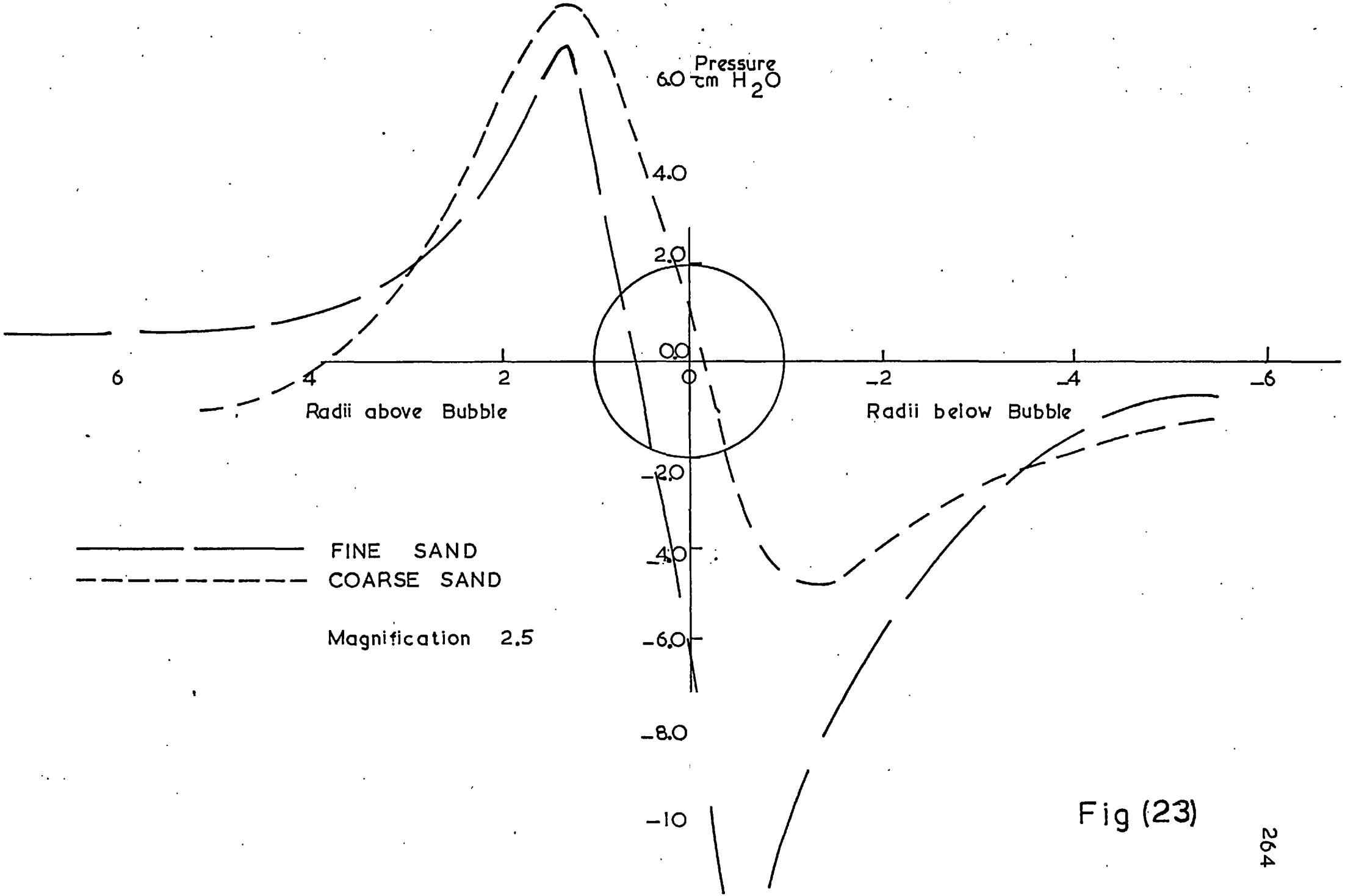
Pressure
cm H_2O
6.0
4.0
2.0
0.0
-2.0
-4.0
-6.0
-8.0
-10
6
4
2
0
-2
-4
-6
Radii above Bubble
Radii below Bubble
FINE SAND
COARSE SAND
Magnification 2.5

Fig (23)

ballotini grade 8 and 10 are present. The pressure peak for coarse sand is higher and the corresponding part behind the bubble falls above that of fine sand. The position of the pressure centre is slightly below the geometrical centre but distinctly below that of the fine sand in agreement with the results of ballotini grade 8 and 10. The agreement of the observed trend of the pressure curves in the case of spherical particles and in this case is remarkable. Exactly the same explanations are applicable.

By now we have provided satisfactory answers to some of the questions which were posed in the beginning of the work. A certain amount of information and evidence have been presented which provides a clear picture of the pressure distribution around a rising bubble. For some of the anomalies observed in the literature satisfactory explanations have been provided. In the next section we concentrate on the pressure gradient studies around a rising bubble.

4.6 PRESSURE GRADIENT AROUND A RISING BUBBLE

The ultimate purpose in the study of pressure distribution around a bubble in a fluidized bed is to obtain relevant information which would advance the understanding of the fluid flow pattern and magnitude into and out of the bubble. So far we have obtained a fairly accurate knowledge of the pressure distribution around a bubble in fluidized beds. We have also studied and explained what happens when the bubble size, particle size and shape change. Now, we are going to extend this information further by studying the pressure gradient distribution around a freely rising bubble.

In order to obtain experimental data for the pressure gradient around a bubble there are two different experimental techniques. One way is to measure the absolute pressure at various distances from the probe. Then from these data the pressure gradient can be assessed. This is an indirect way of assessment. The second method is directly to measure the pressure gradient at various distances from the bubble. We are going to employ both these techniques and compare the obtained results with each other.

4.6.1 PRESSURE GRADIENT MEASUREMENT

Indirect Measurement

The pressure-distance curves obtained in the previous chapter give the difference between the pressure at a point on the vertical axis of the symmetry of the bubble and the pressure at the same level but away from the bubble. This pressure is in fact purely due to the presence of the bubble. Now in order to obtain the pressure gradient at various distances from the bubble one has to convert these curves in such a way that the absolute pressure can be obtained from the curve. In Fig.(23a) a typical example of the pressure-distance curves presented in the previous chapter, and the corresponding bubble tracings are given. As was previously explained this curve can be converted to the form given in Fig.(23b) which is a more informative way of representation of the same data. On the same graph a straight line has been drawn which represents the hydrostatic pressure at each point in the bed far away from the bubble. This line is drawn in such a way to pass through the bubble centre of pressure where the pressure inside the bubble and the pressure far away from the bubble but on the same horizontal level is the same. Now if we read the hydrostatic pressure from curve (2) for a point and add to the pressure given by curve (1) for the same point, the result would be the absolute pressure at that point. If we repeat the same process for a number of points and plot the results as a function of the distance from the bubble we get the curve which represents the absolute pressure for each point above, inside and below the bubble. A curve constructed in such a way is given in Fig.(24). The continuous line gives the hydrostatic pressure at each point away from the bubble. As is seen from Fig.(24) the pressure on the axis of symmetry far below the bubble is the same as the hydrostatic pressure at that level,

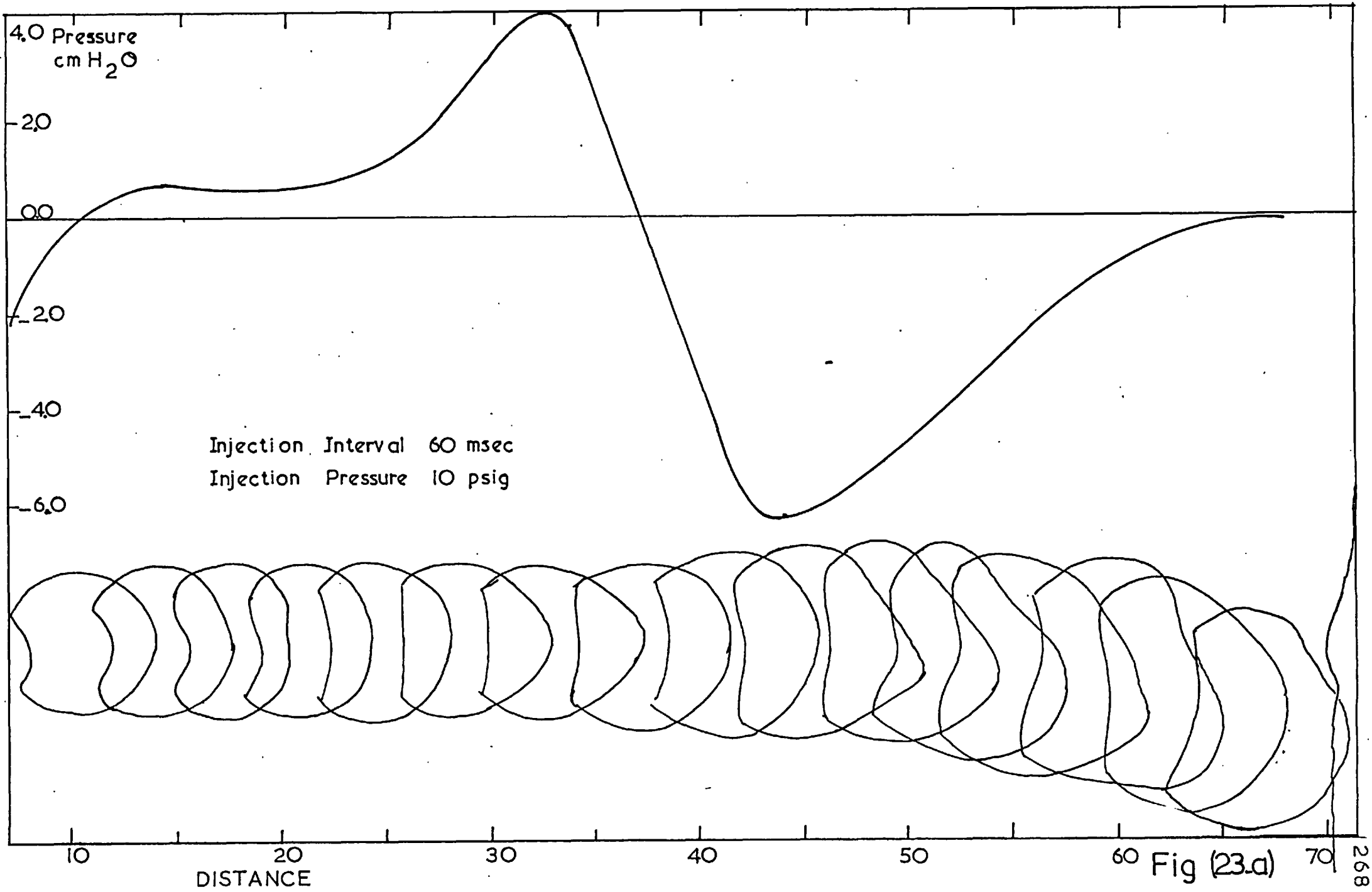
4.0 Pressure
cm H_2O
2.0
0.0
-2.0
-4.0
-6.0
Injection Interval 60 msec
Injection Pressure 10 psig
10
20
30
40
50
60
70
DISTANCE

Fig (23.a)

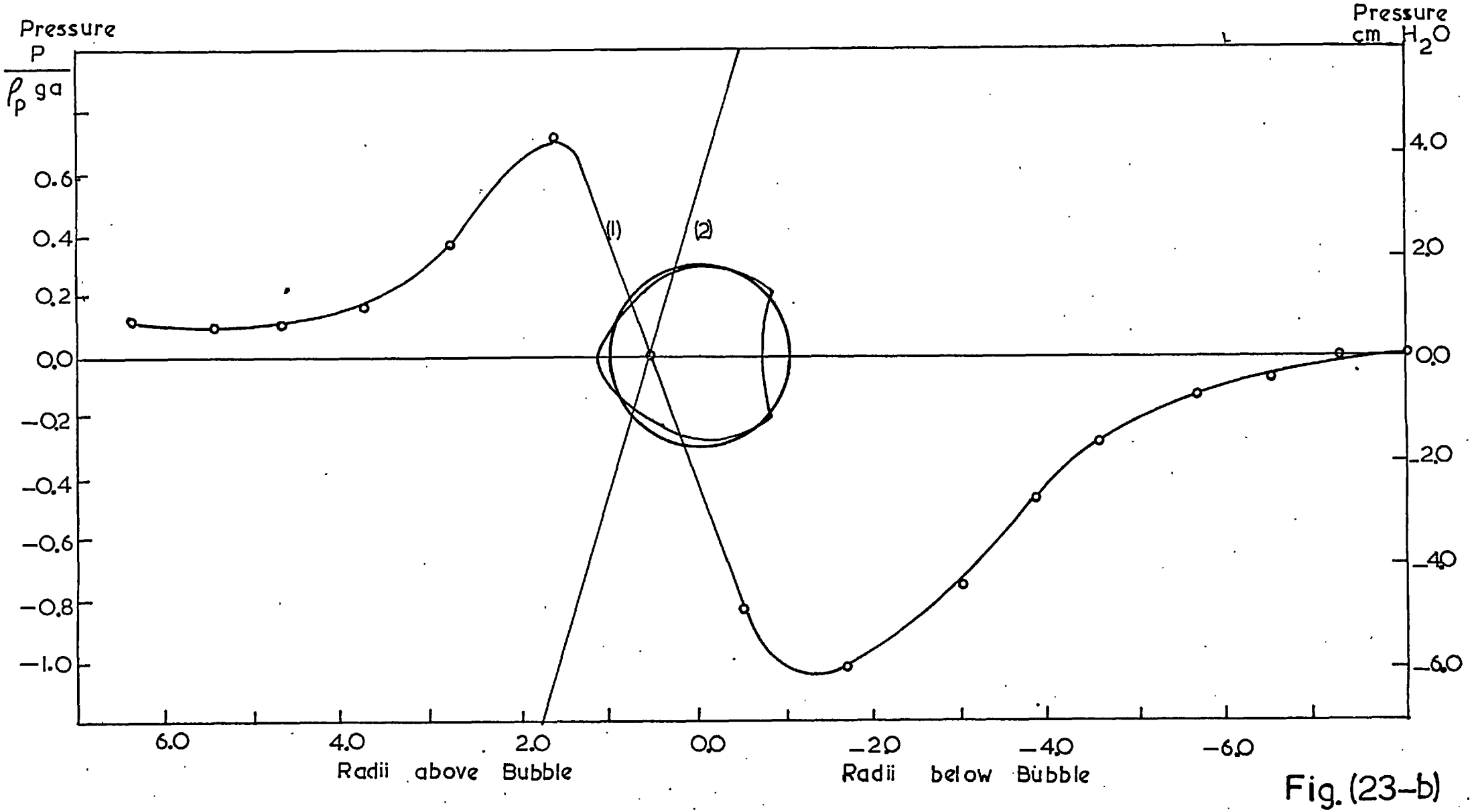
Pressure
P
ρp ga
Pressure
cm H2O
0.6
0.4
0.2
0.0
−0.2
−0.4
−0.6
−0.8
−1.0
4.0
2.0
0.0
−2.0
−4.0
−6.0
(1)
(2)
6.0
4.0
2.0
0.0
−2.0
−4.0
−6.0
Radii above Bubble
Radii below Bubble

Fig. (23–b)

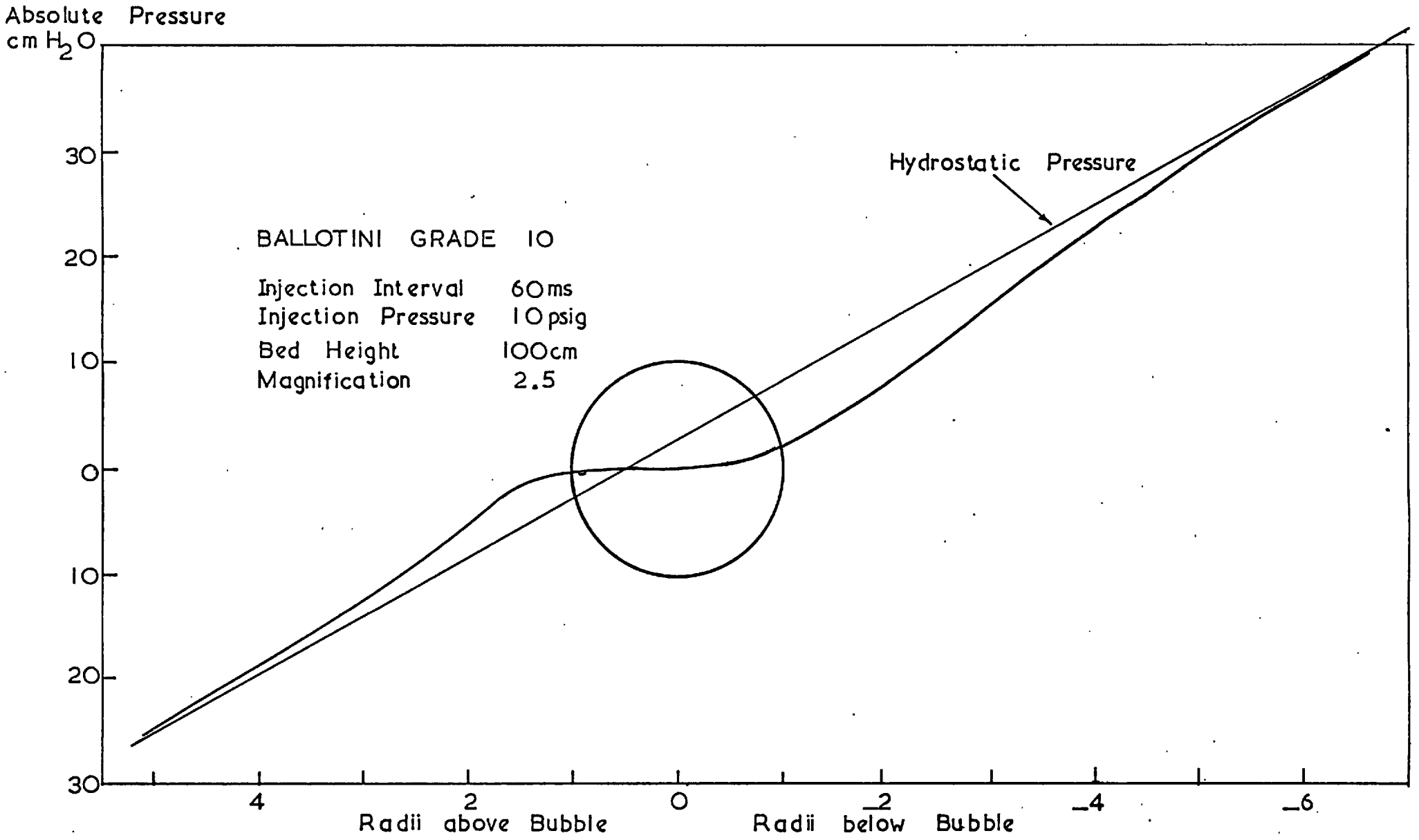
Absolute Pressure
cm H_2O
30
20
10
0
10
20
30
Hydrostatic Pressure
BALLOTINI GRADE 10
Injection Interval 60ms
Injection Pressure 10psig
Bed Height 100cm
Magnification 2.5
4
2
0
-2
-4
-6
Radii above Bubble
Radii below Bubble

Fig.(24)

towards the bubble the pressure deviates from the hydrostatic pressure and inside the bubble the pressure remains approximately constant. Just above the bubble the pressure is higher than the hydrostatic pressure of the same level. Away from the bubble pressure gradually approaches the hydrostatic pressure and becomes identical to it at a large distance above the bubble.

The next step is to find the pressure gradient at each point from the curve in Fig.(24). The pressure gradient at each point is given by the tangent of the curve at that point. If we choose two points on the curve which are fairly close together and read off the corresponding pressures, the difference can be considered as the pressure gradient for the point half way between these points. Here we choose a distance of 5 mm on the distance axis on either side of the points at which the pressure gradient is to be assessed in the way just explained. This is a fairly small distance compared with the size of the bubbles around which the pressure gradient is to be assessed. The bubble in Fig.(24) is of diameter about 10 cm. Strictly speaking the true pressure gradient is obtained when this distance is decreased down to an infinitely small distance. Then the joining line becomes the tangent and the points, hence the mid points coincide. If we repeat the above mentioned procedure for a number of pairs of points and plot the results as a function of the distance from the bubble, the curve so obtained gives the pressure gradient distribution along the vertical axis of the symmetry of the bubble. A curve constructed in such a way is given in Fig.(25). The continuous horizontal line shows the pressure gradient in the particulate phase far away from the bubble. As is seen the pressure gradient along the axis of the symmetry of the bubble far above the bubble, is equal to the normal bed pressure gradient. Towards the bubble it starts to

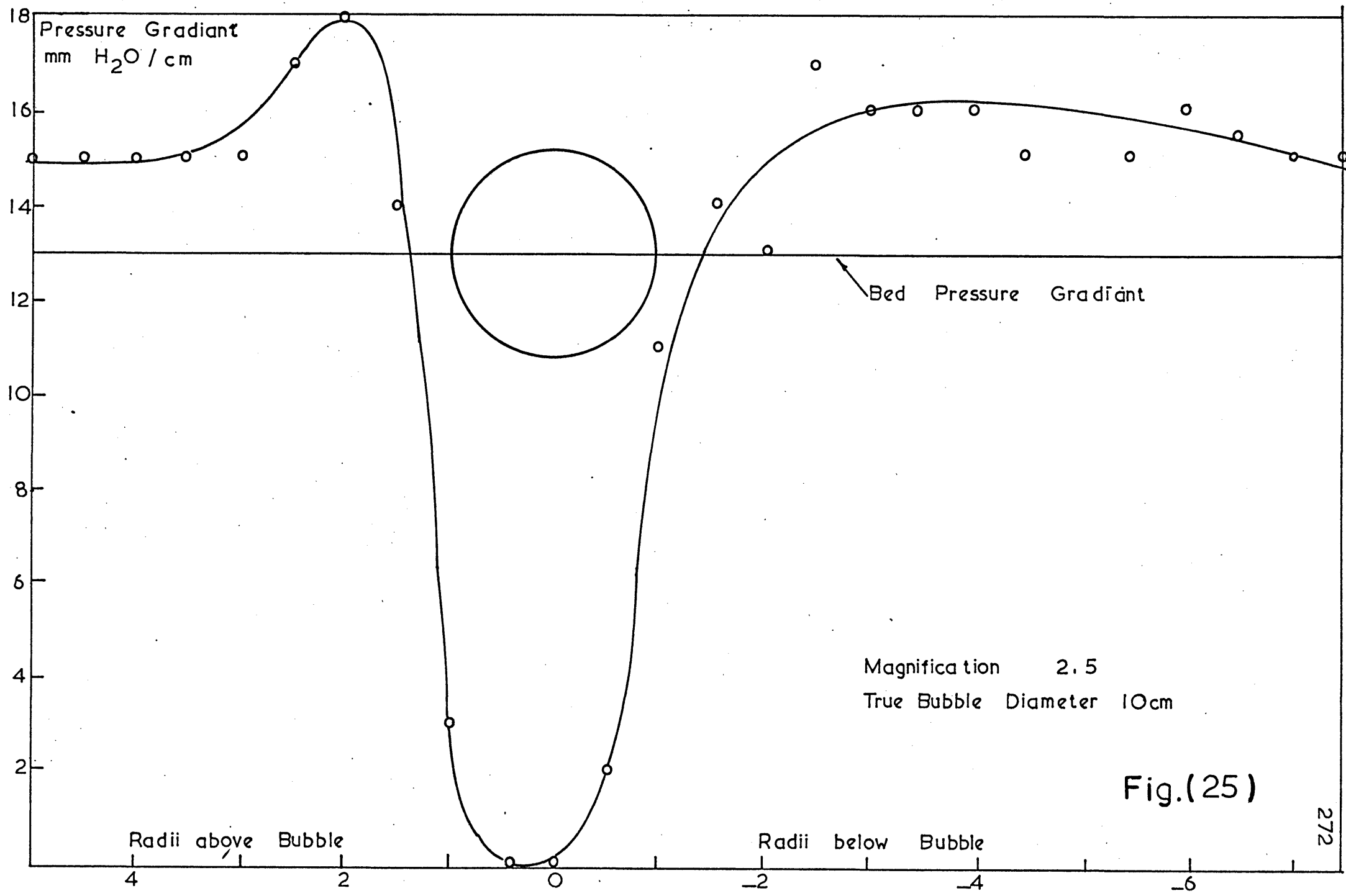
Pressure Gradiant
mm H_2O / cm
18
16
14
12
10
8
6
4
2
Bed Pressure Gradiant
Magnification 2.5
True Bubble Diameter 10cm
Radii above Bubble
Radii below Bubble
4
2
0
−2
−4
−6

Fig.(25)

rise gradually. It falls off inside the bubble. Below the bubble again it has a value greater than the normal bed pressure gradient and approaches this value far away below the bubble.

As was pointed out earlier the bubble diameter in this experiment was about 10 cm which is quite a large bubble. In order to investigate the effect of the size of a bubble on the distribution and magnitude of the pressure gradient it was decided to repeat the experiment for smaller bubbles. It was noticed however that when the size of the injected bubble was too small the pressure-time curve on the output of the recorder was of such small dimensions that the transformation of the curves to pressure-distance curves and also subsequent handling of them caused extraordinary relative error. Therefore, there was a minimum bubble size of 5 to 6 cm which could be studied while making sure that the data were not necessarily subjected to extra errors. In Fig.(26) the result of pressure recordings for two bubbles of diameters 5.1 and 6.7 cm are presented. The vertical axis gives the pressure in P/ρ_p g a and the horizontal axis gives the dimensionless distance $S = \frac{r}{a}$. The curve is drawn through the averaged data. The straight line which passes through the centre of pressure of the bubble gives the particulate phase pressure at each level away from the bubble. The data on Fig.(26) when plotted to large scale was used to obtain the absolute pressure data on the axis of the symmetry of the bubble. The data so obtained were plotted on a very large scale. Fig.(27) gives the same curve but at smaller scale. The original curves were drawn to a scale ten times bigger in pressure dimension and four times bigger in distance dimension. It was essential to plot the curves in such a large scale for the next stage when the pressure gradient was to be measured. Some of the details of Fig.(27) are not seen, particularly inside the

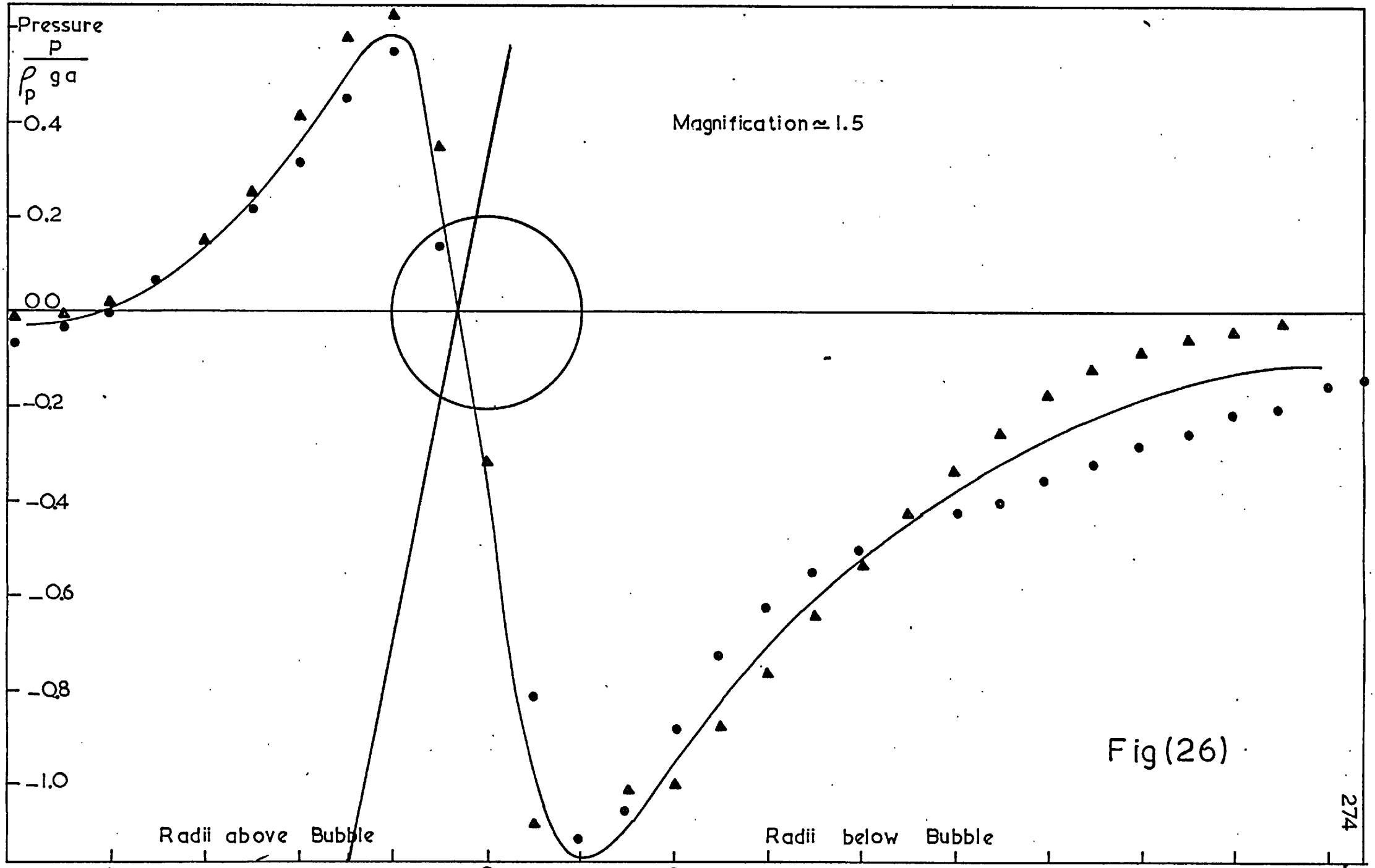
Pressure
P
ρp g a
0.4
0.2
0.0
-0.2
-0.4
-0.6
-0.8
-1.0
Magnification ≃ 1.5
Radii above Bubble
Radii below Bubble
4
2
0
-2
-4
-6
-8

Fig (26)

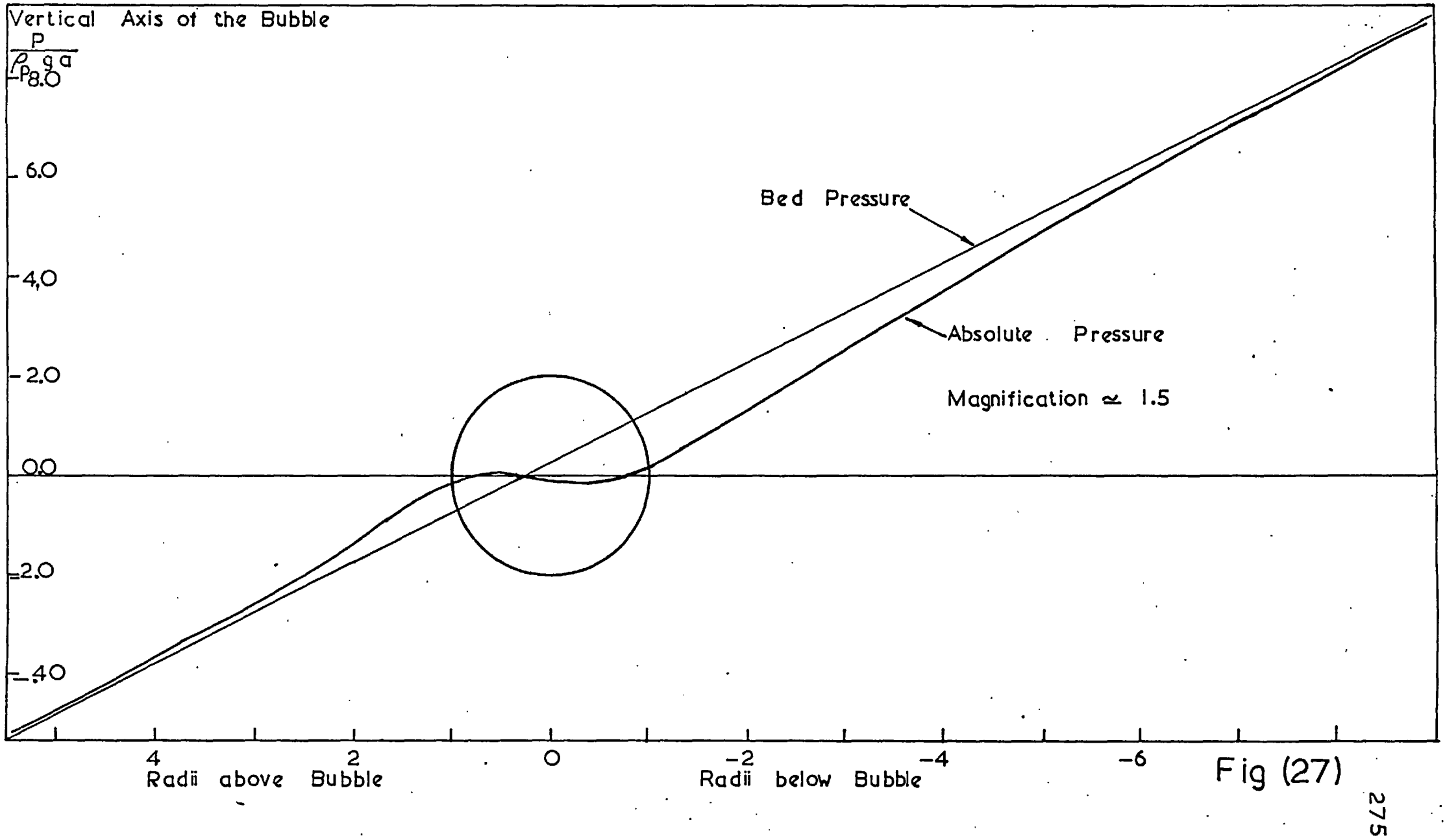
Absolute Pressure on the Vertical Axis of the Bubble
P / ρ g a
8.0
6.0
4.0
2.0
0.0
-2.0
-4.0
Bed Pressure
Absolute Pressure
Magnification ≈ 1.5
4
2
0
-2
-4
-6
Radii above Bubble
Radii below Bubble

Fig (27)

bubble. The data are also presented in Table (2).

TABLE (2)

S	$P^*_H/\rho_p ga$	$\Delta P^*/\rho_p ga$	$(P/\rho_p ga)_{Abs}$	Pressure Gradient cm H_2O/cm
5.5	-5.2	-0.062	-5.262	15.2
5.0	-4.7	-0.040	-4.740	15.2
4.5	-4.2	-0.019	-4.219	15.2
4.0	-3.7	0.011	-3.689	15.2
3.5	-3.2	0.073	-3.127	15.2
3.0	-2.7	0.148	-2.552	15.8
2.5	-2.2	0.234	-1.966	15.0
2.0	-1.7	0.362	-1.338	16.8
1.5	-1.2	0.522	-0.678	16.8
1.0	-0.7	0.594	-0.106	12.0
0.5	-0.2	0.249	0.049	- 2.0
0.0	0.3	-0.314	-0.014	- 3.2
-0.5	0.8	-0.945	-0.145	0.0
-1.0	1.3	-1.162	0.138	13.2
-1.5	1.8	-1.094	0.706	15.6
-2.0	2.3	-0.942	1.358	16.4
-2.5	2.8	-0.802	1.998	17.2
-3.0	3.3	-0.697	2.603	16.0
-3.5	3.8	-0.593	3.207	16.0
-4.0	4.3	-0.516	3.784	15.0
-4.5	4.8	-0.439	4.361	14.2
-5.0	5.3	-0.380	4.920	15.2
-5.5	5.8	-0.327	5.473	16.0
-6.0	6.3	-0.266	6.034	15.2
-6.5	6.8	-0.221	6.579	13.2
-7.0	7.3	-0.180	7.120	13.2
-7.5	7.8	-0.150	7.650	13.2
-8.0	8.3	-0.116	8.184	13.2
-8.5	8.8	-0.081	8.711	13.2

P^*_H = hydrostatic pressure ; P^*_{ABS} = absolute pressure ; $\Delta P = P^*_{ABS} - P^*_H$

One of the striking features of Fig.(27), although not seen here because of the smallness of scale, was that the pressure curve inside the bubble and below the centre of the bubble had its minimum very nearly at the top of the wake. The part of the pressure between -0.5 to -1 bubble radius is clearly the part corresponding to the wake inside the circular bubble. Although not distinguishable here, the slope of the curve inside the wake and near its top was steeper than the line of the normal bed pressure. The slope of the curve lower in the wake, however, was close to the slope of the straight line representing the particulate phase pressure.

The pressure gradient was measured from the absolute pressure curve (original of Fig.(27)) at half-bubble-radius intervals by reading the pressure difference between points at 5 mm distance on either side of the point. The results are given in Table (2) and plotted in Fig.(28). Several ways of representation have been chosen in order to facilitate the comparison of results obtained by different methods.

Direct Measurement

A special pressure probe and assembly was designed for this purpose. A cylinder 6 cm tall, 1.4 cm diameter was made out of brass, which could be fitted with minimum tolerance inside copper couplings mounted on the rear face of the bed at several heights above the distributor. The cylinder was drilled parallel to its axis of symmetry and at 5 mm on each side of it. The holes were 3 mm. diameter and inside them two pieces of brass tubes of size 2 mm I.D. were fitted with minimum tolerance. The opening of the brass tube was covered by a fine gauze (the same as the probes) in order to prevent the particles from entering the tubes. A pointer was mounted on the other end of the cylinder which showed, on a protractor

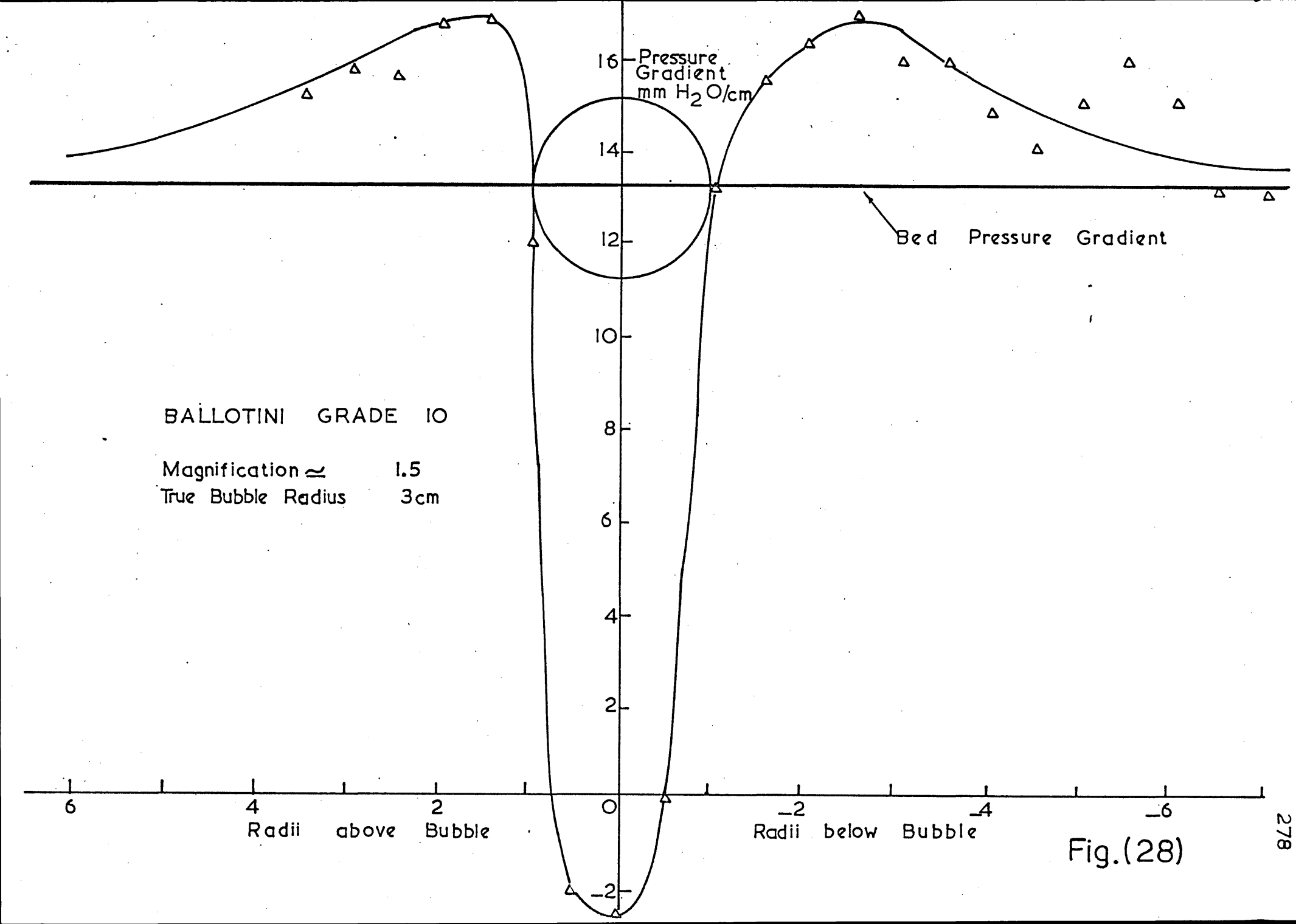
16
14
12
10
8
6
4
2
0
-2
Pressure Gradient mm H_2O/cm
Bed Pressure Gradient
BALLOTINI GRADE 10
Magnification ≃ 1.5
True Bubble Radius 3cm
6
4
2
0
-2
-4
-6
Radii above Bubble
Radii below Bubble

Fig.(28)

mounted on the rear wall of the bed, the angle of the line of centres of the tubes with the vertical. The cylinder was inserted into the copper coupling's body in such a way that its surface (and also the surface of the tubes) was flush with the inside surface of the rear wall of the bed. Two plastic tubes connected the other ends of the brass tubes to the openings of the micromanometer head. In these experiments the sensitivity of the micromanometer was selected to be ten times as much as the previous case. Particles were then poured into the bed and the air was introduced. When the pointer on the cylinder showed 90 degrees, i.e., pressure probes in horizontal position, no adjustment of the reading of the micromanometer was necessary. When the angle was other than zero, i.e. one probe at higher position, the reading of the micromanometer was adjusted to show a zero pressure difference reading at incipient fluidization. The rest of the procedure was the same as the previous experiment. A bubble was injected and while the ultra-violet recorder produced the corresponding pressure-time data, a cine camera, 16 francs/sec, recorded the position of the bubble and the usual synchronization technique was employed. Here for the purpose of comparison with the results of the previous method we represent the data when the angle shown by the pointer was zero, i.e. one probe 10 mm directly above the other.

In Fig.(29a) two typical tracings obtained when bubbles of different size were injected are presented. As is seen there is an injection effect. After that provided the bubble is fairly small it comes into equilibrium with the bed and the pressure difference reading goes to zero. Then as the bubble approaches the probe a gradual increase in pressure difference takes place. There is a sharp decrease in the reading which will be shown to be when the lower probe is inside

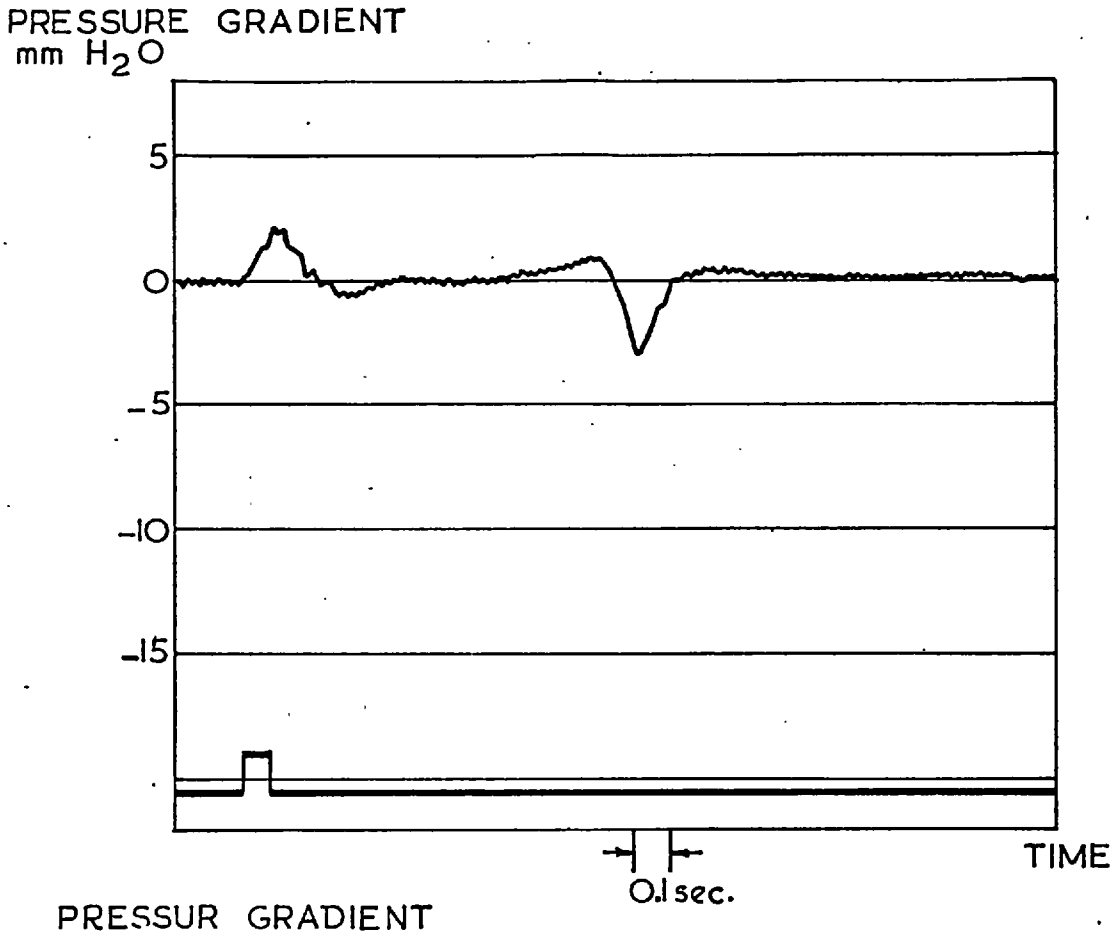
PRESSURE GRADIENT
mm H_2O
5
0
-5
-10
-15
TIME
0.1 sec.

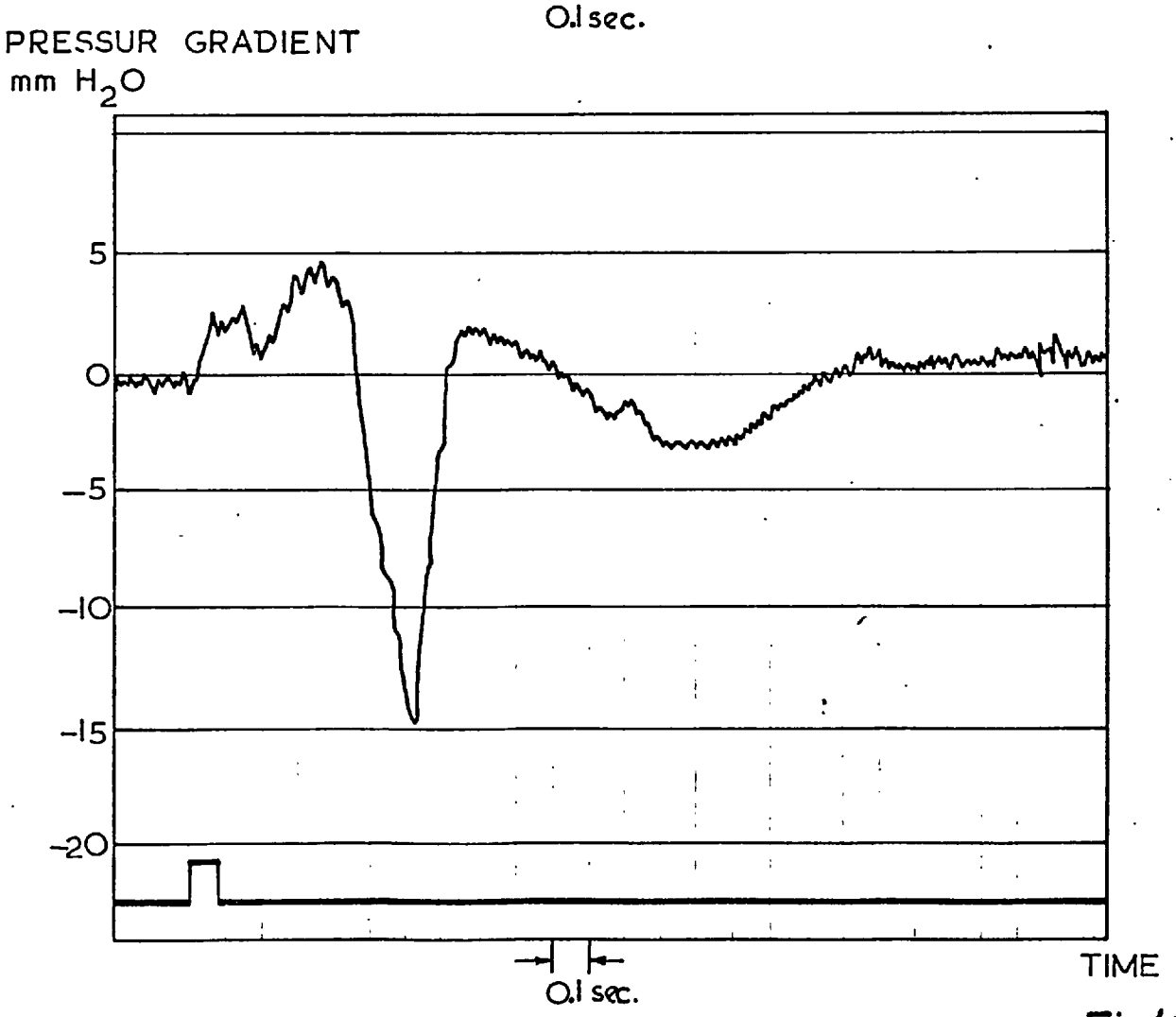
PRESSUR GRADIENT
mm H_2O
5
0
-5
-10
-15
-20
TIME
0.1 sec.

Fig (29-a)

the bubble. When the bubble is just about to leave the upper probe and shortly after that the pressure reading is also higher than zero. After the bubble has completely left the probe the pressure difference comes to zero. The effect of various factors on the tracings were more or less the same as discussed previously.

Now one notices, very clearly, the similarity between the pressure difference results obtained by the direct method in Fig.(29a) and the results obtained by the indirect method in Figs.(25) and (28). In order to obtain reliable results several bubbles were injected and filmed while the pressure readings were being recorded. The pressure-time curves were transformed to pressure-distance curves as was explained previously. A typical such curve is given in Fig.(29) which gives the pressure readings at the probe as a function of the distance of the top of the bubble from the centre of the assembly (i.e., midway between the lower and upper probes). The bubble tracing is also provided. We notice that in Fig.(29) the vertical axis gives exactly the pressure-difference recorded by the recorder. In order to get the actual value of the pressure difference we have to add to these readings a constant pressure difference for a height of 10 mm particulate phase. This is because the pressure reading was adjusted to be zero before injection. Also we choose the horizontal axis to represent the distance as multiples of the bubble radius. Thus we obtained the pressure-distance curve presented in Fig.(30). The summary of all the data obtained from these graphs is given in Fig.(31). The size of the bubbles injected varied between 3.8 to 4.7 cm. Although the size varies the data are fairly close together. In order to detect any possible effect of the size variation in this small range, the same data is plotted as dimensionless pressure difference in Fig.(32). It is seen that the effect of bubble size becomes distinguishable.

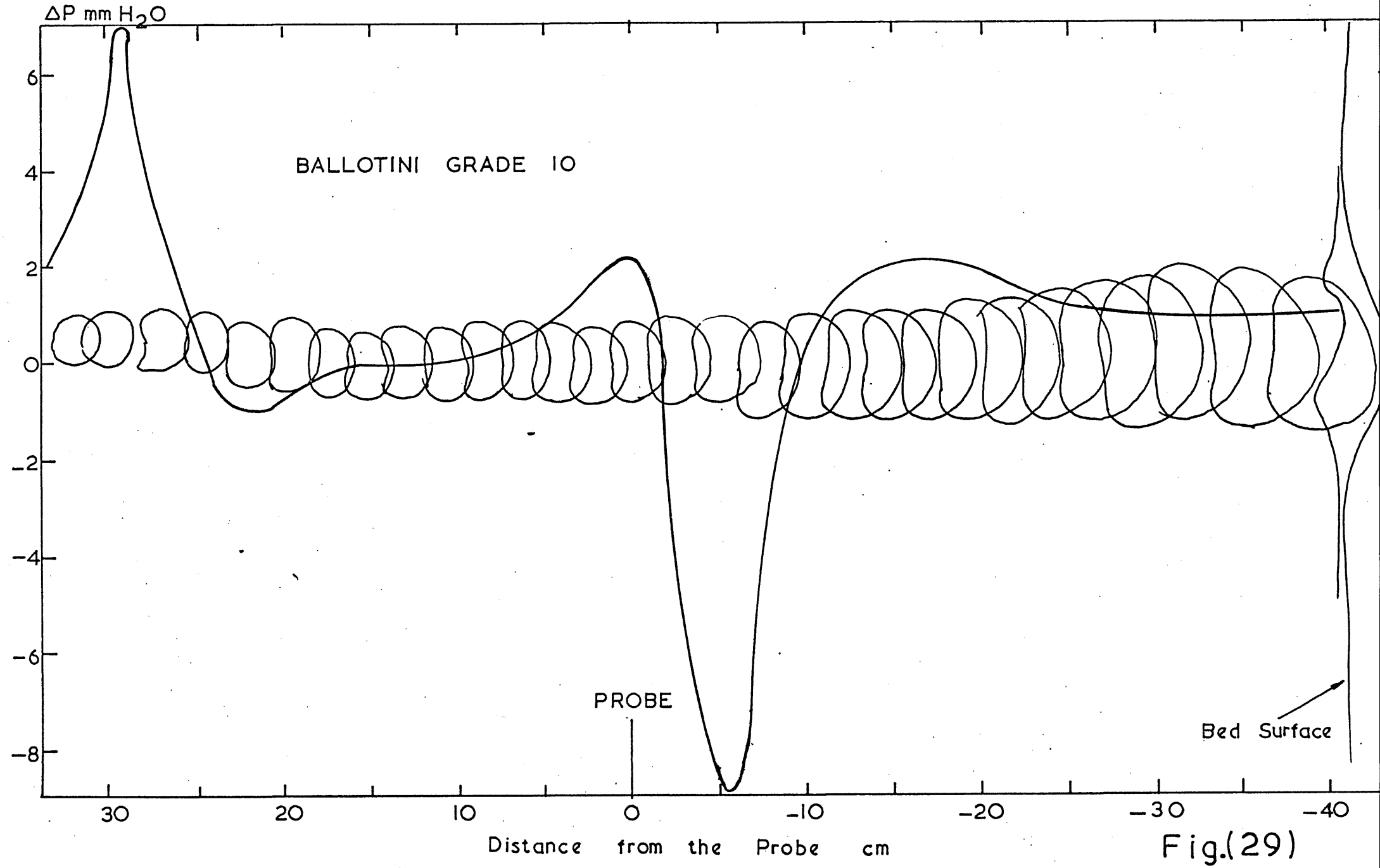
ΔP mm H2O
6
4
2
0
-2
-4
-6
-8
BALLOTINI GRADE 10
PROBE
Bed Surface
30
20
10
0
-10
-20
-30
-40
Distance from the Probe cm

Fig.(29)

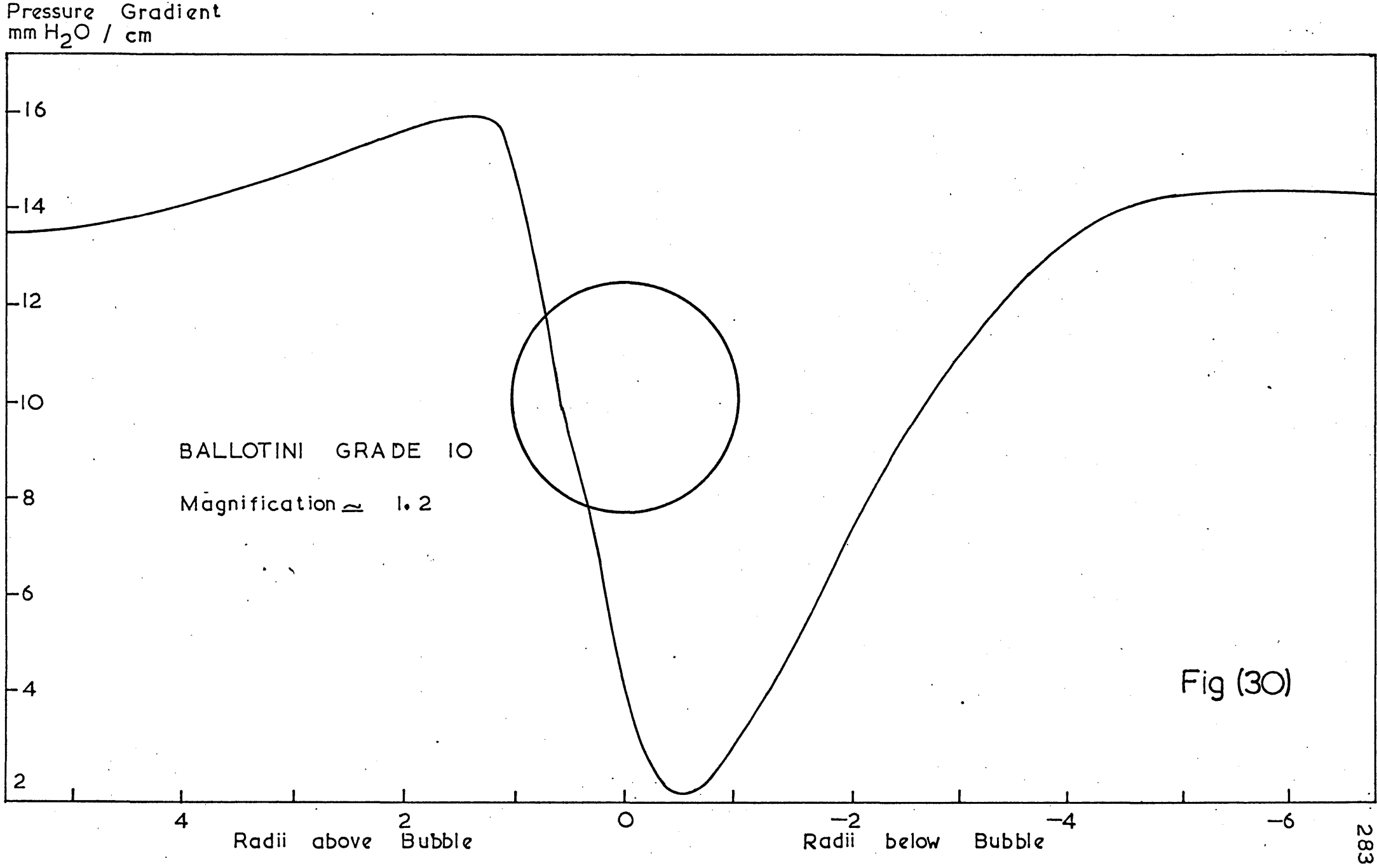
Pressure Gradient
mm H_2O / cm
16
14
12
10
8
6
4
2
BALLOTINI GRADE 10
Magnification ≃ 1.2
4
2
0
−2
−4
−6
Radii above Bubble
Radii below Bubble

Fig (30)

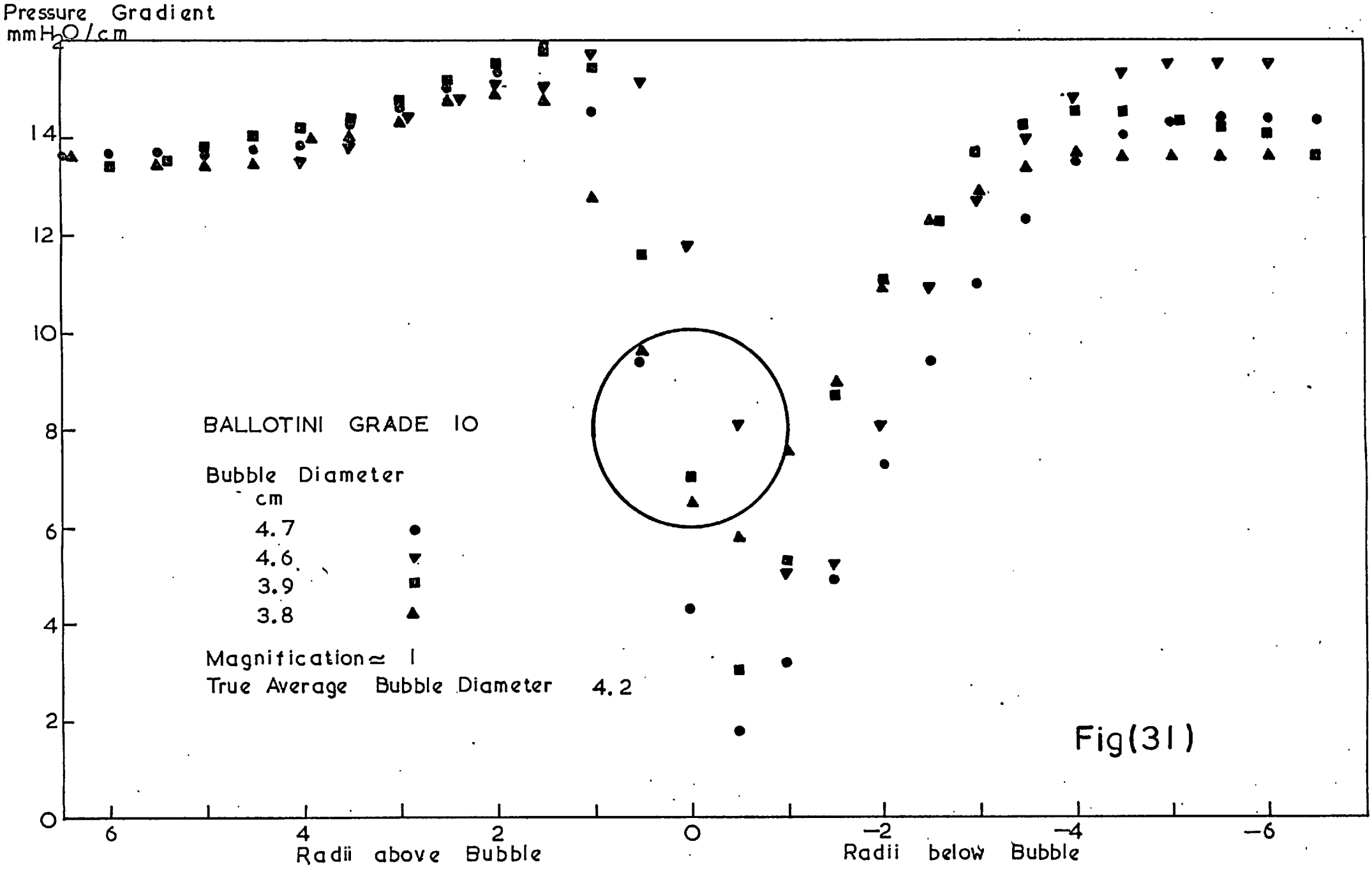
Pressure Gradient
mmH2O/cm
14
12
10
8
6
4
2
0
BALLOTINI GRADE 10
Bubble Diameter
cm
4.7
4.6
3.9
3.8
Magnification ≃ 1
True Average Bubble Diameter 4.2
6
4
2
0
−2
−4
−6
Radii above Bubble
Radii below Bubble

Fig(31)

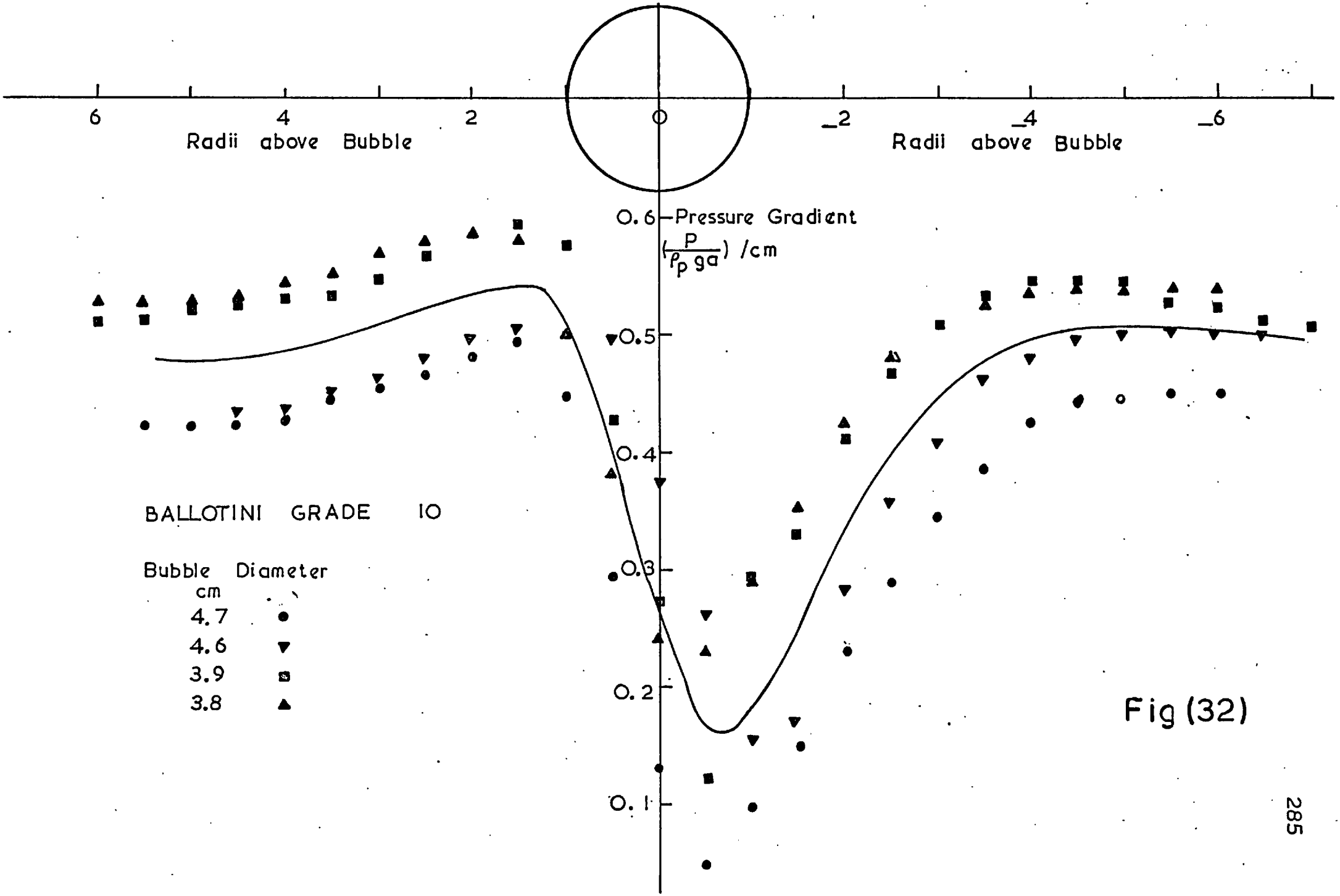
6
4
2
0
_2
_4
_6
Radii above Bubble
Radii above Bubble
0.6
0.5
0.4
0.3
0.2
0.1
Pressure Gradient
$(\frac{P}{\rho_p g a})$ /cm
BALLOTINI GRADE 10
Bubble Diameter
cm
4.7
4.6
3.9
3.8

Fig (32)

However, the average value would be almost the same as Fig.(31).

For the purpose of further study of the effect of bubble size on the distribution of pressure gradient obtained by this method, bubbles of diameter of about 10 cm were injected. Pressure-time curves were obtained for the bubble from the recorder while the position of the bubble was recorded by the cine camera synchronized with the recorder. The curves were transformed to pressure-distance curves. All the data so obtained are represented in Fig.(33). The horizontal axis gives the distance from the centre of the bubble in multiples of bubble radius and the vertical axis gives the pressure gradient in mm of water/cm.

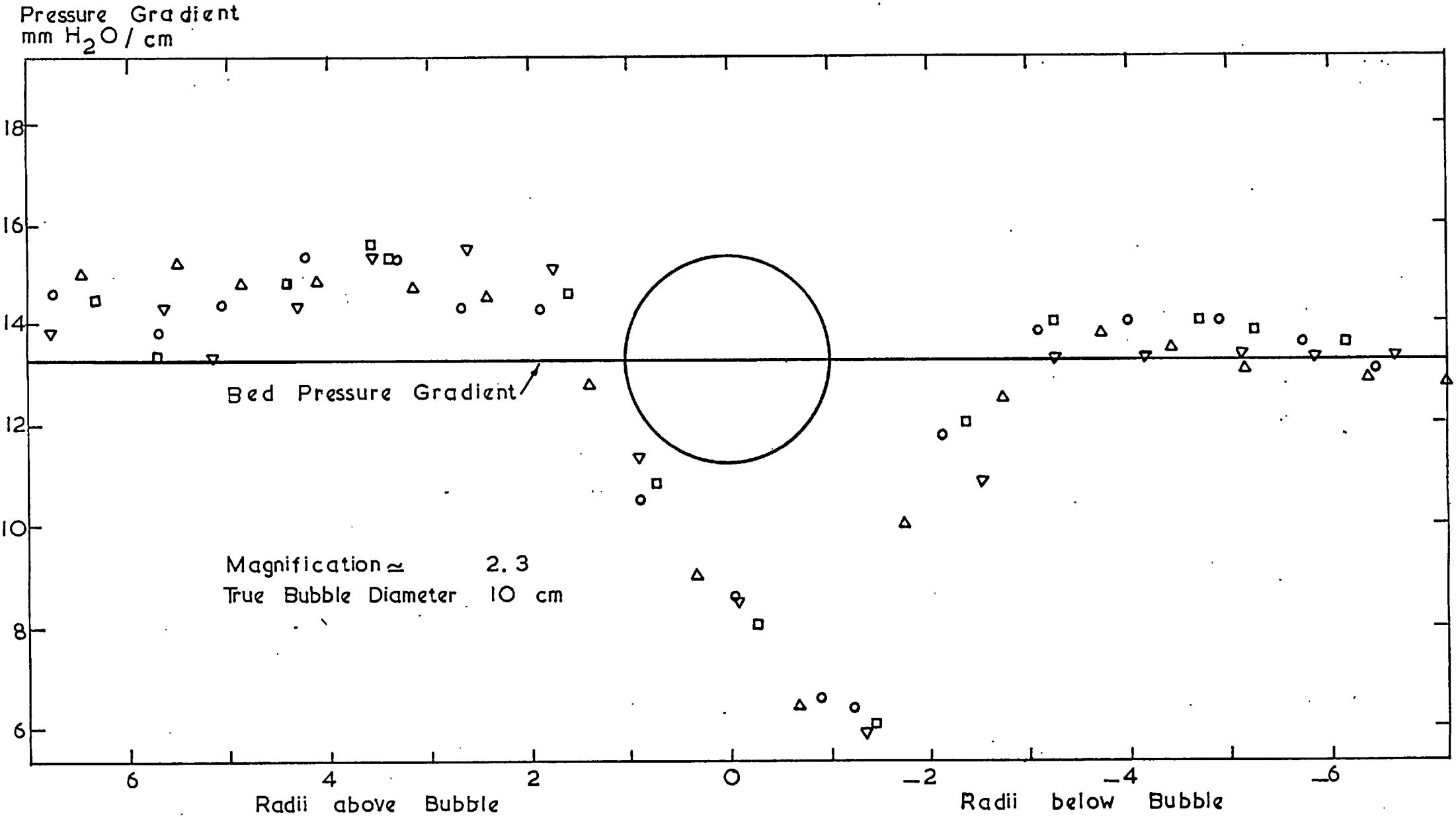
Pressure Gradient
mm H_2O / cm
18
16
14
12
10
8
6
Bed Pressure Gradient
Magnification ≃ 2.3
True Bubble Diameter 10 cm
6
4
2
0
−2
−4
−6
Radii above Bubble
Radii below Bubble

Fig(33)

4.6.2 COMPARISON OF RESULTS

First we compare the results for bubbles of different size obtained by either method separately. In Fig.(34) the pressure gradient data obtained by the indirect method for bubbles of 6 and 10 cm diameter are given. There is no systematic dependence on the bubble size. It is realized that distance of a point on the horizontal axis from the tip of the bubble is quite different, in absolute magnitude, for bubbles of different size. The distance is given as multiples of the bubble radius. The pressure gradient distribution around a bubble is completely independent of the bubble size. This of course is anticipated. For a particle to stay on the boundary of a bubble, and also for the particles above that to be supported, a certain amount of drag is necessary. This means that a certain pressure gradient across a layer of particles is necessary if that layer is to be supported. This pressure gradient is the same so long as the particle size is the same. Then it does not matter if the bubble, the through-flow of which maintains the necessary pressure gradient, is of small or large size. It should be pointed out that in the present experiments the bubble velocity in either case was distinctly above the interstitial velocity. It is also realized that the independency of pressure gradient on bubble size is in spite of the fact that the actual pressure distribution is dependent on bubble size. This of course is expected. It is true that a particle needs the same amount of drag, and hence pressure gradient, to be supported irrespective of the bubble size. However, a particle at, or near the boundary of a large bubble goes through a wider trajectory, and hence needs a bigger force, than when it is on the boundary of a small bubble. It is noticed that for the region corresponding to the inside of the bubble, in the case of the bubble of 6 cm diameter, negative

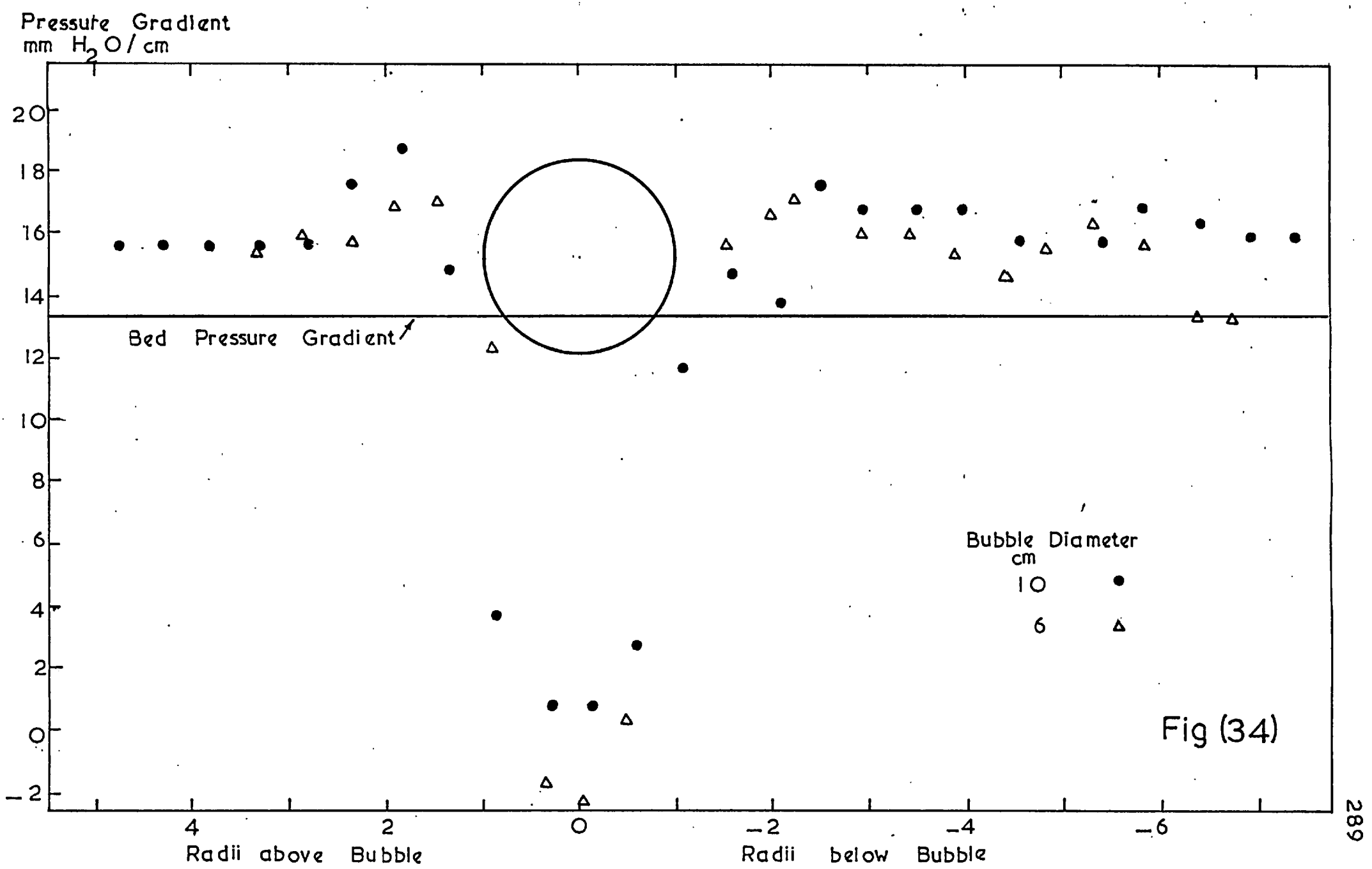
Pressure Gradient
mm H_2O / cm
20
18
16
14
12
10
8
6
4
2
0
−2
Bed Pressure Gradient
Bubble Diameter
cm
10
6
4
2
0
−2
−4
−6
Radii above Bubble
Radii below Bubble

Fig (34)

magnitudes of pressure gradient are also reported. This of course is not surprising at this stage and could have been anticipated from the examination of Fig.(27). The absolute pressure curve inside the bubble has a point of inflection, and the magnitude of the pressure for a small region below and very close to this point is smaller than the corresponding region above the point. In other words the pressure curve is sloping downwards for a very short region and hence the pressure gradient is negative. That the shape of the curve in Fig.(27) is reproducible can be established by the examination of the similar data. REUTER ([46]) also reported the absolute pressure curve of the same shape. However, the pressure gradient inside a bubble is unusually difficult to measure with a good degree of reliability, as the magnitude of the absolute pressure inside the bubble in Fig.(27) is very small and therefore the measurement is subjected to relatively extra error. This is the main reason why the data were plotted to a much larger scale than that in Fig.(27). This partly reduced the error which would have been inevitable on a small scale plot. Error can also arise from uncertainty in the determination of the exact position of the pressure centre. This would be much more accentuated in the case of the data corresponding to inside the bubble. Therefore the observed discrepancy between the results of different cases and in particular the fact that the negative magnitudes of pressure gradient have been observed is not very significant and meaningful in view of all the uncertainties particular to the data of this region.

In Fig.(35) the data obtained by the direct measurement of pressure gradient for various bubble sizes are presented. Bubbles in this experiment were of size 4 and 10 cm in diameter. Four bubbles of almost identical sizes at each case were studied. It is noticed

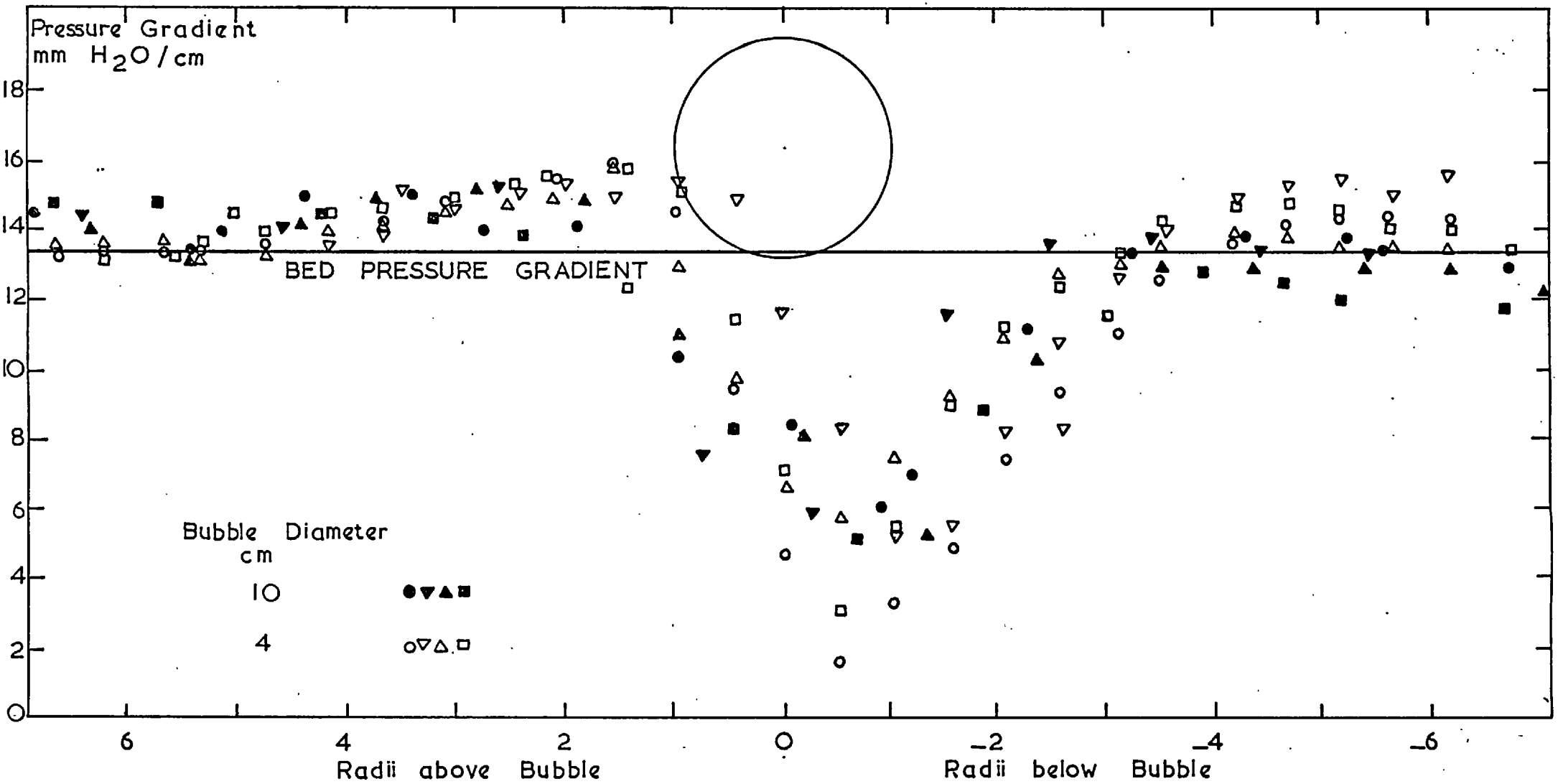
Pressure Gradient
mm H_2O / cm
18
16
14
12
10
8
6
4
2
0
BED PRESSURE GRADIENT
Bubble Diameter
cm
10
4
6
4
2
0
−2
−4
−6
Radii above Bubble
Radii below Bubble

Fig (35)

that there is no significant difference for data of different bubble sizes. This is also in support of previous findings that size of the bubble has no effect on the pressure gradient.

In Fig.(36) all the pressure gradient data obtained by different methods for various bubble sizes are represented. Here for the data obtained by each method, we make no distinction between the data for different bubble sizes and consider them as being due to one bubble size. We are here only concerned with comparison of different results due to different methods. The agreement between the results above the bubble is satisfactory although those obtained by the indirect method fall slightly above those obtained by the direct method. The data due to the latter however fall above those due to the former for the region corresponding to inside the bubble. There is a significant difference between the data for the region below the bubble down to 1.5 bubble diameter below the centre. From this point the agreement is again very good.

It has already been established that there is a considerable difficulty in the assessment of pressure gradient data through indirect methods particularly inside the bubble. Therefore it may be that these difficulties contribute to the observed discrepancy between the results for the region corresponding to inside the bubble. In addition to this we realize that the data due to this method is subjected to a much greater error. The reason for this extra error can easily be seen. We realize that in the assessment of the bed hydrostatic pressure there is significant error because of the inevitable inaccuracy in the determination of the exact position of the bubble centre of pressure, through which the straight line of the bed hydrostatic pressure is drawn. When this pressure at a point is added to the pressure obtained from the pressure curve, at same point,

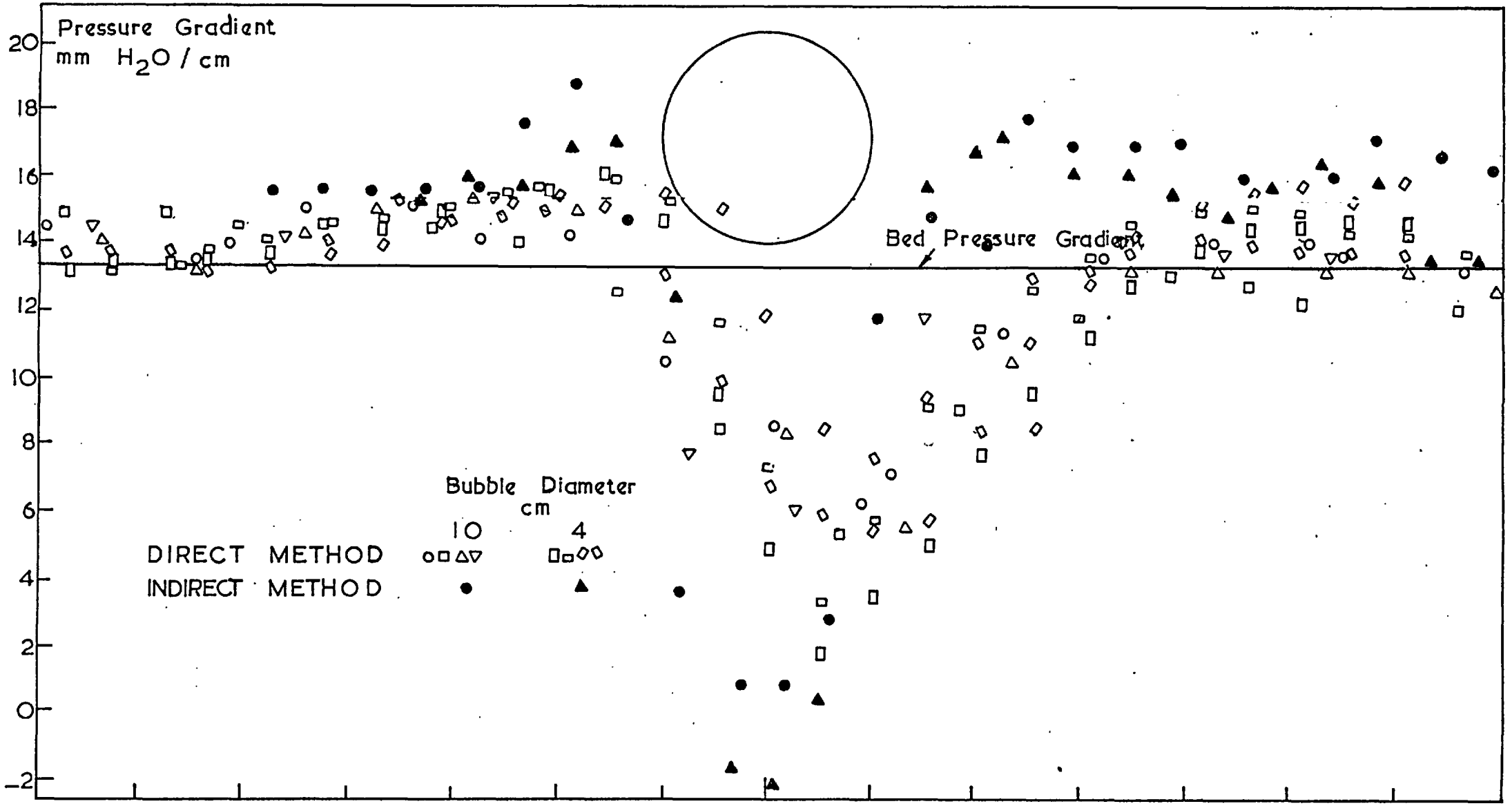
Pressure Gradient
mm H_2O / cm
20
18
16
14
12
10
8
6
4
2
0
−2
Bed Pressure Gradient
Bubble Diameter
cm
10
4
DIRECT METHOD
INDIRECT METHOD
6
4
2
0
−2
−4
−6
Radii above Bubble
Radii below Bubble

Fig(36)

the respective errors are added. Since the assessment of the pressure gradient at a point requires two pressure readings, one on each side of the point, therefore the error is again doubled. Now this amount of error is bound to cause some serious scatter and discrepancy between the results obtained by different methods. The direct measurement of the pressure gradient has also some disadvantages. The most significant drawback of this method is that the pressure drop across one centimeter is considered as the pressure gradient at the mid-point. Ideally one wishes to choose these two points to be very much closer than this. However, it is not possible in view of practical consideration to decrease the distance much below one centimeter. The choice of one centimeter is a reasonable selection with respect to the bubble size studied, however would produce some inaccuracy in the assessment of the exact magnitude of the pressure gradient at a point. Another possible explanation for the observed discrepancy can be presented as follows:

The pressure curves plotted in Fig.(23a) and Fig.(26) give the magnitude of the pressure difference between a point on the axis of the symmetry of the bubble and a point on the same horizontal level but far away from the bubble. Here in the assessment of pressure gradient data the assumption is made that the above mentioned curves are representative of the pressure difference between points on the axis of symmetry of the bubbles and corresponding hydrostatic pressures at the same levels. This assumption is strictly justifiable provided the movement of bubble does not affect the readings of the reference probe at all, i.e. the reference probe always represents the hydrostatic pressure. Supposing that the movement of the bubble has some effect on the readings of the reference probe, this effect, if any, would be more or less of the same type, but of much smaller magnitude

than the effect on the pressure picked up by the probe in the path of the bubble. If this was the case the absolute magnitude of the pressure data in Fig.(23a) and Fig.(25) would be bigger. Similarly it can be shown that in such a case the pressure rise and fall above and below the bubble would have occurred at a longer distance from the bubble in Fig.(24) and Fig.(27). But since the absolute pressure curves, Fig.(24) and Fig.(27), would approach the zero pressure line, under any condition, asymptotically, it follows that at the condition considered above, the resulting curves would have been more flattened just above and below the bubble. As a result of this the pressure gradient data just above and below the bubble would have been smaller than those reported in Fig.(36. In other words the data obtained by the indirect method corresponding to regions very close to the bubble in Fig.(36) are over-estimated. This can very well explain the discrepancy between the results in Fig.(36). However, it must be realized that error in the indirect method cannot be the only factor contributing to the observed discrepancy. Indeed the data obtained by this method give a much more sensible picture of the pressure gradient inside the bubble. Ideally for flow inside a fixed bubble it can be shown, as in APPENDIX (II), that the pressure gradient is negligibly small. Now the magnitude of the pressure gradient suggested by the indirect method is very close to zero inside the bubble. Considering all that has been said about the experimental difficulties particular to the measurement in this region, one realizes that the method is quite capable of giving reasonable results. Therefore there is no reason to believe that the data due to this method are necessarily inaccurate. Indeed that degree of agreement between the results obtained by two entirely different methods is all which can be expected. The exact situation, however, is something

inbetween what have been suggested by these two methods. The fair agreement between the results suggests that neither of these methods are in serious inaccuracy.

From what has so far been said the following points emerge:

(i) The data presented in Fig.(36) give a reasonable representation of the pressure gradient distribution round a freely rising bubble,

(ii) The fair agreement between the results obtained by two different methods indicates that both methods are capable of providing a fairly accurate picture of the situation, the exact picture being somewhere in between. This in turn means that A) the underlying principles and assumption involved are correct, and, B) the pressure-distance data from which the pressure gradient data were assessed are reasonably accurate.

4.6.3 DISCUSSION

To summarize all the information which was presented in previous sections, we may say that the pressure gradient far above a bubble is equal to the normal bed pressure gradient. Its magnitude gradually increases towards the bubble and has a peak very close to the bubble. Inside the bubble it effectively drops to near zero. In the region below the bubble it has a magnitude above that of the particulate phase far away and comparable with that of the nose of the bubble. Away from the bubble it drops gradually until it reaches the normal bed pressure gradient. These regions of rise and fall, above and below the bubble are about 2 to 3 bubble diameters from the centre.

REUTER'S (54) argument concerning the voidage distribution around a bubble was based on a statement about the pressure gradient distribution more or less the same as the above statement. REUTER deduced that the stability of bubbles in fluidized beds was due to the formation of transient layers of particles of low voidage around them. This deduction, as was pointed out earlier, is clearly contradictory to the theoretical predictions of JACKSON (28) and the experimental evidence supplied by LOCKETT & HARRISON (51) in regard to the existence of regions of higher voidage around bubbles. As one of the tasks undertaken in this part of the present work we are going to see why this conflict exists. Also we are going to look into the problem of the stability of bubble boundaries in fluidized beds.

REUTER (54) starts with the statement that "the increased pressure gradient around the bubble leads, according to DARCY'S law, to an increased gas velocity...." Now to begin with, it is much more appropriate, and indeed necessary, to consider the CARMAN-KOZENY equation when the flow problems in fluidized beds are considered, i.e.

$$\text{grad } P = \frac{K (1 - \varepsilon)^2 U_o}{\varepsilon^3}$$

where ε = voidage fraction,

U_o = superficial velocity at incipient fluidization,

K = a constant depending on the properties of fluid and particles.

The important implication is that in drawing any conclusion regarding the change in one variable with respect to change in the other, one is aware of any possible effect of voidage change on the whole situation. REUTER continued, "an increased gas velocity means an increased drag force on neighbouring particles". It is quite possible to have an increased gas velocity without the drag being necessarily increased, by only increasing the voidage in an appropriate way. In fact this is exactly what happens in liquid fluidized systems and gas fluidized systems of fine particles. The observed continuous expansion of the particles within the respective limited regions of those systems when the flow is increased is due to the fact that the particles space themselves more loosely to accommodate the increased flow and hence keep the drag constant. For the region around a bubble in a gas fluidized system one can think of the increased voidage reported in the literature. Therefore the above statement made by REUTER is strictly correct only when the voidage is constant, which is not the case of course (LOCKETT & HARRISON (51)). The experimental work of ROWE & HENWOOD (62) and ROWE, referred to earlier, has shown that the drag experienced by particles in an array is inversely proportional to the separation distance between them. The drag experienced by a particle when surrounded by others is 68 times of that when in isolation, at the same superficial velocity. In other words when a particle in an array increases its separation distance by a small amount, the drag

experienced falls enormously. In such a case if the particle is to be supported there needs to be an enormous increase in the velocity of the fluidizing fluid in such a way that the reduced drag is compensated. ROWE has shown that for an incremental change in the separation ratio, defined as the ratio of the separation distance to the particle diameter, of about 0.01, the velocity has to be increased by almost 100% to keep the drag constant, and hence support the particle. It is quite clear that an increased velocity does not necessarily increase the drag. Again we see that REUTER'S statement is strictly correct only when the voidage is constant. REUTER continued that, "for the pressure gradient around the bubble to be higher than in the undisturbed bed far from the bubble, it is necessary for the solid packing density around the bubble to remain at least equal to the packing density in the undisturbed bed." This statement is not necessarily correct. That the increased pressure gradient near a bubble is compatible with lower solid packing density, i.e. higher voidage, can be shown as follows: Consider the hypothetical situation in a fluidized bed where there are two identical bubbles, around one of them the voidage is equal to the incipient value, and around the other one higher than the incipient value. For the particles around the roof of the latter bubble to be supported, a gas velocity through the bubble roof higher than through the roof of the former bubble is necessary. With the downstream pressure far away from the bubbles being identical, a higher pressure at the boundary of the latter bubble (i.e. with higher voidage) is necessary. This means that the pressure gradient near a bubble is higher when the voidage around it is higher. Since the pressure falls uniformly as one goes away from the bubble, then the local pressure gradient, too, would be greater when the voidage is greater. The above argument,

though not strictly meant to explain the observed high pressure-gradient around bubbles, however, shows that high voidage and high pressure-gradient not only are compatible, but are even necessary for the sake of the stability of bubble's roof. REUTER suggested that "in no cases is it possible for even a small loosening of the particles to take place in the vicinity of bubble since as was shown by ROWE, even a small increase in the interparticle distance leads to an enormous drop in the drag force of the fluid on the particle". Here the author clearly misinterprates the evidence derived from the excellent work of ROWE on the drag studies. We have already shown that these experimental evidences can be utilized in the explanation of increased voidage around a rising bubble. It is interesting to notice that the author (ROWE (60)) comments that "packed layers of particles in the roof of bubbles do not exist."

It is felt that enough evidence against the idea of decreased voidage around bubbles in fluidized beds has been presented. REUTER also tried to explain the stability of bubbles on the basis of the idea that packed layers of particles around bubbles exist, an idea that we have established to be incorrect. In the explanation of the stability of bubbles some other hypotheses have been put forward by REUTER which do not seem to be realistic. Next we are going to consider the problem of bubble stability in fluidized beds, and in particular the pressure gradient information are going to be used.

The drag measurement experiments performed by ROWE & HENWOOD (62) have provided extremely valuable information with regard to the problem of the stability of bubble boundaries in fluidized beds. Considering a downstream facing surface in a fluidized bed, (i.e. top of the wake), it has been shown that the drag experienced by particles on the top layer of the surface is higher than those on the

other layers. If the flow through the particles becomes so high that one of them is expelled from the surface, the drag on that particle falls drastically, and hence the particle falls back to the surface. Therefore the particles at such a surface space themselves in such a way that the magnitude of the drag experienced remains constant, and just enouth to support them. Since the drag is larger at the top layer and decreases with distance below the surface it is clearly seen why voidage near the bottom of the bubble is higher and falls gradually with distance to the incipient value far below the bubble (LOCKETT & HARRISON). The same type of argument applies to the roof of the bubble. For an upstream facing surface the drag on the particles at the first layer is much larger than that on other particles.

Experimental work of LOCKETT & HARRISON (51) shows that there are regions of high voidage around bubbles. ROWE (61) has shown that for a small increase in the interparticle separation an enormous increase in the velocity of the gas is necessary if the particles are to be supported. The experimental work presented here shows that the pressure gradient has a higher magnitude near the bottom and the roof of bubbles. Next we are going to calculate the magnitude of the velocity through the roof of a bubble by utilising the pressure gradient and porosity information provided by the present work and LOCKETT & HARRISON respectively. If the calculated velocity is in agreement with that suggested by ROWE (61) then we conclude that the question of bubble stability has been satisfactorily solved.

The KOZENEY-CARMAN equation can be presented in the form

$$\frac{\Delta P}{L} = 180 \frac{\mu U (1-\varepsilon)^2}{d^2 \varepsilon^3} \qquad \text{Eq.(13)}$$

where ΔP = pressure difference across a layer L of packing material.

μ = viscosity of the percolating fluid.

ε = voidage.

d = diameter of spherical particles and 180 is the average value given by CARMAN of the constant in the equation.

In the present work we have measured the value of pressure difference, i.e. ΔP, on the vertical axis of bubbles over one cm distances. The magnitude of $\frac{\Delta P}{L}$ is thus given in Fig.(34) and Fig.(35) at various distances from the bubble.(Both methods). In Fig.(37) the same data from Fig.(35) obtained by the direct measurement of pressure gradient are represented. The intermediate data have been obtained by interpolation between those on Fig.(35). In Fig.(37) the extreme left-hand side vertical axis gives the pressure gradient in $(dyne/cm^2)/cm$. The horizontal axis gives the distance from the centre of the bubble in multiples of the bubble radius. Also in Fig.(37) the vertical axis on the right-hand side of the pressure gradient axis represent the voidage, i.e., ε. The corresponding curve designated "ε" is virtually the same as the curve constructed by STEWART (52) on the voidage data obtained by LOCKETT & HARRISON (51) for the narrow size range particles they used. The pressure gradient and voidage data presented in Fig.(37) have been obtained from experiments with spherical glass particles. However, the size ranges are completely different. Although it is not strictly permissible to use this data in Eq.(13), there is no choice since voidage distribution data other than these in Fig.(37) are not available. The following discussion may provide some justification however. The theoretical analysis of JACKSON shows that the voidage distribution is independent of particle size, whereas LOCKETT & HARRISON have observed a slight dependence of the voidage on the particle size distribution and their data were not in complete agreement with JACKSON'S predictions. STEWART (52) has suggested that a more appropriate selection of the

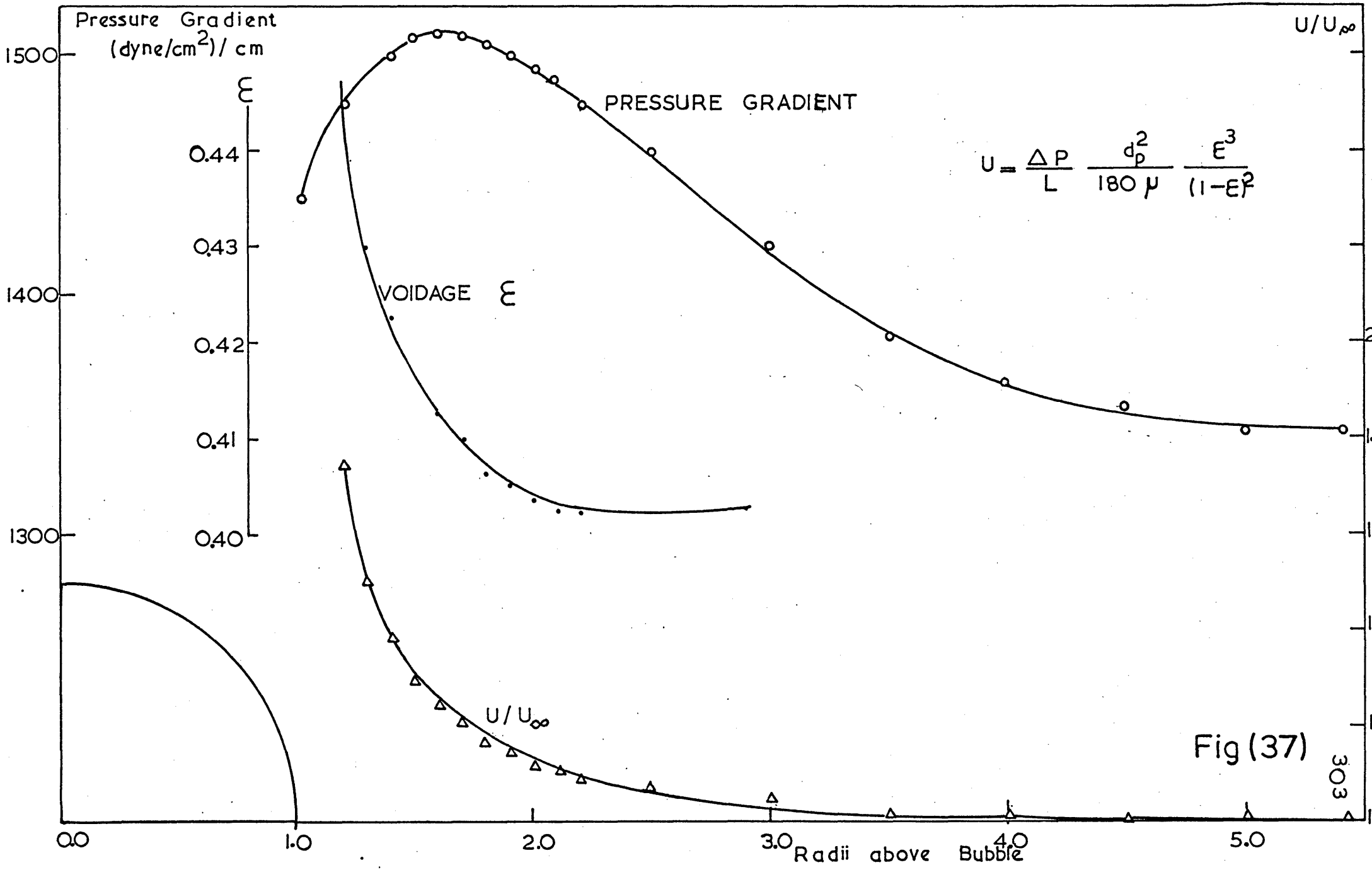
Pressure Gradient
(dyne/cm²)/ cm
1500
1400
1300
ε
0.44
0.43
0.42
0.41
0.40
PRESSURE GRADIENT
VOIDAGE ε
U = ΔP/L · d_p²/180μ · ε³/(1−ε)²
U/U∞
U/U∞
2.0
1.8
1.6
1.4
1.2
1.0
0.0
1.0
2.0
3.0
4.0
5.0
Radii above Bubble
303

Fig (37)

constant in bubble velocity diameter equation would bring satisfactory agreement between the theoretical predictions and the experimental data for the narrow size range. The anomolous behaviour of the wide range size particles could have been due to various inevitable experimental difficulties as suggested by STEWART and therefore not in contradiction with JACKSON'S analysis.

Thus in the light of the above discussion and also due to the fact that the data given by LOCKETT & HARRISON for different size ranges are not wildly different, and that in both cases more or less the same sort of distribution exists, in the absence of any other data we chose the data given in Fig.(37) in the following analysis. Later on it will be shown that this does not invalidate the conclusions.

The next thing to be considered is the particle diameter in Eq.(13). Apparently two choices exist. One is the particle diameter in the present experiments and the other is the one used in the work of LOCKETT & HARRISON. Since we are going to calculate the ratio of U/U_{∞} i.e. the ratio of the velocity of gas at a point near the bubble to that at a large distance from the bubble therefore whatever particle diameter we choose, the magnitude of d^2 in the Eq.(13) can be incorporated in the constant of the equation, which of course has no influence on the magnitude of the calculated U/U_{∞}. Here we choose to employ the size of the particles which were used in the present work. We then write the equation in the following form:

$$U = \left(\frac{d^2}{180\mu}\right) \frac{\varepsilon^3}{(1-\varepsilon)^2} \frac{\Delta P}{L}$$

The calculated values of U/U_{∞} are presented in Fig.(37) where the right-hand vertical axis is graded in U/U_{∞}. It is seen that U is almost constant from far above the bubble down to three bubble radii from the centre. Between 3 to 2 bubble radii it significantly differs

from U_o and from 2 bubble radii sharply increases and reaches a value almost 80% bigger than its value far away from the bubble. As was pointed out earlier the ΔP data were those obtained from the direct measurement of pressure gradient. This method, as it was seen, gives results which are smaller than those given by the other method. If we had used, in the above calculation, the average value of the pressure gradient given by the two different methods we would have obtained a magnitude of U/U_∞ near the bubble greater than what we have obtained now. Also if we had employed the voidage data given by LOCKETT & HARRISON corresponding to the wide size range particles, which indeed are relatively closer to the present particle size range, the calculated magnitude of U/U_∞ near the bubble would have been bigger. (Judged by the graphs in Fig.(1) STEWART (52)). Therefore the magnitude of U/U_∞ near the nose of the bubble as given in Fig.(37) is the smallest possible which could have been obtained. This means that we expect to get about some 80% increase in the velocity of gas near the top of a bubble from the velocity far away from the bubble. We realize that this magnitude of the velocity near the roof of a bubble is in remarkable agreement with the magnitude of the velocity of gas through the roof of a bubble suggested by the analysis of DAVIDSON & HARRISON (4). The authors suggested an average flow of gas twice the incipient value through the roof of bubbles in fluidized beds. The correctness of this predicted value has been checked and completely established as it was discussed in the first part of the present work. Here the remarkable agreement between the predicted value suggested by DAVIDSON & HARRISON and the value presented here, suggests that the present experimental technique is accurate and gives confidence in the results. ROWE has shown that a local increase in the voidage in a fluidized bed of about 3% requires that the

velocity approximately doubles. Here we see that the velocity of gas almost doubles for about 10% increase in voidage. In view of all the experimental difficulties and inevitable errors in the treatment and handling of data and also the number of assumptions involved in the calculation of velocity near the roof of a bubble this degree of agreement is satisfactory.

It is seen from Fig.(37) that the voidage of the particulate phase increases as one gets closer to the nose of the bubble. As it was previously pointed out, for particles to be supported there needs to be an enormous increase in the velocity of gas because the drag falls rapidly with increasing separation between particles as shown by ROWE & HENWOOD. At the same time the pressure gradient increases towards the nose of the bubble, as shown in the present work, and this maintains a high rate of gas flow through the roof of the bubble which is required by the loosened particle in that region. The situation near the roof of the bubble is thus that for a region within one bubble radius all the particles are loosened and at the same time supported by the drag imposed by the flow. These loosened particles are in a more free state, and move under the influence of the flow in such a way that the bubble appears to be rising. At the top of the wake particles are also loose. It has been shown by ROWE et al that the drag on the top layer particles of a downstream facing surface is more than any other layer. We have shown from pressure gradient data that the flow through the roof of the bubble is almost twice the value far away from the bubble. The same thing has to happen for the bottom of the bubble. The pressure gradient data also confirms this. There is, thus, a high rate of flow through the bottom and the wake of the bubbles. This flow may impose such a large drag on the top layer of the wake that the particles may move away from the wake. But once

they have increased their separation distance the drag falls very rapidly and then the particles fall back again to the surface. Therefore the particles in the wake only increase their distance in such a way that they still remain supported by the high rate of gas flow.

In the above argument, we have explained the stability of the upper and lower boundary of a bubble in a fluidized system. All this has taken place in the light of the pressure gradient information provided by this work, and also the well established drag and voidage information. We see that ideas such as "dam or arch formation" and also formation of "barriers" between the bubbles "against the motion of solids" in the absence of which "the fluid flowing from below would drag particles upwards with it, and these particles would immediately fill up the void", proposed by REUTER to account for the stability of the lower part of the bubble, are unnecessary. For the stability of the upper boundary of bubbles we have established that the idea of formation of packed layer of particles above the roof of bubbles is also incorrect. The analogy between the motions of solid bodies in fluids and movement of bubbles in fluidized beds, although helping the understanding of the problem, must be used with extreme caution. The apparent motion of so-called bubbles in fluidized systems is purely an orderly motion of particles, governed by the dynamics of the system. There is no such a thing as a bubble being an entity in a fluidized bed. Once we realize that any observed property associated with a so-called "bubble" is a direct consequence of the dynamic behaviour of the system many problems may be solved. There is no reason to think that there must be a physical thing in the foot of the "bubble" which would stop the particles from being drawn into it. The particular behaviour of the system near the lower

part of a so-called bubble requires that a tongue of particles be projected into the bubble. The extend of this tongue is defined purely by the dynamics of the motion. That the particles in this tongue do not go further is because the dynamics of the system do not allow such a thing. To be more explicit the combination of factors such as drag, pressure gradient, interstitial flow, etc. brings about the observed behaviour of the system near the boundary of the "bubble" and indeed everywhere in a gas fluidized system.

Here, by presenting the necessary knowledge about the pressure gradient and in conjunction with the other well established information we have provided a very satisfactory insight into the problem of how the dynamics of the system bring about some of the most interesting behaviour and properties of gas fluidized systems.

CHAPTER 5

CONCLUSION

INJECTION EFFECT

Injection of a high pressure puff of gas into a two-dimensional gas fluidized bed at its midspan and near the foot, perturbs the bed at the point of injection. The perturbation travels at some velocity, specified by the overall conditions, in all directions. The effect is more pronounced at points away from the walls and hence, a pair of pressure probes, one near the wall and the other at the midspan record a pressure change as the wave front approaches and an extremum as it reaches the level of the probes. After this the effect dies out gradually. For an injection interval of about a few m.sec. the whole pressure variation takes place in a few tenths of a second. The actual form of the pressure variation although very reproducible under carefully controlled conditions, is very sensitive to slight changes in the properties of the system.

SURFACE EFFECTS

Near the surface of a gas fluidized bed, an approaching bubble is accelerated to twice its average velocity during a short interval of time about a few tenths of a second. A high rate of gas removal, more than what can be supplied under normal conditions, takes place which causes:

(i) local defluidization of the particulate phase below the bubble which provided the surface is not too far above the just

mentioned pair of pressure probes causes a reduction in pressure to be sensed by them,

(ii) stabilization of the thinning roof of the bubble prior to burst by increasing the flow through the constituting particles,

(iii) the top layers of the particles at the surface to be exhausted from gas and hence become defluidized. The characteristic shape of the wake of a bubble is therefore preserved, until the redistribution of the flow evens out the surface.

PRESSURE DISTRIBUTION AROUND A RISING BUBBLE

The presence and movement of a bubble influences the pressure distribution (i.e. the distribution of the pressure difference between a point on the vertical axis of a bubble and the pressure at the same level but far away from the bubble) inside a two-dimensional gas fluidized bed significantly within a region from between 3 to 4 bubble radii above down to almost same distance below the centre of the bubble. As a bubble approaches a point the pressure at that point gradually increases, a peak occurs when the bubble is very close to that point. There is a linear decrease in the pressure corresponding to the time when the point is inside the bubble. The pressure recovery takes place when the bubble has passed the point. The pressure difference at a point between situations when the tip and the bottom of the bubble are at that point is equal to the pressure head corresponding to one bubble diameter height of the incipiently fluidized particulate phase. This pressure difference is divided with a ratio of 2/1 between the lower and the upper part of the bubble. A bigger bubble produces a bigger pressure drop. However, from 1.5 bubble diameter below the centre, where an inflection point on the pressure curve is observed, the situation is independent of the bubble size. This is an indication of the extent

of the activity of the wake, and is in remarkable agreement with evidence obtained from completely different experiments.

From all of the theoretical expressions, DAVIDSON expression, and JACKSON modified (in which the experimental bubble velocity is employed instead of the theoretical one) expression predict results which are in reasonable agreement with experiment. For down to one radius above the tip of the bubble DAVIDSON predictions are in good agreement with experiment. From this point the JACKSON modified expression gives results which are in better agreement. This agreement is very good at the tip of the bubble. The pressure centre falls above the geometrical centre of the circular bubble. Near the bottom of the circular bubble the agreement between DAVIDSON predictions and the experimental results is good but declines down to 1.5 bubble diameter below the centre, from there it improves again. This shows that the activity of the wake is more pronounced below the bubble than inside the circular bubble. The agreement between COLLINS predictions below the bubble and the experiment is very poor in spite of the imposition of the wake in this model. As far as pressure prediction is concerned this model is not advantageous to the DAVIDSON model, i.e. the circular bubble.

For bubbles of identical size but in beds of particles of different size, the pressure at the nose and at the bottom of the bubble is higher when the particle size is bigger. The pressure centre falls below that of the finer particles. All these hold good also when the shape of particle is irregular.

The absolute pressure on the axis of the symmetry far below the bubble is the same as the normal bed pressure. Towards the bubble it deviates more and more, and becomes less than the normal bed pressure at the same level. Inside the bubble but very close to the

bottom, the pressure curve has the same slope as the straight line of the normal bed pressure. In the upper part of the wake the absolute pressure curve has a steeper slope, and very close to the surface of the wake has its minimum. From there the curve slopes upward and after an inflection point, it passes through the centre of the pressure. The pressure reaches to its maximum shortly after this and then slopes downward. In this region the pressure on the axis of the symmetry of the bubble has a higher magnitude than the normal bed pressure. Far above the bubble again it becomes identical with the particulate phase pressure at the same level.

PRESSURE GRADIENT DISTRIBUTION AROUND A RISING BUBBLE

The pressure gradient far above a bubble is the same as the normal bed pressure gradient. Towards the bubble it increases and has a peak at the nose of the bubble. Inside the bubble it drops effectively to zero. There is also another peak near the bottom, below the bubble from there the pressure gradient gradually decreases and becomes identical with the bed pressure gradient far below the bubble. The region of the rise and fall is about 2-3 bubble diameters from the centre above and below the bubble.

The pressure gradient distribution is independent of the dimensionless bubble size, i.e. at identical multiples of the bubble radius from the centre of the bubble the pressure gradient is identical.

Both methods of the assessment of the pressure gradient (i.e. the direct measurement and the indirect method, in which the pressure distribution data are being utilized), are capable of providing a fairly good picture, the exact one being somewhere in between.

GENERAL

When a high pressure puff of gas is injected into an incipiently

gas fluidized bed, a bubble is formed. The longer the injection interval and/or higher the injection pressure, the bigger the bubble. However, when the pressure is kept constant but the interval is increased rather drastically, the bubbles so obtained are not necessarily as big as expected, due to double bubble formation and extra leakage associated with the present method of injection.

Selection of the reference pressure probe to be outside the bed is not necessarily advantageous.

The calculated magnitude of the velocity of the gas through the roof of a bubble in a gas fluidized bed is in remarkable agreement with the predicted magnitude by DAVIDSON model. The agreement with the suggested value, for change in the velocity of the gas required by particle displacement, by ROWE is also satisfactory.

Particles on the top and bottom of a bubble are loose but supported by the high rate of gas flow through them. In a region about one bubble radius from the tip of the bubble the voidage is higher than the incipient value. Particles in that region can move freely under the influence of the resultant force in such a way that the bubble appears to rise.

The effect of the wake is extended down to 3-4 bubble radii below the centre of the bubble.

The stability of the bubble boundaries can be well explained in the light of the drag, porosity and the pressure gradient information.

The analogy between the movement of solid bodies in fluids and bubbles in fluidized beds helps the understanding of some of the associated features, but must be treated very cautiously. A bubble in a fluidized bed is not an entity. The apparent motion of a so-called bubble in a gas fluidized system is purely an orderly motion of particles governed by the dynamics of the system.

It is quite possible to have an increased gas velocity without the drag being necessarily increased, by increasing only the voidage in an appropriate way.

High voidage and high pressure gradient near a bubble are not only compatible, but even are necessary for the sake of the stability of the bubble.

All the evidences are in conflict with the existence of packed layers of particles, i.e. low voidage, around bubbles. Ideas such as arch, dam, barrier, and grid formation for the explanation of the stability of bubbles are unnecessary. There is no reason why there should be a physical barrier which would stop the particles from being brought up into and fill the bubble.

APPENDIX (I)

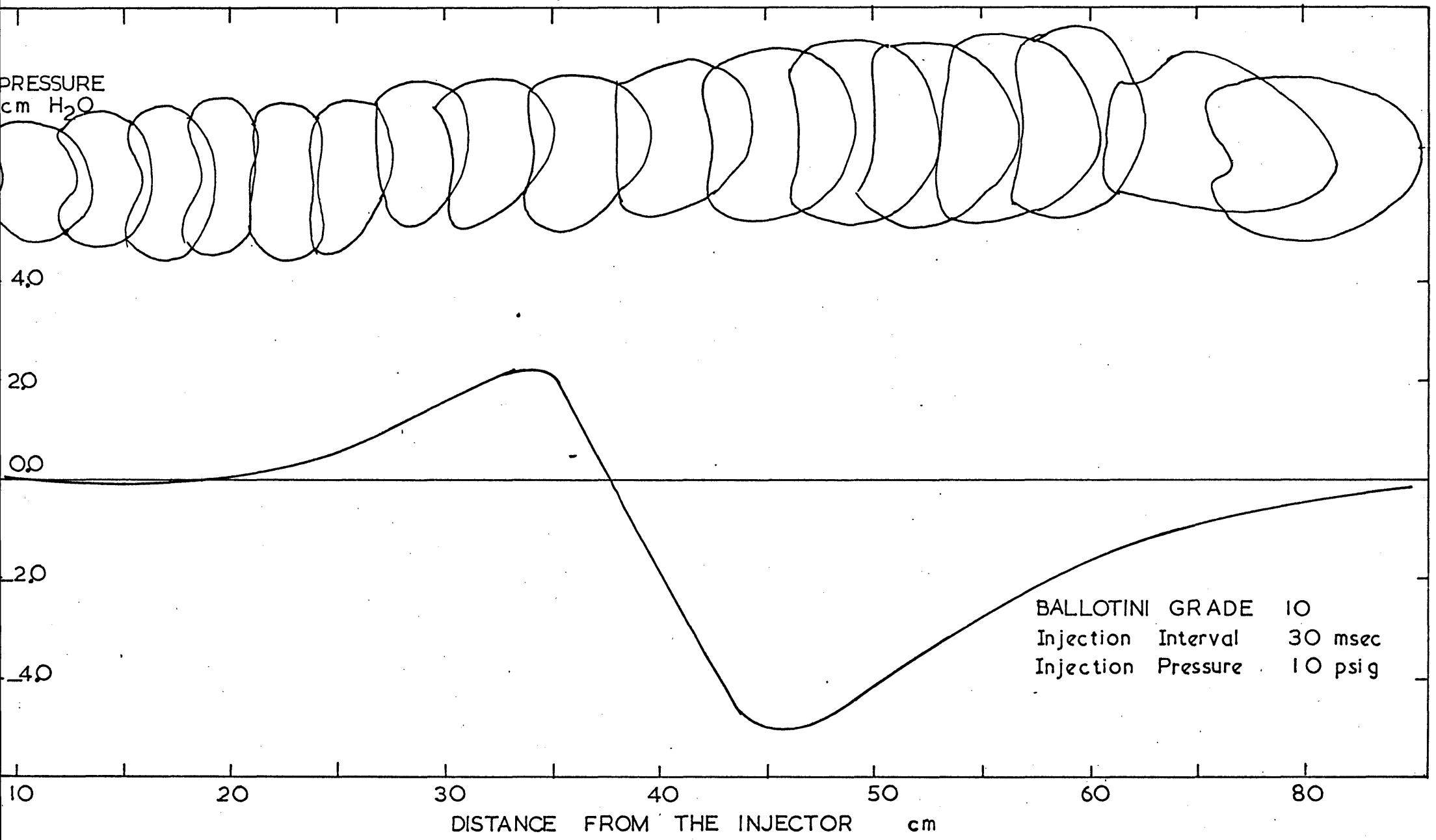
PRESSURE
cm H_2O
4.0
2.0
0.0
-2.0
-4.0
BALLOTINI GRADE 10
Injection Interval 30 msec
Injection Pressure 10 psig
10
20
30
40
50
60
80
DISTANCE FROM THE INJECTOR cm

APPENDIX (I)

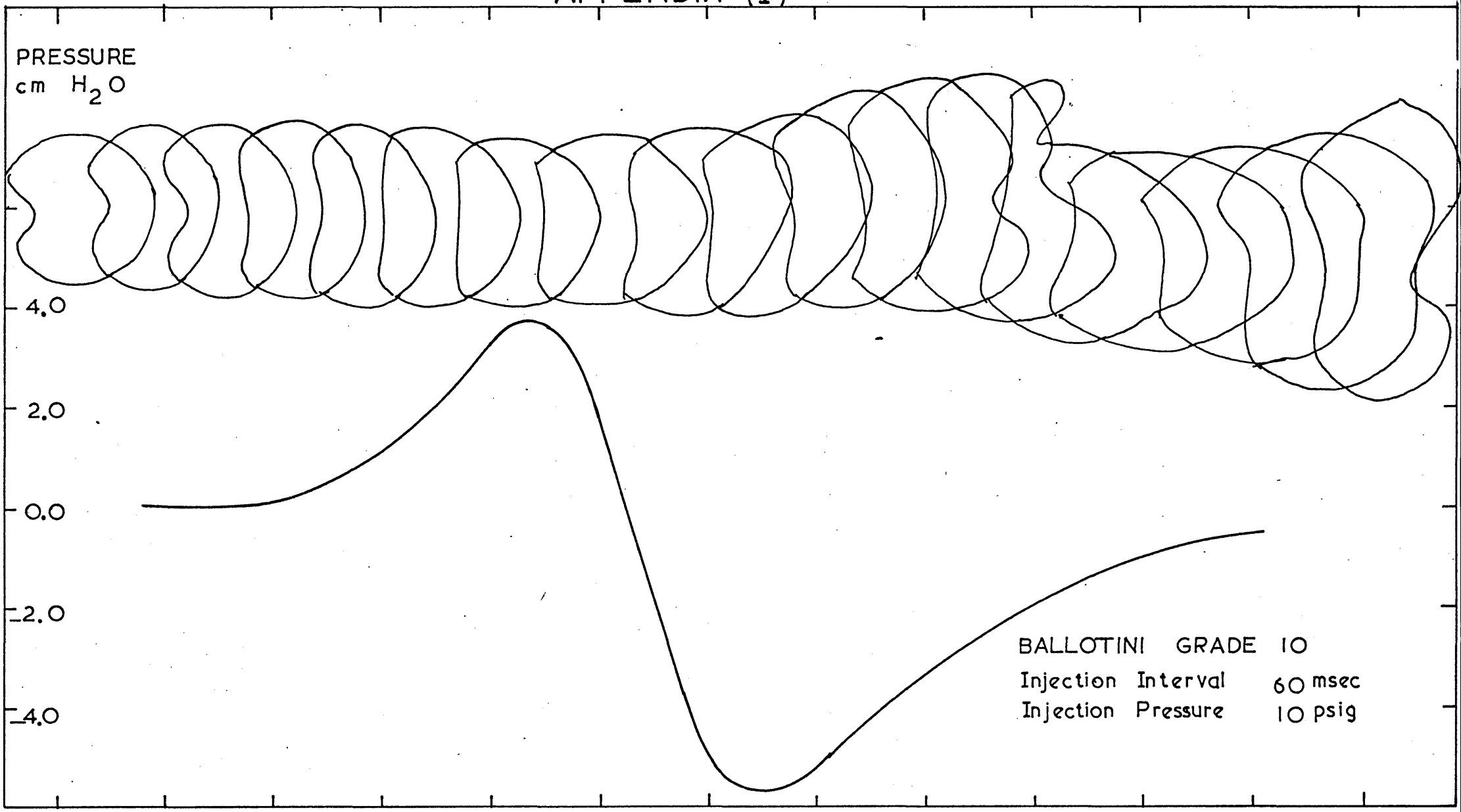
PRESSURE
cm H_2O
4.0
2.0
0.0
-2.0
-4.0
10
20
30
40
50
60
70
DISTANCE FROM THE INJECTOR cm
BALLOTINI GRADE 10
Injection Interval 60 msec
Injection Pressure 10 psig

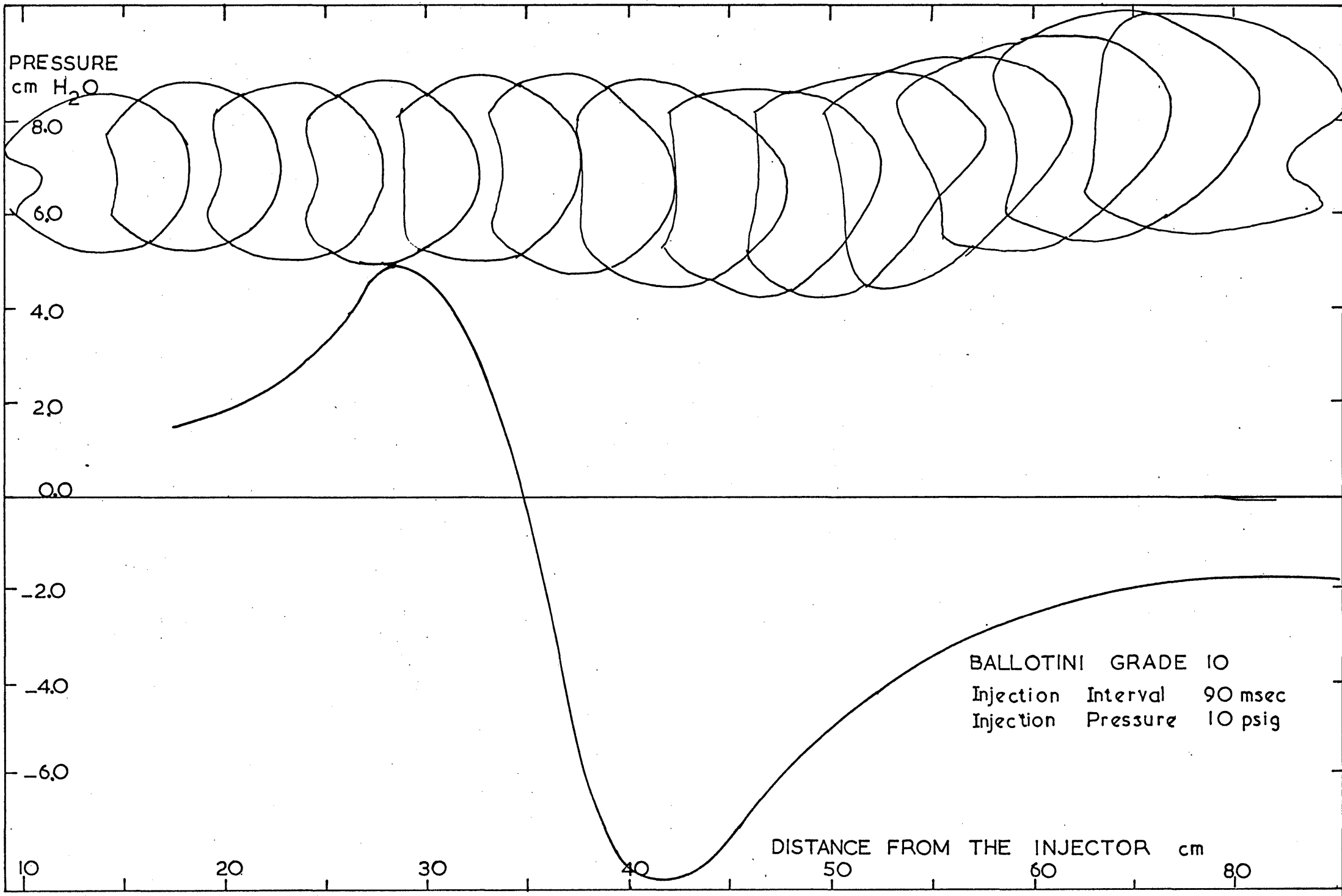
PRESSURE
cm H_2O
8.0
6.0
4.0
2.0
0.0
-2.0
-4.0
-6.0
BALLOTINI GRADE 10
Injection Interval 90 msec
Injection Pressure 10 psig
10
20
30
40
50
60
80
DISTANCE FROM THE INJECTOR cm

APPENDIX (I)

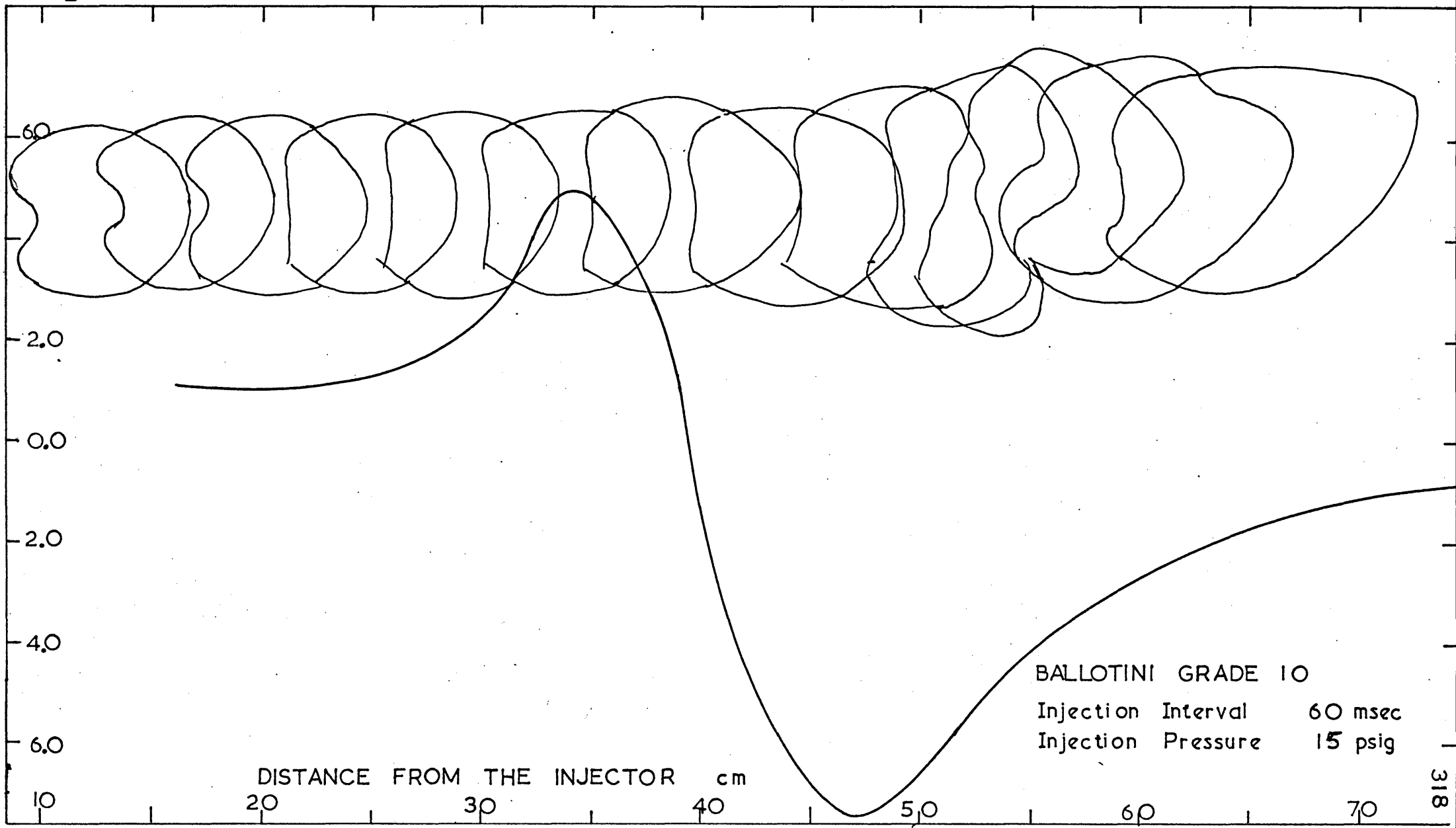
PRESSURE
cm H_2 O
6.0
2.0
0.0
2.0
4.0
6.0
DISTANCE FROM THE INJECTOR cm
10
20
30
40
50
60
70
BALLOTINI GRADE 10
Injection Interval 60 msec
Injection Pressure 15 psig

APPENDIX (II)

PRESSURE INSIDE A BUBBLE

The stream function for the flow outside the bubble given by DAVIDSON (44) is:

$$\psi = (U_B - u_o)(1 - \frac{A^2}{r^2})\sin\theta$$

with $$\frac{A^2}{a^2} = \frac{U_B + u_o}{U_B - u_o} .$$

Assuming that the stream function for the flow inside a bubble is of the form:

$$\psi = (Dr + Er^2) \sin\theta$$

and that at the boundary of the bubble:

(i) $V_{\theta i} = V_{\theta o}$

(ii) $V_{ri} = V_{ro}$

where $V_{\theta i}$, V_{ri}, $V_{\theta o}$ and V_{ro} are the tangential and radial components of the fluid velocity inside and outside the bubble respectively, PYLE & ROSE (63) have shown that the stream function inside the bubble is given by:

$$\psi = 2 U_o \quad (1 + \beta) \frac{r}{a} - (2 + \beta) \quad r \sin\theta \qquad \text{Eq.(A1)}$$

where:

$\beta = U_B/U_o$

U_B = bubble velocity

U_o = incipient velocity (superficial)

Some of the stream lines for the flow are given in Fig.(A1).

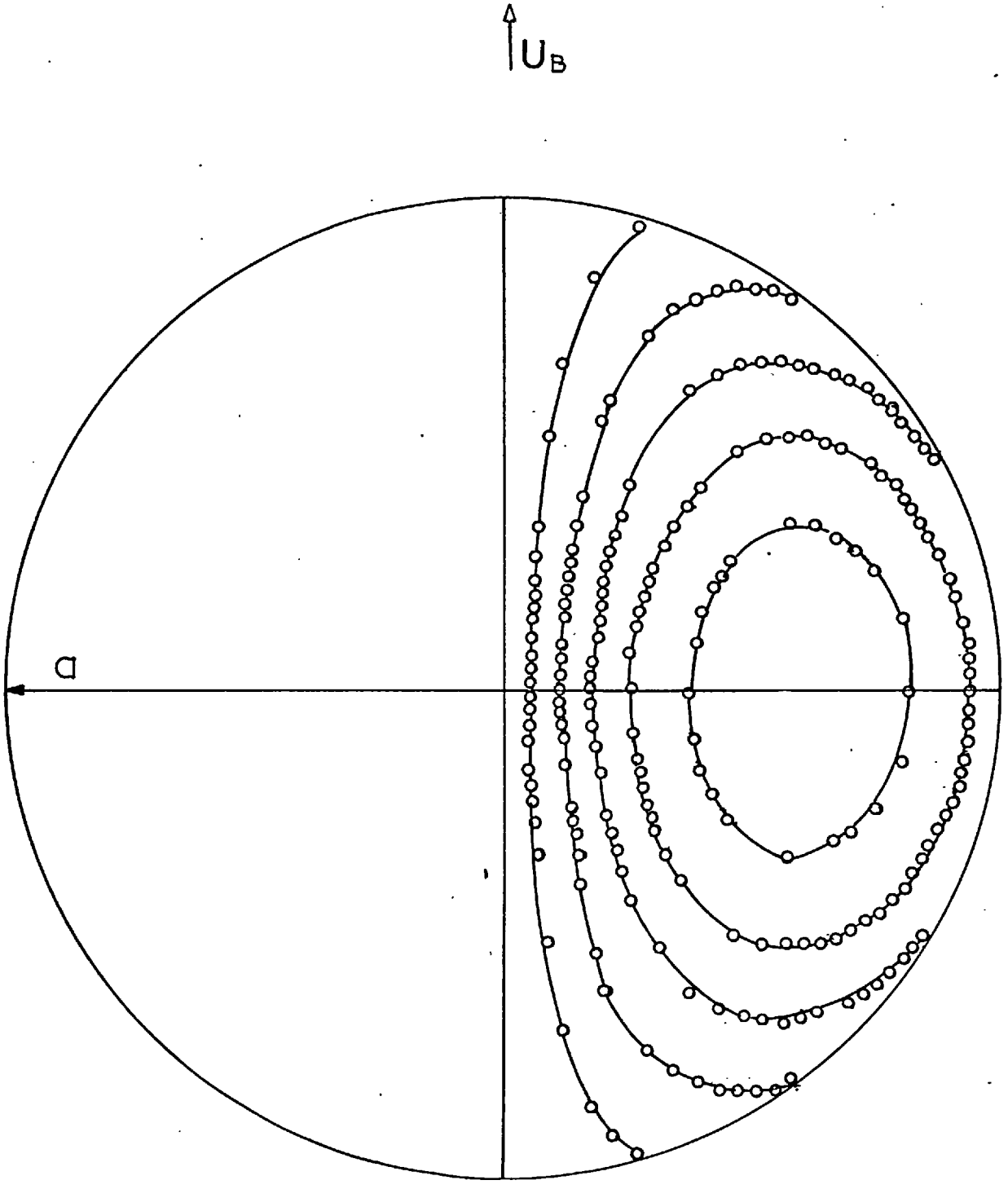

Fig(A-1)

In order to find the pressure at different points inside the bubble we apply the Bernoulli equation along a streamline. We have:

$$\frac{P}{\rho} + g\,Z + \frac{q^2}{2} = \text{constant} \qquad \text{Eq.(A2)}$$

where

g = gravitational acceleration,

q = velocity in space,

P = pressure along the streamlines,

ρ = fluid density,

Z = distance in vertical direction.

For the space velocity: $q^2 = V_r^2 + V_\theta^2$, where r and θ are the directions as given in Fig.(A2), and

$$V_\theta = + \frac{\partial \Psi}{\partial r}$$

$$V_r = - \frac{1}{r} \frac{\partial \Psi}{\partial \theta}$$

where Ψ is as given in Eq.(A1), and also $Z = r \cos\theta$. Thus the pressure along a streamline is:

$$\frac{P}{\rho} = - g\,r\cos\theta - 2\,U_o^2 \left\{ \cos^2\theta \left[2(2+\beta)(1+\beta)\frac{r}{a} - 3(1+\beta)^2 \frac{r^2}{a^2} \right] + 4\left[(1+\beta)^2 \frac{r^2}{a^2} + (2+\beta)^2 - 4(1+\beta)(2+\beta)\frac{r}{a} \right] \right\}$$

$$+ \text{constant} \qquad \text{Eq. (A3)}$$

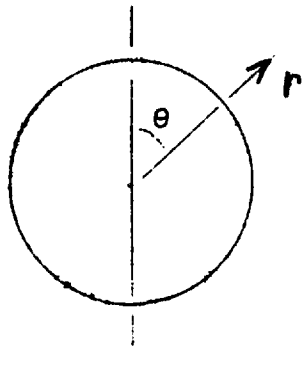

Fig. (A2)

A program was written to find values of "r" and "θ" which would satisfy Eq.(A1), for specified values of the stream function, and the corresponding pressure from Eq.(A3). In Fig.(A3) the pressure data are plotted as function of position on the corresponding streamline. For each streamline the magnitude of the pressure at θ = o is taken as the reference pressure, so that the pressure data are $(P_\theta - P_{qo})$ for each case. The following points are noticeable:

(i) For a streamline completely inside the bubble the corresponding pressure curve is completely closed. Starting from the lowest point on the streamline and moving up in the direction of the flow, the pressure keeps decreasing until it reaches to a minimum at the highest point. From there moving downward in the flow direction the pressure keeps increasing up to a maximum on the lowest point of the streamline. It is clearly seen that for the innermost streamlines the pressure is identical at pairs of points where the streamline is cut by a horizontal level.

(ii) For outer streamlines the region of identical pressure at each level, shrinks from the top and foot. For those streamlines which are not completely closed inside the bubble, the down-coming and up-going branches of the pressure curves are well separated. There is a discontinuity which corresponds to the part of the streamline outside the bubble.

(iii) The maximum drop in pressure from near the bottom of the bubble to near the top is about 10 dyne/cm^2 under present conditions. For such a bubble (8 cm diameter) in ballotini grade 10 the pressure drop across a height of one bubble-diameter of the particulate phase would be 10000 dyne/cm^2. We see that the pressure drop inside the bubble is negligibly small and 10^{-3} times the amount outside the bubble. This is almost equal to the ratio of the densities of the

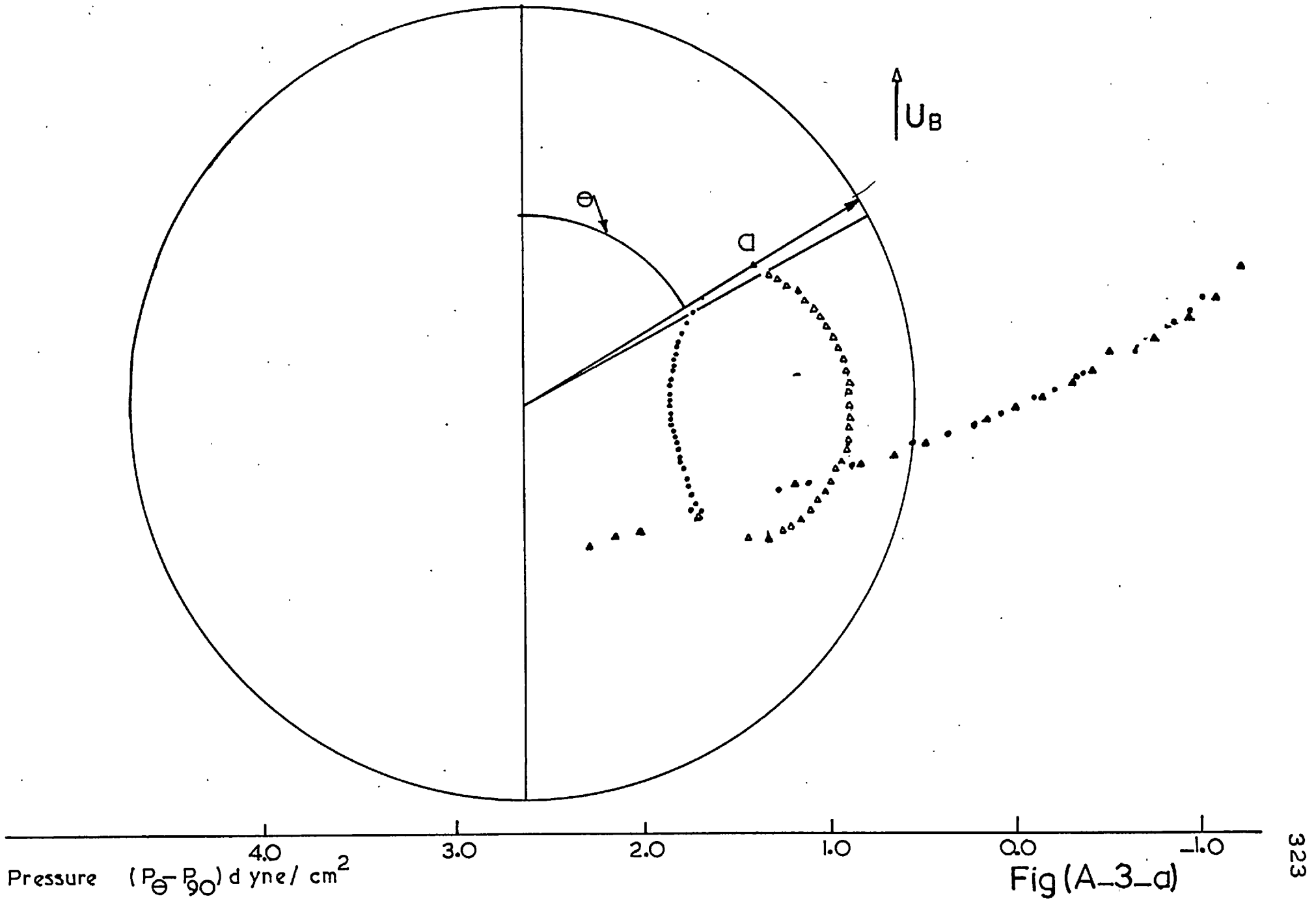

Fig (A-3-a)

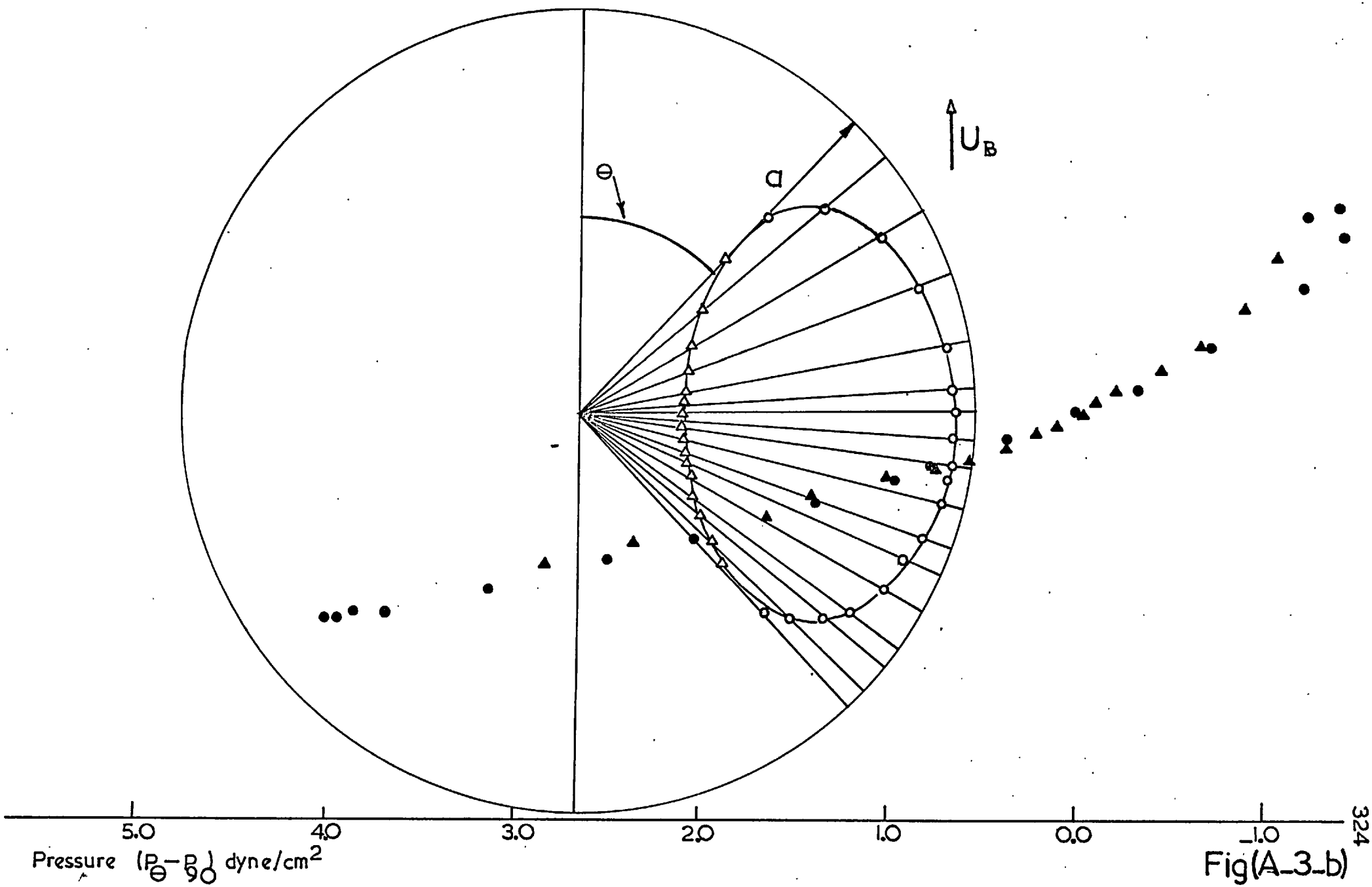

Fig(A_3_b)

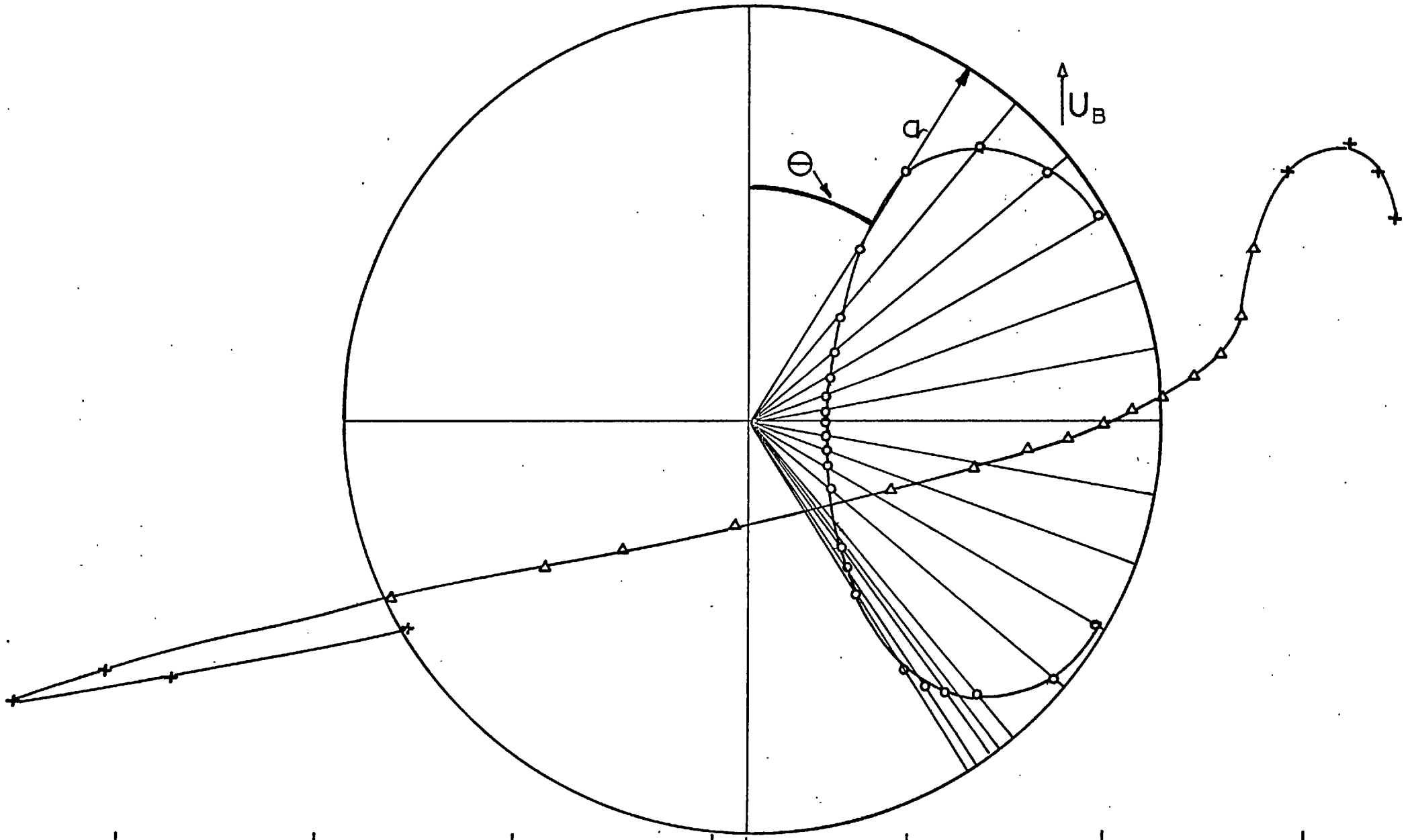

Fig(A-3-c)

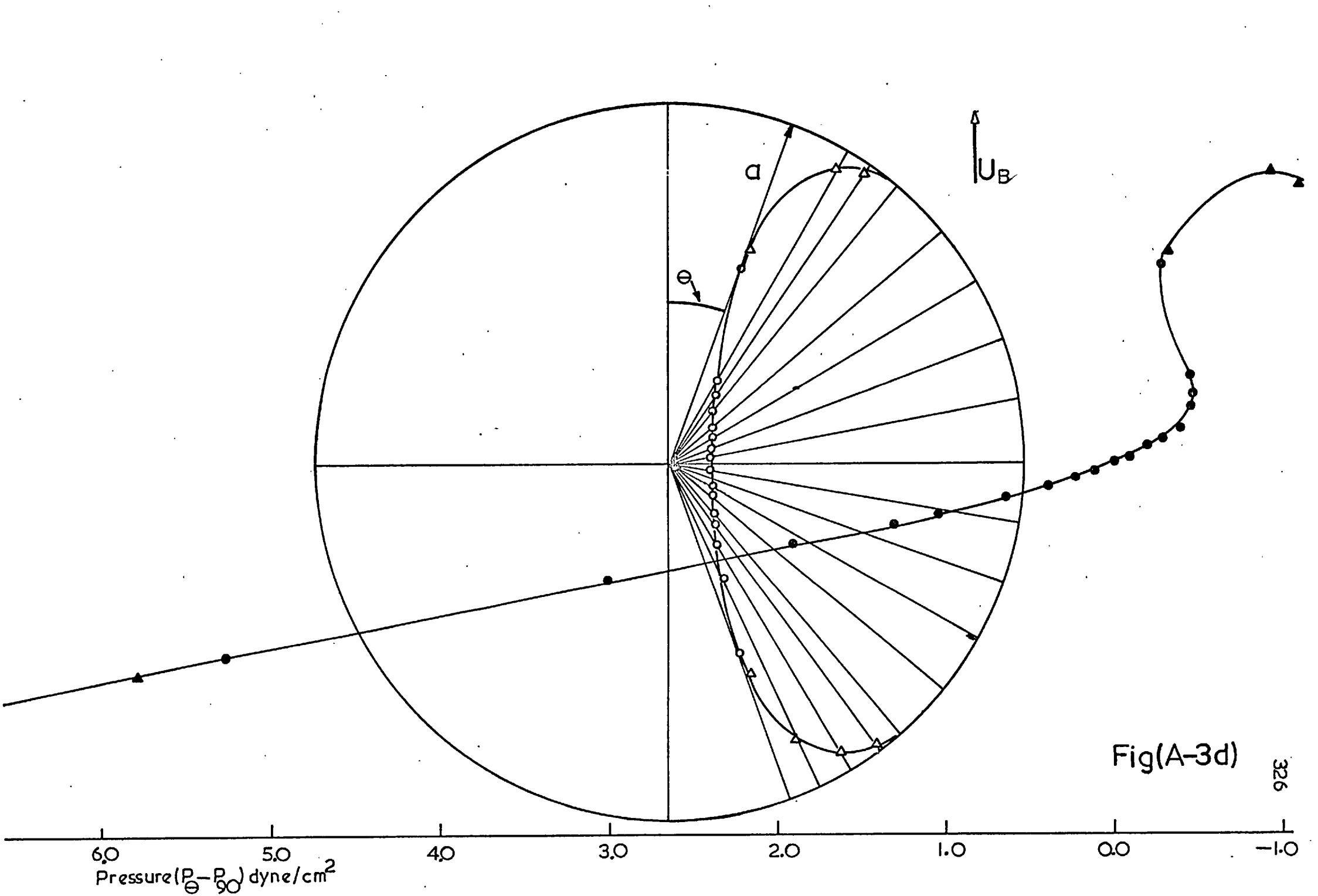

Fig(A-3d)

phases inside and outside the bubble.

(iv) As is seen from Fig.(A4) the pressure at $\theta = 90^{\circ}$, i.e. on the horizontal radius of the bubble has a lower magnitude near the centre. Moving towards the boundary, the pressure increases and has a maximum in the intermediate region, but decreases again near the boundary of the bubble. This behaviour is quite expected and is consistent with the high velocity near the centre and the boundary of bubble, i.e. closely spaced streamlines, and low velocity in the middle. The maximum in pressure occurs at a point where the fluid particle has no movement other than rotation around its axis.

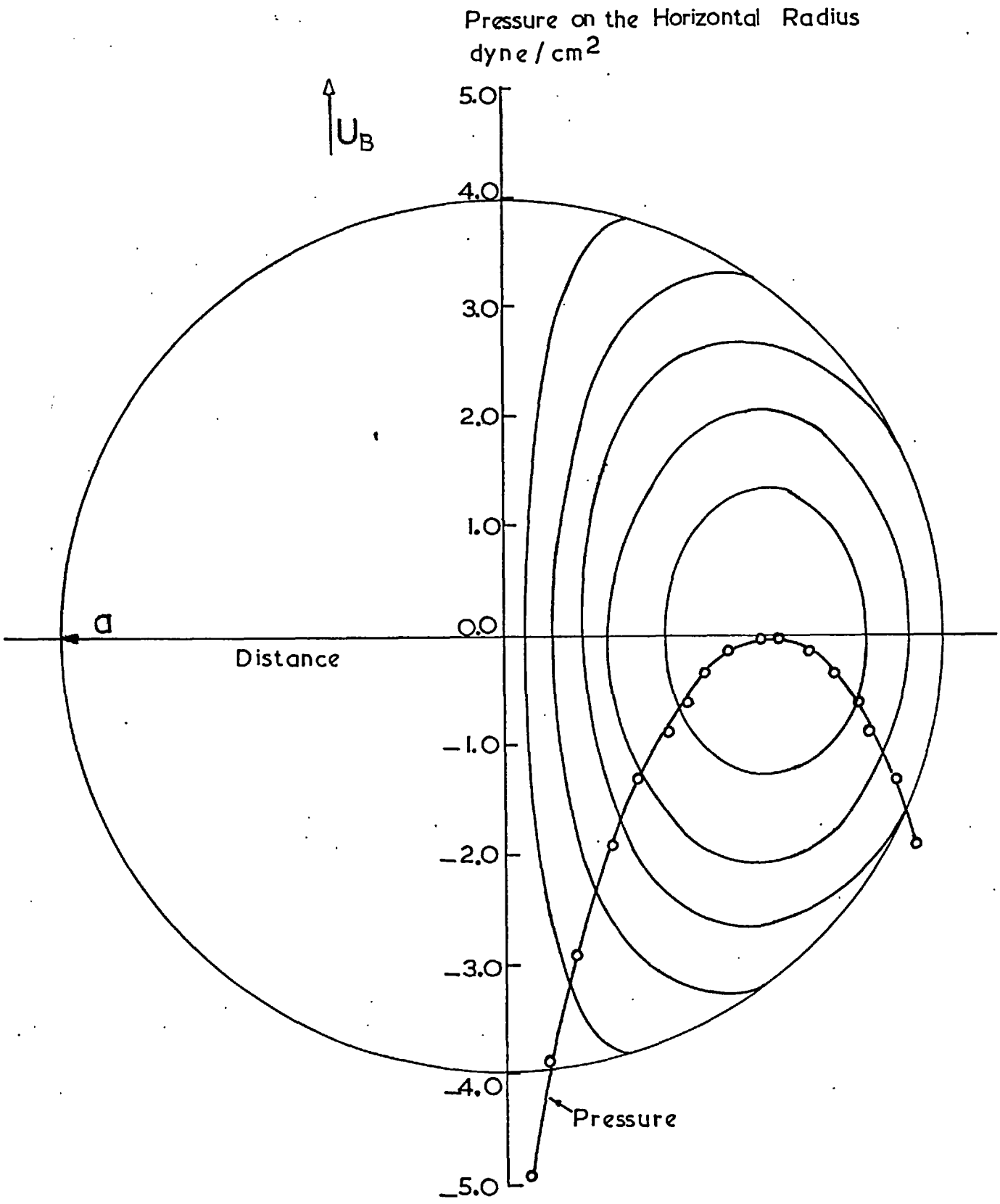
Pressure on the Horizontal Radius
dyne / cm2
UB
5.0
4.0
3.0
2.0
1.0
0.0
-1.0
-2.0
-3.0
-4.0
-5.0
a
Distance
Pressure

Fig(A.4)

REFERENCES

(1) BOTTERILL, J.S.M., et al, Symp. On Interaction between Fluids and Particles Inst. Chem. Engrs. London 1962

(2) ROWE, P.N., et al, Trans. Instn Chem. Engrs. 1965 43, T271

(3) TOOMEY, R.D. and JOHNSTON, H.F., Chem Engng Prog. 1952 48 220.

(4) DAVIDSON, J.F. and HARRISON, D., Fluidised Particles, Cambridge University Press 1963.

(5) BAUMGARTEN, P.K. and PIGFORD, R.L., A.I.Ch.E. Jl 1960 6 115

(6) LANNEAU, K.P., Trans. Instn. Chem. Engrs. 1960 38 125

(7) ROWE, P.N. and SUTHERLAND, K.S., Trans. Instn Chem. Engrs. 1964 42 T55

(8) DAVIES, L. and RICHARDSON, J.F., Trans. Instn Chem. Engrs 1966 44 T293

(9) TURNER, J.C.R., Chem. Engng Sci. 1966 21 971

(10) DAVIDSON, J.F. and HARRISON, D., Chem. Engng Sci. 1966 21 731

(11) PARTRIDGE, G. and ROWE, P.N., Trans. Instn Chem. Engrs 1966 44 T349

(12) LOCKETT, M.J., DAVIDSON, J.F., and HARRISON, D., Chem. Engng Sci. 1967 22 1059

(13) PYLE, D.L., and HARRISON, D., Chem. Engng Sci. 1967 22 1199

(14) NICKLIN, D.J., WILKES, J.O., and DAVIDSON, J.F. Trans. Instn Chem. Engrs 1962 40 61

(15) GRACE, J.R. and HARRISON, D., Chem. Engng Sci. 1969 24 497

(16) GELDART, D., Powder Technol 1968 1 355

(17) TOEI, R., MATSUNO, R., Proc. Intern. Symp. on Fluidization, Netherland - Univ. Press. Amsterdam 1967

(18) KUNII, D., YOSHIDA, K., and HIRAKI, I., Proc. Intern. Symp. on Fluidization, Netherland - Univ. Press. Amsterdam 1967

(19) KOBAYASHI, H., and ARAI, F., Preprint for the 6th Symposium on Chemical Reaction Engrng., Soc. Chem. Engrs., JAPAN, NAGOYA, No. (1962)

(20) COULSON, J.M., and RICHARDSON, J.F., Chemical Engineering Vol. 2 P.392 Pergamon Press 1955

(21) MURRAY, J.D., J. Fluid Mech. 1965 22 57

(22) JUDD, M.R., Ph.D. dissertation, University of Cape Town 1965

(23) BENNETT, C.A., and FRANKLIN, N.L., Statistical Analysis in Chemistry and Chemical Industry. JOHN WILEY & SONS, INC.

(24) SNELL, J.E., LECTURE NOTES IMPERIAL COLLEGE LONDON 1970

(25) DE KOCK, J.W. Ph.D. dissertation University of Cambridge 1961

(26) ROWE, P.N., Atomic Energy Research Establishment, Harwell, 1962

(27) ROWE P.N., and WACE, P.F., Nature, Lond. 1960, 188, 737

(28) JACKSON, R., Trans. Instn Chem. Engrs. 1963, 41 T13

(29) PYLE, D.L., and HARRISON, D., Chem. Engng Sci. 1967 22 531

(30) TOEI, R., and MATSUNO, R., Proc. Intern. Symp. on Fluidization, Netherland Univ. Press. Amsterdam 1967

(31) HARRISON, D., and LEUNG, L.S., 3rd Congr. Europ. Fed. Chem. Engrs P.127, Instn Chem. Engrs., London 1962

(32) WHITEHEAD, A.B., and YOUNG, A.D., Proc. Intern. Symp. on Fluidization, Netherland Univ. Press. Amsterdam 1967

(33) BOTTERILL, J.S.M., GEORGE, J.S. and BESFORD, H. CEP Symposium Series, Vol. 62, 1966 A.I.Ch.E.

(34) PARTRIDGE, B.A., and ROWE, P.N., Trans. Instn Chem. Engrs 1966 44, T335

(35) RIETMA, K., Proc. Intern. Symp. on Fluidization, Netherland Univ. Press, Amsterdam 1967

(36) ROWE, P.N. Proc. Intern. Symp. on Fluidization. Netherland Univ. Press, Amsterdam 1967

(37) KUNII, D., and LEVENSPIEL, O., Fluidization Engineering, JOHN WILEY & SONS, INC. 1968

(38) LITTMAN, H., Paper presented at A.I.Ch.E. meeting Chicago 1962

(39) MUCHI, I., and SHICHI, R., Preprint for 4th Annual Symposium, Soc. Chem. Engrs., JAPAN, TOKYO, NOV 1965

(40) WHITEHEAD, A.B., DENT, D.C., and BHAT, G.N., Powder Technol 1967 1 143

(41) MOTAMEDI-LANJANI, M. M.Sc. Thesis University of London 1967

(42) BERG, A., KLASSEN, J. and GISHLER, P.N., Can. J. Res. 1950 F28 287

(43) MOTAMEDI, M., and JAMESON, G.J. Chem. Engrng Sci. 1968 23 791

(44) DAVIDSON, J.F., Symposium on Fluidization - Discussion Trans. Instn Chem. Engrs. Lond 1961, 39, 230

(45) WACE, P.F., and BURNETT, S.J., Trans. Instn Chem. Engrs 1961, 39, 168

(46) REUTER, H., Chemie-Ingenieur-Technick 1963, 35 98

(47) ANGELINO, H., CHARZAT, C., and WILLIAMS, R., Chem. Engng Sci. 1964, 19, 289

(48) PYLE, D.L., STEWART, P.S.B., Chem. Engng Sci. 1964, 19, 842

(49) STEWART, P.S.B., Trans. Instn Chem. Engrs. 1968, 46, T60

(50) COLLINS, R., Chem. Engng Sci., 1965 20 747

(51) LOCKETT, M.J., and HARRISON, D. Proc. Intern Symp. on Fluidization Netherland Univ. Press. Amsterdam 1967

(52) STEWART, P.S.B., Chem. Engng Sci 1967 45 611

(53) ROWE, P.N., and PARTRIDGE, B.A., Trans. Instn Chem. Engrs. 1965 43 157

(54) REUTER, H., C.E.P. Symposium Series 1966, Vol. 92 No 62

(55) RIETMA, K., Proc. Intern. Symp. on Fluidization, Netherland Univ. Press Amsterdam 1967

(56) HIMSWORTH J.R., Proc. Intern. Symp on Fluidization - Discussion Netherland Univ. Press. Amsterdam 1967 p 168

(57) BUYSMAN, P.J. and PEERSMAN, G.A.N., Proc. Intern. Symp. on Fluidization Netherland Univ. Press Amsterdam 1967

(58) LITTMAN, H., and HOMOLKA, A.G., Preprint 64th National A.Ich.E. Meetings New Orleans 1969

(59) ROWE, P.N., PARTRIDGE, B.A., and LYALL, E., Trans Instn Chem. Engrs. 1964, 19, 973

(60) ROWE, P.N., and PARTRIDGE, B.A., Proc. Symp. On Intraction between Fluids and Particles, Instn Chem. Engrs., London 1962

(61) ROWE, P.N., Trans. Instn Chem. Engrs, 1961, 39, 175

(62) ROWE, P.N. and HENWOOD, G.A. Trans. Instn Chem. Engrs. 1961, 39, 43

(63) PYLE, D.L., and ROSE, P.L., Chem. Engng Sci. 1965, 20, 25